Enhancement of the submerged membrane electro-bioreactor (SMEBR) for nutrient removal and membrane fouling control

Sharif Ibeid

A Thesis

In the Department of

Building, Civil and Environmental Engineering

Presented in Partial Fulfillment of the requirements

For the Degree of

Doctor of Philosophy (Civil Engineering) at

Concordia University

Montreal, Quebec, Canada

December 2011

CONCORDIA UNIVERSITY

School of Graduate Studies

This is to certify that the thesis prepared
By: Sharif Ibeid
Entitled: Enhancement of the submerged membrane electro-bioreactor (SMEBR) for nutrient removal and membrane fouling control

and submitted in partial fulfillment of the requirements for the degree of

Doctor of philosophy (Civil Engineering)

complies with the regulations of the University and meets the accepted standards with respect to originality and quality.

Signed by the final Examining Committee:

Dr. A. K. Waizuddin Ahmed Chair

Dr. M. Heitz External Examiner

Dr. S. Williamson (ECE) Examiner to Program

Dr. C. Mulligan (BCEE) Examiner

Dr. A. Zsaki (BCEE) Examiner

Dr. M. Elektorowicz (BCEE) Supervisor

Approved by Dr. M. Elektorowicz
Chair of Department or Graduate Program Director

December/2011 Dr. R. Drew

Dean of Faculty

Abstract

Enhancement of the submerged membrane electro-bioreactor (SMEBR) for nutrient removal and membrane fouling control

Sharif Ibeid, Ph.D.

Concordia University, 2011

A submerged membrane electro bioreactor (SMEBR) to enhance effluent quality and to reduce membrane fouling was patented by Elektorowicz et al (2009). In this system, activated sludge biological treatment, membrane filtration and electrokinetics are working together in one hybrid unit. The first objective of this research aimed to remove the major unwanted nutrients (Phosphorus and Nitrogen) in addition to the carbon in one single electro-bioreactor unit. The second objective was to investigate the relationship between the electrical input parameters (voltage gradient, current density and exposure mode) on sludge characteristics and therefore membrane fouling. This study consists of three phases: Phase 1 (batch tests), Phase 2 (lab-scale continuous flow) and Phase 3 (pilot-scale continuous flow). The results showed that the direct current (DC) field of medium current density (15 to 25 A/m^2) has the potential to substantially improve sludge characteristics in terms of better dewaterability and high removal of soluble microbial products (SMP) and organic colloids. However, the electrical inputs should be selected based on the concentration of the mixed liquor suspended solids (MLSS). Subsequently, a high reduction of membrane fouling was obtained. The degree of membrane fouling reduction was ranging between 1 to 5 times based on the concentration of soluble microbial products (SMP) and the volatile suspended solids (VSS). This study demonstrated substantial removal efficiencies of nutrients up to more than 95% for carbon, 99% for phosphorus and 97% for nitrogen. However, the removal efficiency of nitrogen was found to be highly influenced by the temperature and the C/N ratio. High temperature (> 18^o C) and high concentration of carbon in the influent wastewater led to a better removal efficiency of nitrogen. SMEBR showed outstanding results that make it a promising technology that can reduce fouling and remove all major macro nutrients at high efficiency in one single reactor.

Acknowledgment

The authors acknowledge the financial support from NSERC STPGP 350666 grants awarded to:

Dr. M. Elektorowicz and Dr. J. Oleszkiewicz.

The help from the cities of Montreal, Laval, Repentigny and l'Assomption

The help and cooperation of the employees and staff of the St. Hyacinthe treatment plant

The help of Microsa Asashi, Japan for providing the pilot membrane

Dedication

I dedicate this thesis to my beloved wife, beautiful daughters, sincere parents and parents-in-law. Their caring, support and encouragement in the last four years was the driving force in helping me achieve my goals and fulfill the requirements of my degree. Special thanks go to my wife who stood behind me all the time and was there when I needed someone to talk to. I would like to extend my dedication to Dr. Maria Elektorowicz, my supervisor, for her support and understanding of a husband and a father living a student life.

Table of Contents

List of figures

List of tables

Chapter 1

Introduction - wastewater treatment plant challenges

1.1 Background

Effluent from wastewater treatment plants poses an environmental hazard to the receiving water bodies mainly due to its richness in nutrients (phosphorus and nitrogen), particularly if the plant is not designed to perform tertiary nutrient treatment. These nutrients are the major eutrophication stimulants that should be eliminated from the effluent before discharging into the aquatic ecosystems, so as to prevent any environmental hazard. Currently, new treatment facilities are designed to remove these nutrients to extremely low levels (< 50 μm and < 2 mg N/l) as a part of sustainable water management. Nevertheless, the more stringent regulations, Quebec in particular, require the retrofitting of the existing ones to meet the disposal requirements and reduce the concentration of these nutrients as much as possible. In conventional treatment plants, the removal of carbon, phosphorus and nitrogen requires several biological reactors working simultaneously at different operating conditions to create the optimum environment for the removal of each single nutrient.

The aerobic activated sludge reactor is by far the most widely applied method to remove carbon (c) through the oxidation of the organic materials by the microbial biomass (flocs). Phosphorus removal involves the recycling of microbial flocs into anaerobic and aerobic zones in order to promote the accumulation of phosphate by

micro-organisms in a process known as enhanced biological phosphorus removal. Biological phosphorus removal can produce an effluent with total phosphorus as low as 0.1 to 0.2 mg/l. Chemicals such as Aluminum sulfate and ferric chloride are common precipitants that are used as alternatives to the biological process or in cases where lower phosphorus concentrations are demanded. On the other hand, nitrogen removal involves sequential aerobic and anoxic reactors to achieve complete transformation of the influent ammonium into nitrogen gas. Carbon source is added into the anoxic reactor to promote the heterotrophic denitrifies responsible for the conversion of nitrate into gas, which is costly and could be detected in the effluent due to incomplete oxidation. However, eliminating all nutrients in one single reactor is undoubtedly a challenging task. But once established, it would reduce the infrastructure cost and plant footprints, which are the major obstacles of building high standard facilities.

Currently, membrane bioreactors (MBR) to separate suspended solids from the liquid in the conventional activated sludge process are used successfully in wastewater treatment plants. MBR reduces the plant footprint and produce high effluent quality through either the micro or ultra-filtration. However, MBR has no contribution in the removal of phosphorus and nitrogen. In addition to that, the reduction of flux over time because of fouling is the major obstacle that requires an immediate solution. Many studies on MBR illustrated that organic colloids and extrapolymer substances (EPS) are the major materials responsible for membrane fouling. Subsequently, removing these organics is the key solution to membrane fouling reduction.

Recently, another system was developed at Concordia University to generate a high quality (Elektorowicz et al. 2009). In this system, activated sludge treatment with membrane filtration is subjected to an electrical direct current (DC) field in the same chamber. In this system, called submerged membrane electro-bioreactor (SMEBR), electrodes are placed around the membrane, which permit on the dissolution of the anode and producing aluminum hydroxides. The combination of biological, membrane filtration and electrokinetics demonstrated high phosphorous, chemical oxygen demand (COD) and ammonia removal and reduction in membrane fouling (Bani-Melhem et al., 2010 and 2011). The SMEBR shows a very high potential to response to the contemporary needs of the wastewater treatment market preserving the principle of sustainability. Yet, SMEBR has not been optimized for the removal of nitrogen, and the mechanisms of membrane fouling reduction are not fully characterized.

1.2 Objectives

In order to build a large scale SMEBR that satisfies the challenges of wastewater treatment plants, the objectives of this research were prioritized in the following order:

1- To study the relationship between DC field parameters such as voltage gradient, current density and electrical exposure mode (time-ON/time-OFF) on sludge characteristics.

2- To determine the SMEBR electrical operating parameters that can improve sludge characteristics, reduce membrane fouling and enhance effluent quality.

3- To promote simultaneous removal of carbon, phosphorus and nitrogen in a single electro-bioreactor.

4- To determine the removal pathways of each nutrient.

To achieve the aforementioned objectives, three phases were needed. The experimentation started with series of batch tests (Phase 1) to provide the best conditions for the continuous flow bench SMEBR reactors (Phase 2). In Phase 3, the SMEBR was tested at a pilot scale level with raw wastewater in the wastewater treatment plant in l'Assomption, Quebec.

Chapter 2

Literature review

2.1 Introduction

Since the reduction of membrane fouling is a major objective of this study, the literature review will start out through defining the soluble microbial products (SMP) due to its direct impact on membrane fouling. Afterward, membrane fouling will be defined in conjunction with elaborated description of the factors affecting its propensity and the current applied methods to mitigate its hazard. In the end, a brief description of some nutrients removal methods that are related to the objectives of this study.

2.2 Microbial products (EPS and SMP) in the activated sludge

Extra-polymer substances (EPS) and soluble microbial products (SMP) represent the pool of organic fractions produced by microorganisms. These organics are considered the major materials responsible for membrane fouling as will be discussed later. By definition, EPSs are organic components located at the surfaces or outside of the microbial cell surfaces that help the aggregation of cells into flocs. EPSs allow the stabilization of the floc structure, provide resistance to toxins, retain water and oxygenous organic compounds, accumulate enzymes and facilitate communication among cells (Laspidou and Rittmann, 2002). EPSs are divided into two main categories; the bound (extractable) EPS and the soluble EPS. The first category composed of condensed capsular polymers tightly associated with the cells and loosely bound

compounds called slimes. The second category represents the soluble organic macro molecules and colloids that are not connected to the cell and move freely between microbial flocs in the liquid phase of the sludge (Nielsen et al., 1997; Hsieh et al., 1994; Nielsen and Jahn, 1999). Dissociation and hydrolysis of the bound EPS in addition to the shearing off from the cell surfaces are the major sources of soluble EPS (Hsieh et al., 1994). Polysaccharides and protein are the major constituents of EPS in any biomass solid surface. However, Nielsen et al. (1997) reported that protein is the predominant fraction of EPS formed in biofilters and trickling filters. Dignac et al. (1998) illustrated that protein is the predominant fraction in activated sludge EPS. Protein has a high density of negatively charged amino groups, which act electro-statically with cations to form stable flocs, yet, protein is the structural unit of enzymes involved in biochemical reactions (Ramsesh et al., 2006). Leung (2003) showed that, most EPS extraction procedures cited in the literature can effectively extract loosely and tightly bound EPS.

On the other hand, SMPs are the fraction of organic compounds released into the sludge supernatant during substrate metabolism (substrate-utilization-association products) and biomass decay (biomass associated products) (De Silva and Rittman, 2000a; Rittman et al., 1987 and 1994). Since SMP and soluble EPS have the same organic nature and come from the same origin, they have been considered synonymous reflecting the same organic pool (Laspidou and Rittman, 2002; Ramsesh et al., 2006). These SMPs or soluble EPS are biodegradable and form the majority of chemical and biological oxygen demands of the biological secondary treatment (De Silva and Rittman, 2000a, 2000b). Barker and Stuckey (1999) reviewed several studies on SMPs and

reported that a secondary effluent contains greater amounts of high molecular weight compounds (<0.5 to >50 kDa) than in the influent. The concentration of SMPs in secondary effluent is likely to increase at a rate proportional to the concentration of biomass because of cell lysis (Rittman et al., 1987; Hao and Lao, 1988). Baskir and Hansford (1980) and Pribyl et al. (1997) concluded that there is an optimum range of food/mass ratio of 0.3 to 1.2 g COD/g MLSS. d to keep the SMP at minimum concentration. A high food/mass ratio enhances microbial growth; low food/mass ratio enhances biomass decay and both of these pathways cause higher concentrations of SMP.

2.3 Membrane fouling

Fouling is the deposition of particles and colloids onto membrane surface combined with the precipitation of the dissolved materials inside the pores and on the membrane surface to eventually cause pore blocking (Bremere et al., 1999; Cho et al., 1999; Crozes et al., 1997). Activated sludge contains different fractions contribute to membrane fouling; namely, suspended solids, colloids and solutes. Some studies claimed that suspended solids are the major fouling contributors (Defrance et al., 2000), others mentioned solutes as the major contributors (Wisniewski and Gramsick, 1998) and others stated that colloids are the main cause of fouling (Bouhabila et al., 2001). These discrepancies in conclusions are related to the differences in operating conditions, sludge characteristics, composition of synthetic water and the type of the membrane used in their studies. In addition, suspended solids, colloidal and solutes are interrelated

components, for example, soluble microbial products (SMP), highly correlated to membrane fouling, comprise the major fraction of sludge dissolved organic carbon (solutes) and have a nano-colloidal size. SMP components could be retained on top of the membrane surface and become part of the cake layer or block membrane pores or adsorbed onto membrane surface or inside pore walls.

The reversible fouling is caused by the deposition of the activated sludge flocs and large particles onto membrane surface to form a cake layer. Reversible fouling is easily removable by appropriate physical cleaning like backwashing (Chang et al., 2008; Wang et al., 2008; Watanable and Kimura, 2006). Irreversible fouling, on the other hand, is the fouling caused by adsorption of dissolved organic material and solutes into membrane pores that lead to the formation of gel layer onto membrane surface. This gel layer is composed of SMP, EPS, colloids, solutes and biofilm. This kind of fouling is persistent and could be partially removed by chemical cleaning (Chang et al., 2008; Wang et al., 2008; Watanable and Kimura, 2006). The hydraulic permeability of the cake layer decreases with the increase of electrolyte in the feed water, increase of permeate flux, (higher flux lead to more compressed cake layer), decrease of surface charge (due to electrical repulsion) and decrease of floc size (Petsev et al., 1993). Reversible fouling could be converted into irreversible if not cleaned continuously and on time.

The physicochemical interactions between membrane module and foulants lead to flux decline and an increase of the filtration resistance. Resistance in series model is the

simplest expressing membrane fouling mechanisms (Lee et al., 2001; Silva et al., 2000). According to this model,

$$R_t = R_m + R_c + R_f \quad (2.1)$$

$$R_f = R_{pb} + R_a \quad (2.2)$$

Where, R_t is the total membrane resistance (m^{-1}), R_m is the intrinsic membrane resistance (m^{-1}), R_c is the cake layer resistance (m^{-1}) (reversible fouling), R_f is the irreversible fouling resistance (m^{-1}), R_{pb} is the pore block resistance (m^{-1}), and R_a is the adsorption resistance (m^{-1}). The resistance can be calculated according to Darcy's law (Equation 2.3)

$$R = TMP/\mu . J \quad (2.3)$$

Where, R is the resistance of any fouling mechanism of interest (m^{-1}), TMP is the transmembrane pressure cause by this fouling mechanism (Pa), μ is permeate dynamic viscosity in Pa.s and J is the permeate flux in $m^3/m^2.s$. In order to calculate all values of resistances caused by different fouling mechanisms, a series of filtration tests are conducted to calculate the value of each resistance compound. Pure water filtration to calculate R_m, sludge filtration to calculate R_c and pure water filtration immediately after cake layer removal to calculate R_f.

2.4 Factors affecting membrane fouling

Any membrane fouling is controlled by membrane module properties, sludge characteristics and the operating conditions. Unfortunately, studying the impact of these factors on membrane fouling was not conducted under a standard method that

facilitates the exchange of results and comparisons. Different scientific approaches, sludge properties, wastewater composition, operation conditions, membrane modules were used in these studies leading to the impossibility of making an absolute conclusions. In addition to that, these factors are interrelated and act simultaneously. This makes the assessment of each fouling contributor separately subject to a certain degree of experimental error. Nevertheless, understanding the fouling mechanism of these factors and their interactions with the membrane module is the best way towards outlining the required criteria of reducing the fouling phenomenon.

2.4.1 Membrane module properties vs. fouling

Three major materials are used in manufacturing membrane modules; cellulose acetate, polyamide and polysulfone polymers (Table 2.1). Currently, thin film composite membranes made of a mixture of polymers are dominating the commercial markets. Membrane properties play an important role in the first stages of adsorption of organic molecules and biofilm initiation. Before the initiation of any biofilm on membrane surfaces, the absorption of macromolecules onto membrane surface should proceed to serve as carbon source for the first attached cells; this preparation step is called membrane conditioning. Membrane surface properties such as electrical charge (zeta potential), roughness and hydrophobicity govern the speed and the strength of fouling formation. Most membranes gain their negative charge in water by protonation and polarization of their functional groups (Kang et al., 2006). Membranes with more negative charges are likely to repel particles that are negatively charged and thus

mitigate the adsorption potential of these compounds. However, the exact effect of membrane charge on fouling is still unclear. Some researchers (Pasmore et al., 2001) reported minimum fouling when the surface charge is minimal, other studies found that more negatively charged membranes are more effective in reducing cell adhesion and reduce fouling rate (Kang et al., 2001). Surface roughness enhances the attachment of foulants through increasing the surface area and reducing the shear velocity on the surface proximity (Kang et al., 2006; Vrijen Hoek et al., 2001). Regarding hydrophobicity, it is highly accepted that hydrophilic membranes exhibit higher fouling resistance than their hydrophobic counterparts (Fan et al., 2001; Pasmore et al. 2001). This is mainly because of their higher affinity to water than compounds of hydrophobic nature. Pasmore et al. (2001) tested 31 membranes with different surface properties and reported that hydrophilic, electrically neutral and smooth surfaces reduce the adsorption of organic molecules and biofilm formation rate. Their results are consistent with the findings of Knoll et al. (1999). Yamamoto et al. (2006) tested two membrane materials polyethylene (PE) and polyvinylidene fluoride (PVDF) having the same nominal pore size. They found that after 140 days of operation under the same conditions and physical cleaning that the filtration resistance for PVDF membranes was much less than PE despite that the amount of material adsorbed on the PVDF membrane was higher than that for PE, because PVDF adsorbed organic materials with less fouling potential.

Table 2.1: Major manufacturing materials used in membrane industry (Escobar et al., 2005)

Group-1	Group-2	Group-3	Others
Cellulose acetate Cellulose diacetate Cellulose triacetate	Polyamid Aromatic polyamide Polyether amid Polyether amines Polyetherurea	Polysulfone polyethersulfone	Polyvinylidene fluoride (PVDF) Polypropylene Polyethylene (PE)

2.4.2 Sludge properties vs. fouling

Meng et al. (2006) reviewed the literature and found that the mixed liquor suspended solid (MLSS) concentration, bound EPS, SMP, floc particle size distribution, sludge viscosity, flocs and colloids relative hydrophobicity and surface charge (zeta potential) are the major sludge properties correlated with membrane fouling.

2.4.2.1 Mixed liquor suspended solids (MLSS)

Theoretically, increasing the concentration of MLSS is expected to increase fouling. Ross et al. (1990) showed that MLSS of 40,000 mg/l would severely reduce permeate flux. The concentration of 30,000 to 40,000 mg/l was set by Yamamoto et al. (1989) as the critical flux beyond which severe fouling is witnessed. Other studies showed that low and medium concentrations of MLSS has no significant differences on its effect on membrane fouling, 3600 to 8400 mg/l (Hong et al., 2002), 4000 to 8000 mg/l (Le Clech et al., 2003). Rosenberger et al. (2005) reported after reviewing different studies that

low concentration of MLSS (<6000 mg/l) exhibit low fouling, high MLSS (>15000 mg/l) has a high fouling potential and the intermediate values has no significant difference. Meng et al. (2006) found an exponential relationship between MLSS (2000 to 25,000 mg/l) and fouling formation rate. Based on the previous studies, it is recommended to operate SMBR at MLSS lower than 15,000 mg/l in order to avoid membrane fouling as much as possible. On the other hand, some studies found that increasing MLSS from 3000 to 8000 mg/l reduced fouling probably due to reducing the deposition of small particles onto the membrane surface (Li et al., 2008). Therefore, studying the relationship between MLSS and membrane fouling is a necessity in our study.

2.4.2.2 Viscosity

According to Darcy's law (Equation 2.3) the permeate flux will decrease as the sludge dynamic viscosity increased. The dynamic viscosity reflects the amount of polymeric substances with viscous nature such as protein, polysaccharides and other SMP. The increase of these biopolymers increase the viscosity and thereby reduce permeate flux (Meng et al., 2006). Itonaga et al. (2004) illustrated that MLSS of 10,000 mg/l represents the turning point above which the viscosity increases linearly. They also indicated that the removal of colloidal organics through coagulation has substantially reduced sludge viscosity. This means that, at the same MLSS the major components affecting the magnitude of sludge viscosity are the organic substances. Low temperature increases viscosity and reduces permeate flux as well (Chiemchaisri and Yamamoto, 1993).

2.4.2.3 Particle size distribution (PSD) and structure

The increase of particle size distribution (PSD) is highly believed to increase permeate flux (Li et al., 1998). Smaller particles, particularly smaller than 50 μm, deposit on membrane surface or inside the voids of the cake layer causing an increase of membrane resistance (Bai and Leow, 2002). Microbial flocs destruction caused by any reason increases the amount of micro flocs and the release of EPS into the sludge supernatant, which in return increases membrane resistance and permeate flux (Wisniewski and Grasmick, 1998). Chang et al. (1999) found that irreversible fouling is independent of floc structure, size and shape, on the other hand, reversible fouling as a function of these factors. Floc structure has a major influence with the following order; bulking sludge, pinpoint sludge and normal sludge.

2.4.2.4 Microbial flocs hydrophobicity and surface charge

Hydrophobic surfaces repel water molecules and attach to surfaces with hydrophobic affinity. The attachment of microbial flocs onto membrane surface increases as the hydrophobic interactions between the two surfaces increase (Meng et al., 2006; Chang et al., 1999; Van et al., 1987). The existence of non-polar amino acid groups as a part of protein polymers substantially influence microbial flocs hydrophobicity, carbohydrates have no major influence (Jorand et al., 1994). Lee et al. (2003) found that flocs hydrophobicity is highly positively correlated to protein/carbohydrate ratio than the total EPS, which confirms the role of protein in shaping microbial flocs hydrophobicity.

In regard to flocs surface charge, Liao et al. (2001) and Wilen et al. (2003) reported that the amount of EPS embedded in microbial flocs is highly associated to more negative charge on the surface. Lee et al. (2003) reported a positive correlation ($r=0.8$ $p<0.05$) between protein/carbohydrate ratio and flocs surface charge, which means that protein is the major constituent influencing the flocs negative charge. Ionization of EPS functional groups such as carboxylic, sulfate and phosphate are responsible for microbial flocs negative charge (Sutherland, 2001). A highly negative correlation between microbial flocs surface charge and membrane fouling was reported (Meng et al., 2006; Lee et al. 2003). The previous studies indicates that microbial flocs having less EPS are carrying a lower magnitude of negative charge and exhibit less fouling potentiality.

2.4.2.5 EPS-bound and SMP

Bin et al. (2008) found that organic fouling comprise the majority of fouling fractions deposited on the membrane, minor inorganic contribution was observed. Also, they reported that EPS, protein, and polysaccharides concentration (mg TOC/g SS) on membrane surface were 3, 2 and 4 times, respectively, higher than the bulk solution. EPS provided membrane flocs with highly hydrated gel matrix, which acts as a barrier to permeate flux. The major components of EPS are protein and polysaccharides (Lee et al., 2003; Geng, 2006). Membrane fouling starts off by the adsorption of SMP, organic colloids and macromolecules onto membrane surface (irreversible fouling) followed by the attachment of the suspended bacterial flocs, which form a cake layer (reversible

fouling). Considering short term operation of MBR, the cake layer represent the major fraction contributing to filtration resistance, while colloids and solutes has no dominant initial fouling effect (Lee et al., 2003). Defrance et al. (2000) reported 65% suspended solids, 30% colloids and 5% dissolved material contributing to membrane fouling. Lee et al. (2001) recorded 80% cake resistance, 12% membrane resistance and 8% irreversible resistance. Wisniewski (1996) reported 50% contribution of dissolved materials when backwashing was done more frequently.

Theoretically, since EPSs are key components of suspended microbial flocs, the reduction of membrane permeability caused by the deposition of microbial flocs onto membrane surface (reversible fouling) is expected to be strongly correlated to the bound EPS. Many studies reported strong and positive correlation between bound EPS and total membrane resistance (Nagaoka et al., 1996; Chang and Lee, 1998; Yun et al., 2006; Meng et al., 2006). Cho et al. (2005) found a positive correlation between bound EPS and filtration to resistance within the range 20 to 80 mg EPS/g (MLVSS). Yamatoo et al. (2006) stated 20 to 130 mg EPS/g (SS) as a range of high correlation with fouling. High levels of EPS produce higher floc size with larger voids between the flocs of the cake layer, which allow better hydraulic permeability. Decreased levels of EPS cause floc breakage and deterioration (Liu and Fang, 2003). The previous studies claimed that bound EPS is the major factor responsible for membrane fouling. This is true for reversible fouling under short operating period. However, for long operating periods, irreversible fouling dictates the lifetime of the membrane. Although, the initial percentage contribution of irreversible fouling is insignificant, the continuous

adsorption of SMP on membrane surface and between the voids of the cake layer makes SMP a major fraction enhancing fouling propensity.

Many recent studies revealed a strong correlation between SMP and the increasing membrane filtration resistance (Rosenberger and Kraume, 2003; Evenlij and Van der Graaf, 2004; Holbrook et al., 2004; Lim and Bai, 2003; Yamato et al., 2006). Geng and Hall (2007) proposed a new theory saying that bound EPS is not directly related to membrane fouling but through the release of SMP into the liquid phase. Rosenberger et al. (2005) showed that the adsorption of SMP conditioning the membrane for future build-up of a biofilm, which is characterized by a gel structure, hinders the passage of water through the membrane. Lesjean et al. (2005) found in a pilot scale SMBR operated for two years a linear relationship between SMP and fouling formation rate. Many studies reported carbohydrate as the major SMP fraction accumulate on membrane surface and cause fouling (Lesjean et al., 2005; Evenblij et al., 2005; Rosenberger et al., 2005; Tarnacki et al., 2005). On the other hand, fewer studies reported a strong positive correlation between protein and fouling despite its existence on membrane surface in a range of 15% (Evenblij et al., 2005) to 90% (Drews et al., 2005). Hernandez Rojas et al. (2005) confirmed a substantial increase of membrane resistance as the soluble protein increased from 30 to 100 mg/l. Arabi and Nakhla (2008) showed that protein/carbohydrate ratio of 4 and 8 caused higher hydrophobic EPS, better attachment onto membrane surface and therefore reduced membrane filterability. High molecular weight components of SMP>10 kDa contribute significantly to fouling, while compounds with a low molecular weight have insignificant influence

(Jang et al., 2005). Organic compounds like humic substances in the liquid phase have low molecular weight and smaller size than the membrane nominal size, which make it easy for such organic compounds to pass through without causing any noticeable fouling (Drews et al., 2005). The above discussion indicates the significant role of SMP as a major fouling contributor. Thus, the removal of such organic material from the sludge liquid phase is likely to reduce the reversible and irreversible fouling.

2.4.2.6 Sludge filterability and dewaterability

Dewaterability of sludge represents either the rate of filtration or the percentage of bound water content of the sludge after dewatering (Jin et al., 2004). In other words, filterability corresponds to the dewaterability of the sludge, which is one of the most difficult and costly process in treatment plants. Currently, the most common methods used to determine sludge filterability are capillary suction time and specific resistance to filtration (SRF). Sludge bound water is divided into different pools: bulk water, interstitial water, surface water and chemically bound water, which is strongly attached within the floc by chemical bonds and removed at 105^{o} C (Smollen, 1990; Vesilind and Martel, 1990). Bulk water represents the part of water surrounds the flocs, interstitial water represent the part that is held by capillary forces. These two pools of water can be easily removed by physical means such as vacuum filtration, belt filter presses, drying beds or centrifugation. On the other hand, surface water represents the part that is

adsorbed or absorbed by organic particles inside the flocs (mainly EPS). Christensen and Characklis (1990) described EPS as a hydrated matrix with 98% water content.

Different sludge properties determine its filterability; soluble EPS, bound EPS, floc size, viscosity and cations concentrations. Liming et al. (2009) reported that CST decreases as the floc size increases. Their results were consistent with previous studies (Karr and Keinath, 1978; Novak et al., 1988). Highly viscous sludge exhibits lower filterability (Jin et al., 2004; Li and Yang, 2007). Other studies reported a decrease in filterability with increasing soluble EPS (Kim et al., 2001) and increasing bound EPS (Nagaoka et al., 1996). Jin et al. (2004) showed that increased amounts of bound EPS in the flocs contribute significantly to more water binding ability of the flocs, which is highly lowering the filterability of the sludge. Li and Yang (2007) studied bound EPS in more detail and reported that loosely bound EPS contain more bound water than tightly bound EPS. Moreover, loosely bound EPS is highly responsible for higher viscosity due to its distribution in the outer parts of the cells and flocs.

2.4.3 Operating conditions (SRT and HRT)

Generally, the operating conditions affect membrane fouling through their impact on sludge properties. SRT regulates the concentration of MLSS, HRT determines the organic loading and both of them determine the final steady state food/mass (F/M) ratio. Cross flow velocity over the membrane module is another key operating parameter affecting sludge properties and the propensity of membrane fouling.

SRT indirectly affects the propensity of membrane fouling through changing sludge properties. Jinsong et al. (2006) reported that the increase of SRT from 10 to 30 days increased the MLSS by 3 to 4 g/l , increased viscosity, reduced SMP, 100% lower polysaccharides concentration in the supernatant and lower fouling rate propensity. How et al. (2006) found that SMP bound-EPS, total organic carbon (TOC), protein, polysaccharides, UVA_{254} and membrane fouling rate decreased with increasing SRT. Grelier et al. (2006) reported that membrane fouling is more dependent on SRT than MLSS concentration, lower membrane fouling was observed after increasing the SRT from 8 to 40 days due to the reduction of protein and polysaccharides concentrations in the sludge supernatant. Pollice et al. (2008) operated the MBR at SRT higher than 40 days without showing any drawbacks in term of biological activity, filterability and cleaning needs. Ahmad et al. (2007) attributed the removal of colloidal and soluble organics to the increased growth of microorganisms belonging to the α and β sub-classes as the SRT increased from 20 to 60 days at which membrane biofouling was minimum. On the other hand, other studies found opposite results. Yamamatoo et al. (1989) found an increase of membrane fouling with increasing SRT due to the increase of MLSS. However, the increase of MLSS concentration does not necessarily cause higher fouling rate as illustrated earlier.

In conventional activated sludge treatment, short SRT is adopted to prevent the accumulation of biomass (MLSS) and to ensure fast gravity solid-liquid separation. Undoubtedly, the possibility of operating MBR under long SRT is the key parameter toward minimizing sludge production. This led to a great temptation among researchers

to investigate the possibility of zero sludge production at long SRT. Consequently, many MBR studies were operated at long SRT or even at complete sludge retention (SRT=∞). Longer SRT ends up with high MLSS and low F/M ratio. At low F/M ratio, the substrate limitation dominates the system. Thus, the limited carbon sources in the feed water are degraded to support the biomass with the energy needed for maintenance and survival with little sludge production. Bhatta et al. (2004) reported a very low sludge yield of 0.04 to 0.09 kg MLSS/kg BOD at SRT equal to 500 days and low organic loading of 0.5 kg BOD/m^3.d. Meanwhile, the MBR operated at considerably stable state for 200 days at low suction pressure (< 25 kPa). Pollice et al. (2008) operated the MBR at SRT higher than 40 days without showing any drawbacks in terms of biological activity, filterability and cleaning needs. Rosenberger et al. (2000) operated MBR for 3 years at complete sludge retention resulting in highly concentrated biomass of 15 to 23 g MLSS/l and F/M ratio of 0.07 kg COD/kg MLSS. d. On the other hand, longer SRT is likely to increase the concentration of MLSS to a harmful level as discussed earlier. Longer SRT leads to the accumulation of inert materials of fouling potential (like hair and lint), which are not completely removed in the pre-treatment (Le Clech et al., 2006). Han et al. (2005) reported a two fold increase of fouling propensity rate as SRT increased from 30 to 100 days due to the increase of MLSS from 7 to 18 g/l accompanied with another increase of sludge viscosity. An increase of sludge viscosity is probably the major shortcoming of operating MBR at long SRT due to the limitations imposed on the oxygen mass transfer (Lubbeck et al., 1995) leading to poor oxygenation and increased aeration cost. The

increase of aeration intensity at high viscous medium increases the risk of microbial flocs breakage.

These studies indicate that fouling was reduced by increasing SRT due to the reduction of materials having fouling potential. The reduction of soluble compounds could be attributed to the larger and stronger microbial flocs forming at higher SRT, which can resist the shear forces and the breakdown. In addition to that, more diverse microbial community at longer SRT is another factor increasing the degradability and removal efficiency of soluble and colloidal organics. In the end, the selection of SRT to produce the lowest sludge without increasing membrane fouling rate is a function of the other operating conditions, mainly the organic loading. The lower the organic loading the longer the SRT without fouling consequences. The organic loading, on the other hand, is proportional to the substrate concentration in the feed wastewater and inversely proportional to the HRT. Thus, the upper limit of SRT is determined by the concentration of biodegradable organics of the feed wastewater and the HRT. Theoretically, Yoon et al. (2004) determined that a minimum HRT of 11.4 h is required for the treatment of typical wastewater of COD equal to 400 mg/l to produce zero sludge (SRT = ∞) when the target MLSS is less than 15,000 mg/l, at which no significant increase of membrane fouling is expected to take place.

2.5 Control of membrane fouling

Work has been dedicated to find out feasible ways to mitigate membrane fouling such as increasing the hydrophilicity of the membrane surface by the introduction of polar

groups, intermittent aeration (Hasar et al. 2001), changing the depth of the membrane (Kim et al., 2008) module, air as a backflushing medium (Visvanathan et al., 1997), addition of adsorbent material like powdered activated sludge (Kim and Lee, 2003) and many more. Hereafter, the most common methods applied in MBR technology will be discussed.

2.5.1 Critical flux

By definition, the critical flux is the flux below which no deposition of foulants or decline of permeability is observed over the operating time. The critical flux based on the back transport of microbial flocs and other particles provided by the cross flow velocity (CFV) along the membrane module. The concept of avoiding membrane fouling by operating at filtration rate below the critical flux was first proposed by Field et al. (1995). However, the increase of trans-membrane pressure (TMP) as a result of fouling after a critical time at fluxes lower than the critical flux was reported by many investigators (Ognier et al., 2004; Le Clech et al., 2006). Thus the so named critical flux by its original definition does not exist in MBR. Brookes et al. (2006) supported the concept of transitional flux as an alternative to the critical flux, which represents the flux at which fouling rate is changing from low to high. Likewise, Kim and Digiano (2006) described the critical flux as “a relative rather than absolute”. Ng et al. (2005) introduced the concept of sustainable flux at which the TMP increases gradually at a low rate to limit severe and rapid membrane fouling.

A flux step method technique is commonly used to determine the value of the critical flux. In this method the flux is incrementally increased, but kept constant for a specified time (usually between 0.25 to 2 h). Next, the TMP is recorded over the time. Finally, the lowest flux that exhibits a remarkable increase of TMP over time represents the membrane critical flux under the tested conditions. Different critical flux values for the same membrane module might be obtained depending on the MLSS concentration, CFV or aeration intensity, membrane length and the filtration time (Kim and DiGiano, 2006). Kim and DiGiano (2006) tested three permeate fluxes (29.7, 19.1 and 9.5 $l/m^2.h$), the highest value was the critical flux determined by the short term operating time. The TMP decreased sharply after 10 h at the critical flux and after 40 h for the 19.1 $l/m^2.h$, while the 9.5 $l/m^2.h$ sub-critical flux showed stable TMP to the end of 50 h. This study indicates that the critical flux determined based on short term operating time causes fouling after long time of operation. On the other hand, the lower the flux from the critical value, the less the fouling rate is likely to be.

The flux along the membrane length is the highest near the open end of the fiber and decreases gradually down the fiber (Chang and Fane, 2001). Therefore, the flux close to the open end is higher than the average length flux at which the critical flux is determined, which means higher fouling at this part of the membrane. This variation of fouling along the membrane fiber is more obvious for a large scale MBR and hardly noticeable at the small scale experiments conducted with short membrane modules (Kim and DiGiano, 2006).

2.5.2 Cross flow velocity (CFV)

Generating high cross flow velocities (CFV) parallel to the membrane module is advantageous to mitigate the formation of cake layer on the membrane surface. The uplifting of bubbling air generates the shear stress needed to remove the deposited microbial flocs out of the membrane surface. Thus, improving the hydrodynamic around the membrane surface has been proven to alleviate sludge deposition onto membrane surface (Chellam and Weisner 1997; Ueda et al., 1997). The degree of preventing the formation of the cake layer depends on the magnitude of the cross flow velocity, the membrane filtration flux and the MLSS concentration (Liu et al., 2003). Generally, decreasing the MLSS concentration and filtration flux or increasing the CFV are helpful approaches to control the formation of the cake layer (reversible fouling). Higher filtration flux leads to more compressed cake layer and therefore less permeability (Le-Clech et al., 2006). The actual CFV around the membrane module is measured with a velocity-meter; however, the magnitude of the CFV could be estimated using an equation obtained through multiple regression analysis (Liu et al., 2003). Aeration intensity (Q/A) is another way to express the CFV, where Q is the flow rate and A is the effective cross section area of the reactor.

Le-Clech et al. (2003) revealed that increasing the air flow velocity always led to an increase of membrane critical flux (due to lower deposition of microbial flocs on the membrane surface) at 8 different combinations of MLSS, membrane pore size and aeration intensity. Meng et al. (2007) reported that aeration intensity has a small impact

on the formation of the reversible fouling at MLSS below 10,000 mg/l. However, membrane fouling was significantly reduced at MLSS higher than 10,000 mg/l by increasing the air intensity from 200 l/h to 600 l/h in a reactor of 12 l working volume. Liu et al. (2003) showed an exponential relationship between cross flow velocity and sludge viscosity. Meng et al. (2007) demonstrated that aeration intensity has a small effect on CFV as long as the MLSS is below 12,000 mg/l or sludge viscosity below 3 mPa.s. At higher values of sludge viscosity or MLSS, a severe drop of CFV is expected to dominate around the membrane module.

Ueda et al. (1997) suggested that there is a critical CFV beyond which no effect on the cake layer removal efficiency could be achieved. Liu et al. (2000) reported 0.3 m/s as the critical CFV. Choi et al. (2005) reported linearly increase of permeate flux with increasing the CFV at MLSS of 5000 mg/l. Furthermore, the reversible fouling was prevented at cross flow velocity of 3 m/s for the micro-filter membranes and 2 m/s for the ultra-filter membranes.

On the other hand, controlling membrane fouling through adopting the CFV has some limitations. Firstly, for each value of CFV there is a microbial floc cut-off diameter at which the shear forces are unable to prevent smaller particles depositing on the membrane surface. Smaller particles have higher inter-particle repulsion forces that hinder the passage of water and decrease the permeability of the cake layer. In addition to that, smaller pore size between the particles is likely to be blocked faster as the organic materials deposited inside the pores. Thus, the membrane should be back

washed more frequently to get rid of the deposited particles that are not repelled by the CFV. Secondly, CFV energy consume is costy. Approximately 70% of the energy input in MBR is consumed through the aeration to prevent the formation of the cake layer (Prieske et al., 2008). Therefore the magnitude of the CFV should not exceed the critical value to minimize energy consumption.

2.5.3 Membrane backwashing

Backwashing is the major physical means to clean the membrane of the deposited foulants, mainly the loosely attached cake layer. In this process, filtration is stopped for a specified time and part of the permeate water is pumped in the reverse direction. The cleaning efficiency obtained by backwashing is a function of its frequency, duration and intensity. Many studies were conducted to optimize these parameters under different operating conditions. For example, Jing et al. (2005) found that the frequency of 600 s filtration/45 s backwashing is more efficient than (200 s filtration/15 s backwashing). Psosch and Schiewer (2008) revealed that a combined air sparging and backwashing has provided 4 times better permeability than the conventional air sparging alone at CFV of 2 m/s.

2.5.4 Chemical cleaning

Different chemical cleanings are recommended to reduce the accumulation of the irreversible fouling: Chemically enhanced backwash (daily basis), maintenance cleaning (weekly basis) and the intensive chemical cleaning once or twice a year (Le-Clech et al., 2006). The concentration of the chemical is the lowest for the daily cleaning and the

highest for the intensive cleaning. Le-Clech et al. (2005) summarized in Table 2.2 the intensive chemical cleaning protocols for different membrane modules.

Table 2.2: Intensive chemical cleaning protocols for MBR suppliers (Le-Clech et al., 2005)

Supplier	Type	Chemicals	Concentration (%)	Protocol
Mitsubishi	CIL	NaOCl	0.3	Backflow through membrane (2h)+ soaking (2 h)
		Citric acid	0.2	
Zenon	CIP	NaOCl	0.2	Backpuls and recirculate
		Citric acid	0.2 to 0.3	
Memcor	CIP	NaOCl	0.01	Recirculate through lumens
		Citric acid	0.2	
Kubota	CIL	NaOCl	0.5	Backflow and soaking
		Citric acid	1	

CIL= cleaning in line where chemical solutions are generally backflow (under gravity) inside the membrane.

CIP= cleaning in place where membrane tank is isolated and drained; the module is rinsed before being soaked in the cleaning solution and rinsed to remove excess chlorine.

NaOCl = sodium hypochlorite

2.5.5 Coagulation

Removing of SMP and colloidal organics from around the membrane surface is very desirable to reduce fouling and improve the filtration rate. The addition of coagulants like aluminum sulfate (alum) and ferric chloride, commonly used in wastewater treatment plants, induce the flocculation of these submicron particles and subsequently improve the performance of MBR. Once these coagulants are ionized, they form complex hydroxides, which adsorb the suspended solids and the colloidal and soluble organics. Holbrook et al. (2004) found a substantial reduction of SMP as a result of alum addition. Mishina and Nakajama (2009) reported an effective SMP removal (particularly

the SMP fraction between 1 µm and 0.4 µm) and increase of microbial flocs size distribution by coagulant addition. Meanwhile, Fe-coagulant was more effective than Al-coagulant. Lee et al. (2001) reported that colloids between 0.1 µm to 2 µm coagulated into larger aggregates with the addition of alum. Ivanovic et al. (2008) tested a flocculation zone integrated in the MBR. They found that membrane fouling was reduced by the reduction of the submicron organic particles. Song et al. (2008) revealed that at 200 to 500 mg/l aluminum sulfate, the permeate flow rate increased as well as the phosphorus removal efficiency and the specific resistance to filtration decreased. However, In SMEBR where aluminum anode is used, Al-coagulant is released into the reactor by the corrosion of the anode.

2.5.6 Electro-coagulation

This process starts by electrolysis reactions at the anode electrode surface to produce trivalent cation coagulants that helps in the removal of the soluble colloidal organics. Aluminum electrodes were found to be more appropriate than iron electrodes. However, iron easily oxidized by air and colouring the water (Lin et al., 2005).

The release of Al^{+3} causes the flocculation of colloidal organics through reducing the absolute value of zeta potential to a level where the Van der Waal's forces are greater than the repulsive forces between the negatively charged colloids. In addition to that, the produced Al^{+3} reacts with the free OH^- in water to initially form monomeric species such as $Al(OH)^{+2}$, $Al(OH)_2^{+1}$ and $Al(OH)_4^-$. Afterward, these species converted into polymeric species such as $Al_8(OH)_{20}^{+4}$, $Al_{13}(OH)_{34}^{+5}$, which eventually transform into a

long chain of $Al(OH)_{(s)}$. These cationic hydroxide complexes can effectively remove the negatively charged organic materials through the electrostatic forces to neutralize the charge. Moreover, these complexes have large surface area up to 1 μm (Balkan and Kolesnikova, 1996) capable of adsorbing and trapping the soluble and organic colloidal particles, which are easily separated from the liquid medium by sedimentation or H_2 flotation (Kobya et al., 2006; Can et al., 2003; Bayramoglu et al., 2004). In addition to the formation of aluminum hydroxide complexes, electrokinetic system enhances the interactions between the solid surfaces to facilitate the flocculation process (Mollah et al., 2001; Larue and Vorobiev, 2003; Matteson et al., 1995). The effectiveness of electrocoagulation depends primarily on the current density (CD) calculated as the current (A)/anode area (m^2), which regulates the dosing rate of metal into the liquid medium and the gas bubble density. The majority of CD cited in the literature ranges between 10 to 150 A/m^2, higher current density is required when flotation is the separation mechanism of the coagulated particles, while low current densities are suitable for electro-coagulation processes equipped with other separation facilities such as sedimentation tanks, sand and coal filters or membrane filtration (Holt et al., 1999).

Electro-coagulation is a technology that is easy to operate with no chemical coagulants addition (Kobya et al., 2006) and most importantly, the liquid does not enrich with salts and ions left over after the chemical treatment (Mollah et al., 2001; Chen, 2004). Larue et al., (2003) found that electro-coagulation produces flocs of bigger size and density. Due to these advantages, electro-coagulation was performed successfully to treat different types of wastewaters such as decolorization of the dye (Daneshvar et al.,

2004), oil in water (Canizares et al., 2008), textile wastewater (Bayramoglu et al., 2007), poultry slaughterhouse (Bayramoglu et al., 2006) and many others.

Inserting the electrodes inside the activated sludge to enhance the flocculation of colloida and other solid surfaces is a risky process due to adverse effect of the direct current field on the biomass viability. Esmaily et al., (2006) and Huang et al., (2008) used the electrokinetic to inactivate the pathogens in the sludge. Therefore, the electrokinetic that is combined with any biological treatment should be performed cautiously at low current density and intermittent exposure mode (Bani-Melhem et al., 2011).

2.6 Nutrient removal

Different methods have been suggested for the removal of N and P from the wastewater over the last two decades. The sequential anoxic/oxic membrane bioreactor was proposed and applied for the removal of nitrogen (Cho et al., 2005; Ahn et al., 2003; Adam et al., 2002). This system contains two separate reactor zones (oxic and anoxic) that require the recycling of the mixed liquor between the two zones. The system is not suitable for the removing of phosphorus to a desired level. Sequential batch reactors have shown the possibility of N removal in one reactor (Jianlong et al., 2008; Udert et al., 2008; Chiu et al., 2007; Wu et al., 2007). The process starts by a period of anoxic conditions that is followed by a period of oxic conditions. The alternation of the oxic/anoxic conditions enables the removal of nitrogen but not phosphorus.

Autotrophic denitrification using hydrogen as electron donor worked successfully in many researches (Sunger and Bose, 2009; Rezania et al., 2007, 2006). Intermittently aerated membrane bioreactor for nitrogen removal has also shown promising results (Choi et al, 2009; Yoo et al., 1999) for the removal of nitrogen. Phosphorus could be removed through the addition of chemical coagulant directly in the activated sludge reactor. The coagulant could be added before or after the activated sludge reactor. Biological removal of phosphorus is performed through the recycling of the wastewater between the anaerobic and aerobic reactors to promote the phosphorus accumulating bacteria. In some occasions, the chemical coagulants are added to complement the removal of phosphorus to lower concentrations. A separate electro-chemical unit for phosphorus removal in a separate unit before the wastewater flows into the activated sludge reactor was investigated by Kim et al. (2010) at lab scale level. To enhance the nutrient removal efficiency, a fermentation unit to produce volatile fatty acids (VFA) that are desirable by the phosphorus accumulating bacteria as well as the denitifiers (Jeyanayagam, 2005). All of the above mentioned technologies required more than one unit or reactor zone to effectively remove nitrogen and phosphorus. One suggested design for nutrient removal is given in Figure 2.1

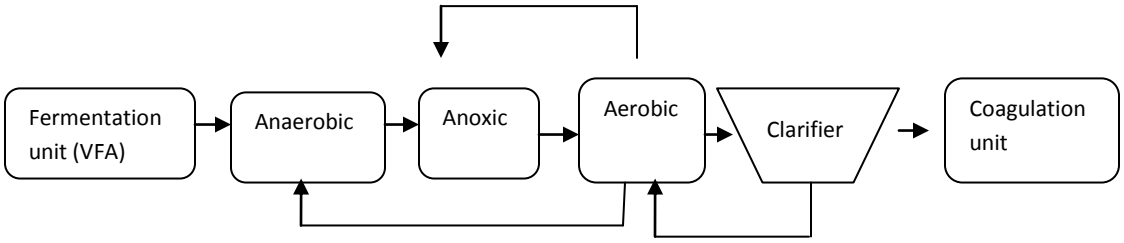

Figure 2.1: Conventional tertiary treatment process for nutrient removal

2.7 Anaerobic ammonium oxidation (anammox)

Removal of ammonium through anaerobic ammonium oxidation (anammox) in conditions of high-ammonia concentrated streams was confirmed by many studies (Yang et al., 2010; Tsushima et al., 2007; Trigo et al., 2006). In this process, ammonium is oxidized into N_2 gas using the nitrite as electron acceptor under strictly anaerobic conditions (Van de Graaf et al., 1996). Thus, nitrogen removal through anammox process requires the partial nitrification of ammonium to obtain an ammonium/nitrite ratio equal to 1. The anammox bacteria are autotrophic belong to the order *Planctomycete* (Strous et al., 1999). The most challemging task of adopting anammox process in wastewater treatment is the start up period due to the slow growth rate with a doubling time equal to 14 days (Isaka et al., 2006). The optimum temperature at which the anammox bacteria exhibit the maximum activity is 30 to 40 ^{o}C (Strous et al., 1999). However, the anammox was proved to work successfully at 20 ^{o}C (Cema et al., 2007; Isaka et al., 2007). Dosta et al. (2008) reported that the anammox bacteria operated successfully at 18 ^{o}C and the activity decreased at 15 ^{o}C. Anammox bacteria are likely to be activated in the electro-bioreactor due to the ability of this reactor to create an alternate aerobic and anaerobic conditions.

Chapter 3

Research hypothesis

3.1 Mechanisms of nutrient removal in the electro-bioreactor

Electro-bioreactor is basically composed of two electrodes immersed in a conventional activated sludge. In this research, aluminum was selected as the material of the sacrificial anode and iron as the cathode. In this reactor, different electrochemical reactions are taking place once the DC field is activated. Each reaction plays its role in removing the targeted nutrients if the system is adjusted for this goal. In this context, three major operating conditions should be considered in order to create the optimal conditions for the removal of carbon, phosphorus, and nitrogen:

1- Current density (CD- the current (A) passing between the two electrodes divided by the anode surface area (m^2)). The strength of the current density determines the amount of Al^{+3} and electrons produced into the system (Equations 3.1 and 3.2) and the amount of hydrogen gas produced at the cathode (Equations 3.3), which all play major role in nutrient removal. Meanwhile, microorganisms cannot tolerate continuous exposure to the current and should be given enough time-OFF to recover from the electrical shock and resume its biological role in the system. Therefore, intermittent exposure to the electrical field can prevent the adverse effect on microbial activity.

2- Electrical exposure mode (time-ON/time-OFF) that also affects the production rate of Al^{+3}, electrons and H_2 gas over the operating time.

3- Dissolved oxygen (DO) concentration should be within limits, neither too low nor too high, in order to create different levels of oxidation-reduction potential (ORP) and promote different bacterial genotypes responsible for the transformation of nitrogen in the system. These limits of DO depends on the operating conditions, generally, it should be between 0 to 1.5 mg/l

Reaction at the anode:

$$Al \longrightarrow Al^{+3} + 3\,e^{-} \qquad (3.1)$$

$$2H_2O \longrightarrow O_{2\,(gas)} + 4H^{+}_{(aq)} + 4e^{-} \qquad (3.2)$$

Reactions at the cathode:

$$3H_2O + 3e^{-} \longrightarrow 3/2H_{2(g)} + 3OH^{-} \qquad (3.3)$$

$$½\ O_2 + 2e^{-} + H_2O \longrightarrow 2OH^{-} \qquad (3.4)$$

3.1.1 Carbon removal

Carbon removal can be achieved in the electro-bioreactor through the oxidation of organic material by the microbial activities as they do in any conventional activated sludge reactor. However, the current density should be as low as possible and the time-OFF should be as long as possible in order to maintain the highest performance of

biomass. In electro-bioreactor, biodegradation is not the sole removal pathway of carbon. The produced Al^{+3} reacts with the free OH^- in water to initially form monomeric species such as $Al(OH)^{+2}$, $Al(OH)_2^{+1}$ and $Al(OH)_4^-$. Afterward, these species converted into polymeric species such as $Al_8(OH)_{20}^{+4}$, $Al_{13}(OH)_{34}^{+5}$, which eventually transform into a long chain of $Al(OH)_{(s)}$. These cationic hydroxide complexes can effectively adsorb the negatively charged organic materials through the electrostatic forces, particularly those colloids of non-biodegradable nature.

3.1.2 Phosphorus removal

Phosphorus removal can be achieved through the formation of $AlPO_4$ solids or forming complexes with Al(OH)s. Thus, phosphorus becomes part of the suspended solids of the system that could be recovered after the solid liquid separation using either the clarifier or membrane modules. In addition to the electrochemical removal of P, biological removal is highly expected to take place because of the capability of the system to work at alternating levels of oxidation reduction potential (ORP).

3.1.3 Nitrogen removal

Nitrogen removal can be achieved in the electro-bioreactor through its capability to change rapidly the ORP (Table 3.1) to create simultaneous nitrification/denitrification conditions. The process of nitrogen removal is explained in the following steps:

Table 3.1: Optimal oxidation-reduction potential (ORP) for different biological processes

Biological process	Conditions	Optimum ORP (mV)
Nitrification	Aerobic	+100 to +350
Denitrification	Anoxic	-50 to +50
P-removal	Anaerobic stage	-100 to -225
	Aerobic stage	+25 to +250

Step 1: Once the DC field is activated, the electrons are discharged from the anode zone (Equations 3.1 and 3.2). Since the dissolved oxygen molecules have the highest electro-negativity (affinity to gain electrons) in the system, most of these discharged electrons react with the dissolved oxygen (Equation 3.4) to produce hydroxide. In the electrochemical systems, Equation 3.4 proceeds Equation 3.3 until DO is consumed at the cathode surface. Therefore, DO concentration decreases over time as long as the current is on the time-ON mode.

Step 2: In the case that the concentration of DO in the reactor is too high, the high buffering capacity of the reactor would consume all the electrons and still hold enough oxygen to act as the major electron acceptor for the biological reactions. In that case,

the ORO stays high (> +100) and promotes only the autotrophic nitrification process that transforms ammonium into nitrate in the system (Equations 3.5 and 3.6).

$$NH_4 + 3/2O_2 \rightarrow NO_2^- + H2O + 2H+ \qquad \textit{Nitrosomonas} \text{ bacteria (3.5)}$$

$$NO_2^- + H_2O \rightarrow NO_3^- + 2H^+ + 2e^- \qquad \textit{Nitrobacter} \text{ bacteria (3.6)}$$

Step 3: In the case that the dissolved oxygen in the reactor is not too high, the discharged electrons react with DO until not enough oxygen is available to support the aerobic condition to act as the major electron acceptor. As a result, nitrate as e-acceptor appears in the system and the ORP drops from the aerobic limit to the anoxic limit (+50 to -50 mV). At this level of ORP, the heterotrophic denitrifiers become active and start the conversion of nitrate into N_2 gas (Equation 3.7).

$$NO_3^- \rightarrow NO_2^- \rightarrow NO + N_2O \rightarrow N_2 \qquad \text{(Denitrification process)} \quad (3.7)$$

Step 4: To make the system even more powerful and enhance the nitrification potential of the system, the influx of electron and dissolved oxygen levels could be adjusted to lower the ORP to -150 mV. At this level of redox potential, the autotrophic anaerobic ammonium oxidation (anammox) is activated and starts to nitrify the ammonium using the already existing nitrite in the system as electron acceptor (Equation 3.8). Since the rate of anammox is higher than the aerobic autotrophic nitrification, it is expected to achieve a higher nitrification potential than the reactor operated only at aerobic nitrification as it does in the conventional biological activated sludge.

$$NH_4^+ + NO_2^- \longrightarrow N_2 + 2H_2O \quad \text{(anammox)} \qquad (3.8)$$

Step 5: In order to achieve complete and enhance N removal, the system should fluctuate between a redox potential of -150 mV and +150 mV. Nearly, 50% of the time the reactor should work at strictly aerobic conditions in order to give enough time for nitrification to partially convert ammonium into nitrite and nitrate. The other 50% of the time should be given to support the anoxic heterotrophic denitrifers and the anammox, which can work simultaneously. This changing of ORP profile is achievable through activating the DC field for some time (time-ON) at a current density strong enough to produce enough electrons to satisfy oxygen needs of electrons and neutralize its function as the major electron acceptor. Afterwards, NO_3^- starts to take over the role as the major electron acceptor and later nitrite at the anammox conditions. Once this limit is reached, the DC field is deactivated so that no more electrons are discharged. Then, the system should be given enough time (time-OFF) to recover its oxygen content to a level that can support the aerobic conditions after which another cycle starts to repeat the process once again.

Step 6: Another pathway of N removal in the system is the hydrogen trophic denitrification in which some bacteria species are capable of using the H_2 gas produced at the cathode (Equation 3.3) as e-donor and nitrate as electron acceptor to denitrify it into N_2 gas (Equation 3.9).

$$2NO_3^- + 5H_2 + 2H^+ \longrightarrow N_2 + 6H_2O \quad \text{(hydrogen trophic denitrification)} \quad (3.9)$$

3.2 Membrane fouling reduction

In the electro-bioreactor, many electro-kinetic processes take place that help reducing the concentrations of soluble and colloidal organics in the sludge supernatant. Electro-coagulation caused by the release of Al^{+3} ions and the formation of aluminum hydroxides is likely the major mechanism contributing to the removal of organic materials of high fouling potential from the activated sludge supernatant. On the other hand, the released Al^{+3} reduces the magnitude of zeta potential and allows the colloids and soluble solutes to attach to each other and forming larger particles. In addition to that, the current field enhances the motion of the charged particles (soluble or colloidal) and forces them to contact with each other and therefore improves the coagulation. Electrophoresis, the movement of charged colloids toward the oppositely charged electrode at which they deposit, is another removal mechanism of organic materials. The removal of solutes and colloids is expected to reduce the membrane fouling.

To verify the above hypothesis, a series of multiple runs of batch (Phase 1), lab scale (Phase 2) and pilot scale (Phase 3) tests were conducted.

Chapter 4

Phase 1: Methodological approach: Batch tests

Phase 1 consists of two stages in order to fully achieve its objectives (Figure 4.1). As it was illustrated in the hypothesis (Chapter 3), the electrical operating parameters in the SMEBR are crucial for a successful operation process. The main objective of Phase 1 was to determine the electrical operating parameters for Phase 2 (continuous flow) that can cause positive improvements of sludge properties without negatively affecting the microbial activity. These electrical operating parameters include voltage gradient, current density, and electrical exposure mode (time-ON/time-OFF).

Stage 1 and Stage 2 were conducted to study the relationship between the electrical operating parameters and sludge properties. Since Stage 1 provided only the removal efficiencies of organic foulants at the end of the operating period (from 72 h to 150 h), Stage 2 focused on studying the removal efficiencies of organic foulants over time. Furthermore, the impact of electrokinetic processes on microbial activity was investigated in Stage 2.

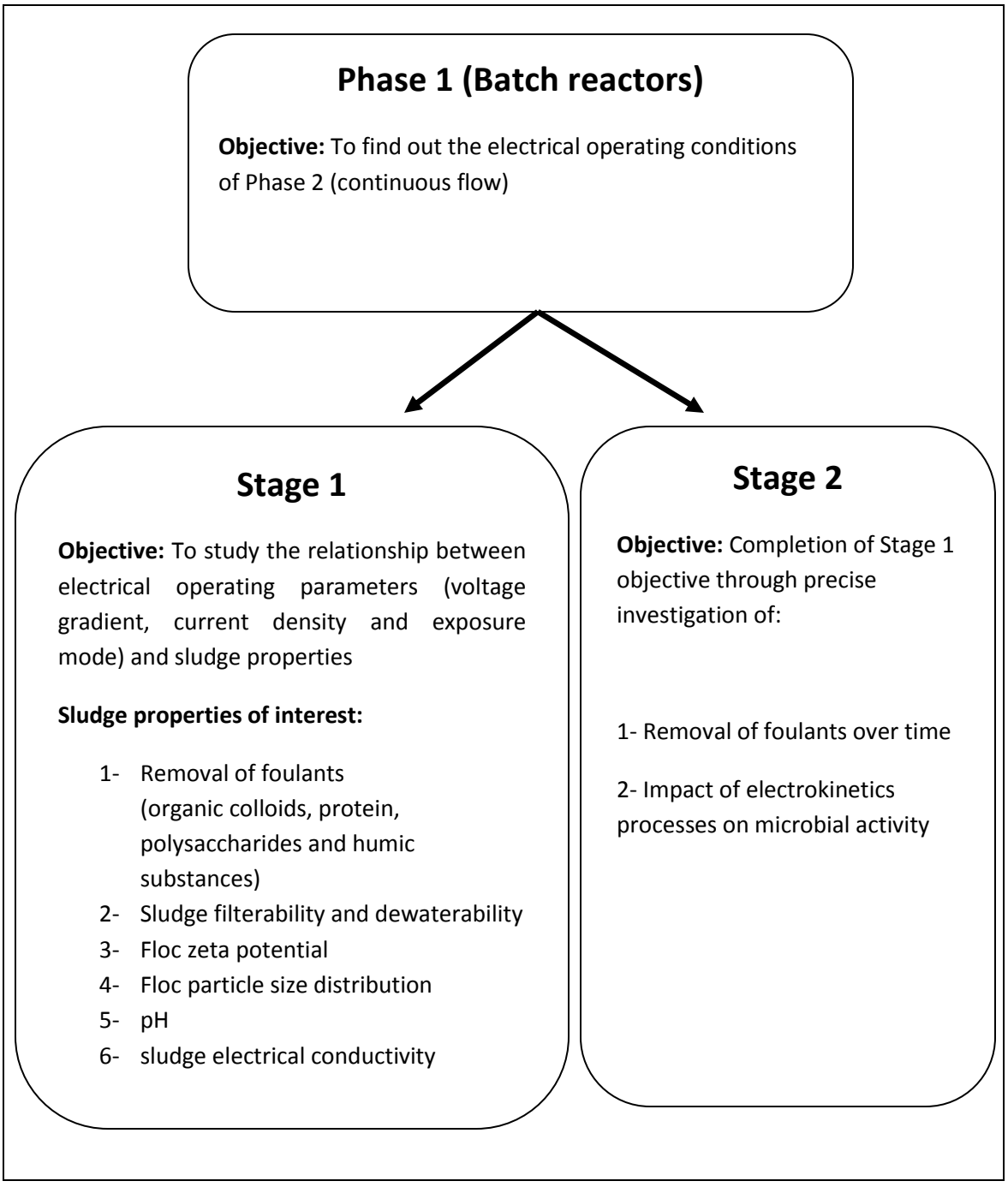

Figure 4.1: Phase 1 (Stage 1): Flow chart of the methodological approach

4.1 Phase 1 (Stage 1): Experiment set up

Experimental setup of Phase 1 consists of a series of 1-l batch electrokinetic bioreactors equipped with a perforated aluminum anode and iron cathode made of stainless steel mesh, aerated from the bottom to maintain the aerobic conditions. The space between the electrodes was adjusted to 5 cm (Figure 4.2). The porous electrodes are chosen to ensure the mixing of activated sludge in the whole reactor. These reactors indeed simulate the SMEBR without membrane module. Activated sludge was brought from the St. Hyacinthe, QC wastewater treatment plant, stored at 4° C for no longer than a month to avoid any likely changes of sludge properties due to the prolonged storage. Three levels of mixed liquor suspended solids (MLSS) concentrations ("low" from 3000 to 5000, "medium" from 8000 to 10,000 and "high" from 13,000 to 16,000 mg/l) were used in this phase. Three voltage gradients were selected based on 0.5, 1.0, and 1.5 V/cm to provide different current densities between the electrodes. The voltage gradients were selected based on the results of a previous study (Bani Melhem et al., 2010). Five different electrical exposure modes (5'-ON/5'-OFF, 5'-ON/10'-OFF, 5'-ON/15'-OFF, 5'-ON/20'-OFF and continuous-ON) were selected to run the bioreactors for a minimum of 70 h for testing electro-kinetic processes. Some runs were operated up to 150 h to project the long term effect of DC field on the activated sludge properties. The 45 combinations of electrical exposure modes, MLSS and voltage gradients (Table 4.1) were conducted at 9 runs. Each run consisted of five electro-bioreactors and one control bioreactor operated side by side as a reference and for

comparison purposes (Figure 4.2). Table 4.1 indicates the electrical parameters and operating conditions. Activated sludge was brought as needed from the wastewater treatment plant in St. Hyacinthe, QC.

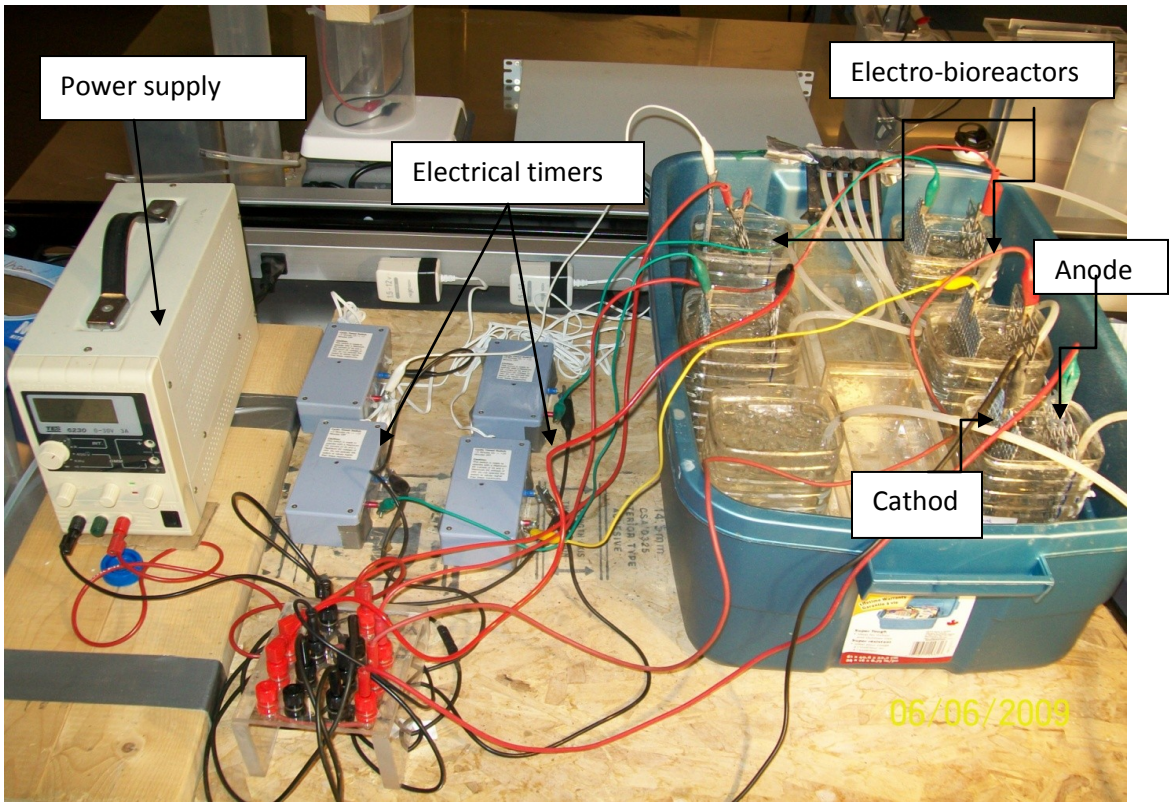

Figure 4.2: Phase 1(Stage-1): Experimental set up of the electro-bioreactors.

Table 4.1: Phase 1(Stage 1): Electrical parameters and MLSS concentrations tested

MLSS (mg/l)	Voltage (V/cm)	Run #	Electrical exposure mode
3,000 to 5,000	0.5	3	Five electrical modes and 1 control will be tested for the nine different combinations of voltage and MLSS. Electrical modes: 1- 5'-on/5'-off 2- 5'-on/10'-off 3- 5'-on/15'-off 4- 5'-on/20'-off 5- continuous -on
	1.0	6	
	1.5	1	
8,000 to 10,000	0.5	9	
	1.0	4	
	1.5	2	
13,000 to	0.5	8	
	1.0	5	

15,000	1.5	7	
Total number of combinations= 45			

4.2 Phase 1(Stage 2): Experiment set up

The same batch electro-bioreactors used in Stage 1 were used in this stage. Two current densities were selected for this experiment, 25 and 50 A/m^2. The former value of current density was selected based on the results of Stage 1 because it has improved sludge properties of interest. Current density of 50 A/m^2 was selected to study the influence of a high current density on the rate of SMP removal efficiency and its impact on microbial activity. Two MLSS of 6000 and 15000 mg/l and the same five electrical exposure modes used in Stage 1 were selected (Table 4.2). These values of MLSS were selected to test the system at different levels that could be adopted in treatment plants. Control reactor without electrical current was run side by side for comparison purposes. Since the lab facilities permit the running of six reactors at once, the whole combinations were completed by 4 runs. Each run was operated for a period of 48 hours. No synthetic water was added into the reactors, the current density was maintained constant by adjusting the voltage. In this stage, SMP were analyzed as an indicative of organic removal efficiency, and oxygen uptake rate (OUR) was measured as an indicator of the microbial activity.

Table 4.2: Phase 1(Stage 2): The operating conditions of batch reactors

MLSS (mg/l)	CD (A/m^2)	Run number	Electrical exposure modes
6000	25	1	5'-ON/5'-OFF
	50	2	5'-ON/10'-OFF
150000	25	3	5'-ON/15'-OFF
	50	4	5'-ON/20'-OFF
			Continuous-ON

4.3 Analytical methods and materials

The following measurements were performed during the Phase 1 tests: Changes of current density, pH, electrical conductivity EC (concentration of soluble salts), floc particle size distribution and floc zeta potential. At the end of the test, the supernatant after centrifugation at 4000 rpm for 20 minutes was analyzed for chemical oxygen demand (COD) (total, soluble and colloidal) and EPS (protein and polysaccharides) and humic substances (UV_{254} absorbance).

Electrical conductivity (EC), pH and dissolved oxygen were measured using a HQ30d single-input multi-parameter meter (Hach, USA). Current density was calculated as current passing between the electrodes (A) divided by the anode surface area (m^2). UVA_{254} was measured using a Lambda 40 UV/VIS spectrometer (Perkin Elmer Instruments, USA). The removal efficiency of humic substances (HS) after applying direct current (DC) field was calculated according to Equation 4.1.

$$\text{HS removal efficiency} = \frac{\text{UVA254 (control)} - \text{UVA254 (after DC field)} * 100\ \%}{\text{UVA254 (control)}} \quad (4.1)$$

4.3.1 Particle size distribution

Electrokinetic is expected to increase the particle size distribution (PSD) through electro-coaugulation and the reduction of the magnitude of zeta potential. The PSD was measured using the Partica LA-950V2 laser diffraction particle size analysis system (Horiba, USA). To avoid the damage of the flocs through sampling, 5 to 10 ml of the activated sludge was taken by a syringe with 2 mm opening. The sample was stirred gently in the syringe before injecting and circulating into the instrument. The refractive index was set to 1.4.

4.3.2 Zeta potential

A sludge sample of 50 ml volume was centrifuged at 4000 rpm for 20 minutes. The supernatant was discarded and mixed with a few drops of the activated sludge. This later mixture was injected into the electrical cell of zeta meter 3.0+ (Zeta -Meter Inc., USA) for microbial floc zeta potential measurement. The final value was given as the average of 10 readings.

4.3.3 Filterability

Sludge filterability was studied because it reflects its dewaterability and its potential to cause membrane fouling. Sludge filterability was evaluated as specific resistance to filtration (SRF). Sample sludge of 100 to 300 ml was filtered in a Buchner funnel under a

vacuum of 100 kPa, Whatman 40 filter paper was used with surface area of 0.01 m^2. The filter paper was wetted with distilled water and then dried by the vacuum pump before the activated sludge filterability test starts. During the filtration, the filtrate volume (V) was recorded versus time (t). The slope (b) of the resulting line of t/V on the Y-axis and V on the X-axis was calculated and inserted in Equation 4.2 to calculate SRF.

$$\mathrm{SRF} = \frac{(2\mathrm{b}\ \mathrm{A2}\ \mathrm{TMP})}{\mu.\ \mathrm{C}} \qquad (4.2)$$

Where, SRF is the specific resistance to filtration (m/kg), A is the filtration area (m^2), TMP is the vacuum pressure (Pa), μ is the dynamic viscosity of the filtrate (mPa.s), C is the mass of solid per unit volume (kg/m^3) and b is the slope of the line (t/V) Vs (V) in s/m^6 .

4.3.4 Chemical oxygen demand (COD)

Due to the existence of different organic fractions in the sludge supernatant, COD was divided into three types: total-COD, colloidal-COD and soluble-COD. Calculating the magnitude of each COD value was conducted following a procedure suggested by Hernandez et al. (2005). The sludge-liquid separation using centrifugation at 4000 rpm for 20 minutes lead to a supernatant that contains soluble and colloidal organic fractions. The measurement of COD for this supernatant represents the total-COD. The colloids could be removed from the supernatant by flocculating them at 250 mg/l alum, followed by a second centrifugation to get a supernatant contains only the soluble organic fractions, the COD for this supernatant is called soluble-COD. Colloidal-COD was

calculated as the difference between the total and soluble COD. COD was measured using the TNT plus vials (method 8000, Hach, USA).

4.3.5 Soluble microbial products (protein and polysaccharides)

Soluble microbial products (SMP) are organic compounds that are likely to be removed from the sludge supernatant through the electrokinetic processes. Protein and polysaccharides were measured calorimetrically following Dubois et al. (1956) and Lowery et al. (1951) methods, respectively. Series of glucose concentrations were used as a standard for polysaccharides measurements, while albumin bovine serum was used as standard for protein measurements.

4.3.6 Microbial activity

The passage of the current through the activated sludge liquor is likely to harm or hinder the microbial activity. The microbial oxygen uptake rate (OUR) was used in this phase to evaluate the changes of the microbial activity as affected by the current. The OUR was measured by directly inserting the dissolved oxygen meter inside the reactor at the end of each operating period. After cutting off the aeration, the reduction of dissolved oxygen (DO) concentrations over the time were plotted. The slope of the best fit line represented the OUR in mg DO/min. The sealed bottle method was not used in this experiment because the OUR was very high and a few minutes were enough to cause severe drop of DO down to zero at MLSS of 15000 mg/l. The time consumed by transferring samples from the reactors into the bottles, inserting the probes, sealing the bottles would consume a valuable time and thus losing the exact OUR. To make sure

that no oxygen exchange between the air and the bioreactor was taking place, in a separate reactor contains only tap water, dissolved oxygen was measured for 1 h period. The OUR for this reactor was zero, which means that the exchange of oxygen between the air and the reactor was zero, thus, direct measuring of OUR in the reactors is very accurate and represents larger volume than the sealed bottle procedure.

4.4 Phase 1: Classification of current density

Charge carrying between the electrodes through sludge liquor depends on the ionic conductance (main contributing mechanism) and surface conductance. Ionic conductance refers to carrying charge by the soluble free ions in the bulk solution, while surface conductance is carried out by the ions in the electric double layer at the solid liquid interface (Khan, 1991). Consequently, the current passing between the two electrodes in SMEBR is proportional to the concentration of soluble ions, the concentration of suspended solids and the voltage gradient applied. These three main factors are interrelated and collectively determine the final value of the current generated. The same value of voltage gradient could produce different currents passing through the reactor based on the concentration of soluble salts and MLSS. However, the magnitude of electrical conductance (current) between the electrodes is the factor affecting the major electrokinetic processes such as electroosmosis, electromigration and electrophoresis. For this reason, current density was used in this research as a base to make comparisons and correlations with the changes of sludge properties, membrane fouling and effluent quality. The current density in this research was

classified into three categories: low (8 to 15 A/m^2), medium (15 to 35 A/m^2) and high (35 to 50 A/m^2). The batch bioreactors in this stage were not fed continuously with wastewater. Occasionally, concentrated synthetic wastewater was added to replenish the depleted ions in order to maintain the same current density over the whole operating period as much as possible. The composition of synthetic wastewater used in Phase 1 is illustrated in Table 4.3. This composition was selected to simulate the real wastewater content of organic materials, P, N and soluble salts. However, some runs were operated without the addition of any wastewater. Nevertheless, these conditions were not an obstacle to understand the relationship between electrical input parameters and the components of interests

Table 4.3: Wastewater characteristics used in Phase 1

Component	Concentration (mg/l)
Glucose	310
Peptone	252
Yeast extract	300
Ammonium sulfate	100
Potassium phosphate	37
Magnesium sulfate	40
Manganese sulfate monohydrate	4.5
Iron sulfate	0.4
Calcium chloride	4
Potassium chloride	25
Sodium bicarbonate	25

Chapter 5

Phase 1(Stage 1) Results and discussion

The discussion of this stage was built on identifying the current densities and exposure modes that can cause the removal of foulants (SMP and colloidal organics) and improve the sludge filterability to ensure a good dewaterability. Meanwhile, maintain the microbial activity.

5.1 Current density (CD) vs. sludge electrical conductivity (EC)

Changes of electrical conductivity (EC) and current density (CD) over the time for each run are illustrated in Figures 4.1 to 4.9. Running the batch bioreactors with occasional feeding caused an increase and decrease of soluble salts over the time as affected by the availability of the food to the sludge biomass. The reduction took place when the carbon source was abundant in the bioreactor and the exponential microbial growth was the dominant phase. At this condition, ions such as ammonium, nitrate and orthophosphate were consumed to build up new cells. The reduction of soluble salts through this pathway was observed in the first operating hours when the sludge still have dissolved organic materials to support building new cells. On the other hand, the increase of soluble salts appeared when the carbon sources were depleted and the indigenous phase dominated. During the indigenous phase where food is limited the microbial die off and cell lysis have released the intra soluble ions into the bulk solution

and therefore increased EC. This kind of ups and downs in soluble salt concentrations due to the availability or lack of carbon sources was more severe at higher MLSS and not related to the electrical parameters. However, the electrical field under all operated current densities (5 to 60 A/m^2) caused a reduction of soluble salts in the bioreactor, mainly due to the migration and deposition of ions on the electrodes.

Based on the above mechanisms affecting soluble salts fate in the occasionally fed batch electro-bioreactors, a few examples will be discussed in detail to describe the whole processes affecting sludge EC and CD. However, the same principles and mechanisms are applied in all operating conditions tested on the batch reactors. At MLSS=4700 mg/l and voltage gradient = 1.5 V/cm (Figures 5.1a and 5.1b), a substantial reduction of EC was observed after 24 hours for all electrical modes up to 39%, while the control exhibited a 25% reduction. This means that in the first operating hours, the majority of soluble salts were consumed to build up new cells, but not due to electrical deposition. After that, sludge EC started to increase in the control as the carbon sources depleted and indigenous phase dominated. After 70 hours of operation, the rate of ions deposition on electrodes exceeded the rate of ions released by cell lysis. The reduction in EC relative to the control reactor was in the following order; 38% for 5'-ON/5'-OFF, 29% for 5'-ON/10'-OFF, 26% for 5'-ON/15'-OFF, 18% for 5'-ON/20'-OFF. The continuous-ON mode in this run exhibited regular sharp drops in the current density despite that the EC was almost stable. This drop in current density indeed is not attributed to the drop in EC, but to the formation of a layer on the anodes, which insulated the passage of the current between the electrodes. The current density was fully recovered once this

layer was washed off the electrodes. This layer was formed on top of the anode as the colloidal organics or the microbial flocs having negative surface charges moved towards it through the electrophoresis process. Depositions on anode surface by this process were mostly observed under continuous-ON electrical mode under high current density and MLSS (Runs 4, 5, 7) and for the 5'-ON/5'-OFF electrical mode at MLSS=14,000 mg/l (Run 5). Thus, the continuous-ON mode and 5'-ON/5'-OFF are not recommended for the long term operation under some conditions because of their strength to attract the suspended particles onto the anode surface. At MLSS=5000 mg/l, voltage gradient=0.5 V/cm (Figures 5.3a and 5.3b) showed a gradual decrease in EC for all electrical modes until the end and no severe drop in current density was observed, because the current density was not strong enough (5 to 12 A/m^2) to attract negatively suspended solids towards the anode. When the current density was between 15 to 30 A/m^2 a severe drop of current density due to anode depositions was only observed for the continuous-ON mode (Runs 1, 4, 5, 6, 7).

It was clear in all runs that current density decreased as the sludge EC decreased unless there was a high rate of releasing ions through cell lysis in the indigenous phase. However, the reduction rate of EC is expected to increase by increasing current density. Unfortunately, knowing the exact reduction percentage for each current density and MLSS is not possible at this stage because measuring sludge EC is not enough to determine the amount of ions deposited on the electrodes. For this reason, studying the fate of soluble ions as affected by different strength of current densities cannot be achieved by just measuring the changes of sludge EC. A mass balance approach to

quantify the mass of ions deposited on each electrode and on the suspended solid surfaces is required to establish this relationship. However, this mass balance was not performed in this research because it was not a major objective.

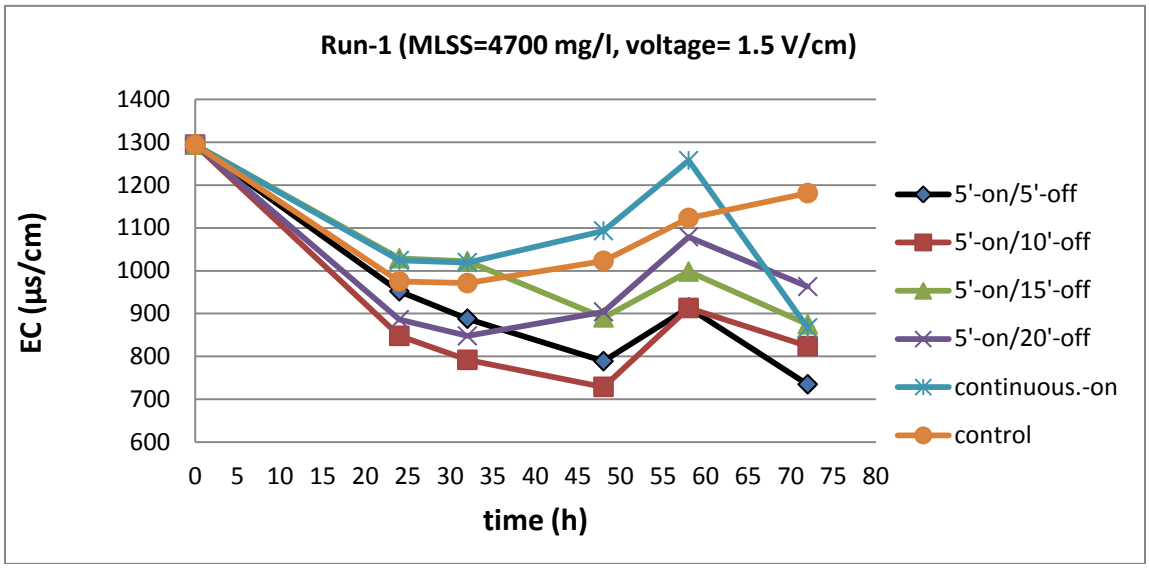

Figure 5.1a: Run 1: Changes of electrical conductivity (EC) over 70 h operating period

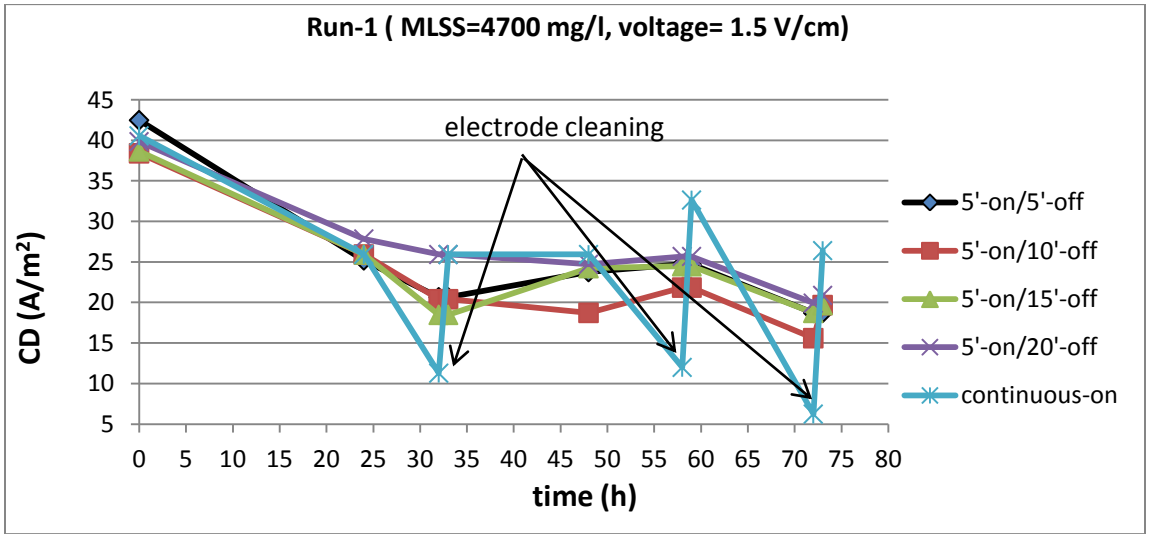

Figure 5.1b: Run 1: Changes of current density (CD) over 70 h operating period

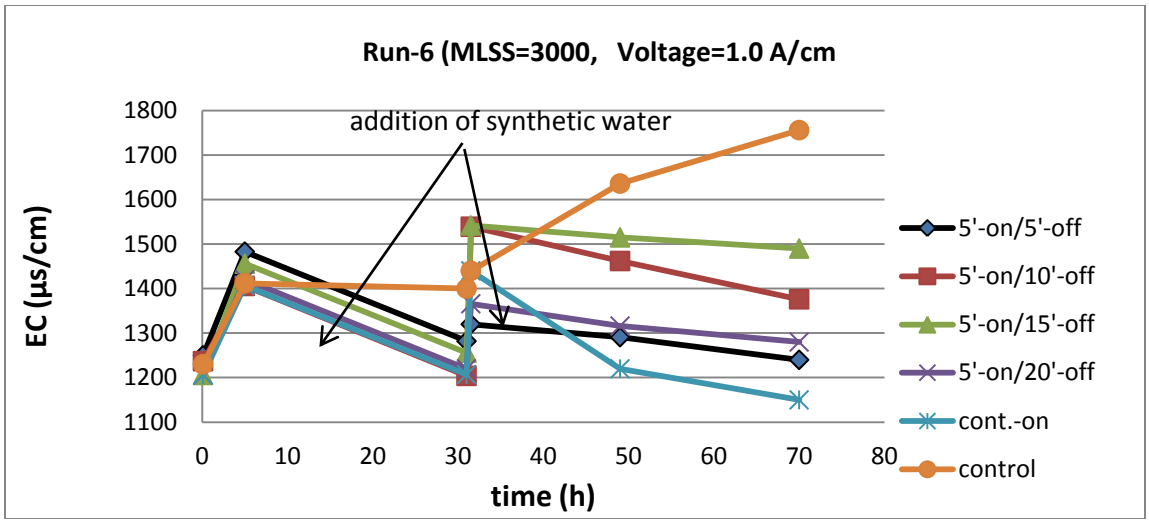

Figure 5.2a: Run 6: Changes of electrical conductivity (EC) over 70 h operating period

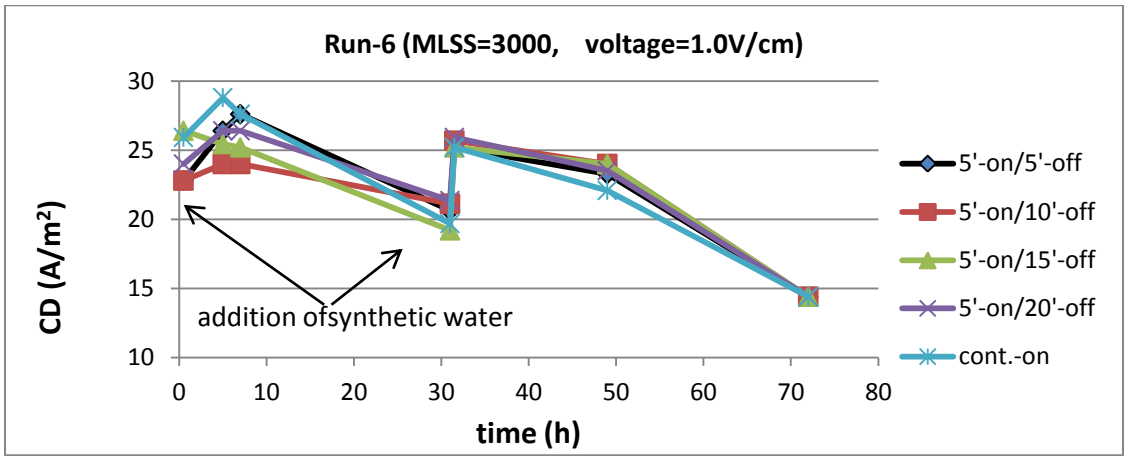

Figure 5.2b: Run 6: Changes of current density over 70 h operating period

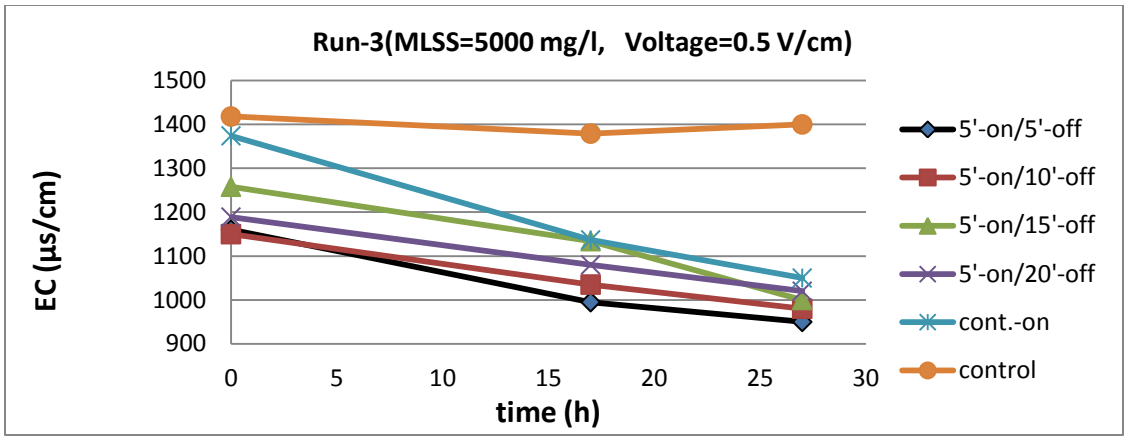

Figure 5.3a: Run 3: Changes of electrical conductivity (EC) over 27 h operating period

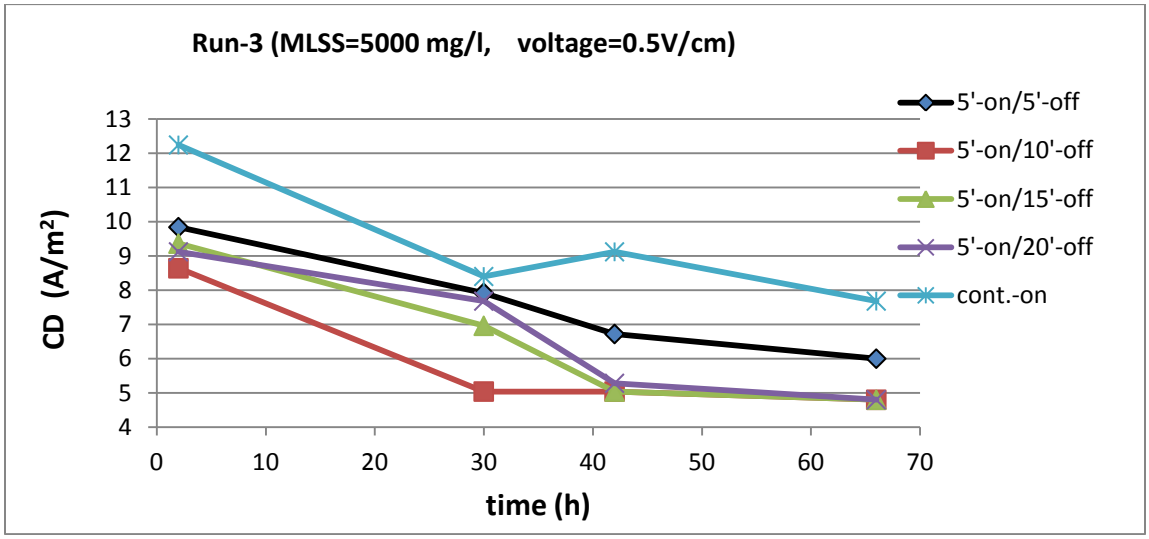

Figure 5.3b: Run 3: Changes of current density (CD) over 68 h operating period

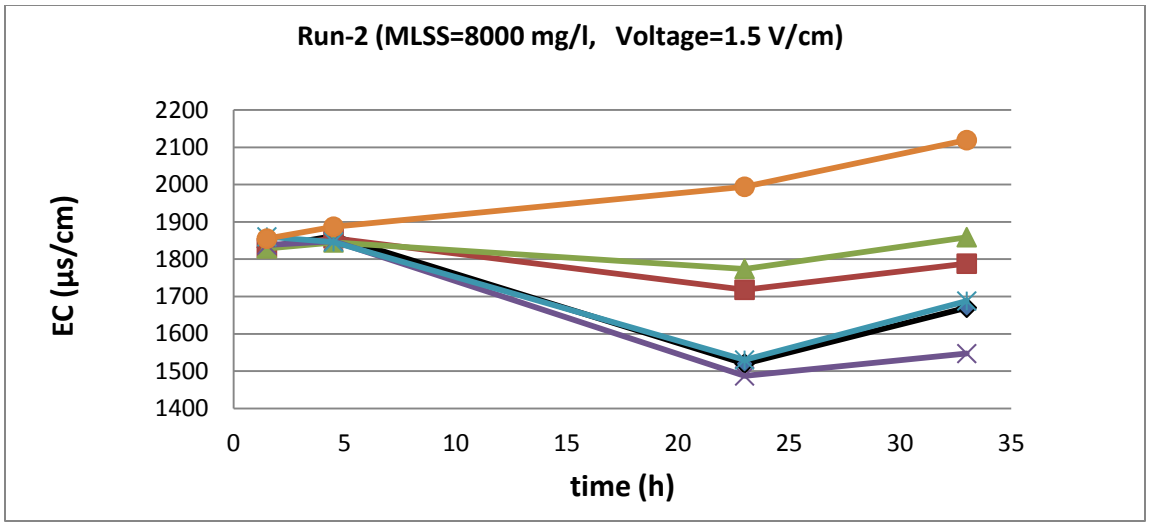

Figure 5.4a: Run 2: Changes of electrical conductivity (EC) over 34 h operating period

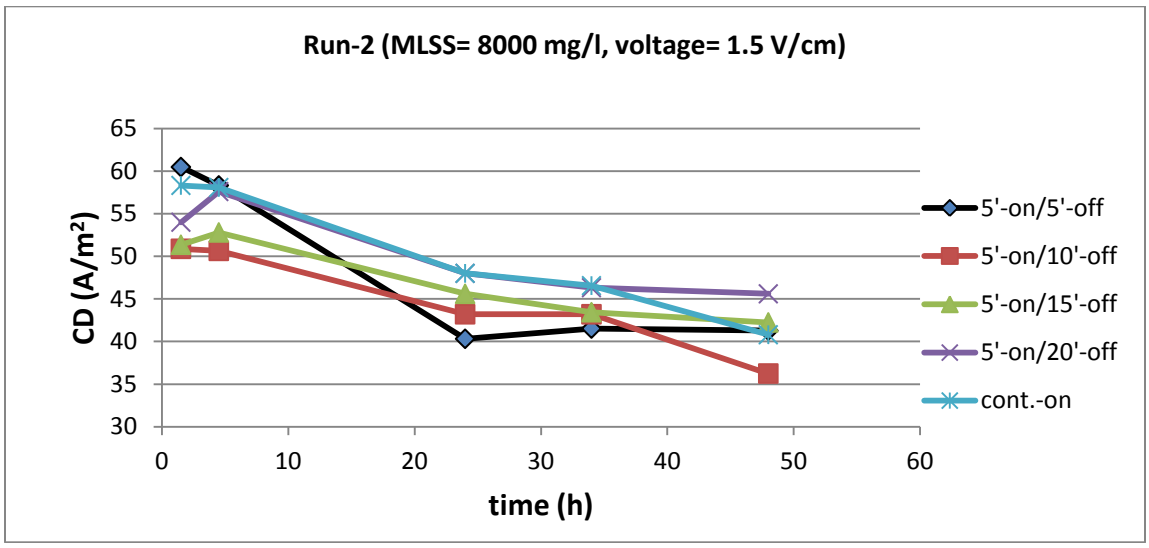

Figure 5.4b: Run 2: Changes of current density (CD) over 48 h operating period

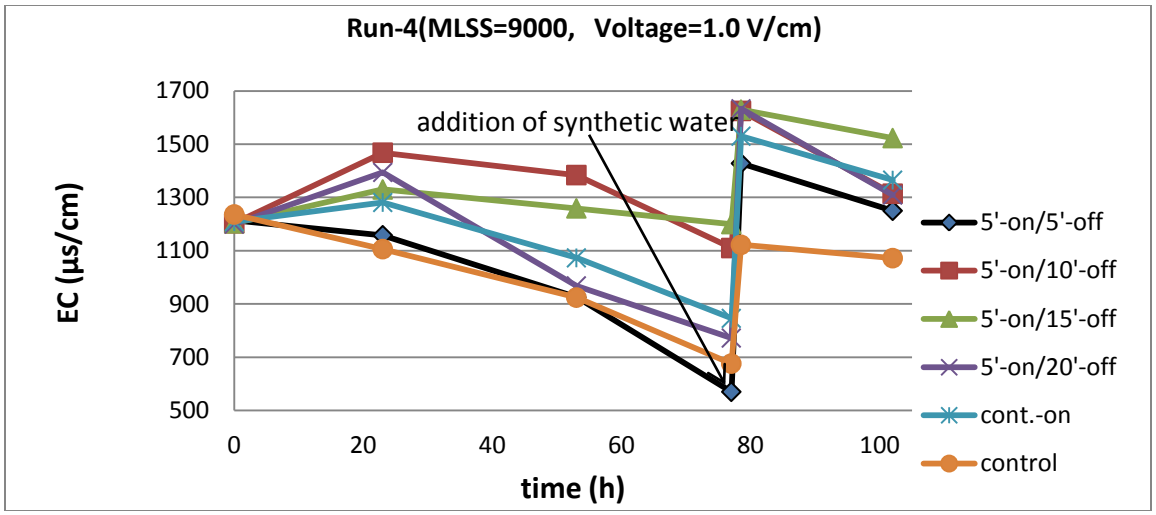

Figure 5.5a: Run 4: Changes of electrical conductivity (EC) over 100 h operating period

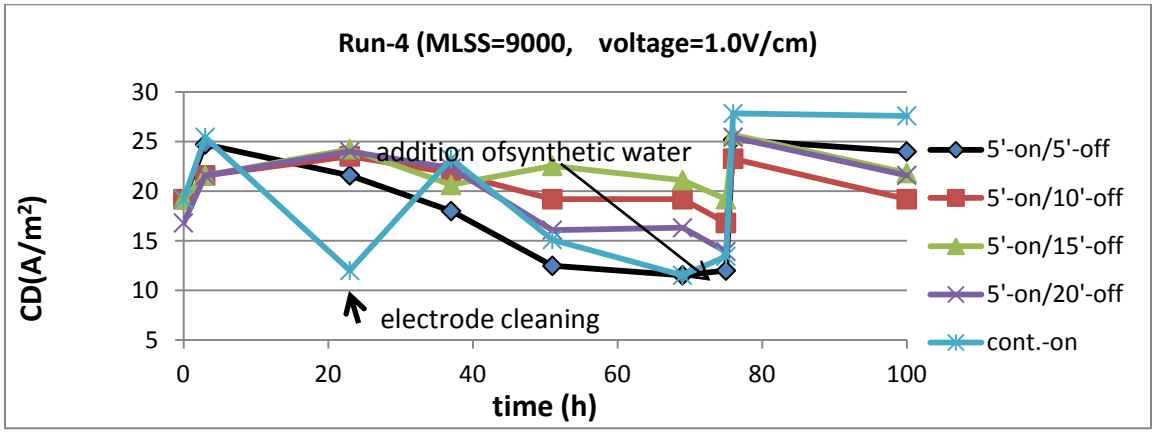

Figure 5.5b: Run 4: Changes of current density (CD) over 100 h operating period

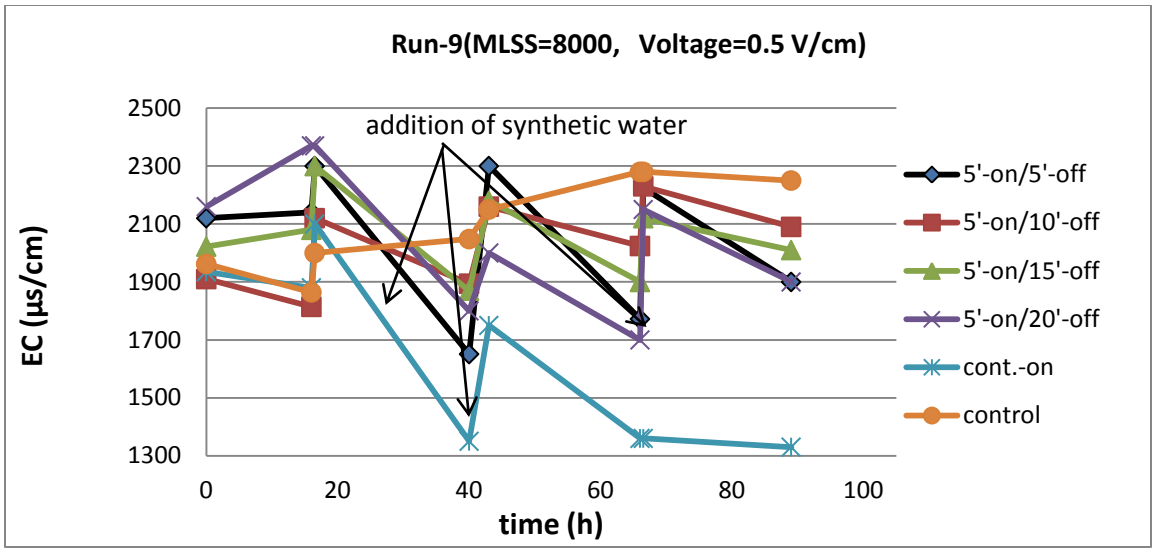

Figure 5.6a: Run 9: Changes of electrical conductivity (EC) over 90 h operating period

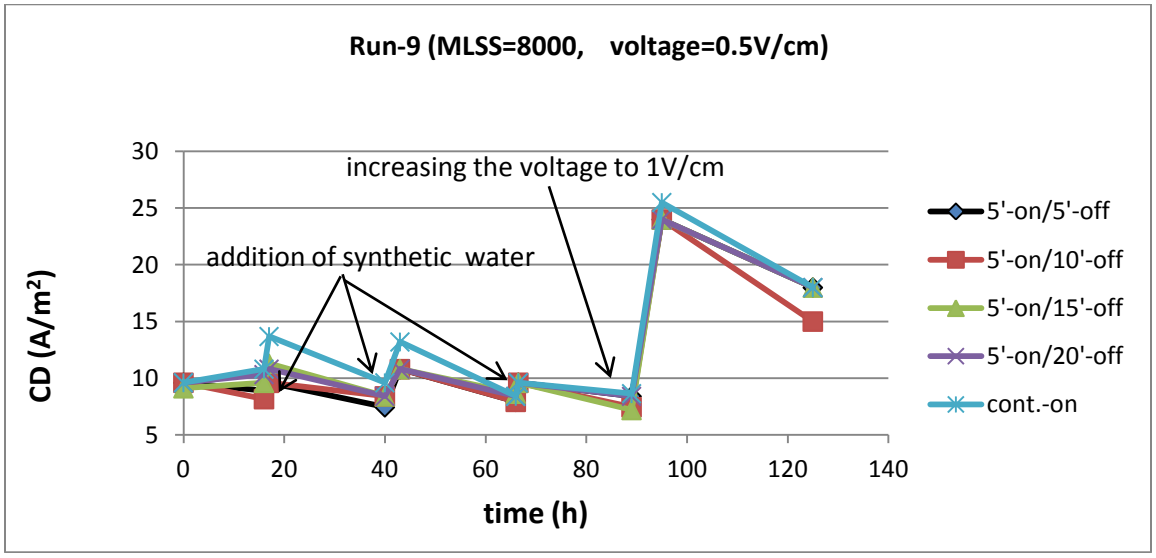

Figure 5.6b: Run 9: Changes of current density (CD) over 130 h operating period

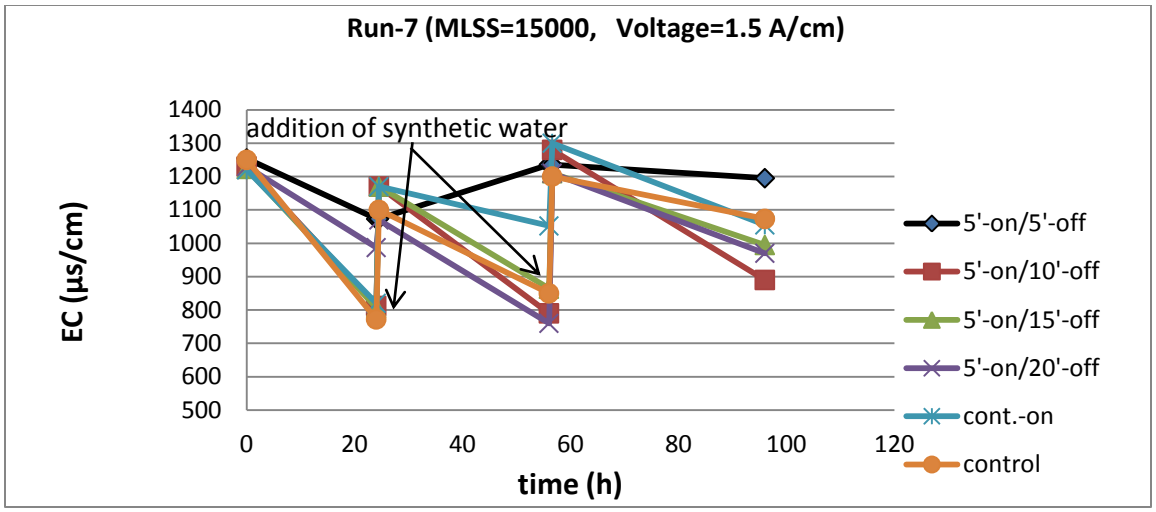

Figure 5.7a: Run 7: Changes of electrical conductivity (EC) over 100 h operating period

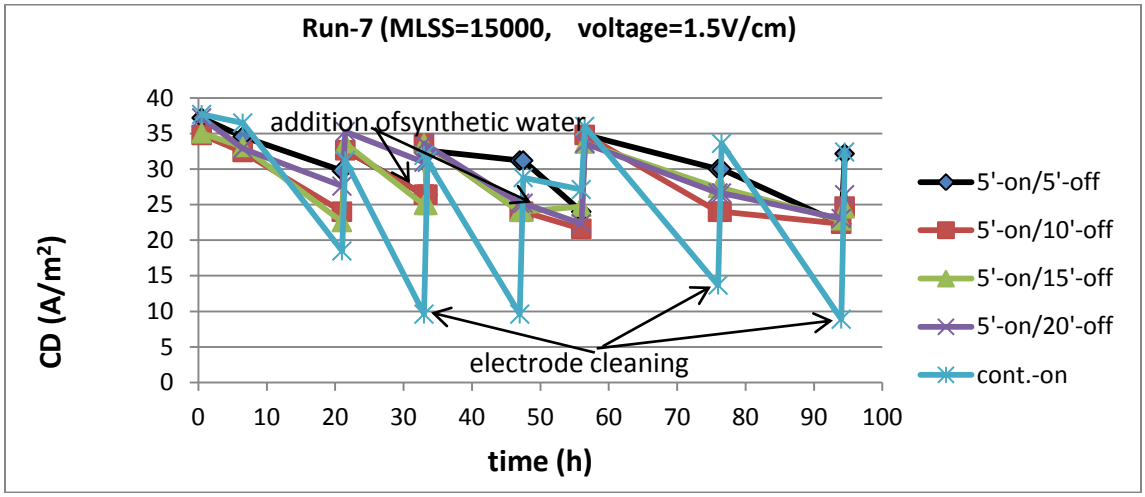

Figure 5.7b: Run 7 Changes of current density (CD) over 94 h operating period.

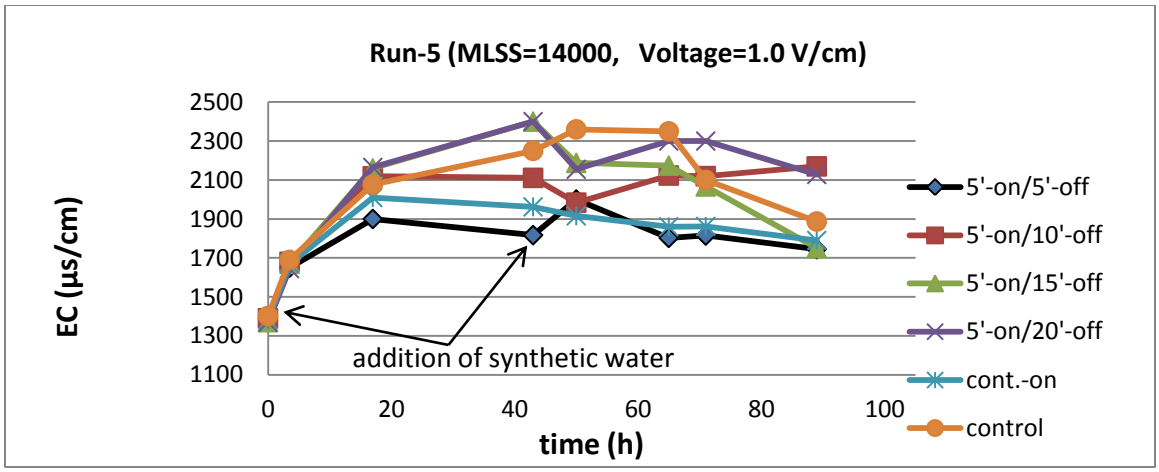

Figure 5.8a: Run 5: Changes of electrical conductivity (EC) over 90 h operating period

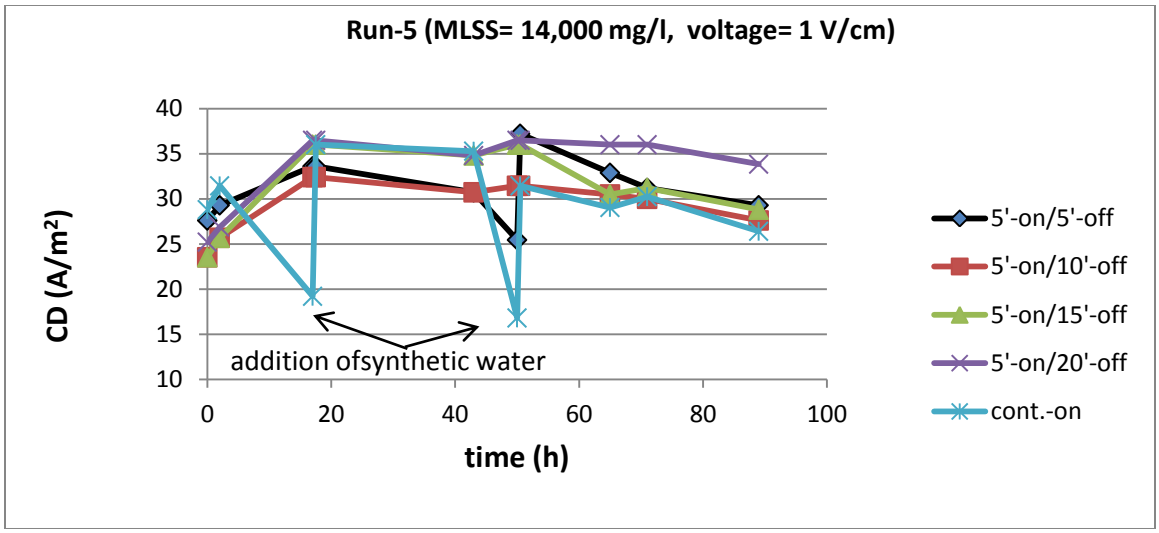

Figure 5.8b: Run 5: Changes of current density (CD) over 90 h operating period

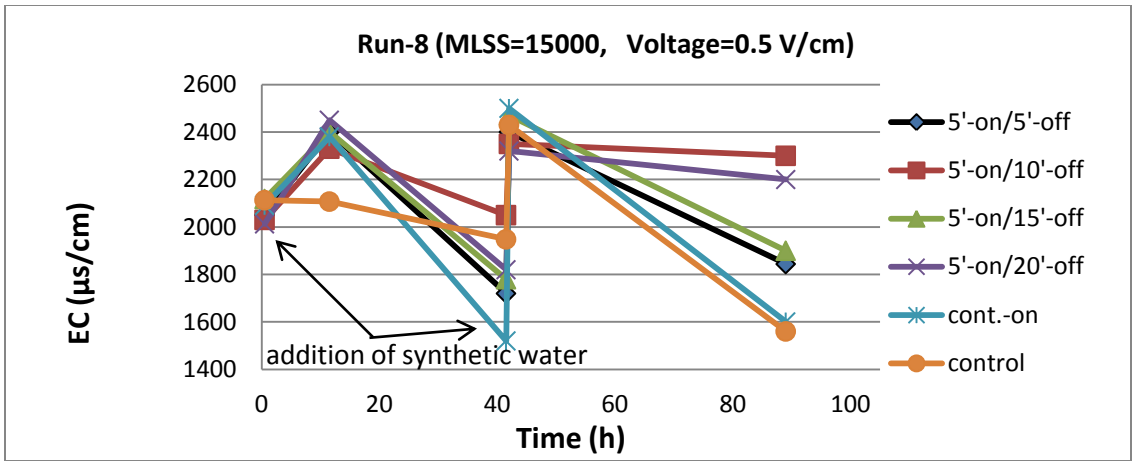

Figure 5.9a: Run 8: Changes of electrical conductivity (EC) over 90 h operating period

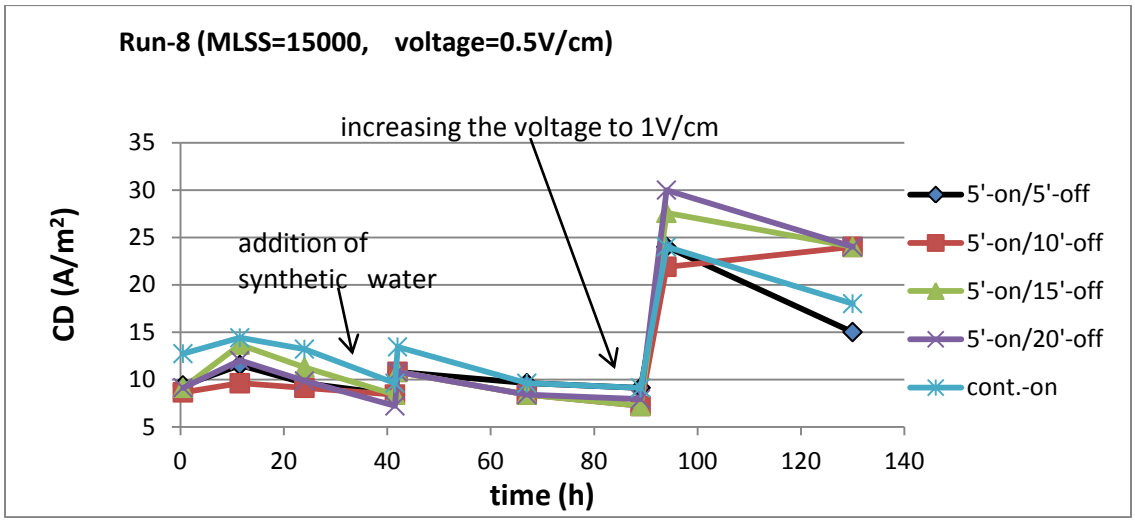

Figure 5.9b: Run 8: Changes of current density (CD) over 130 h operating period

5.2 Relationship between current density and pH

Applying direct current field is expected to decrease pH around the anode through the releasing of H^+ into the sludge liquor, while pH is expecting to increase at the cathode zone due to the production of hydroxide ions. Results showed that current densities

ranging between 5 up to 60 A/m^2 caused a slight increase of sludge pH. The maximum increase that was recorded is 2 degrees under current density of 40 to 60 A/m^2 at the continuous-ON mode (Figure 5.10). Therefore, applying direct current field at current density up to 60 A/m^2 is not likely to cause severe changes in sludge pH to a level that might negatively affect the microbial efficiency. However, this experiment was conducted on batch reactor. Under continuous flow, the changes of sludge pH is expected to be much less than what have been noticed because the liquid phase of the sludge will be replaced continuously by the influent wastewater, which has pH around neutrality. Thus, the slight increase of pH noticed will be neutralized by the large buffering capacity of the feed wastewater.

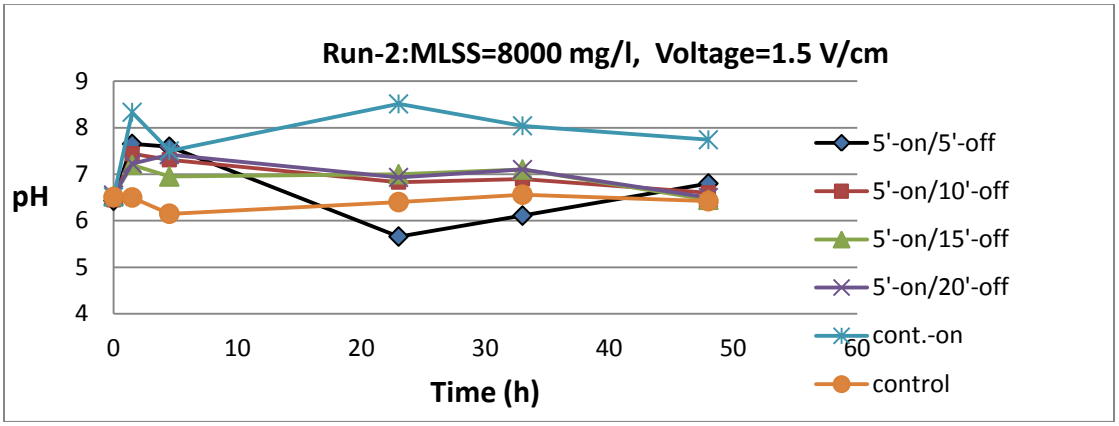

Figure 5.10: Run 2: Changes of sludge pH over the operating period of 48 h at current density ranging between 40 to 60 A/m^2

5.3 Relationship between current density (CD) and COD-colloidal

Changes of COD-colloids as affected by different strengths of current densities are shown in Figures 5.11 to 5.16. At low current density (8 to 12 a/m^2), the removal efficiency of the colloids was in the range of 45 % to 93% (Figures 5.11 and 5.12). The

highest removal at this level of current density was obtained at continuous-ON and 5'-ON/5'-OFF modes at high MLSS. Therefore, low current densities are more effective in the removal of organic colloids at electrical modes cycles with the shortest time-OFF and high MLSS. Short time-OFF at that low CD ensures enough dissolution of Al^{+3} coagulants, while high MLSS provides more solid surfaces to interact electrically with the organic colloids.

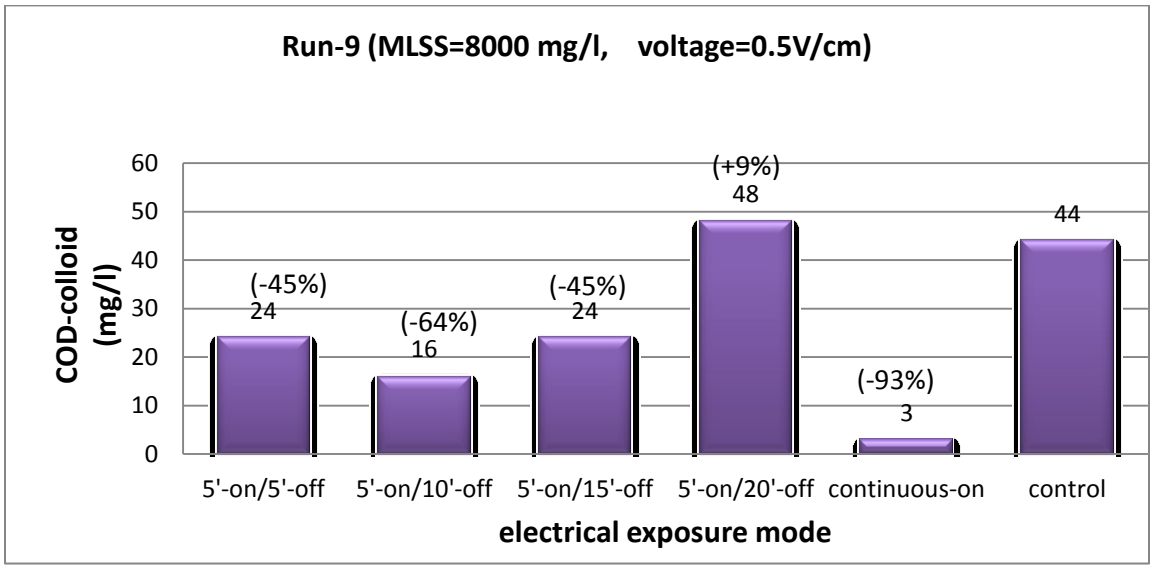

Figure 5.11: Run 9: Changes of COD-colloidal at current densities ranging between 8 to 10 at the end of 109 h operating period. (-) = reduction, (+) = increase

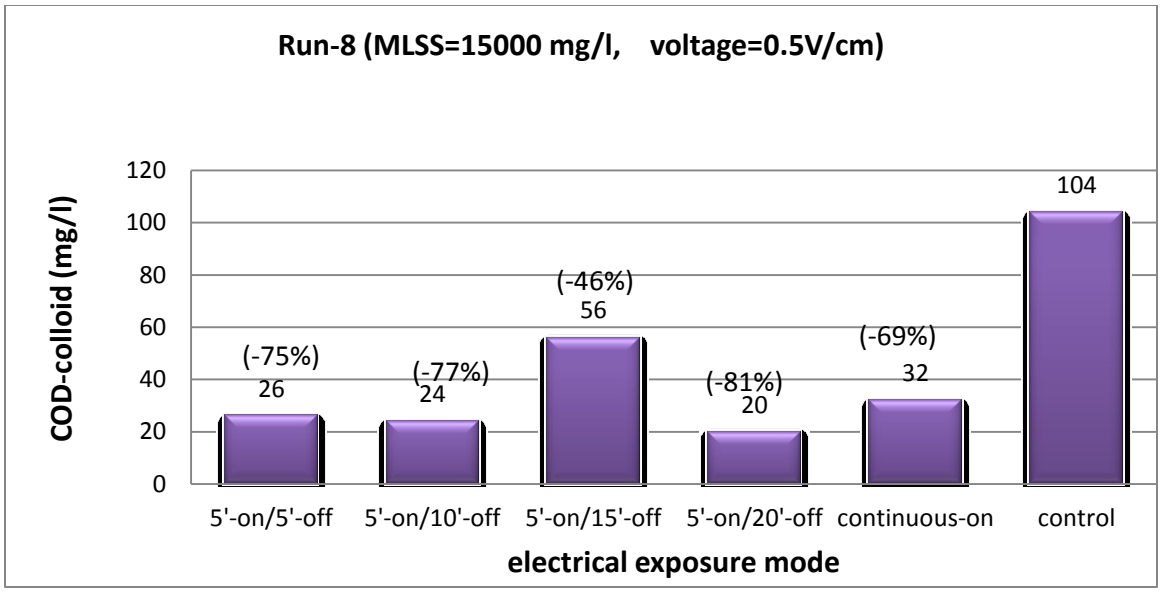

Figure 5.12: Run 8: Changes of COD-colloidal at current densities ranging between 8 to 12 A/m^2 at the end of 90 h operating period. (-) = reduction

On the other hand, higher values of current density between 15 to 25 A/m^2 were very powerful in removing organic colloids at 9000 mg/l MLSS (up to 100%), except for the mode 5'-ON/20'-OFF (Figure 5.13) that exhibited only 20% removal due to the length of time-OFF that did not supply enough Al^{+3}. At the same time, at low MLSS=3000 mg/l and CD of 15 to 25 A/m^2, the removal was very efficient only at 5'-ON/5'-OFF and continuous-ON electrical modes (Figure 5.14). Lower concentration of MLSS provides less solid surfaces; therefore, longer time-ON is required in the electrical cycle to substantially remove organic colloids.

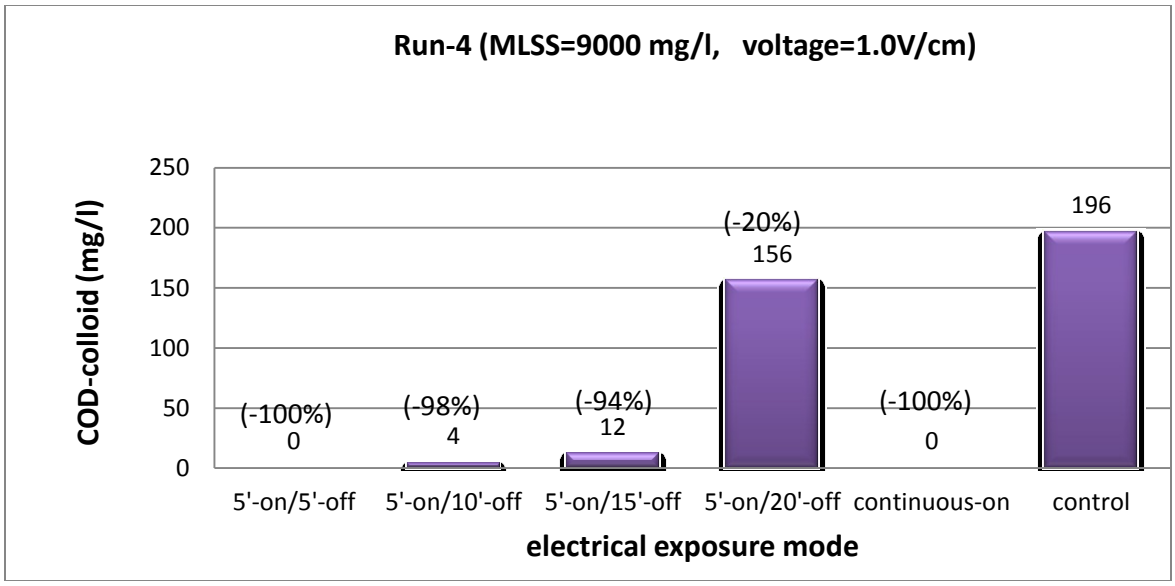

Figure 5.13: Run 4: Changes of COD-colloidal at current density ranging between 15 to 25 A/m^2 at the end of 100 h operating period. (-) = reduction

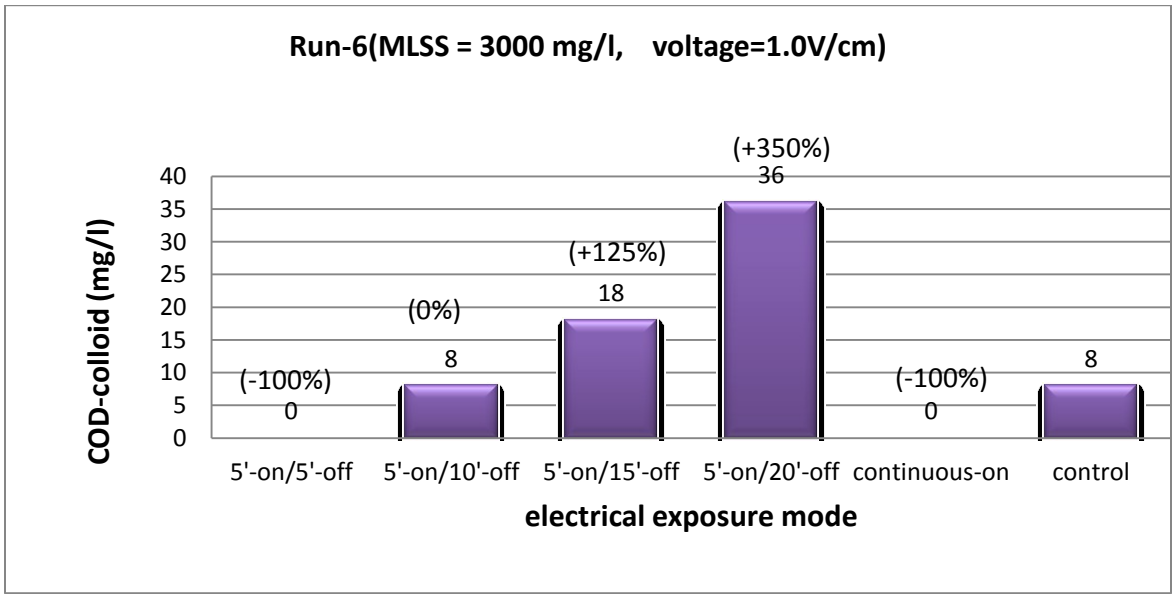

Figure 5.14: Run 6: Changes of COD-colloidal at current density ranging between 20 to 25 A/m^2 at the end of 70 h operating period. (-) = reduction, (+) = increase

At high MLSS of 14000 to 15000 mg/l and current density of 25 to 35 A/m^2, there was a complete contradiction between Run 5 (Figure 5.15) and Run 7 (Figure 5.16), which were operated at the same CD and MLSS, except that Run 5 was operated at voltage gradient of 1V/cm and run 7 at 1.5 V/cm. Run 5 exhibited at least 93% removal for all electrical modes, while Run 7 exhibited higher colloidal concentration up to more than 10 times that of the control at the electrical mode 5'-ON/5'-OFF. The other electrical modes in Run 7 exhibited different increases in organic colloids ranging between 0.5 to 2.7 times compared to the control. However, despite this increase of colloidal organic, most of the other sludge properties were improved by the DC field as will be illustrated later. This indicates that selecting the best electrical operating parameters should be considered collectively but not on one individual sludge property. Furthermore, operating at current densities higher than 30 A/m^2 and electrical mode with short time-OFF such as 5'-ON/5-OFF is not recommended at high concentrations of MLSS due to the high risk of damaging the microbial flocs by the current.

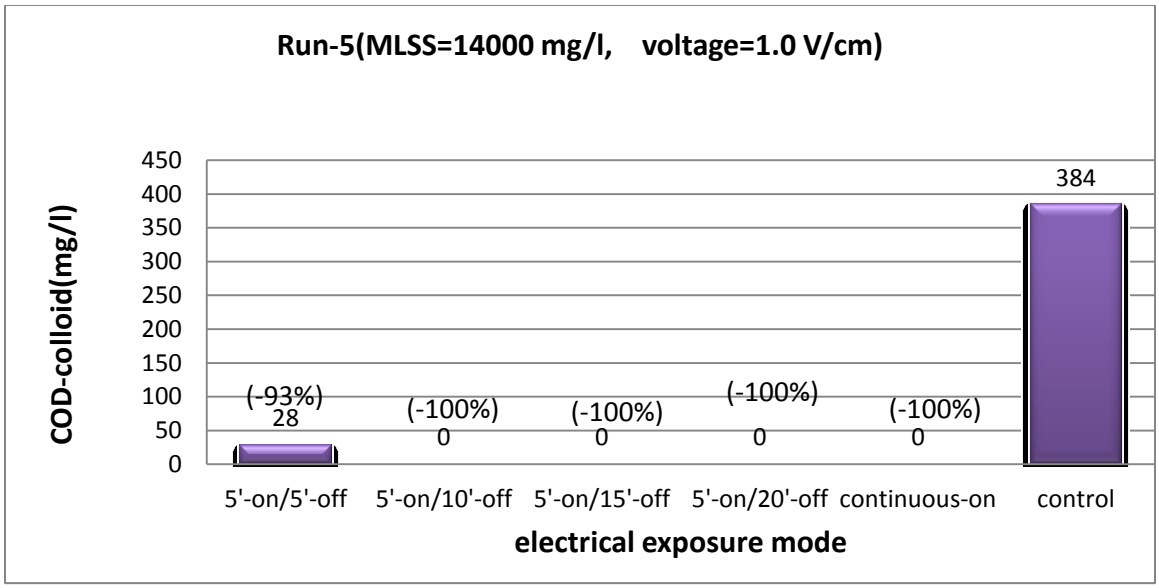

Figure 5.15: Run 5: Changes of COD-colloidal at current density ranging between 25 to 35 A/m^2 at the end of 90 h operating period. (-) = reduction

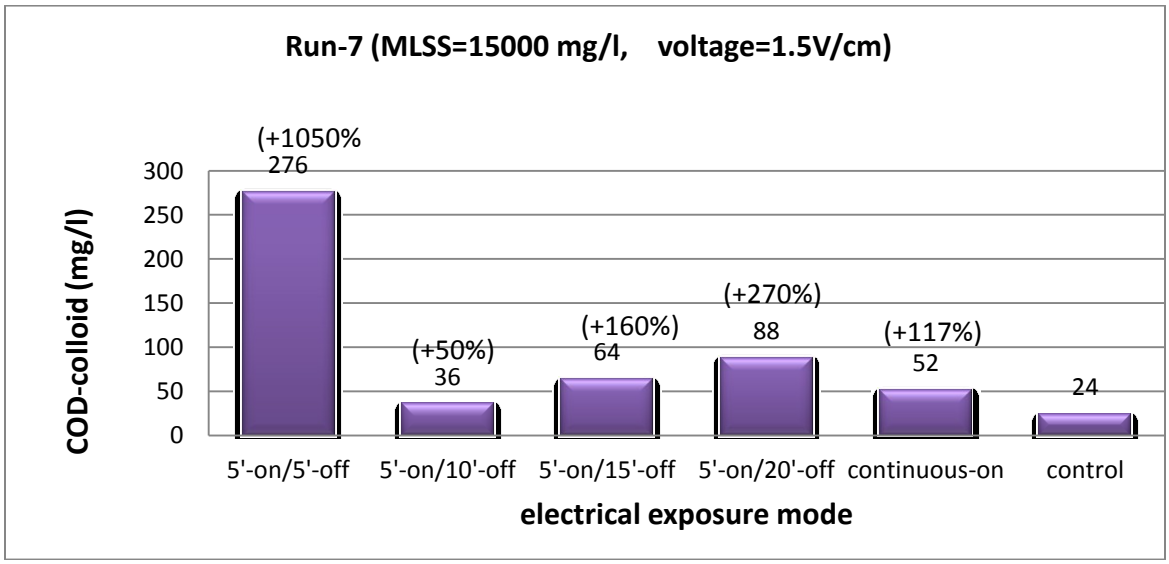

Figure 5.16: Run 7: Changes of COD-colloidal at current densities ranging between 20 to 35 A/m2 at the end of 90 h operating period. (-) = reduction, (+) = increase

5.4 Relationship between current density and SMP

Figures 5.17 to 5.23 represent the changes of SMP (protein and polysaccharides) concentrations in the supernatant at the end of the operating period at different current densities and MLSS. Results showed that the removal of protein and polysaccharides is affected by current density, MLSS and the electrical mode. At low current density between 8 to 12 A/m^2 and high MLSS=15,000 mg/l, the removal efficiency was very low for protein (Figure 4.17a) and polysaccharides (Figure 4.17b) at all electrical modes except for the continuous-ON and 5'-ON/5'-OFF modes. However, the low current density (8 to 12 A/m^2) at MLSS= 8000 mg/l, exhibited less removal efficiency for protein (Figure 4.18a) and polysaccharides (Figure 4.18b) even at the continuous-ON and 5'-ON/5'-OFF. This proves again that lower current density is more effective in removing SMP at higher MLSS concentration than lower levels.

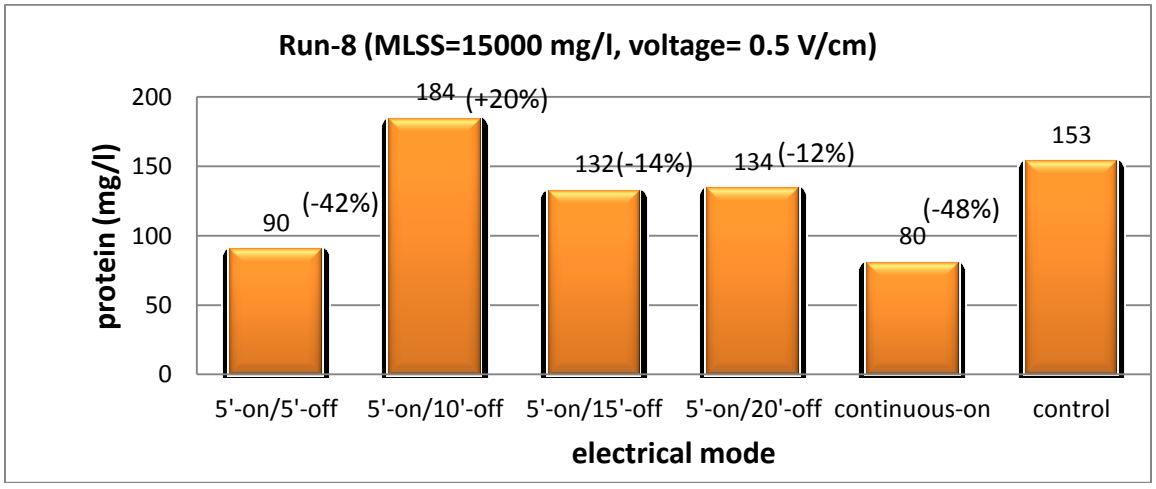

Figure 5.17a: Run 8: Changes of soluble protein concentration at current density ranging between 8 to 12 A/m2 at the end of 90 h operating period. (-) = reduction, (+) = increase

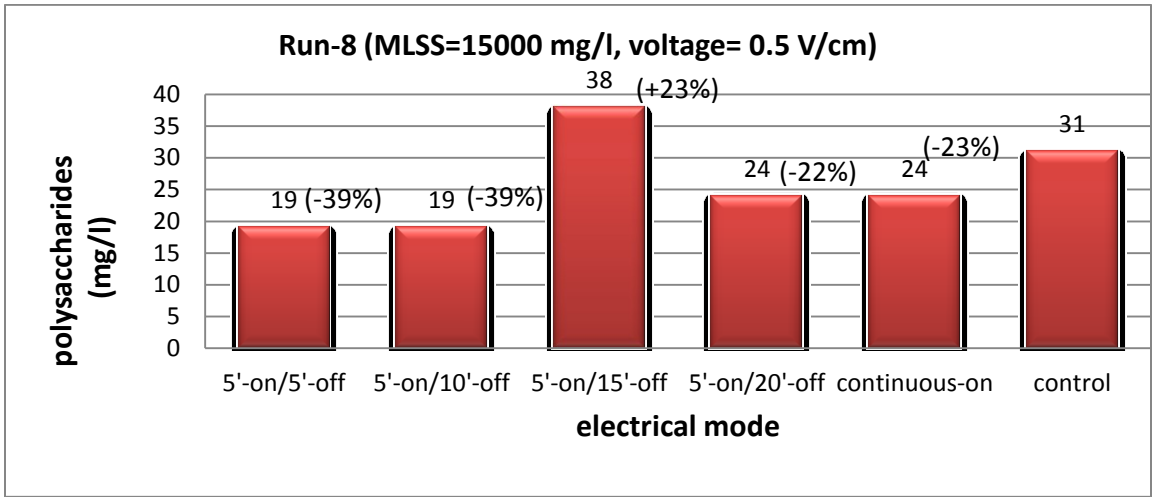

Figure 5.17b: Run 8: Changes of soluble polysaccharide concentration at current density ranging between 10 to 12 A/m^2 at the end of 90 h operating period. (-) = reduction, (+) = increase

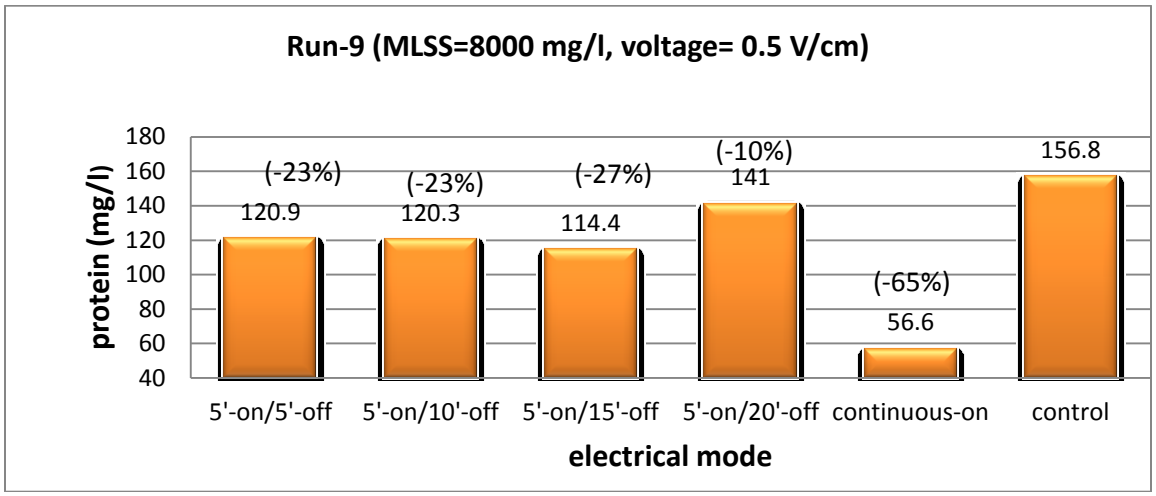

Figure 5.18a: Run 9: Changes of soluble protein concentration at current density ranging between 8 to 10 A/m^2 at the end of 109 h operating period. (-) = reduction

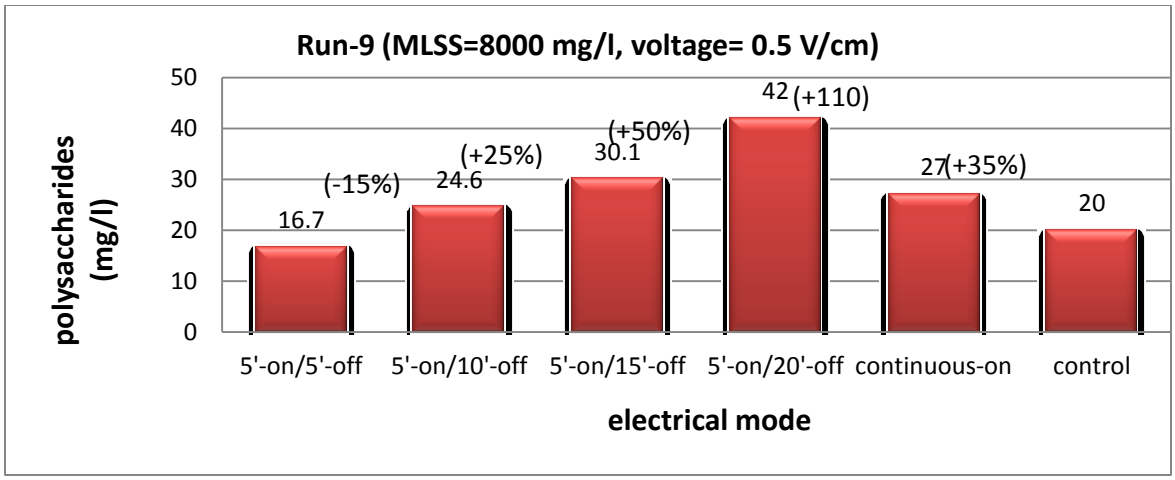

Figure 5.18b: Run 9: Changes of soluble polysaccharide concentration at current density ranging between 8 to 10 A/m^2 at the end of 109 h operating period. (-) = reduction, (+) = increase

Higher magnitudes of current density between 20 to 35 A/m^2 showed a substantial removal for all electrical modes at MLSS ranging between 3000 to 9000 mg/l. The removal efficiency under these conditions was up to 83% for protein (Figures 5.19a and 5.20a) and 69% for polysaccharides (Figures 5.19b and 5.20b).

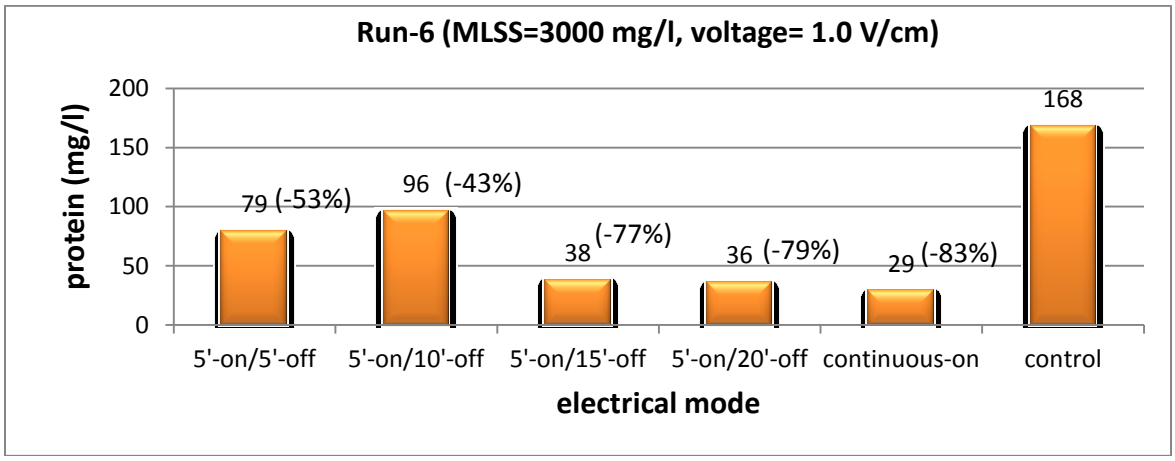

Figure 5.19a: Run 6: Changes of soluble protein concentration at current density ranging between 20 to 25 A/m^2 at the end of 70 h operating period. (-) = reduction

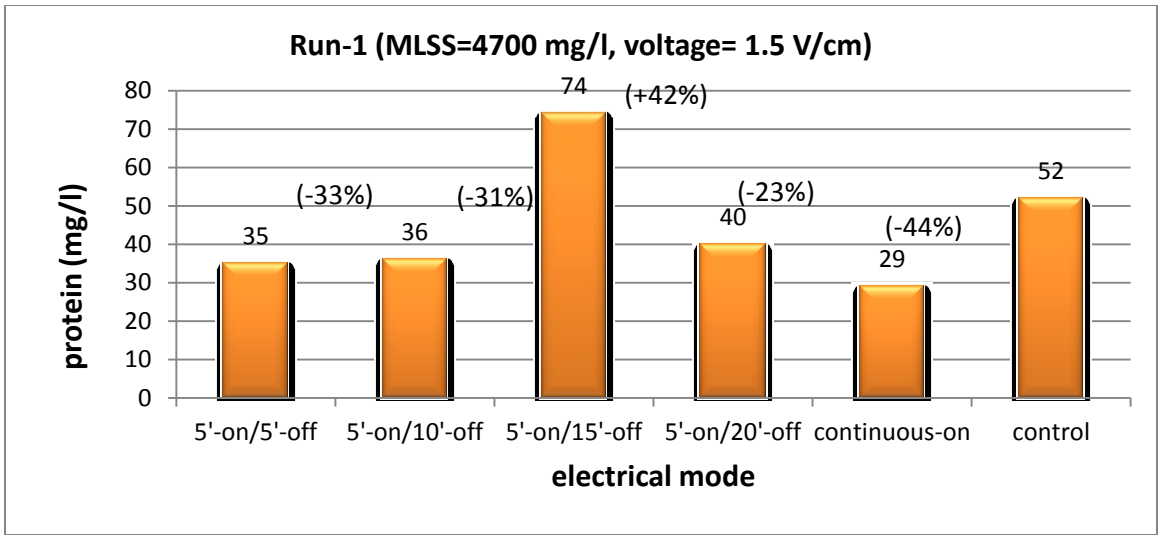

Figure 5.20a: Run 1: Changes of soluble protein concentrations at current density ranging between 20 to 35 A/m^2 at the end of 72 h operating period. (-) = reduction, (+) = increase

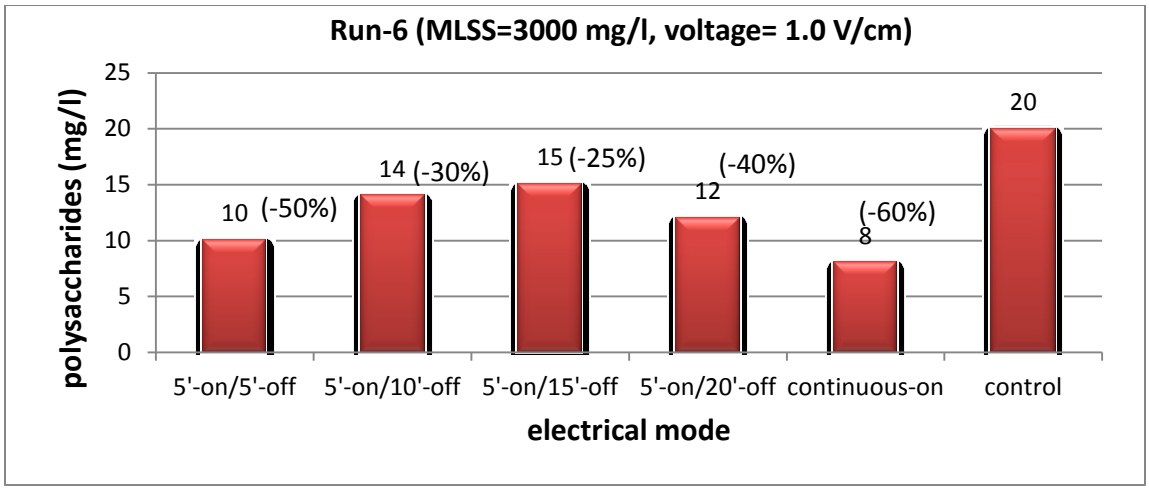

Figure 5.19b: Run 6: Changes of soluble polysaccharide concentration at current density ranging between 20 to 25 A/m^2 at the end of 70 h operating period. (-) = reduction

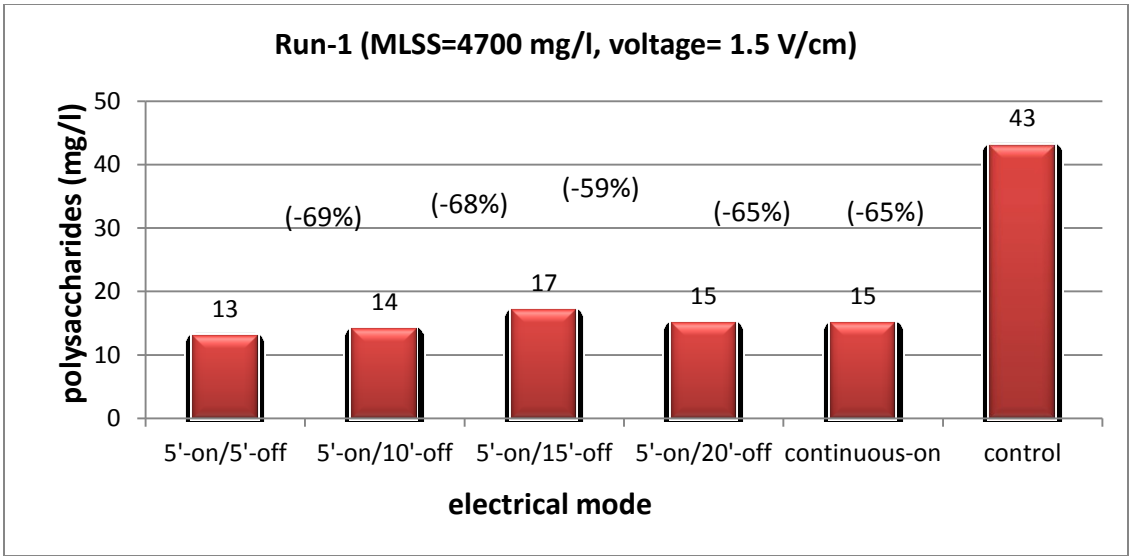

Figure 5.20b: Run 1: Changes of soluble polysaccharide concentration at current density ranging between 20 to 35 A/m2 at the end of 70 h operating period. (-) = reduction

At high values of MLSS around 15,000 mg/l and current density between 25 to 35 A/m^2 (Figures 5.21a,b and 5.22a,b), it was found that electrical modes with higher percentage of time-ON in the electrical cycle showed an increase of SMP due to cell lysis as affected by the current field. Simultaneously, the electrical modes, 5'-ON/10'-OFF, 5'-ON/15'-OFF and 5'-ON/20'-OFF showed a substantial reduction of polysaccharides up to 68% and up to 37% for protein. However, these electrical modes did not show a consistency in the removal of protein and polysaccharides. For example, substantial removal of polysaccharides was accompanied by a slight increase of protein in some cases. The reason for these discrepancies is that at MLSS of high concentration (15,000 mg/l) the sludge viscosity is too high, which makes mixing of the liquor to provide homogeneous concentration of SMP throughout the reactor extremely difficult. Thus, working under high MLSS requires special attention regarding the air distribution in the reactor, yet,

more samples may be needed to minimize the error coming from sludge heterogeneity. Different mechanisms are expected to contribute in the removal of SMP from sludge liquor. SMPs are considered as a nano-colloids having a negative charge under alkaline pH, Therefore, SMP could move and deposit on the anode through electrophoresis. The Al^{+3} produced from the anode forming aluminum hydroxide or acting as a tri-cation coagulant is another removal pathway. In addition to that, the electro-coagulation between the colloids, aluminum hydroxides, and microbial suspended solids is another route of removal.

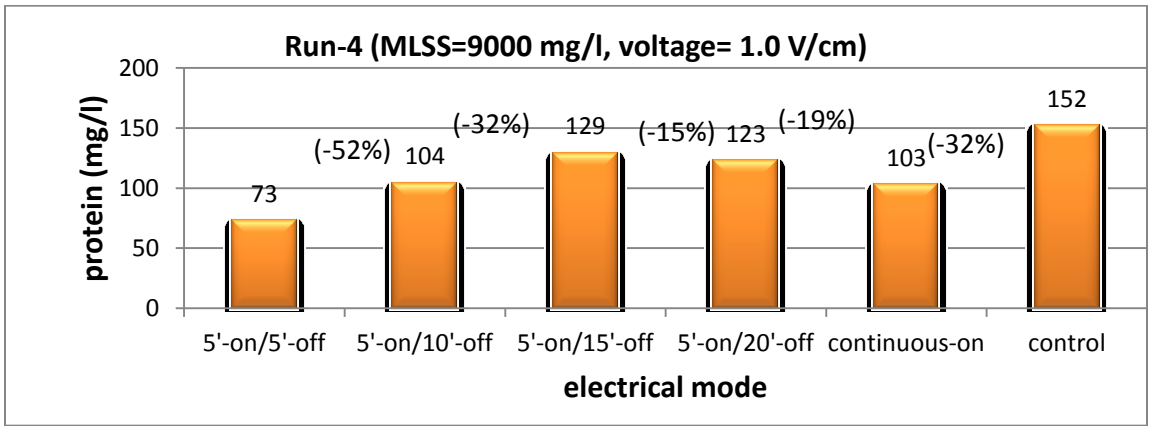

Figure 5.21a: Run 4: Changes of soluble protein concentration at current density ranging between 15 to 25 A/m^2 at the end of 100 h operating period. (-) = reduction

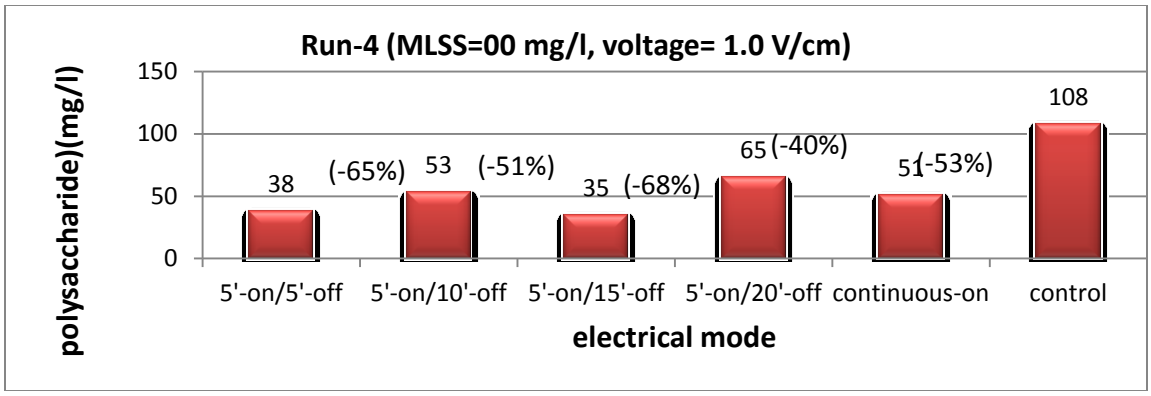

Figure 5.21b: Run 4: Changes of soluble polysaccharide concentration at current density ranging between 15 to 25 A/m^2 at the end of 100 h operating period. (-) = reduction

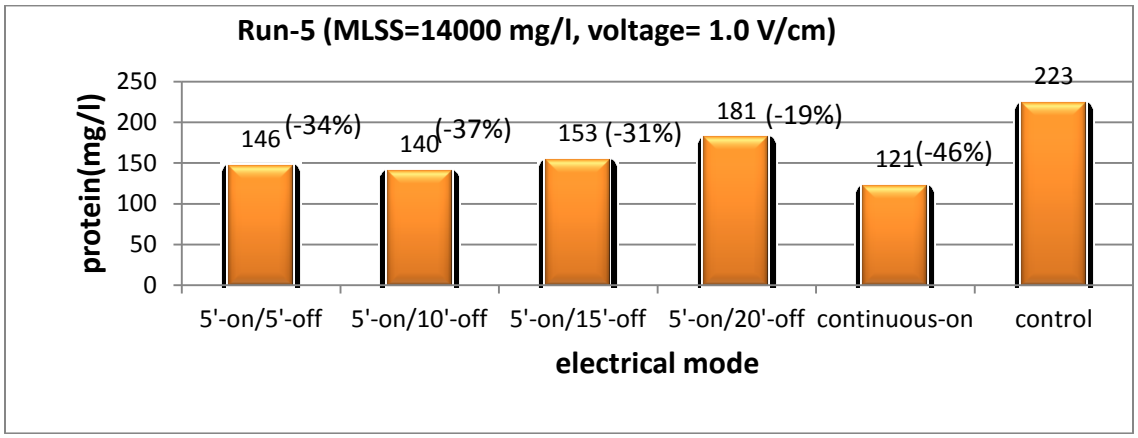

Figure 5.22a: Run 5: Changes of soluble protein concentration at current density ranging between 25 to 35 A/m^2 at the end of 90 h operating period. (-) = reduction

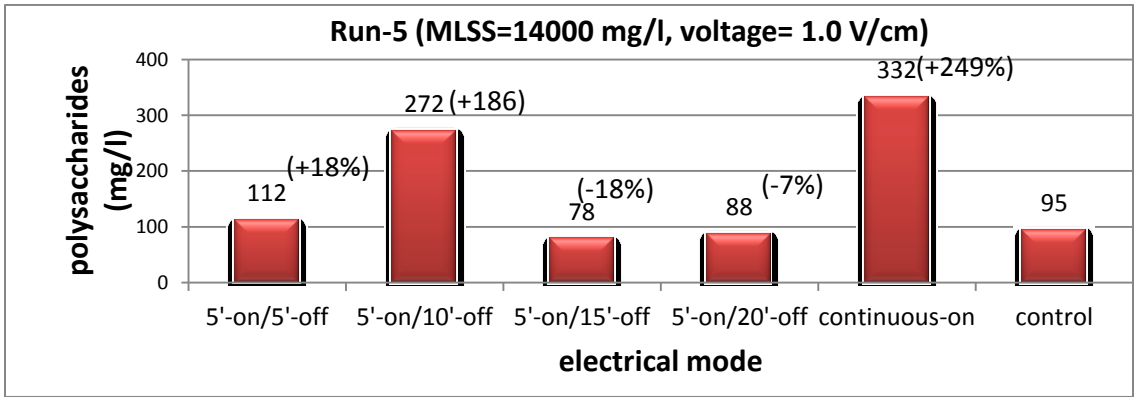

Figure 5.22b: Run 5: Changes of soluble polysaccharide concentration at current density ranging between 25 to 35 A/m^2 at the end of 90 h operating period. (-) = reduction, (+) = increase

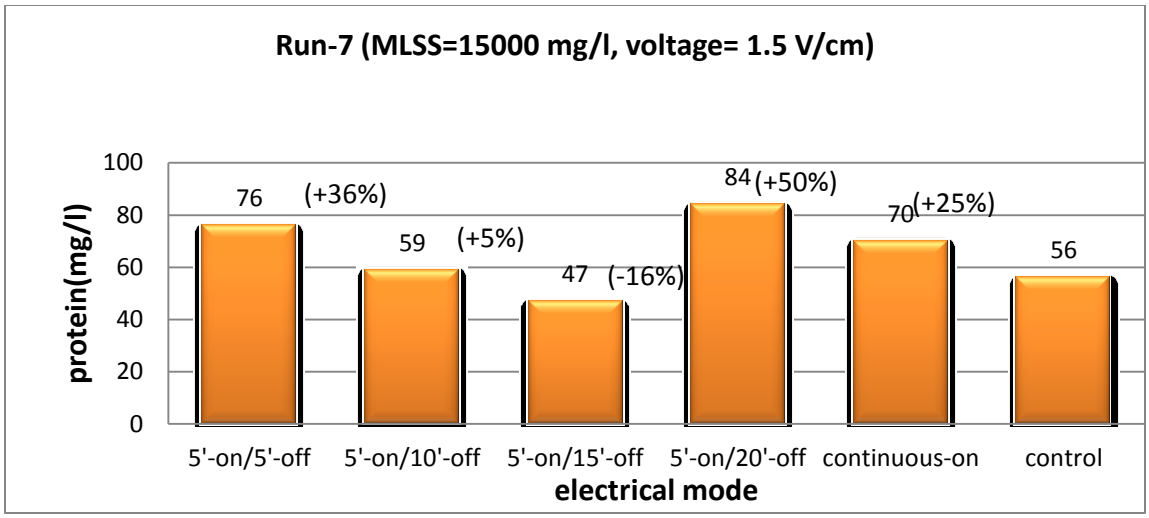

Figure 5.23a: Run 7: Changes of soluble protein concentration at current density ranging between 25 to 35 A/m^2 at the end of 96 h operating period. (-) = reduction, (+) = increase

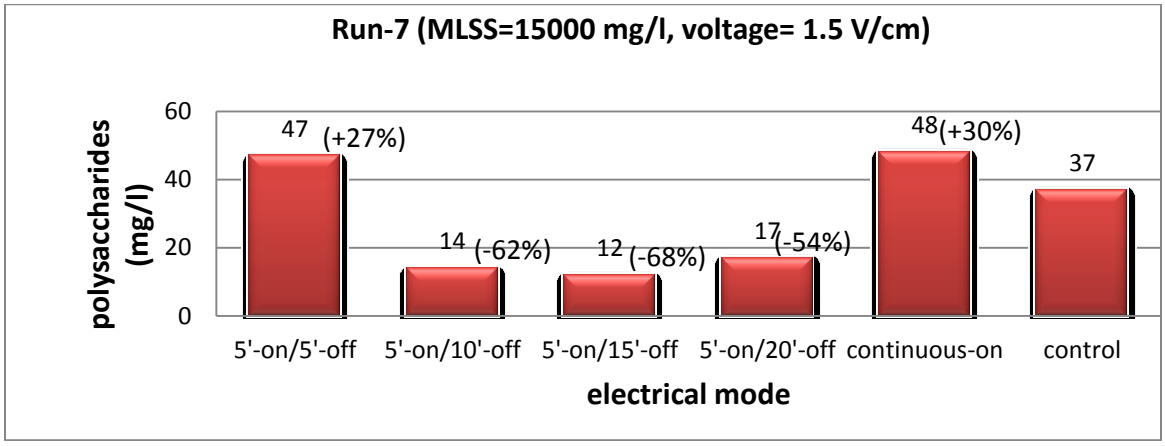

Figure 5.23b: Run 7: Changes of soluble polysaccharide concentration at current density ranging between 25 to 35 A/m^2 at the end of 96 h operating period. (-) = reduction, (+) = increase

5.5 Relationship between current density and humic substances

low current density (8 to 12 A/m^2) showed better removal efficiency of humic substances at MLSS of 15000mg/l (Figure 5.25)than that at MLSS of 8000 mg/l (Figure 5.24), which did not exhibit any removal efficiency whatsoever, except a slight decrease

at the continuous-ON mode. In other words, low current density is not effective in removing humic substances unless the MLSS is around 15000 mg/l; this result is consistent with the removal efficiency of SMP as indicated previously.

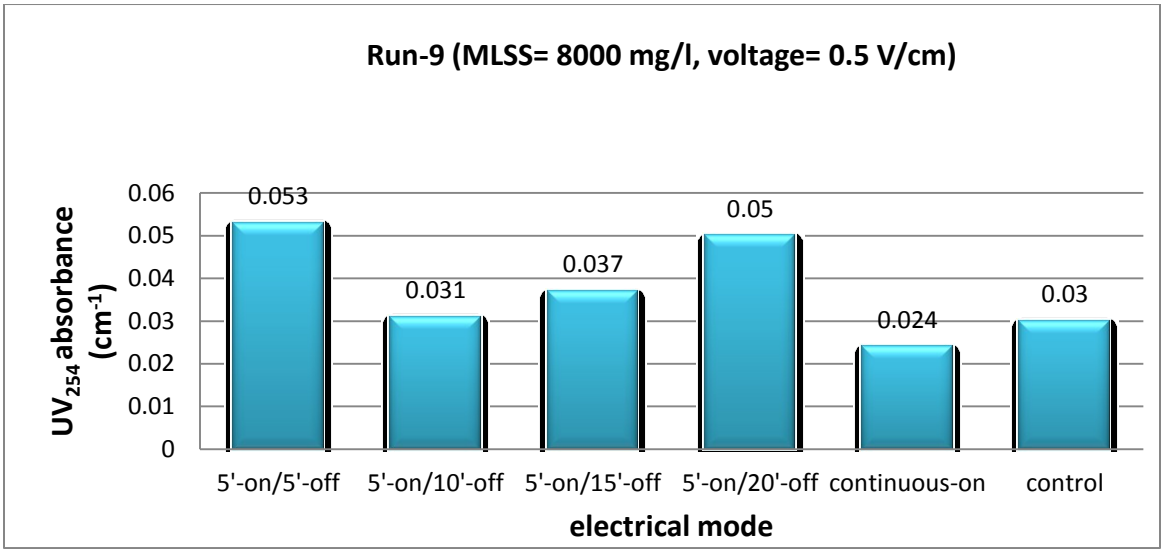

Figure 5.24: Run 9: Changes of humic substances concentration measured as the absorbance at UV_{254} at current density ranged between 8 to 12 A/m^2 at the end of 109 h operating period. (-) reduction

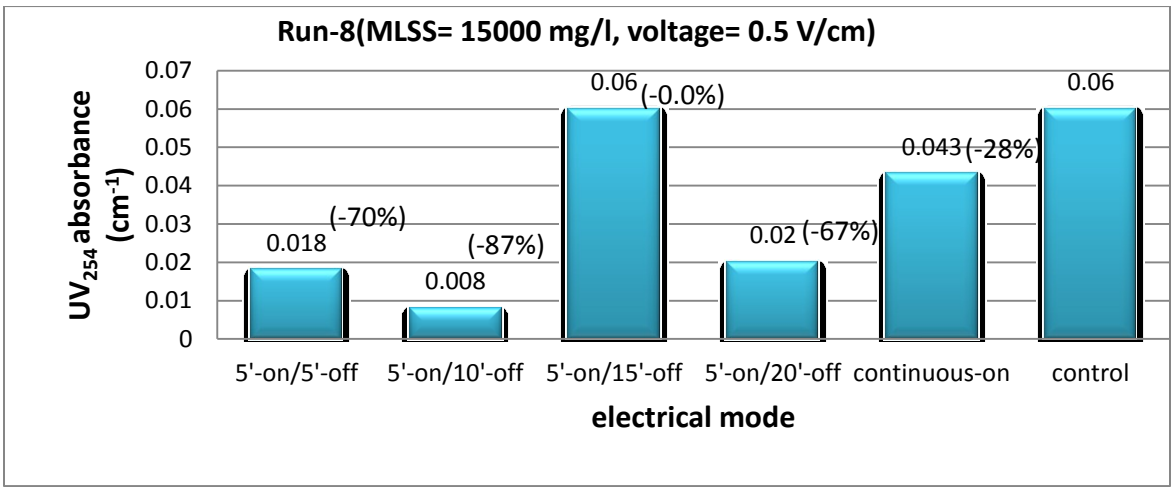

Figure 5.25: Run 8: Changes of humic substances concentration measured as the absorbance at UV_{254} at current density ranged between 8 to 12 A/m^2 at the end of 90 h operating period. (-) = reduction

On the other hand, minimum removal efficiency of 48% was achieved for all electrical modes and for all MLSS concentrations when the current density ranged between 20 to 35 A/m^2 (Figures 5.26 to 5.28). Furthermore, removal efficiencies higher than 90% were obtained at different electrical modes and MLSS concentrations. This is extremely important for reducing the formation of disinfection by-products through the disinfection process. At MLSS of 14000 mg/l, the electrical modes of 5'-ON/10'-OFF and 5'-ON/15'-OFF exhibited better removal efficiencies than the electrical modes with shorter time-OFF (Figure 5.27). However, the continuous-ON mode does not represent the exact effect due to the severe fluctuation in current density at that high level of MLSS. Thus, continuous-ON mode will not be accounted or considered under such conditions where severe fluctuations of current density were taking place. The removal mechanisms of humic substances are not different than that of SMP. It is attributed to the electro-coagulation among the organic materials, microbial flocs and aluminum hydroxides. In the end, the removal of humic substances was calculated based on the UVA_{254}, which is interfered with the presence of protein in the sample due to its capability to absorb the same wavelength. Nevertheless, this criterion is still a good indication of high removal of humic substances.

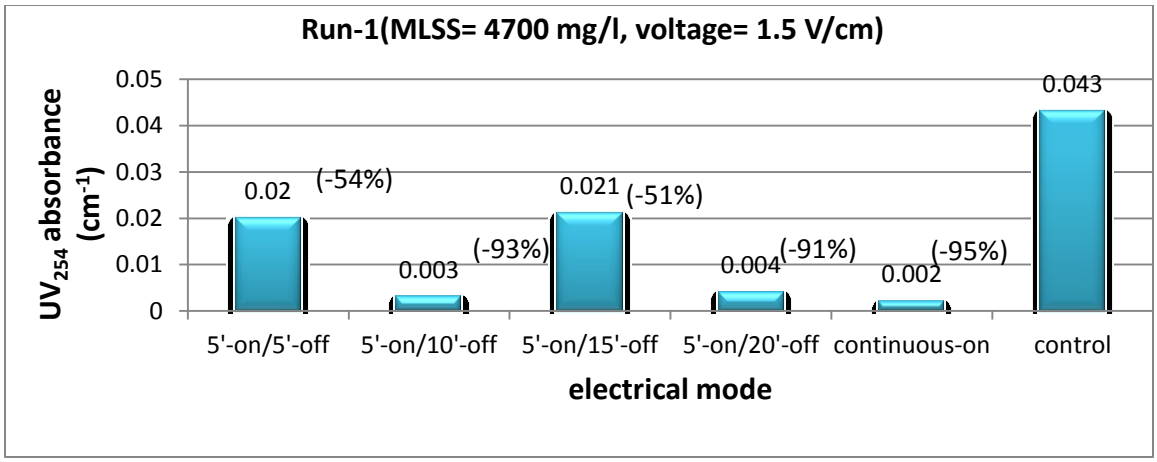

Figure 5.26: Run 1: Changes of humic substances concentration measured as the absorbance at UV_{254} at current density ranged between 20 to 35 A/m^2 at the end of 72 h operating period. (-) = reduction

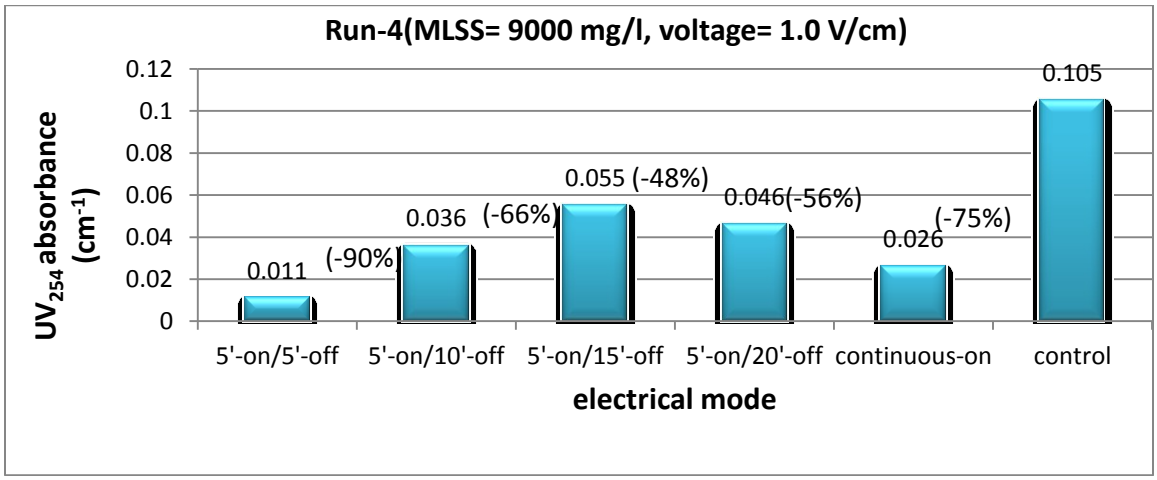

Figure 5.27: Run 4: Changes of humic substances concentration measured as the absorbance at UV254 at current density ranged between 15 to 25 A/m2 at the end of 100 h operating period. (-) = reduction

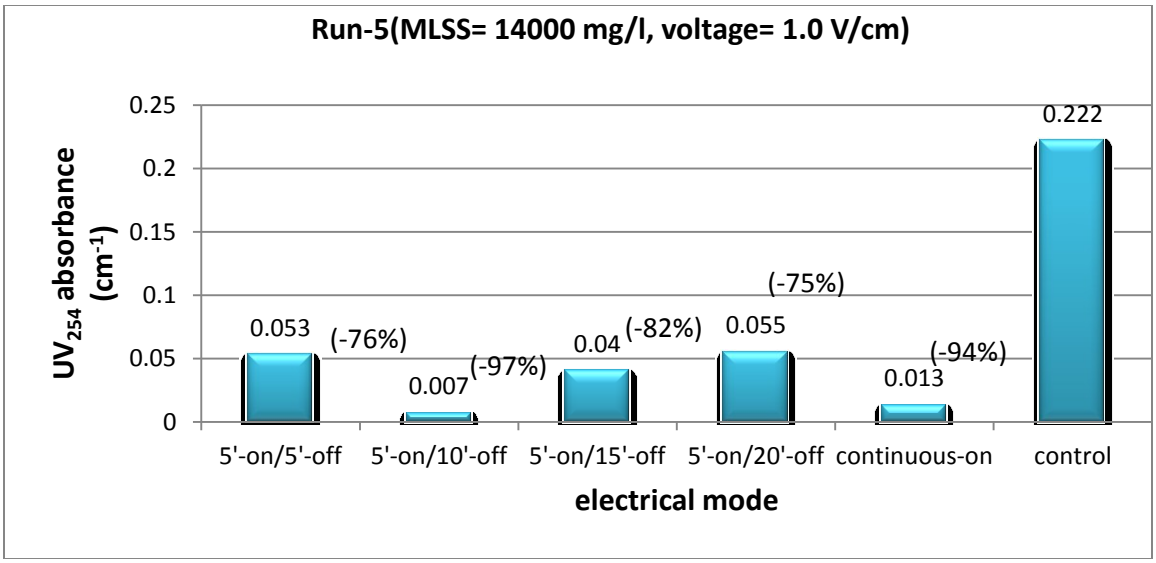

Figure 5.28: Run 5: Changes of humic substances concentration measured as the absorbance at UV_{254} at current density ranged between 25 to 35 A/m^2 at the end of 90 h operating period. (-) = reduction

5.6 Relationship between current density and zeta potential

The magnitude of zeta potential determines the capability of microbial flocs to attach to each other. The closer the magnitude of zeta potential to zero either from the positive or the negative side, the less the repulsive forces between flocs and the higher the opportunity to form larger flocs. Applying a current field using aluminum anode is expected to cause coagulation between the flocs. Aluminum ions are able to neutralize the negative charge on the microbial floc surfaces and thereby reducing the repulsive forces between the flocs. The magnitude of zeta potential of the microbial flocs without applying any electrical field was ranging between -12 to -40 mV. In this study, it was found that there was no single value representing the whole pools of microbial flocs. Microbial flocs exist at different sizes ranging from a few micrometers up to more than 200 μm. this variability in the size of microbial flocs provided different concentrations

and distributions of the functional groups on the flocs surfaces leading to different values of zeta potentials within the same sludge liquor (Ibeid et al., 2010a and 2010b). Therefore, in order to measure the exact range of zeta potential values, all flocs sizes should be tracked when the sample is injected into the zeta meter. In this study, the determination of microbial flocs zeta potential based on tracking all pools of flocs was done only for a few runs, while the other runs were conducted based on giving one value for all microbial flocs, which is misleading for comparison purposes as it is difficult to know which pool was measured every time. Luckily, these runs represent different current densities and illustrated in Tables 5.1 to 5.3. Low current densities did not show any substantial changes in zeta potential, while current densities between 20 to 35 A/m^2 exhibited substantial changes for some pools of microbial flocs. Tables 5.2 and 5.3 show that the magnitude of zeta potential, for some microbial flocs, was reduced significantly under different electrical modes. Though, some flocs even had positive zeta potential. However, the mechanisms that caused such changes in zeta potentials under current densities between 20 to 35 A/m^2 is related to the amount of the Al^{+3} released from the anode. High production of aluminum ions leads to the neutralization of the negative charge on the solid surfaces until a positive zeta potential is reached.

Table 5.1: Changes of zeta potential (mV) after 90 h operating period at current density 8 to 12 A/m^2 and MLSS= 15000mg/l

Time (h)	5'-on/5'-off	5'-on/10'-off	5'-on/15'-off	5'-on/20'-off	Continuous-on	Control
90	-16 to -28	-11 to -30	-19 to -30	-15 to -30	-13 to -30	-12 to -27

Table 5.2: Changes of microbial flocs zeta potential (mV) over 80 operating period at current densities 25 to 35 A/m^2 and MLSS = 14000 mg/l

Time (h)	5'-on/5'-off	5'-on/10'-off	5'-on/15'-off	5'-on/20'-off	Continuous-on	Control
0	-13 to -40	-13 to -40	-13 to -40	-13 to -40	-13 to -40	-13 to -40
20	-8 to -35	-8 to -35	-6 to -35	-6 to -35	-5 to -35	-13 to -40
80	+3 to -14	+2 to -16	-6 to -30	-4 to -20	-16 to -49	-18 to -50

Table 5.3: Changes of microbial flocs zeta potential (mV) over 70 h operating period at current density 20 to 25 A/m^2 and MLSS= 3000 mg/l

Time (h)	5'-on/5'-off	5'-on/10'-off	5'-on/15'-off	5'-on/20'-off	Continuous-on	control
0	-12 to -32	-12 to -32	-12 to -32	-12 to -32	-12 to -32	-12 to -32
50	+30 to -30	-10 to -20	-10 to -22	-8 to -19	+20 to -20	-14 to -31
70	0 to +22	0 to +20	-14 to -6	-16 to -2	+5 to +35	-14 to -23

5.7 Relationship between current density and microbial floc size

The mean particle size distribution (PSD) of floc size changed over the operating period based on the current density. Low strength current densities of 5 to 12 A/m^2 showed a slight increase of flocs size; only at continuous-ON electrical mode at low MLSS (Figures 5.29 to 5.31). At the same time, current densities between 15 to 35 A/m^2 showed a substantial increase of flocs size for all electrical modes and MLSS concentrations, but with different percentages (Figures 5.32 to 5.34). For example, At MLSS= 4700 mg/l and current density of 20 to 35 A/m^2, the mean PSD increased from 49 up to 72 μm(45%) at 5'-ON/5'-OFF, 74 μm(49%) at 5'-ON/10'-OFF, 64 μm (31%) at 5'-ON/15-'OFF, 59 μm (20%) and 58 μm (18%) at continuous-ON , respectively. Higher current densities of 40 to 60 A/m^2 exhibited significant increase of microbial floc size at MLSS of 8000 mg/l as depicted in Figure 5.35. The flocculation of smaller flocs into larger ones is mainly due to

the reducing of the repulsive forces between the flocs by changing the magnitude of zeta potential closer to zero. Generally, as the time went by, floc size decreased due to the removal of bound water from the microbial flocs electrical double layer by electroosmosis (Ibeid et al., 2010a and 2010b). This trend of increasing followed by decreasing of floc size was observed whenever the current density was strong enough to cause flocculation and extraction of bound water.

It should be noted here that the maximum PSD observed over the time in this experiment is not necessarily the maximum size peaked. Once the maximum floc size is reached as affected by current density and electrical mode, the removal of bound water through electroosmosis is likely to cause continuous reduction of flocs size. Since sampling for PSD measurements was taken once or twice per day, it is very unlikely to know the maximum size reached. Furthermore, electrical modes with less time-off showed faster increase of flocs size, which makes studying this relationship more difficult. However, knowing that direct current field is able to cause flocculation and extraction of the tightly bound water from the microbial flocs is extremely beneficial as these changes play crucial role in determining sludge filterability as will be indicated in the next section.

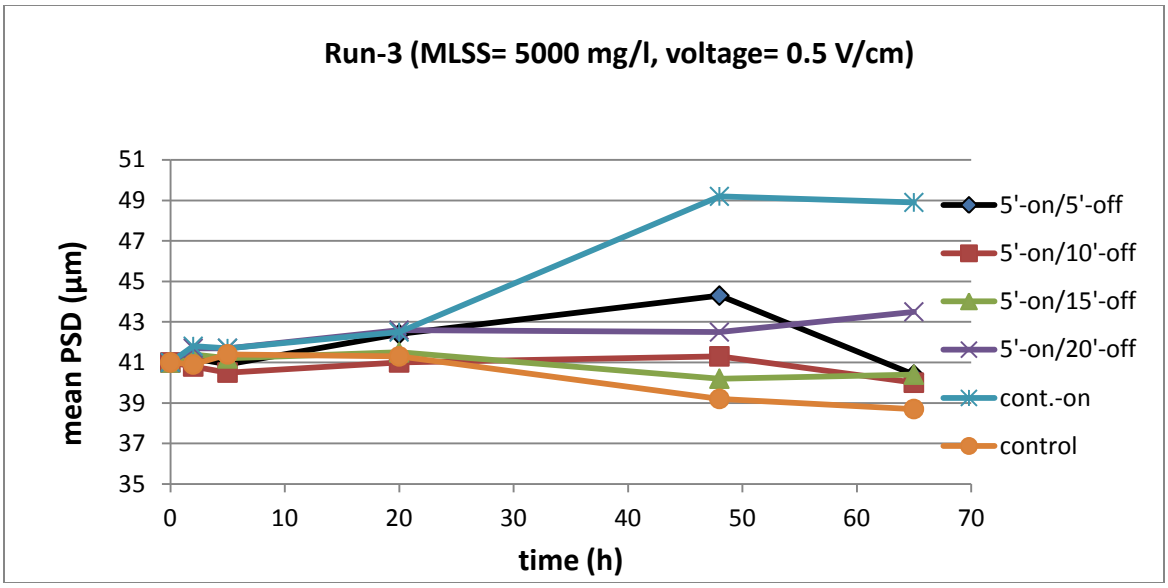

Figure 5.29: Run 3: Changes of microbial flocs mean particle size distribution (PSD) at current density ranged between 5 to 10 A/m^2 over 65 h operating period.

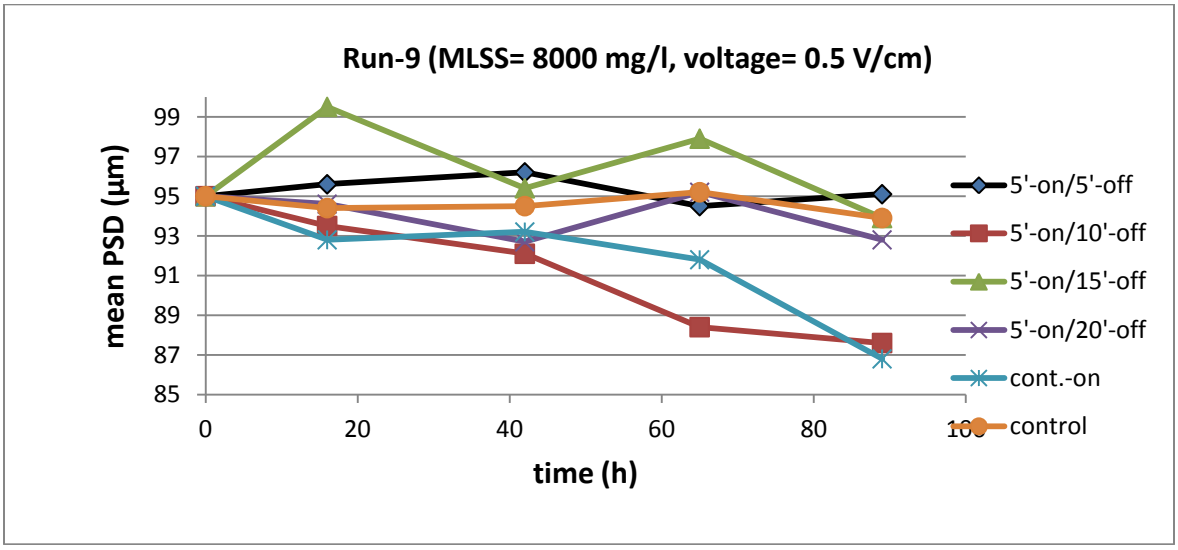

Figure 5.30: Run 9: Changes of microbial flocs mean particle size distribution (PSD) at current density ranged between 8 to 10 A/m^2 over 109 h operating period.

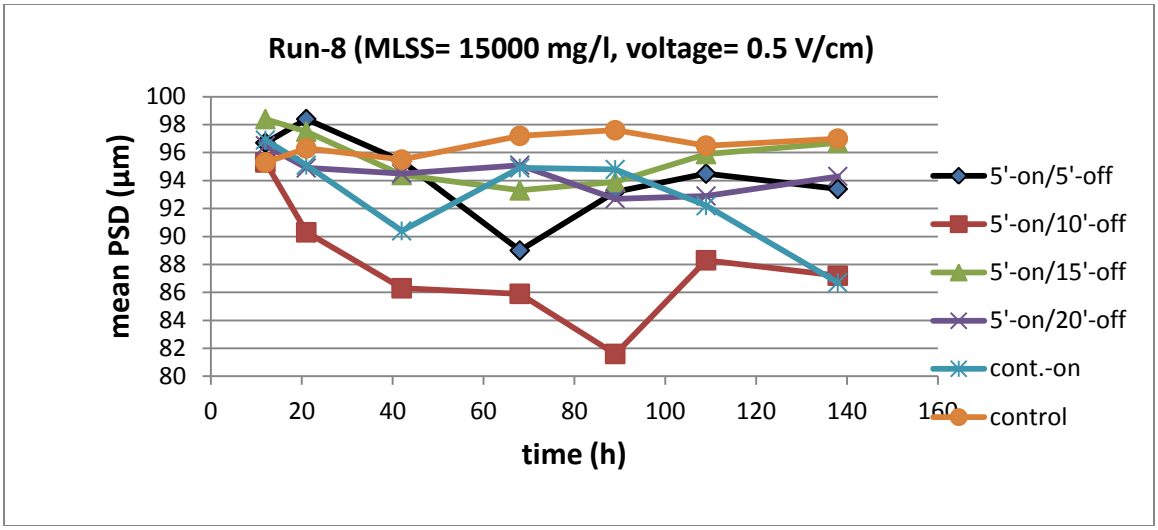

Figure 5.31: Run 8: Changes of microbial flocs mean particle size distribution (PSD) at current density ranged between 8 to 12 A/m^2 over 90 h operating period.

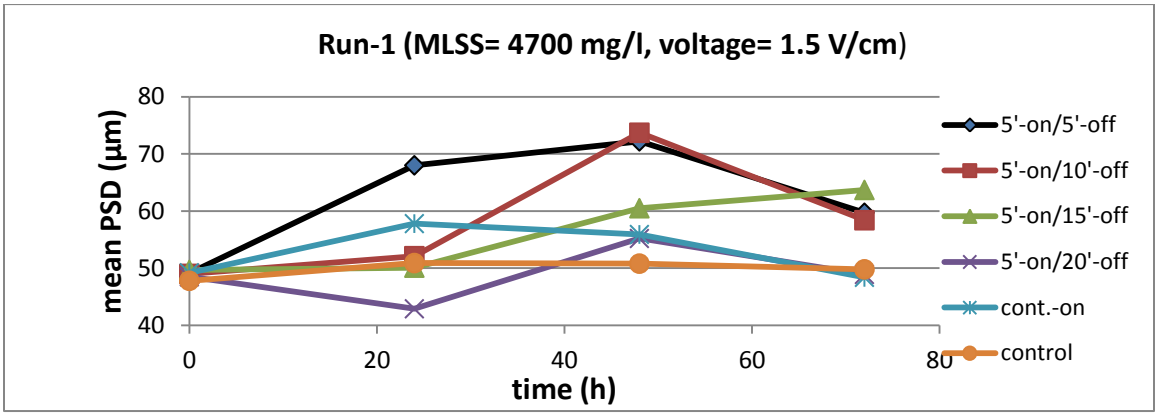

Figure 5.32: Run 1: Changes of microbial flocs mean particle size distribution (PSD) at current density ranged between 20 to 35 A/m^2 over 72 h operating period.

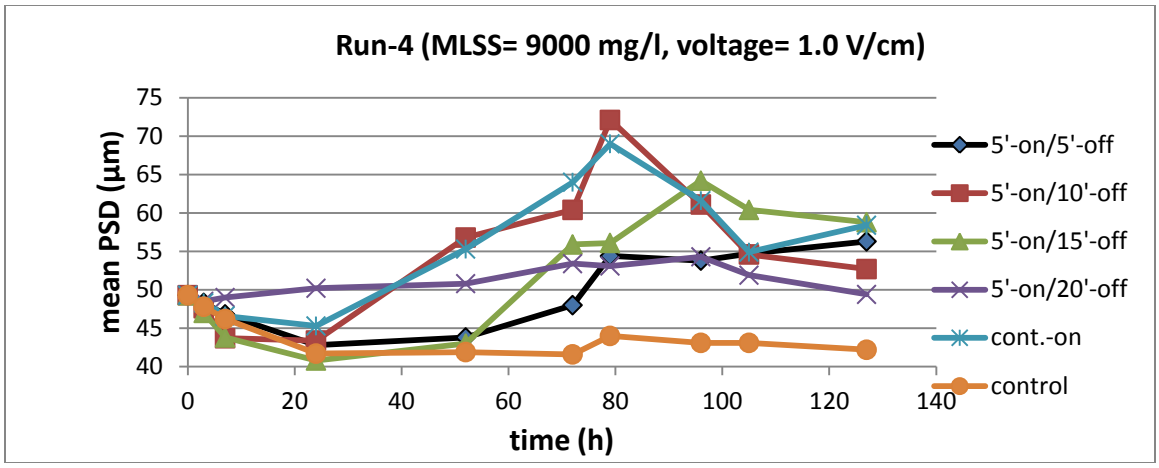

Figure 5.33: Run 4: Changes of microbial flocs mean particle size distribution (PSD) at current density ranged between 15 to 25 A/m^2 over 100 h operating period.

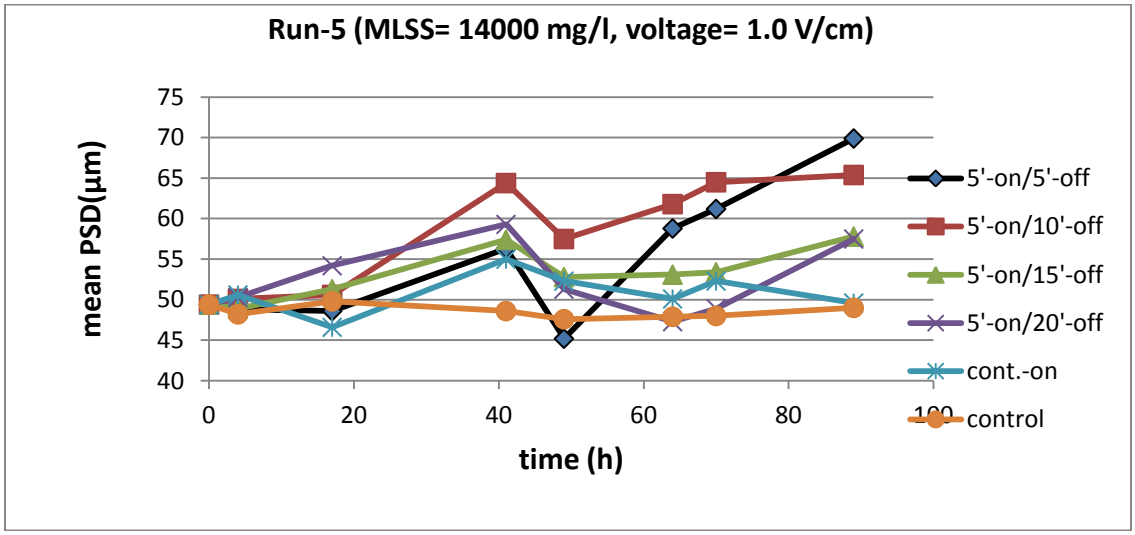

Figure 5.34: Run 5: Changes of microbial flocs mean particle size distribution (PSD) at current density ranged between 20 to 35 A/m^2 over 90 h operating period.

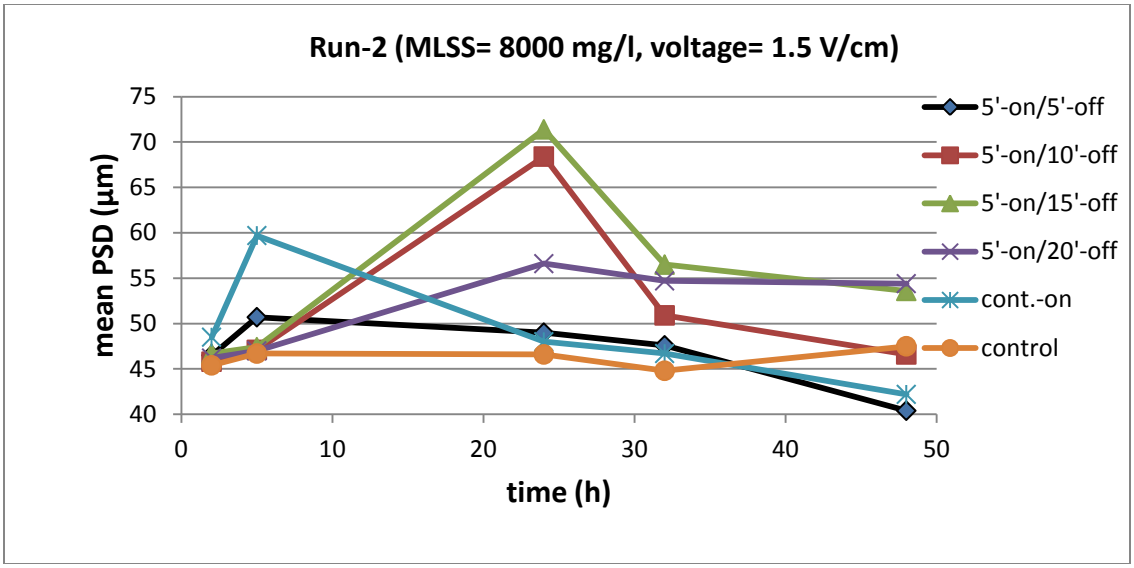

Figure 5.35: Run 2: Changes of microbial flocs mean particle size distribution (PSD) at current density ranged between 40 to 60 A/m^2 over 48 h operating period.

5.8 Relationship between current density and sludge dewaterability

Sludge dewaterability represents either the rate of filtration or the percentage of bound water content of the sludge after dewatering (Jin et al., 2004). Sludge dewatering is considered as one of the most difficult and costly processes in treatment plants. Sludge bound water is divided into four different pools: bulk water, interstitial water, vicinal water and chemically bound water. Chemically bound water is strongly attached within the floc by chemical bonds and could only be removed at 105^{o} C (Smollen, 1990; Vesilind and Martel, 1990). Bulk water represents the part of water surrounds the flocs, interstitial water represents the part held by capillary forces. These two pools are deemed loosely bound water that can be easily removed by physical means such as vacuum filtration, belt filter presses, drying beds or centrifugation. On the other hand,

vicinal water (tightly bound water) represents the part that is adsorbed or absorbed within the electrical double layer of the organic surfaces inside the microbial flocs (mainly EPS). Christensen and Characklis (1990) described EPS as a hydrated matrix with 98% water content. The conductance of charge through the electrical double layer transfers the momentum to water molecules to move towards the electrodes (electroosmosis). Since the sludge liquor pH used in this experiment is slightly alkaline, the solid surfaces are negatively charged and the electrical double layer is filled with cations. Under direct current field, these cations have the tendency to move towards the cathode, simultaneously, giving the momentum to the bound water molecules to move towards the cathode.

In this study it was found that minimum current density is required to provide the driving forces for the bound water to move out of the double layer. Current densities between 15 to 35 A/m^2 were found to cause a substantial removal of the bound water and thus increasing sludge dewaterability by decreasing the specific resistance to filtration (SRF) as depicted in Figures 5.36 to 5.39. A ssubstantial reduction of SRF ranging from a few times up to more than 200 times for almost all MLSS and all electrical exposure modes was observed when the current density ranged between 15 to 35 A/m^2. High MLSS, continuous-ON and 5'-ON/5'-OFF exposure modes showed an increase of SRF due to its negative effect on cells viability and the release of soluble microbial products (SMP) into the sludge liquor. Therefore, continuous-ON mode and 5'-ON/5'-OFF are not recommended operating conditions for MLSS less than 3000 mg/l or MLSS higher than 15000 mg/l.

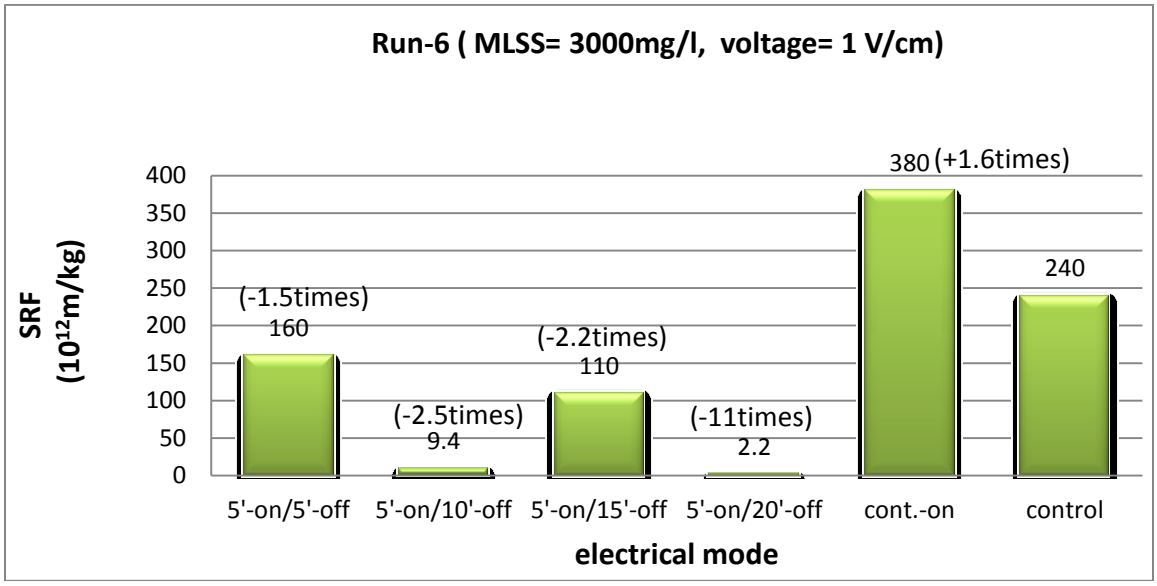

Figure 5.36: Run 6: Changes of sludge specific resistance to filtration (SRF) at the end of 70 h operating period at current densities ranged between 20 to 25 A/m^2. (-) reduction, (+) increase

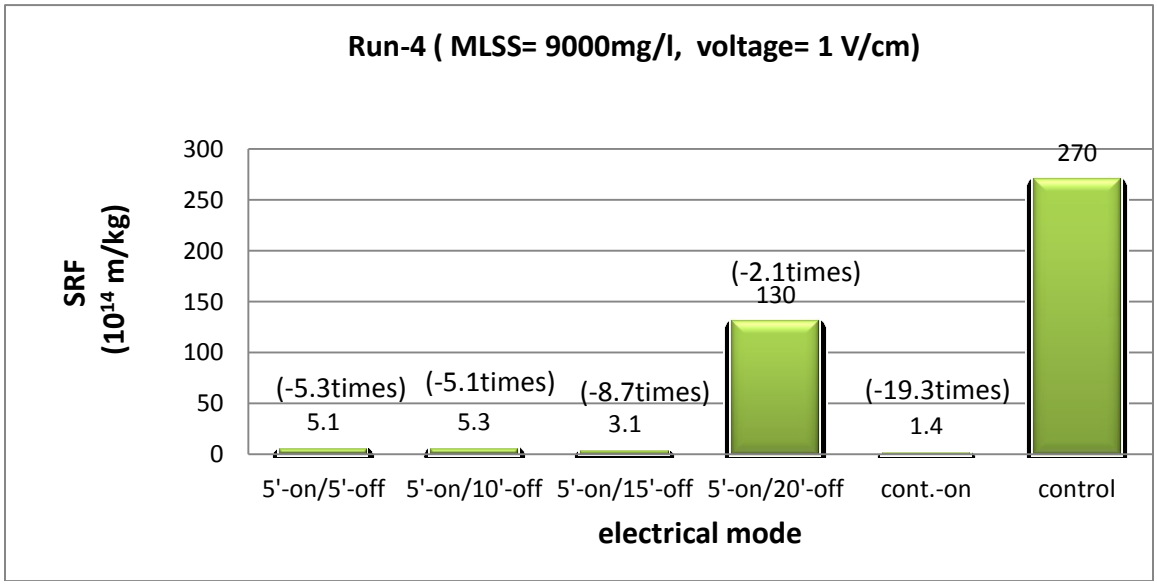

Figure 5.37: Run 4: Changes of sludge specific resistance to filtration (SRF) at the end of 100 h operating period at current densities ranged between 15 to 25 A/m^2.

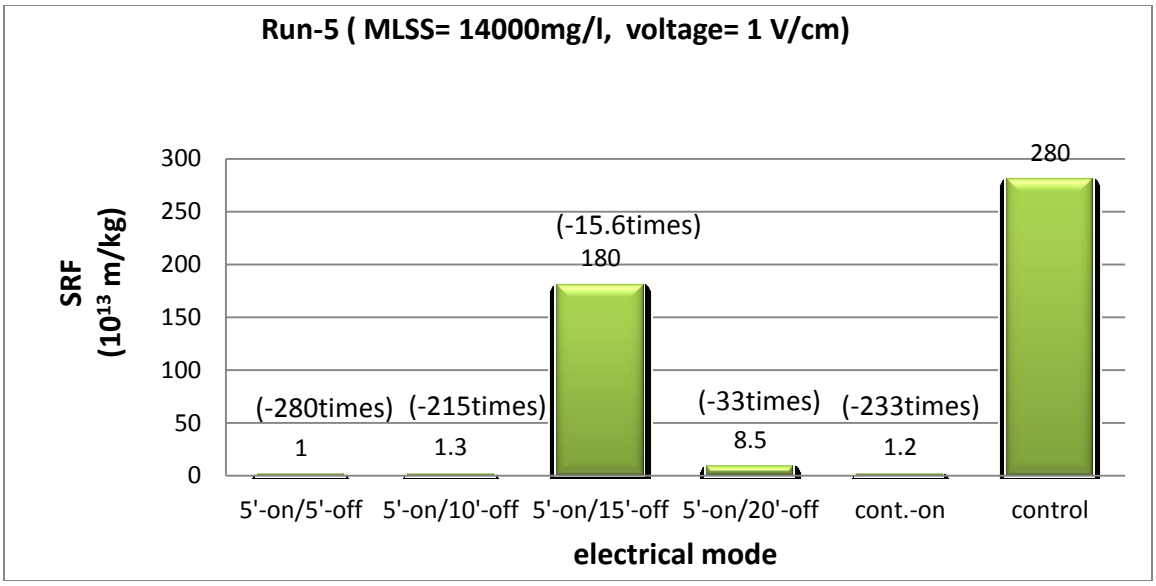

Figure 5.38: Run 5: Changes of sludge specific resistance to filtration (SRF) at the end of 90 h operating period at current densities ranged between 25 to 35 A/m^2.

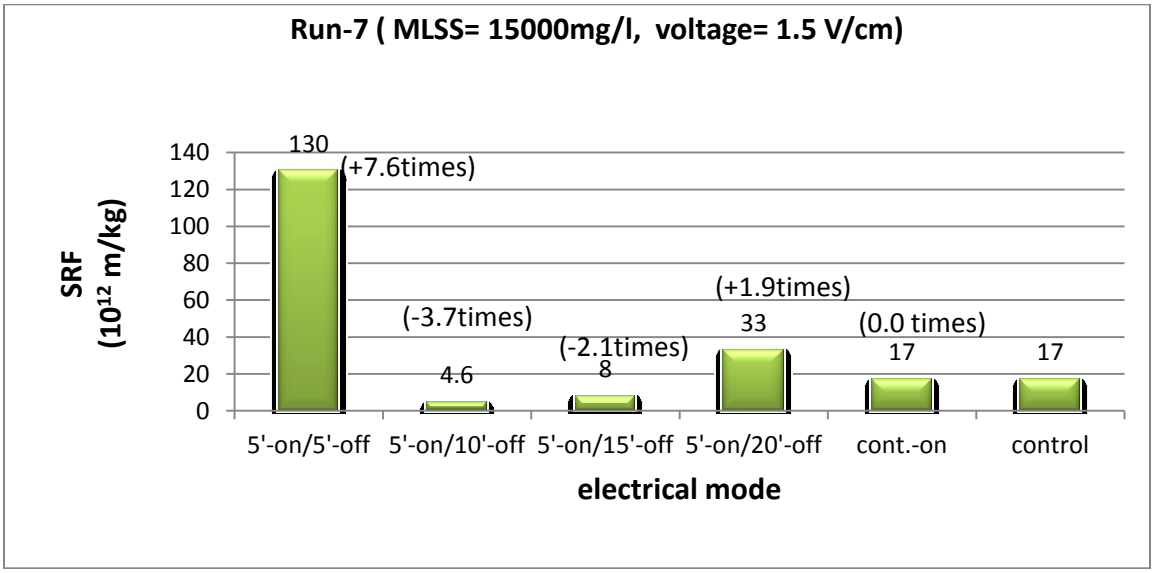

Figure 5.39: Run 7: Changes of sludge specific resistance to filtration (SRF) at the end of 96 h operating period at current densities ranged between 25 to 35 A/m^2.

On the other hand, a current density lower than 12 A/m^2 was found to be insufficient to cause the extraction of bound water except for the 5'-ON/5'-OFF electrical mode at MLSS of 15000 mg/l and for the continuous-ON mode at MLSS of 8000 mg/l (Figures

5.40a and 5.41a). Surprisingly, the other electrical modes caused significant increases of SRF at that low CD. The exact justification of that increase is unclear. Theoretically, low CD is likely to attract and deposit the dication on the cathode leaving more mono-valent cation in the bulk solution. This step is followed by the diffusion of dications within the electrical double layer into the bulk solution due to the changes in the concentration gradient. Afterward, the mono-valent cations replace some of the displaced dications in the electrical double layer and force it to expand and hold more bound water. When the current density was increased up to 25 A/m^2 at the end of that operating period at low current density, the SRF was substantially increased for all exposure modes except for 5'-ON/5'-OFF at MLSS of 15000 mg/l (Figures 5.40b and 5.41b). This mode and intensity is above the tolerance limit of microorganisms that caused the increased SRF because of the release of SMP. These changes of SRF are consistent with the results obtained at similar current density in the other runs. The electroosmosis process was clearly obvious through the reduction of the microbial size over the operating period as shown in the previous section. Current densities between 40 to 60 A/m^2 caused a reduction of flocs size up to 32%, while the maximum reduction of flocs size obtained at current density lower than 12 A/m^2 is 9% at 5'-ON/5'-OFF electrical mode. At current densities between 15 to 35 A/m^2, the reduction percentage was less than 32%, but higher than 9%.

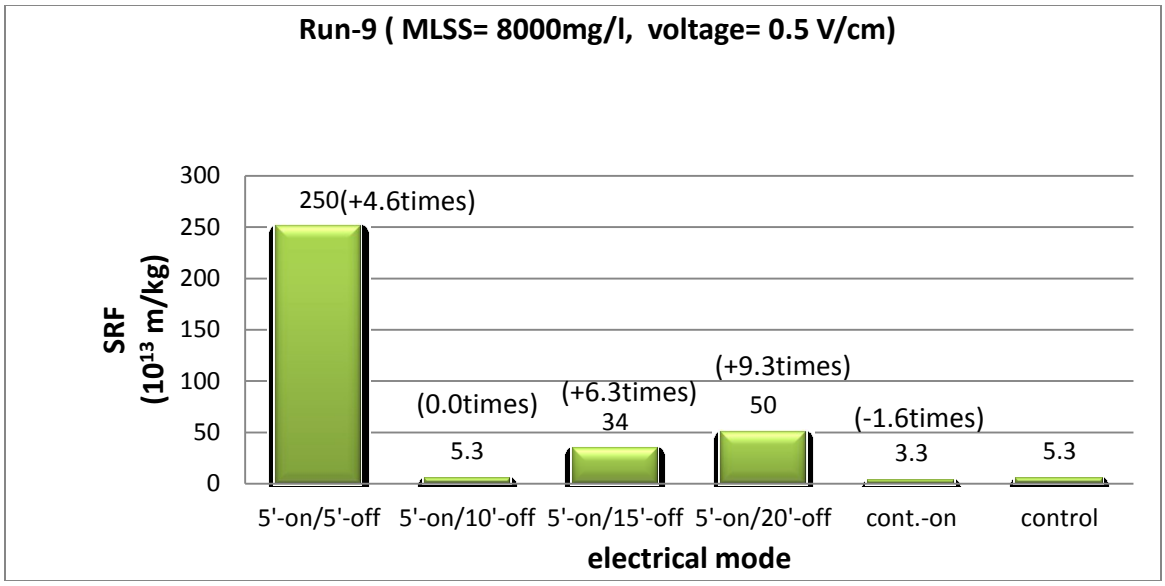

Figure 5.40a: Run 9: Changes of sludge specific resistance to filtration (SRF) at the end of 109 h operating period at current densities ranged between 8 to 12 A/m^2.

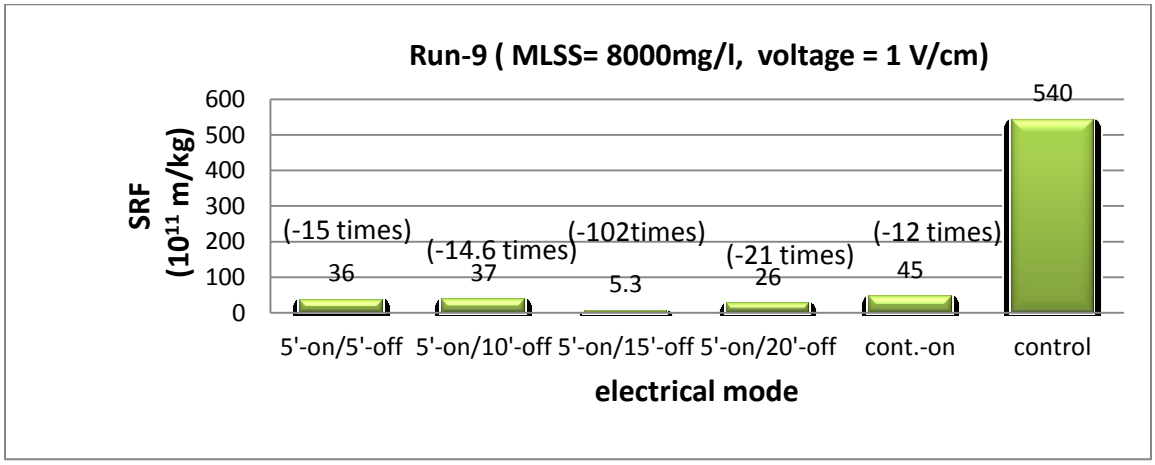

Figure 5.40b: Run 9: Changes of sludge specific resistance to filtration (SRF) after raising the current density from (8 to 12 A/m^2) to 25 A/m^2 by increasing the voltage at the end of the 109 h for an extra 36 h operating period.

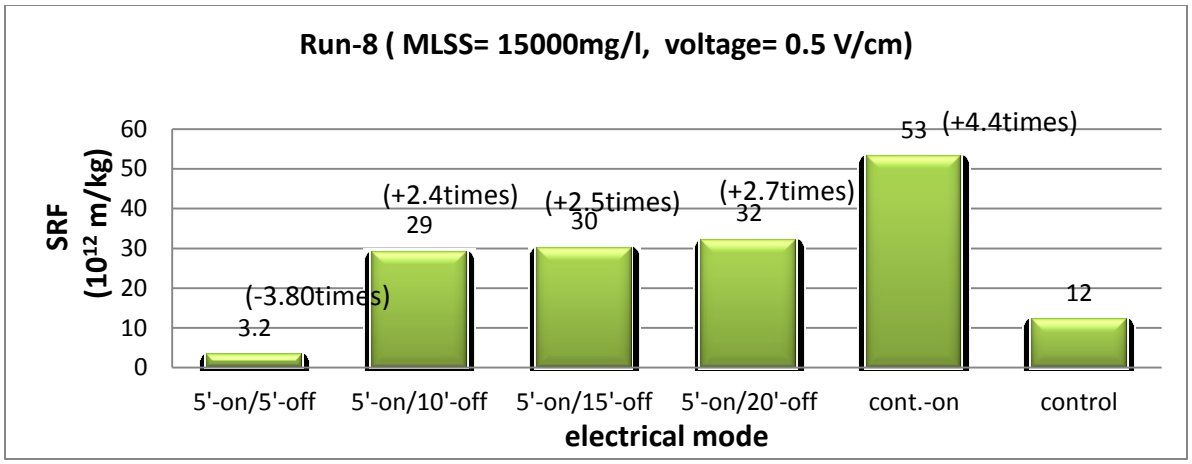

Figure 5.41a: Run 8: Changes of sludge specific resistance to filtration (SRF) at the end of 90 h operating period at current densities ranged between 8 to 12 A/m2.

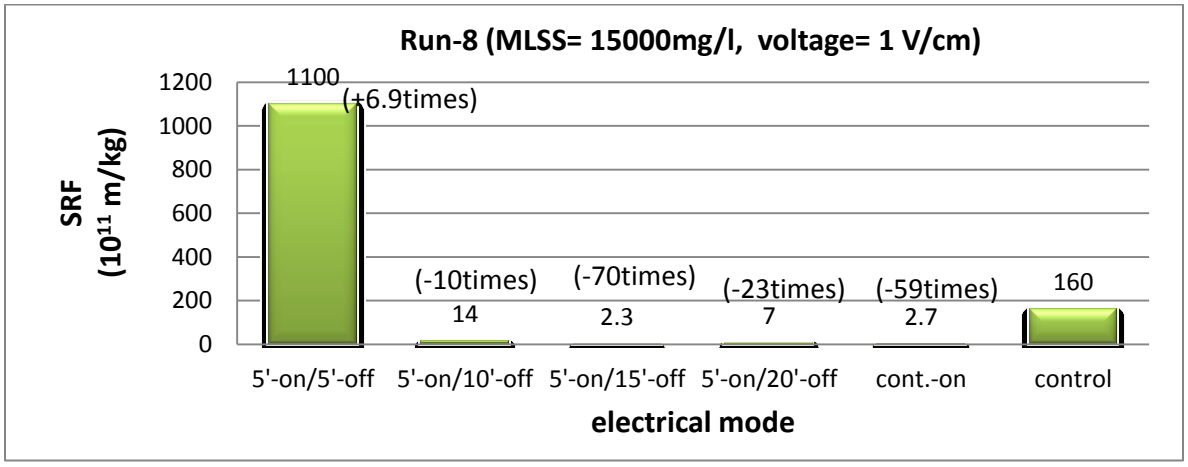

Figure 5.41b: Run 8: Changes of sludge specific resistance to filtration (SRF) after raising the current density from (8 to 12) to 25 A/m^2 at the end of 90 h for an extra 40 h operating period by increasing the voltage.

5.9 Phase 1 (Stage 1): Summary and conclusions

This stage has demonstrated the changes that might happen to the sludge properties as a result of applying direct current field. However, these changes are dependent on the current density, electrical mode, and the MLSS. Some properties were improved, others did not. The results are summarized in Table 5.4. Continuous-ON electrical mode showed regular severe drops in the current density, particularly at high current density

and high MLSS. Furthermore, continuous-ON mode did not show any better changes than the other electrical modes, which means it is possible to reach the same level of sludge polishing at lower energy costs. In addition to that, current densities below 12 A/m^2 are not capable of extracting the tightly bound water except for the continuous – ON and 5'-ON/5'-OFF at MLSS= 15000 mg/l and continuous-ON at MLSS of 8000 mg/l. Thus, working under these modes is very risky since any changes of MLSS would cause negative effects. In addition to that the, the removal of SMP and organic colloids was not as good as it was at higher current densities. Therefore, selecting a current density below 12 A/m^2 as an electrical operating parameter is not recommended. On the other hand, current densities between 15 to 35 A/m^2 were found to cause the targeted changes of sludge properties as long as the electrical exposure mode is selected properly based on the MLSS concentration. For example, at MLSS higher than 3000 and lower than 10000 mg/l, it has been found that 5'-ON/10'-OFF and 5'-ON/15'-OFF electrical modes have reduced the organic colloids, SMP, SRF and humic substances substantially. Likewise, at high MLSS around 15000 mg/l, 5'-ON/15'-OFF and 5'-ON/20'-OFF were found to improve sludge properties at the highest level. These improvements are expected to reduce the membrane reversible and irreversible fouling, enhance the effluent quality and sludge dewaterability. Thus, these electrical modes and current densities will be carried forward for the next phases of the experiment as promising operating conditions.

Table 5.4: Changes of sludge properties under different current densities, electrical exposure modes and MLSS, (-ve = removal %, +ve = increasing %)

Operating conditions	Sludge properties	Electrical modes				
		5'-on/5'-off	5'-on/10'-off	5'-on/15'-off	5'-on/20'-off	Continuous-on
Run-1 4700 (mg/l) 20 to 35 (A/m^2)	Org.Colloids	*	*	*	*	*
	Protein	-33%	-31%	+42%	-23%	-44%
	Polysacch.	-69%	-68%	-59%	-65%	-65%
	SRF	*	*	*	*	*
	HS	-54%	-93%	-51%	-91%	-95%
Run-6 3000 (mg/l) 20 to 25 (A/m^2)	Colloids	-100%	0%	+125%	+350%	-100%
	Protein	-53%	-43%	-77%	-79%	-83%
	Polysacch.	-50%	-30%	-25%	-40%	-60%
	SRF	-150%	-250%	-220%	-1100%	+160%
	HS	-57%	0%	-30%	-97%	+13%
Run-4 9000 (mg/l) 15 to 25 (A/m^2)	Colloids	-100%	-98%	-94%	-20%	-100%
	Protein	-52%	-32%	-15%	-19%	-32%
	Polysacch.	-65%	-51%	-68%	-65%	-40%
	SRF	-530%	-510%	-870%	-210%	-1930%
	HS	-90%	-66%	-48%	-56%	-75%
Run-5 14000 (mg/l) 25 to 35 (A/m^2)	Colloids	-93%	-100%	-100%	-100%	-100%
	Protein	-34%	-37%	-31%	-19%	-46%
	Polysacch.	+18%	+186%	-18%	-7%	+249%
	SRF	-28000%	-21500%	-1560%	-3290%	-23300%
	HS	-76%	-97%	-82%	-75%	-94%
Run-7 15000 (mg/l) 25 to 35 (A/m^2)	Colloids	+1050%	+50%	+160%	+270%	+117%
	Protein	+36%	+5%	-16%	+50%	+25%
	Polysacch.	+27%	-62%	-68%	-54%	+30%
	SRF	+760%	-370%	-210%	+190%	0%
	HS	*	*	*	*	*
Run-9 8000 (mg/l) 8 to 12 (A/m^2)	Colloids	-45%	-64%	-45%	+9%	-93%
	Protein	-23%	-23%	-27%	-10%	-65%
	Polysacch.	-15%	+25%	+50%	+110%	+35%
	SRF	+460%	0%	+630%	+930%	-160%
	HS	+76%	0%	+23%	+66%	-20%
Run-8 15000 (mg/l) 8 to 12 (A/m^2)	Colloids	-75%	-77%	-46%	-81%	-69%
	Protein	-42%	+20%	-14%	-12%	-48%
	Polysacch.	-39%	-39%	+23%	-22%	-23%
	SRF	-380%	+240%	+250%	+270%	+440%
	HS	-70%	-87%	0%	-67%	-28%

Chapter 6

Phase 1 (Stage 2): Results and discussion

The results of Stage 2, in general, were consistent with the main findings of Stage 1. However, the findings of this stage complement the part that was not conducted in Stage 1.

6.1 Relationship between current density and the SMP removal over time

At MLSS=6000 mg/l and current density=25 A/m^2, all electrical modes showed substantial reduction of protein and polysaccharides after 48 h of operation, except for the continuous-ON electrical mode (Figures 6.1 and 6.2). Microorganisms were unable to tolerate continuous exposure to a direct current field of 25 A/m^2; microbial dying off caused the release of SMP. During the first 10 h of operation, no significant reduction of SMP was observed for all electrical modes. Afterward, the removal efficiency increased linearly up to 50 to 60 % for protein and up to 80% for polysaccharides at the end of 48 h operating period. However, electrical modes with shorter time-OFF showed higher and faster removal efficiency.

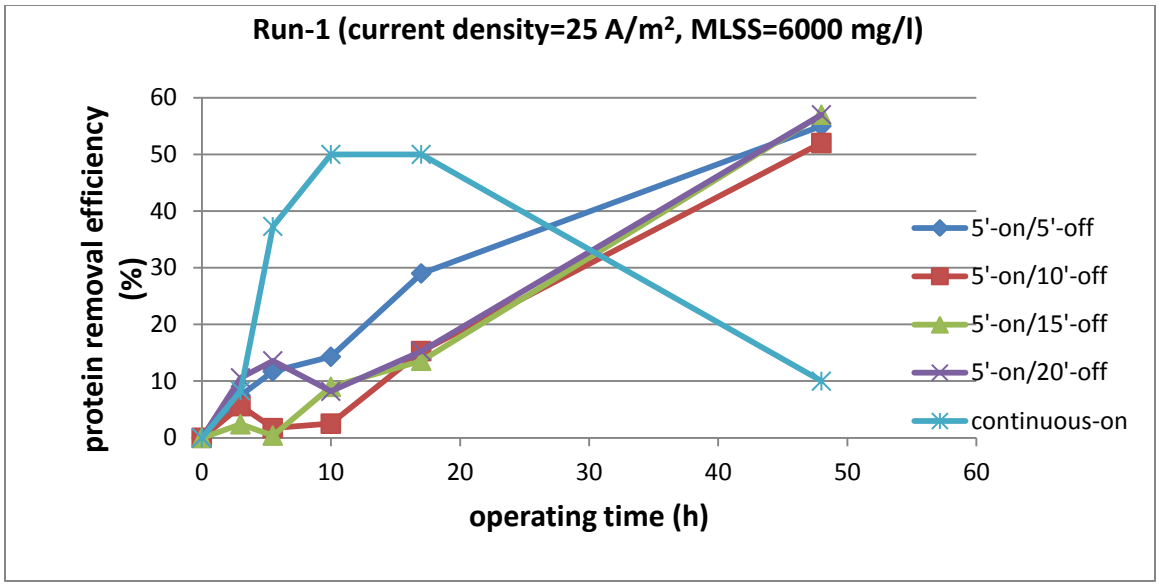

Figure 6.1: Run 1: Protein removal efficiency over 48 h operating period

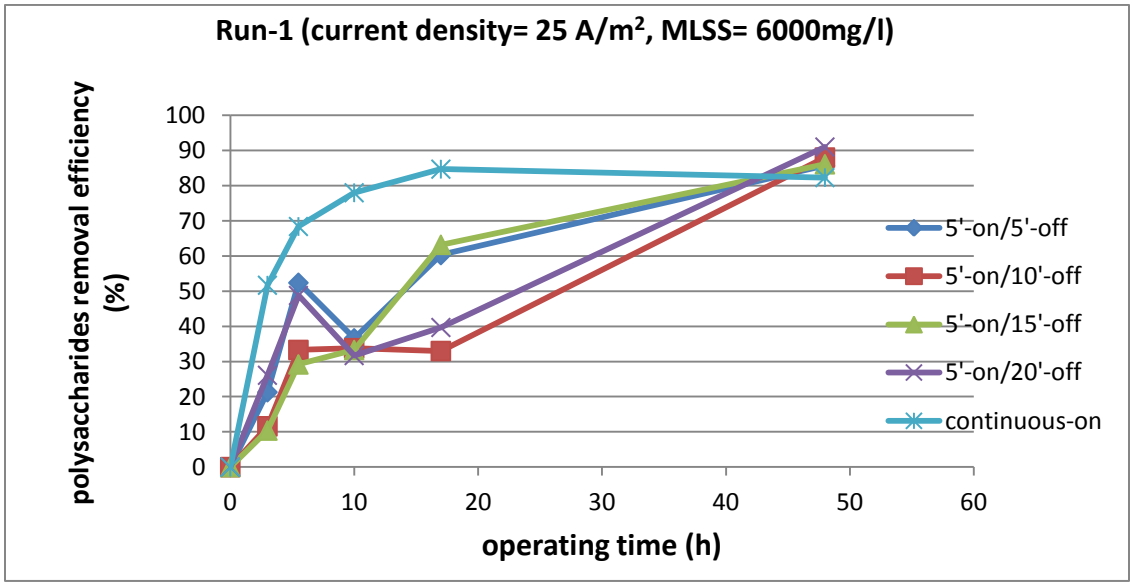

Figure 6.2: Run 1: Polysaccharides removal efficiency over 48 h operating period

On the other hand, for MLSS of 6000 mg/l and 50 A/m^2, the removal efficiency started to increase after 5 h of operation for almost all electrical modes (Figures 6.3 and 6.4) due to the fast dissolution of Al^{+3}. This removal efficiency did not last for a long time as

it declined after 20 h of operation, except for 5'-ON/20'-OFF electrical mode that maintained the maximum level of removal efficiency to the end. Though, more time might be needed for that mode to eventually reach a turning point at which SMP removal efficiency decreases. These findings indicate that 50 A/m^2 is too strong to be considered as an electrical operating parameter due to its direct harm on microrganisms.

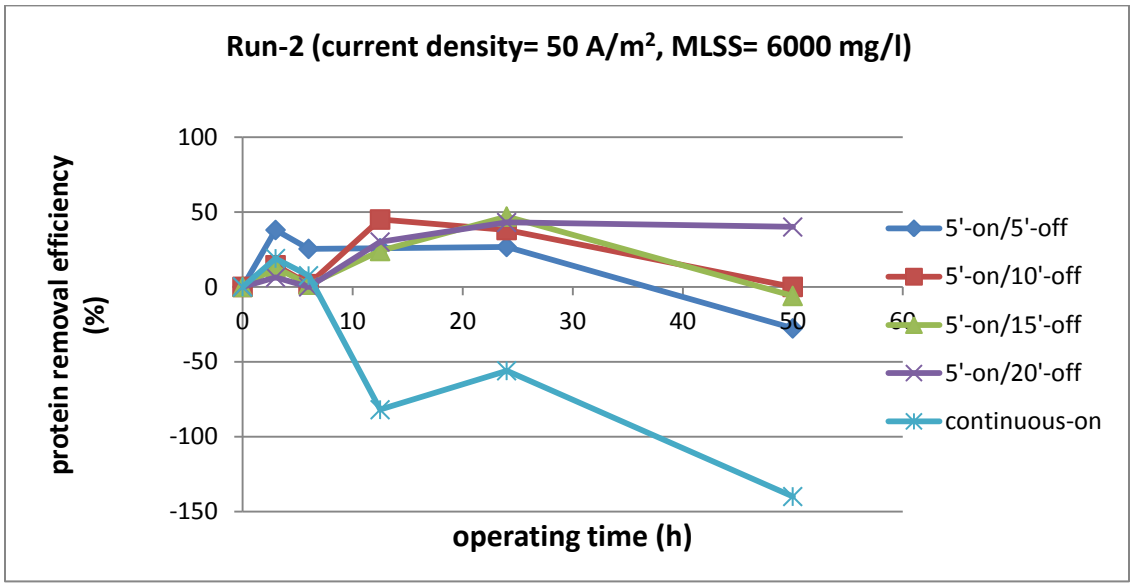

Figure 6.3: Run 2: Protein removal efficiency over 48 h operating period

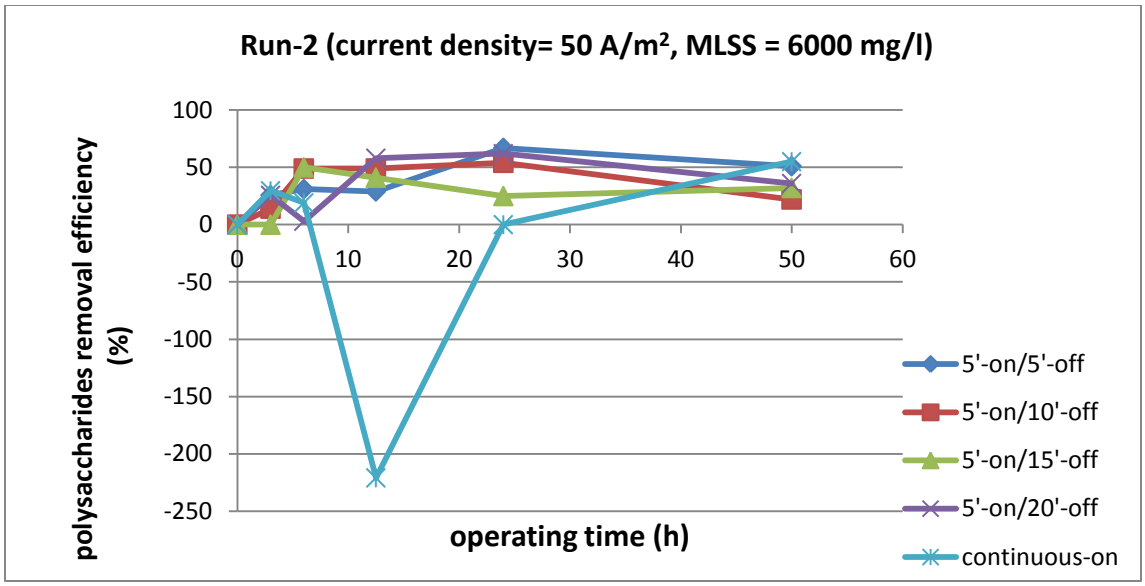

Figure 6.4: Run 2: Polysaccharides removal efficiency over 48 h operating period

At MLSS= 15000 mg/l and current density= 25 A/m^2, the electrical modes 5'-ON/15'-OFF and 5'-ON/20'-OFF did not show any microbial die off or release of SMP (Figures 6.5 and 6.6). In contrast, the electrical modes continuous-ON, 5'-ON/5'-OFF and 5'-ON/10'-OFF showed an increase of SMP due to their capability to negatively affect the microbial viability. As the time went by, the concentration of SMP was decreased at these electrical modes due to the drop in current density to a value that is not harmful to the microorganisms. At MLSS= 15000 mg/l and 50 A/m^2, the system failed completely due to the fast accumulation of microbial flocs on the electrodes causing severe drop in the current density. Thus, maintaining a constant current density under such conditions is extremely difficult, which makes the results of this run meaningless and will not be presented here.

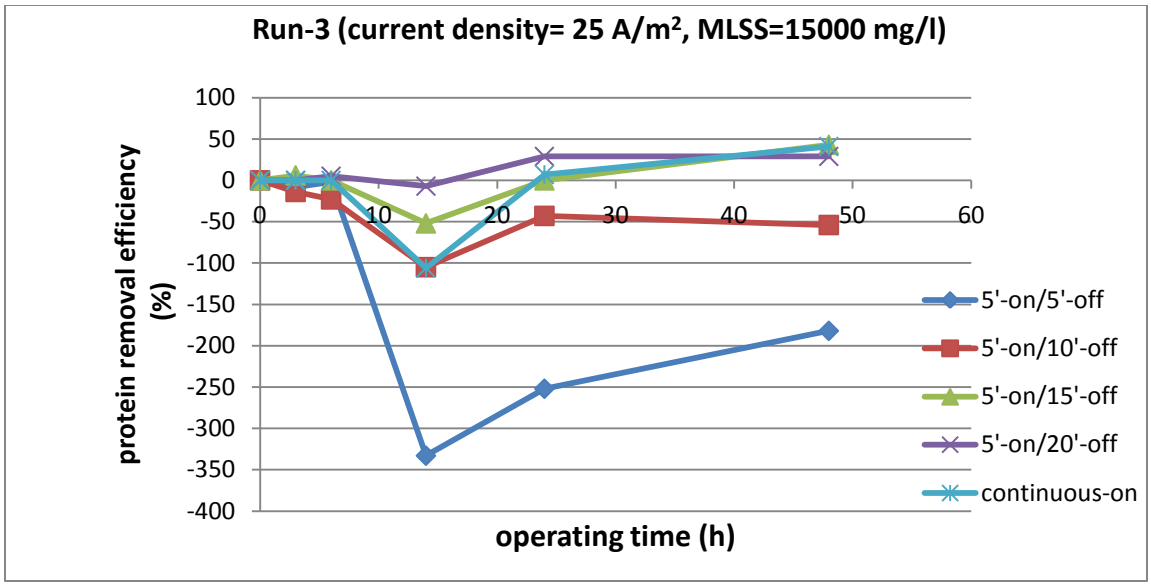

Figure 6.5: Run 3: Protein removal efficiency over 48 h operating period

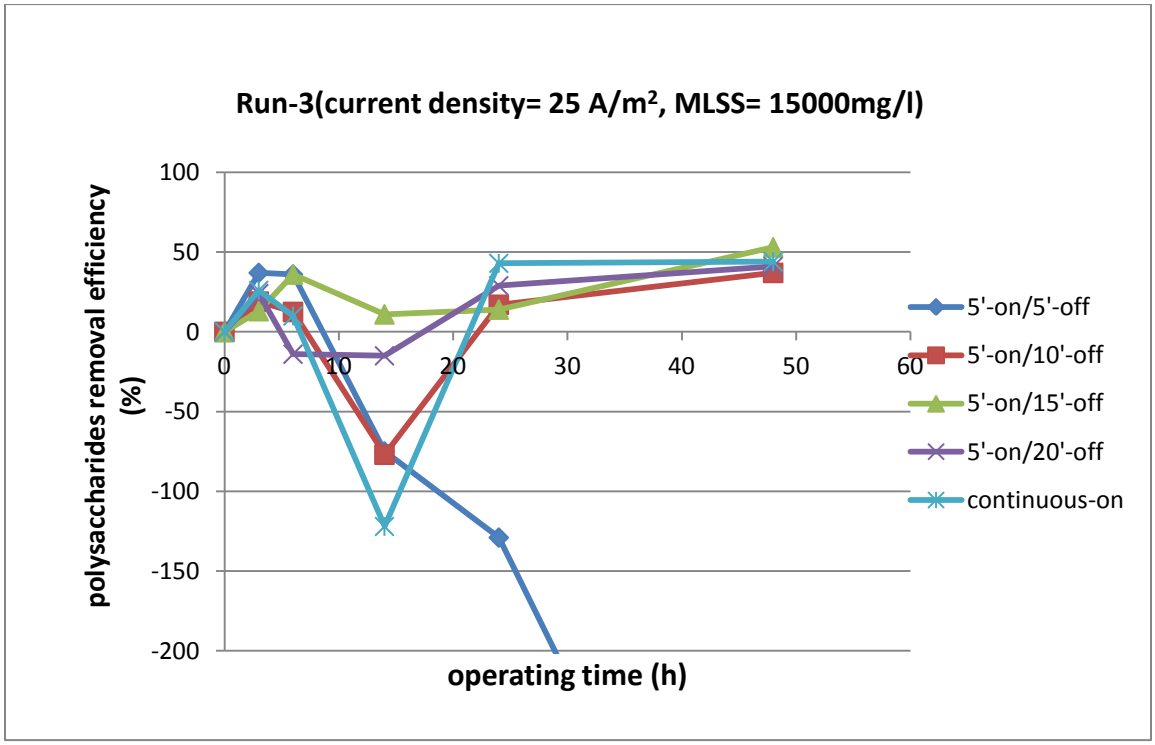

Figure 6.6: Run 3: polysaccharides removal efficiency over 48 h operating period

6.2 Relationship between current density and microbial activity

Surprisingly, the current density of 25 A/m^2 significantly increased microbial activity for all electrical modes at MLSS of 6000 mg/l (Figure 6.7). This increase of microbial activity at these conditions as represented by the OUR was the highest for the electrical mode with the shortest time-OFF. In fact, this increase of OUR in the electrical bioreactor is not because oxygen was consumed by the biomass, but due to the electrochemical reactions. In the electro-bioreactor, the electrons produced at the anode react with the available oxygen to form hydroxyl ions. The electrical mode with high magnitude of CD and short time-OFF produces more electrons leading to high OUR. This abiotic consumption of electrons interfere with the OUR test used to measure the microbial activity (biotic OUR). Thus, OUR method is not a good test to evaluate or measure the microbial activity in the electrical system due to the interference with the electrochemical reactions. However, this test could be still used to study the impact of DC field on biomass activity as will be discussed hereafter.

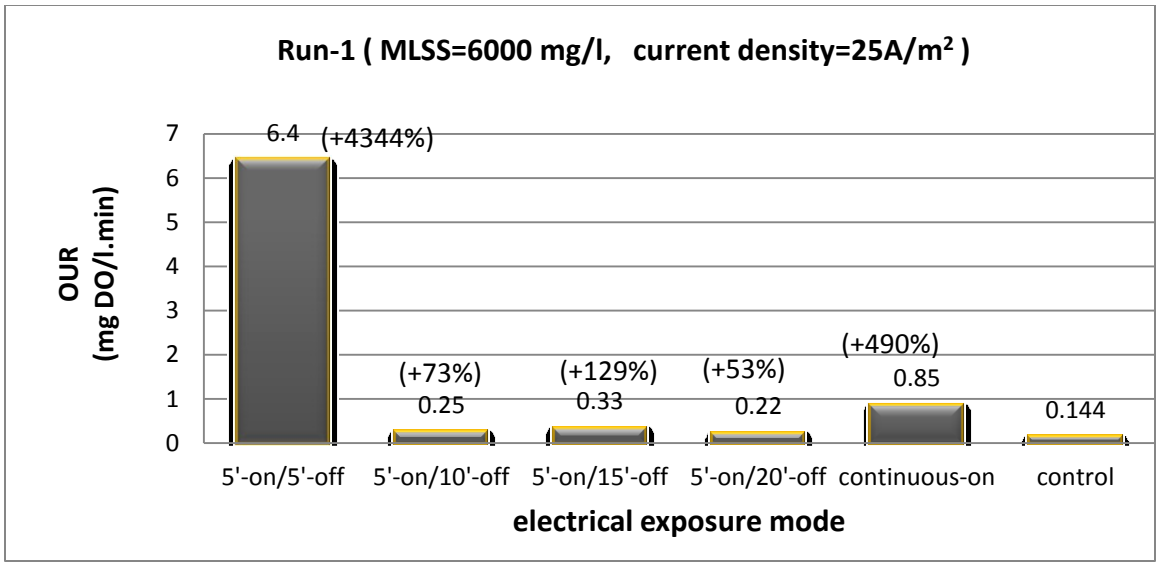

Figure 6.7: Run 1: Microbial activity measured as oxygen uptake rate (OUR) at the end of 48 h operating period

CD of 25 A/m^2 at MLSS = 15000 mg/l, exhibited lower OUR than the control reactor for continuous-ON and 5'-ON/5'-OFF modes (Figure 5.8). This reduction in OUR in these reactors means that the summation of biotic and abiotic consumption of oxygen at these electrical conditions is less than the control, which proves that these two modes have for sure reduced the microbial activity and should not be considered as operating conditions. The other electrical modes that showed higher OUR than the control indicate that the microorganisms are still active and performing very well. However, the degree to which the biotic OUR is affected by the CD is impossible to be evaluated in this test. Yet, the modes with longer time-OFF at CD=25 A/m^2 are the recommended operating conditions.

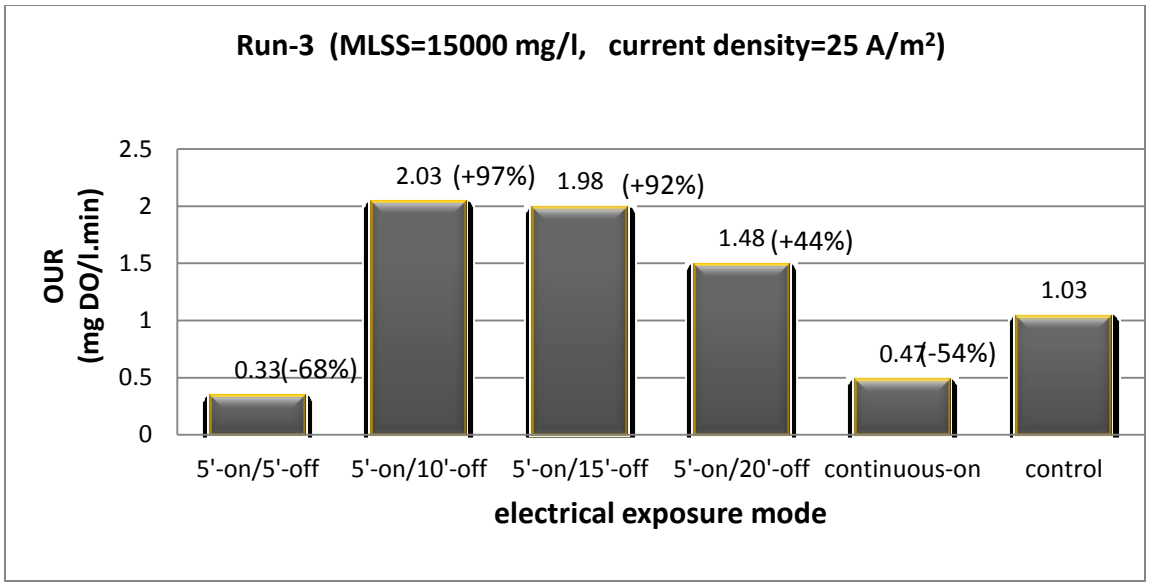

Figure 6.8: Run 3: Microbial activity measured as oxygen uptake rate (OUR) at the end of 48 h operating period

On the other hand, 50 A/m^2 showed a slight reduction of microbial activity for all electrical modes (Figure 6.9). This reduction of OUR was lower than the control reactor in spite of the contribution of abiotic consumption of oxygen in the electro-bioreactor, which indicates that the biotic OUR is much worse than the control reactor. As a conclusion, 50 A/m^2 is a strong CD that should be avoided in order to maintain high biomass activity. These results are also consistent with SMP removal efficiency since the concentration of protein and polysaccharides started to increase after 25 h of operation as the microbial activity declined and die off started to take place.

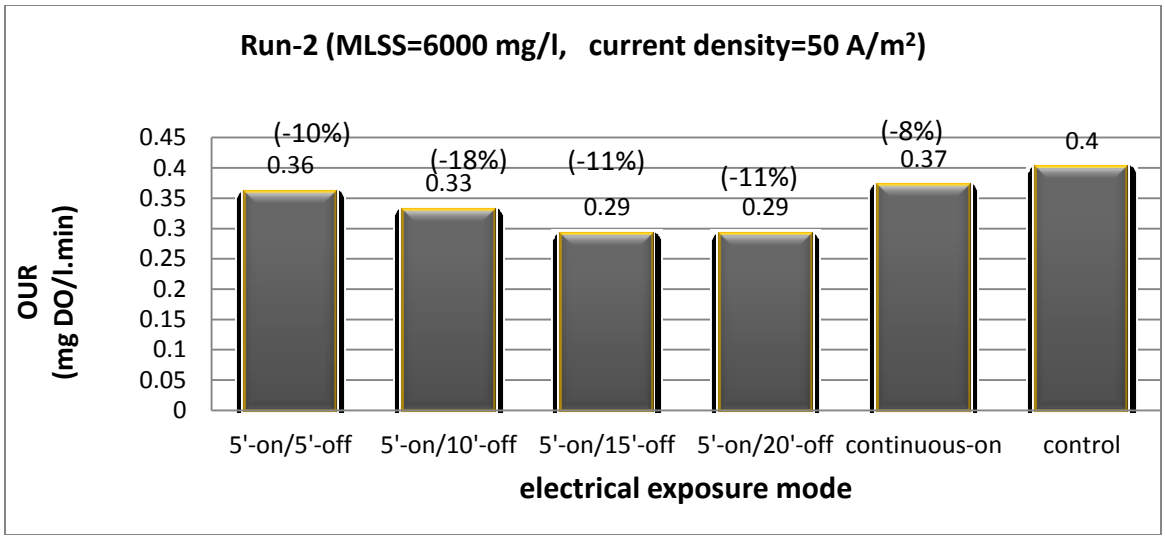

Figure 6.9: Run 2: Microbial activity measured as oxygen uptake rate (OUR) at the end of 48 h operating period

6.3 Phase 1 (Stage 2) Conclusions

The results of this stage indicate that 50 A/m^2 caused microbial dying off, while 25 A/m^2 is a promising current density as long as the electrical exposure mode is selected based on the MLSS concentration. 5'-ON/5'-OFF and 5'-ON/10'-OFF at MLSS- 6000 mg/l and 5'-ON/15'-OFF and 5'-ON/20'-OFF at MLSS= 15000 mg/l are likely to improve sludge properties and eventually reduce membrane fouling and enhance effluent quality of SMEBR. Meanwhile, maintain high microbial activity. Though, it is highly recommended to work at lowest CD with the longest time-OFF possible to preserve the microbial activity and lower the cost as long as it is achieving the targeted changes.

The changes the direct current field can achieve are not instantaneous, but need a minimum time span of operation before substantial changes could be observed. This time span is inversely proportional to the percentage of time-ON in the electrical cycle.

Based on the results of Stage 2,The electrical parameters of current density 15 to 20 A/m^2 and exposure modes 5'-ON/15'-OFF and 5'-ON/20'-OFF were selected as a promising operating conditions for Phase 2.

Chapter 7

Phase 2: Methodology - continuous flow

The main objective of Phase 2 was to examine the performance of the SMEBR under continuous flow in terms of nutrient removal, sludge properties and membrane fouling. The second objective was to evaluate the simultaneous removal of ammonium and nitrate in the SMEBR for a long period of time. The third objective was to confirm the reproducibility of the results under different operating conditions. The objectives of Phase 2 were completed in two stages (Figure 1).

7.1 Experiment setup

In both stages, one submerged membrane electro-bioreactor SMEBR and one submerged membrane bioreactor (MBR) without electrical field to serve as a control were operated simultaneously. They were operated at the same conditions to create perfect comparing conditions. SMEBR (Figure 7.2) outer body was composed of a cylindrical polyethylene container (20 l). The design is similar to a patented SMEBR system (Elektorowicz et al., 2009). In the middle of this reactor, a cylindrical ultrafiltration Zeeweed-1 (GE, Canada) membrane module with 0.04 μm pore size and 0.047 m^2 surface area was placed vertically. Two air diffusers were inserted on top and below the membrane to provide air intensity enough to hinder the accumulation of microbial flocs on the membrane surface. Two cylindrical perforated electrodes (aluminum anode and stainless steel cathode) were placed around the membrane. A

direct current power supply connected with an electrical timer was applied to provide the required current density and exposure mode (time-ON/time-OFF). Vacuum pump was connected to the membrane outlet to extract the liquid phase of the sludge liquor at a constant flow rate. Activated sludge used to fill up the reactors was brought from the wastewater treatment plant in St. Hyacinthe, QC.

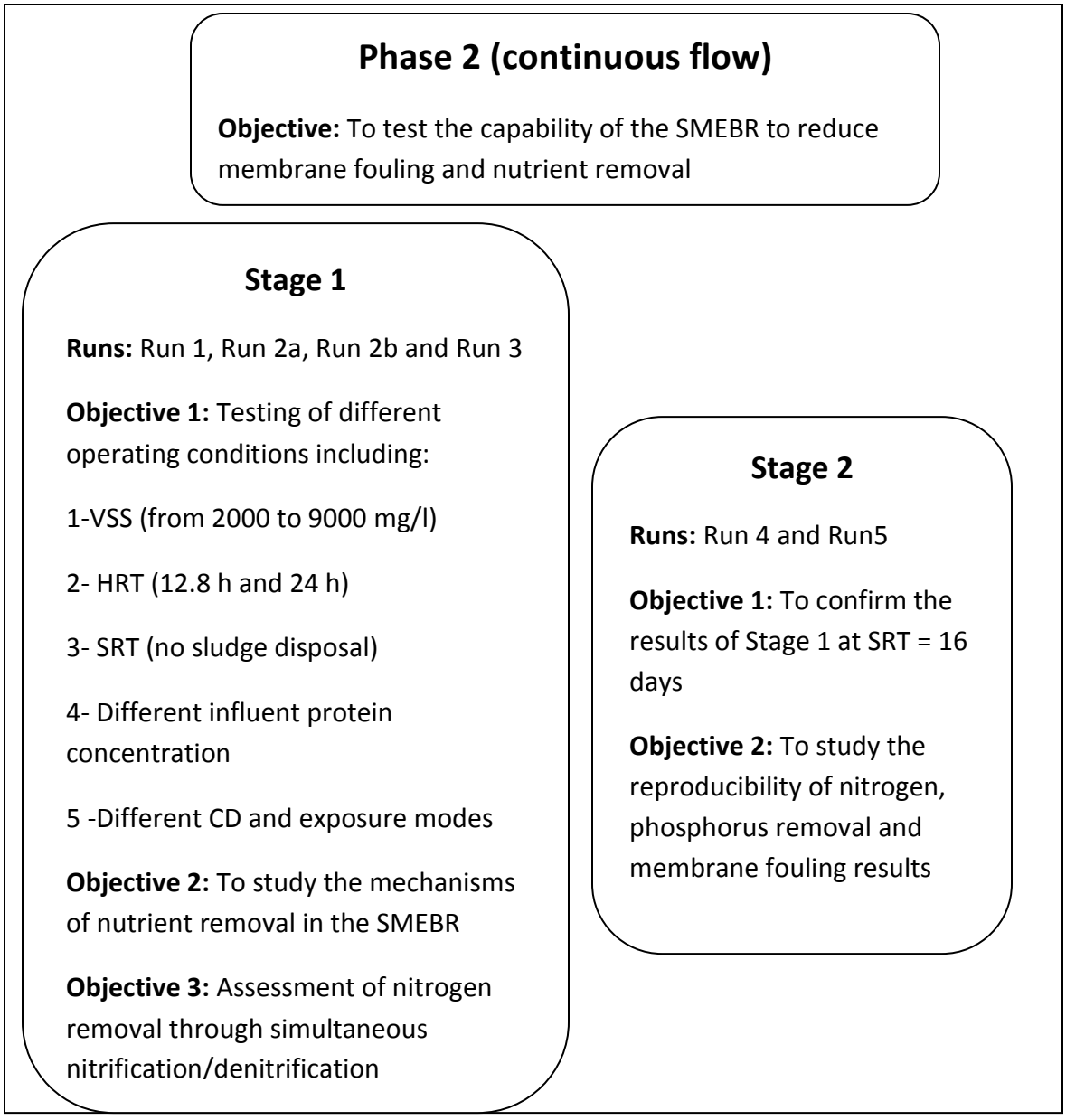

Figure 7.1 Phase 2: Flow chart of objectives and operating conditions

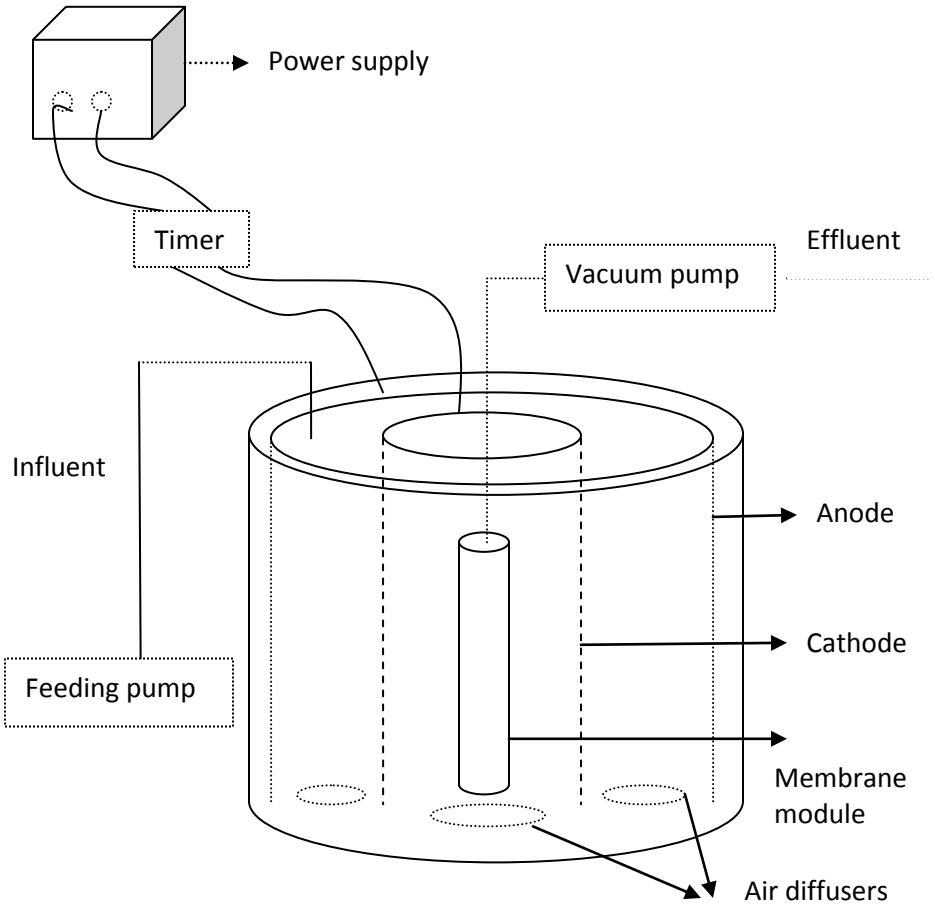

Figure 7.2 Phase 2: Experimental setup of SMEBR

7.2 Operating conditions

Phase 2 (Stage 1):

Based on the preliminary batch reactors tests, it was found that a current density between 15 to 20 A/m^2 and electrical exposure modes 5'-ON/15'OFF and 5'-ON/20'OFF are good enough to generate sufficient concentration of Al^{+3} to cause the removal of phosphorus and enough electron flux to change the ORP profile to fluctuate between -100 to +150 mV and thus transforming N into gases such as nitric oxide (NO), nitrous

oxide (N_2O) and molecular nitrogen (N_2). These electrical parameters were tested in several runs (Table 7.1) to explore the feasibility of C, P and N removal in one single reactor. During the operation, the dissolved oxygen (DO) concentration was fluctuating to verify the influence of oxygen concentration on the ORP profile. In Phase 2, the influent synthetic wastewater has different sources for nitrogen, namely, chemically bound nitrogen (easily dissolving ammonium sulfate) and organic compounds rich in ammonium (yeast extract and peptone) that release nitrogen in the ammonical form once degraded by the biomass.

Several runs were conducted to reach the targeted results. Run 1 was operated at the highest influent concentration of total nitrogen (TN) = 110 mg-N/l. Run 2 at lower concentration of TN= 57mg-N/l to study the removal efficiency at different levels of organic N. Run 2 consisted of Run 2a performed at hydraulic retention time (HRT) of 12.8 h and Run 2b at longer HRT of 24 h. Run 3 was operated based on glucose as a carbon source and ammonium sulfate as the sole source of ammonium in order to know exactly the concentration of ammonium in the influent, thereby, being able to make a mass balance and evaluate the removal efficiency of ammonium. This run was conducted for evaluating the nitrification potential of the SMEBR and the control MBR. SMEBR was expected to exhibit a higher nitrification potential due to the electrokinetic influence (electrical activation of different types of N transforming bacteria). The composition of synthetic water used for each run is given in Table 7.2. This composition was selected to have similar composition of nutrients, organic carbon and soluble salts to those exist in raw wastewater.

Table 7.1: Phase 2 (Stage 1): Operating conditions for each experimental run

Run #	CD (A/m^2)	Exposure mode	HRT (h)	Influent TN (mg-N/l)	Influent NH_4-N (mg/l)	Influent PO_4^{-3} (mg/l)	Influent COD (mg/l)	Operating period (days)
Run 1	20	5'-ON/15'-OFF	12.8	110	22	36	950	14
Run 2a	15	5'-ON/20'-OFF	12.8	57	22	36	950	26
Run 2b	15	5'-ON/20'-OFF	24	57	22	36	950	16
Run 3	17	5'-ON/20'-OFF	12.8 and 24	variable	variable	36	950	23

The activated sludge was brought from the activated sludge reactor in the wastewater treatment plant in St Hyacinthe, QC just one day before starting the experiments. The mixed liquor concentration (MLSS) was adjusted between 2000 to 3000 mg/l before used in the reactors. No sludge was disposed in this phase, except for the sludge sampled for analyses. When the MLSS concentration increased to a sufficiently high level that causes high membrane fouling rate, the MLSS concentration was diluted to maintain a reasonable fouling rate. This allowed studying the impact of electrical operating conditions on the reactor performance at different MLSS and VSS as well.

Table 7.2: Wastewater characteristics used in Phase 2 (Stage 1)

Component	Concentration (mg/l)			
	Run 1	Run 2a	Run 2b	Run 3
Glucose	310	665	665	850
Peptone	252	85	85	0.0
Yeast extract	300	100	100	0.0
Ammonium sulfate	100	100	100	100 to 250
Potassium phosphate	37	37	37	37
Magnesium sulfate	40	40	40	40
Manganese sulfate monohydrate	4.5	4.5	4.5	4.5
Iron sulfate	0.4	0.4	0.4	0.4
Calcium chloride	4	4	4	4
Potassium chloride	25	25	25	25
Sodium bicarbonate	25	25	25	25

Phase 2 (Stage 2)

Stage 2 consists of two runs (Run 4 and Run 5). The SMEBR was operated at 5'-ON/20'-OFF electrical mode at CD of 15 A/m^2. These electrical operating conditions were found to improve the performance of SMEBR at reasonable production of chemical sludge. The other operating conditions are illustrated in Table 7.1. In this stage, the solid retention time (SRT) in the two runs was set to 16 days. This magnitude of SRT simulates the real working conditions of the biological secondary treatment. An average of 500 ml daily

sludge volume was disposed of. This volume compromised 1/16 of the total reactor volume (8 l). The influent wastewater composition used in this stage is the same used in Run 2 of Stage 1 (Table 7.2)

Table 7.3: Operating conditions for each experimental run of Phase 2 (Stage 2)

Run #	CD (A/m^2)	Exposure mode	HRT (h)	influent TN (mg-N/l)	Influent NH_4-N (mg/l)	Influent PO_4^{-3} (mg/l)	Influent COD (mg/l)	Operating period (days)
Run 4	15	5'-ON/20'-OFF	12.8	57	22 to 29	36	950	18
Run 5	15	5'-ON/20'-OFF	12.8	57	22	36	950	30

7.3 Analyses

Measurements and analysis were conducted to evaluate the changes on sludge properties, treatment efficiency, nutrient removal and membrane fouling in both stages of Phase 2.

7.3.1 Treatment efficiency

Samples were taken periodically from the influent, effluent and from the sludge supernatant (after centrifugation at 4000 rpm for 20 minutes) to evaluate the treatment efficiency of nutrient, organic colloids and SMP removal. Methods of analyses are indicated in Table 7.4.

Table 7.4: Analyses for the assessment of the treatment efficiency

Component	Analytical method
Orthophosphate	Reduction by amino acid (method 8178, Hach, USA)
Ammonium	Ammonium electrode using accumet AR-25 ion meter (Fisher Scientific, USA). Or, TNT plus vials (Hach, USA)

Nitrate	Nitrate electrode using accumet AR-25 ion meter (fisher scientific, USA). Or, TNT plus vials (Hach, USA)
Total nitrogen (TN)	TNT plus vials (Hach, USA)
COD(total,colloidal,soluble)	TNTplus vials (method 8000, Hach, USA)
UVA254	Direct measurement using Lambda40 UV/VIS spectrometer (Perkin Elmer, USA)
Protein	Lowery et al. (1951) method. However, this method is widely used in recent publications
Polysaccharides	Dubois et al. (1956) method. However, this method is widely used in recent publications

7.3.2 Sludge properties

Changes of sludge characteristics were analyzed over the operating period. Sludge pH, electrical conductivity (EC) and DO were measured continuously over the operating time. Sludge characteristics of interest are included in Table 7.5.

Table 7.5: Sludge properties analyzed

Sludge property	**Analytical method**
Specific resistance to filterability (SRF)	As described in Phase 1(Stage 1)
Flocs mean size distribution	As described in Phase 1 (Stage 1)
Zeta potential	As described in Phase 1 (Stage 1)
pH	Direct measurement using HQ30d multi-parameter meter (Hach, USA)

Electrical conductivity (EC)	Direct measurement using HQ30d multi-parameter meter (Hach, USA)
Dissolved oxygen (DO)	Direct measurement using HQ30d multi-parameter meter (Hach, USA)
Total suspended solids (TSS)	Filtration + drying at 105° C (method 2540 D, standard methods for the examination of water and wastewater)
Volatile suspended solids (VSS)	burning at 550 °C ((method 2540 E, standard methods for the examination of water and wastewater))
Sludge dynamic viscosity	Direct measurement using viscometer at room temperature
Sludge bound water	Dead-end filtration of 100ml at vacuum (1 bar) to separate the sludge. The difference of mass of the sludge after drying at 105° C represents the amount of bound water.

7.3.3 Membrane fouling

Membrane fouling was studied through calculating the rate of membrane fouling represented as the changes of trans-membrane pressure (TMP) over time (Equation 7.1).

$$\text{Fouling rate} = \frac{\text{TMP (kPa)}}{\text{t (d)}} \qquad (7.1)$$

The SMEBR and the MBR were run at initial TMP of 1to 3 kPa. As the TMP increased over time due to the accumulation of microbial flocs onto membrane surface to a level that reduced the membrane flux significantly (TMP > 10 kPa).Once the TMP reached this point, the membrane was removed and cleaned thoroughly by tap water and then returned back into the reactor. The number of physical cleanings represents the severity of the reversible fouling in each reactor. The frequency of membrane cleaning was used in this research to compare the fouling propensity in each reactor.

Chapter 8

Phase 2 (Stage 1): Results and discussion - nutrient removal

This chapter discusses the removal efficiency of nutrients in the SMEBR and MBR in addition to their removal pathways.

8.1 Carbon removal

The COD removal efficiency was very high in SMEBR (>99%) as well as in MBR (>97%) even after 37 days of operation (Figure 8.1). This indicates that the microbial flocs were able to recover the electrical shock at those operating conditions (CD < 20 A/m^2 and time-OFF > 15'). After 45 days of operations the biomass was highly active and performed the oxidation of organic materials to the highest level as indicated by the high removal efficiency of COD removal. However, slightly higher removal efficiency was achieved in the SMEBR due to the capability of this system to coagulate the colloidal organic materials or even those with high molecular weight.

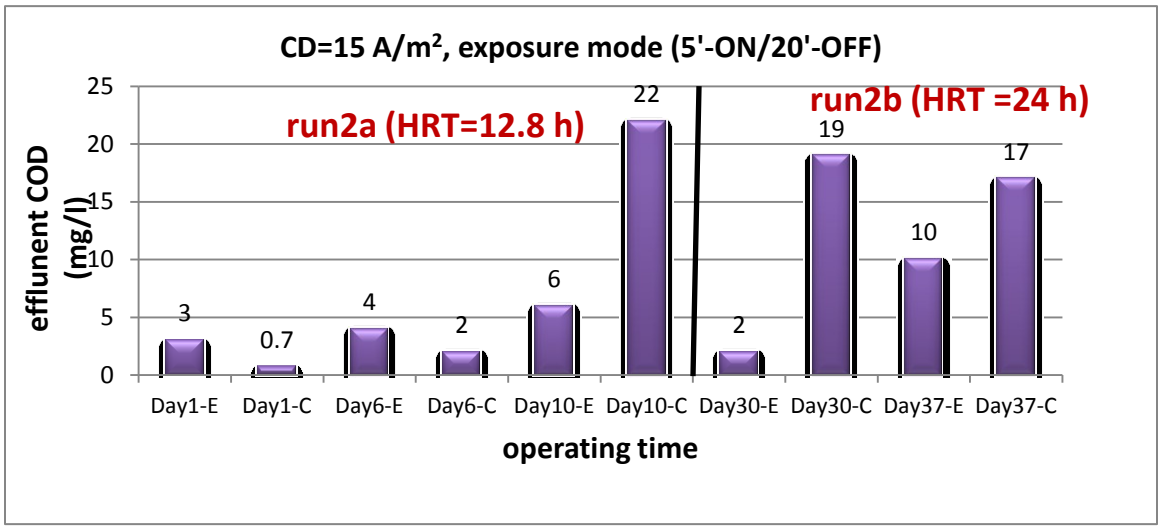

Figure 8.1: Run 2a and Run 2b: COD concentration in the effluent over the operating; E= SMEBR and C= MBR)

The removal of colloidal particles through electro-coagulation from the supernatant (Figure 8.2) is the major reason for better removal of organic materials.

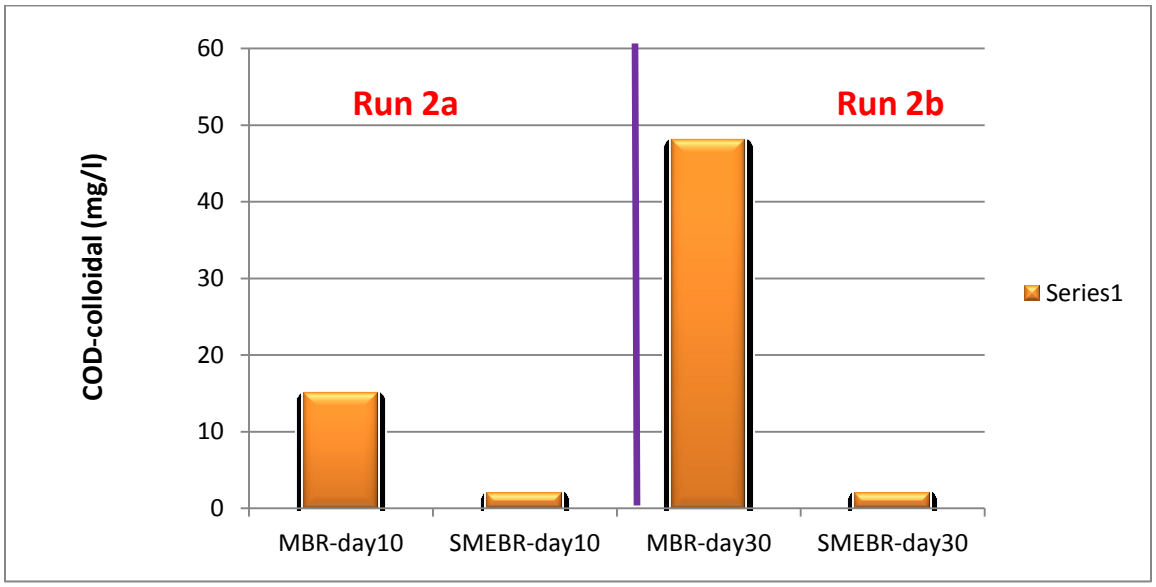

Figure 8.2: Run 2a and Run 2b: Changes of sludge colloidal supernatant COD

8.2 Phosphorus removal

When the SMEBR operated at HRT of 12.8 h (Figures 8.3 and 8.4), a removal efficiency up to nearly 100% (non-detectable limit in the effluent) was achieved. The electro-chemical dosing of AL^{+3} into the system at these electrical parameters was enough to form complexes with phosphorus and extract it from the liquid phase of the activated sludge. On the other hand, the effluent orthophosphate concentration increased in the MBR from around 2.5 at the starting time up to 12 mg $PO4^{-3}$-P because of the high influent P concentration. The maximum removal efficiency in the MBR did not exceed 25%.

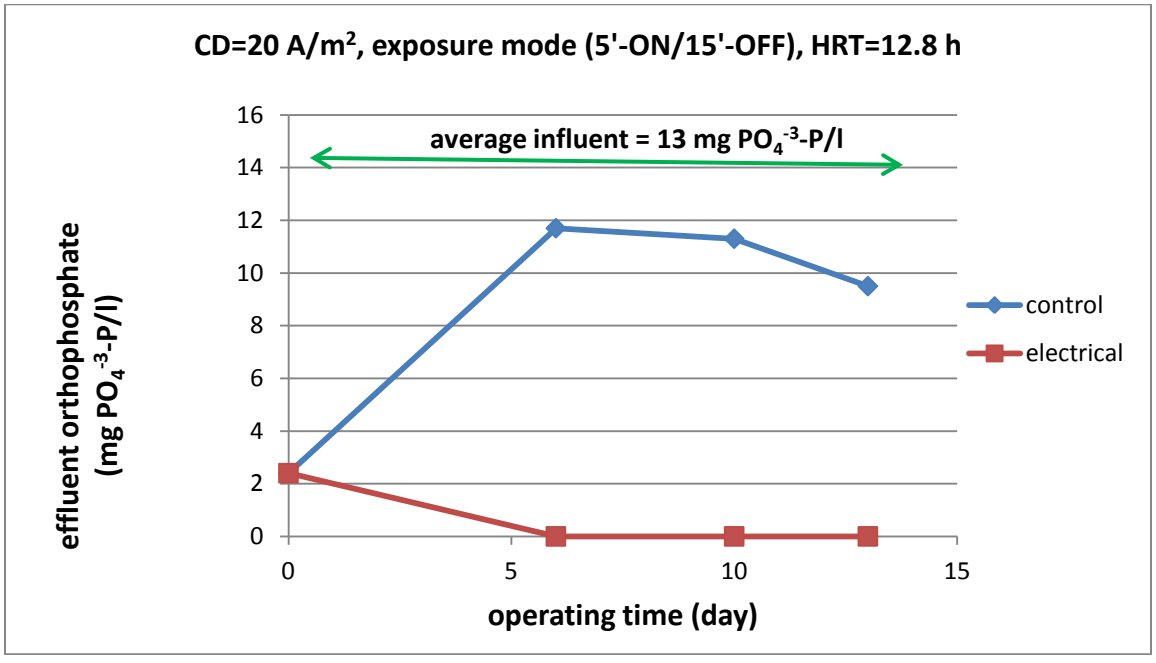

Figure 8.3: Run 1: Phosphorus removal in the SMEBR (electrical) and the MBR (control)

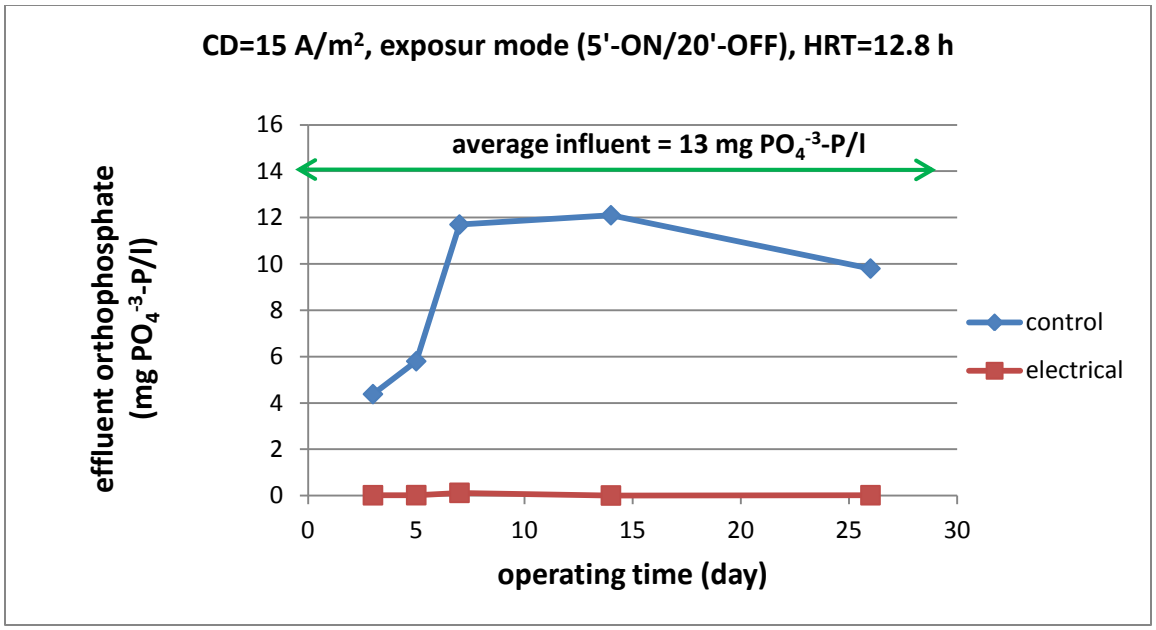

Figure 8.4: Run 2a: Phosphorus removal in the SMEBR (electrical) and the MBR (control)

The exposure mode 5'-ON/20-OFF exhibited nearly complete removal of phosphorus as long as the current density was higher than 15 A/m^2 (Figure 8.5). But, when the HRT increased from 12.8 h to 24 h, the current density dropped to 10 A/m^2 due to the reduction of soluble ions in the sludge. Longer HRT led to less loading of soluble salts into the SMEBR. At this low level of current density, the 5'-ON/20'-OFF exposure mode did not provide the required Al^{+3} ions responsible for P removal. At that current density (10 A/m^2), an exposure mode with shorter time off could be a solution. However, the current density was then increased to 15 A/m^2 by increasing the voltage gradient to compensate for the reduction of the soluble ion concentration. Once the CD was back to 15 A/m^2, no phosphorus was detected in the effluent. These results confirm that CD and electrical exposure mode should be adjusted to produce the critical concentration of Al^{+3} required to remove effectively the incoming phosphorus.

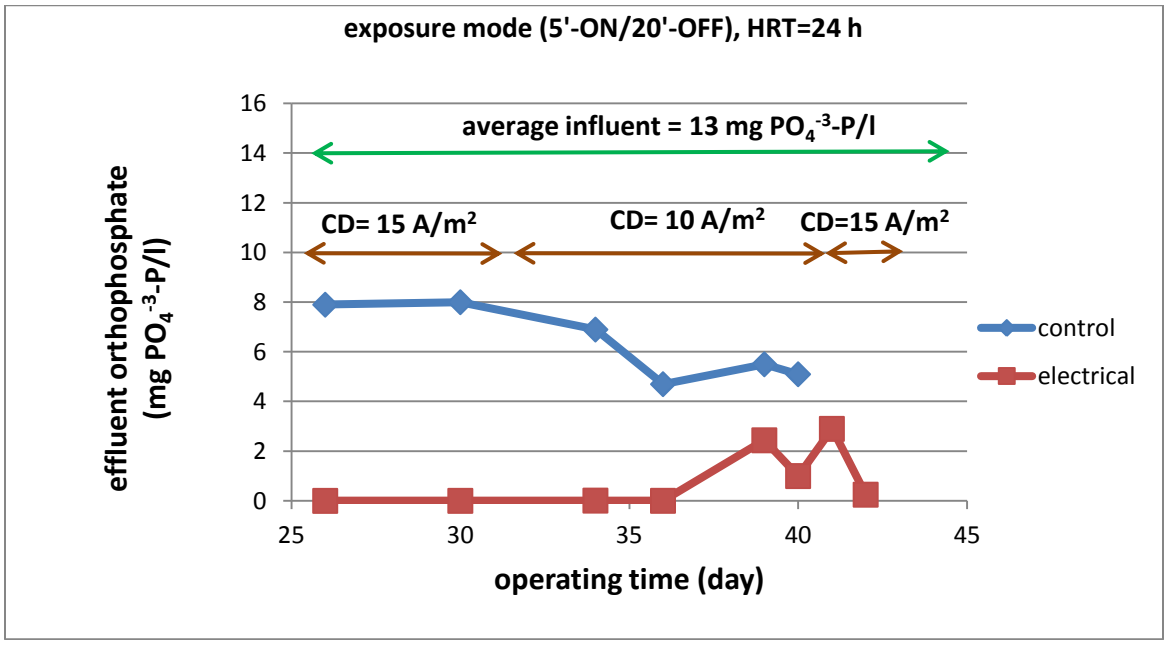

Figure 8.5: Run 2b: Phosphorus removal in the SMEBR (electrical) and the MBR (control)

In order to explore the fate of phosphorus in the sludge, the sludge was extensively explored to determine where phosphorus ends up in the SMEBR. For this purpose, the supernatant of MBR and SMEBR were obtained through centrifugation at 2700 g for 20 minutes. The supernatant was then filtered through 0.45 µm to separate the particulate and soluble P. results depicted in Figurers 8.6 and 8.7 show that the majority of P in the system was in the form of soluble phosphorus (orthophosphate) that disappeared almost completely from the supernatant and the effluent of SMEBR. A small percentage of P existed in the particulate form.

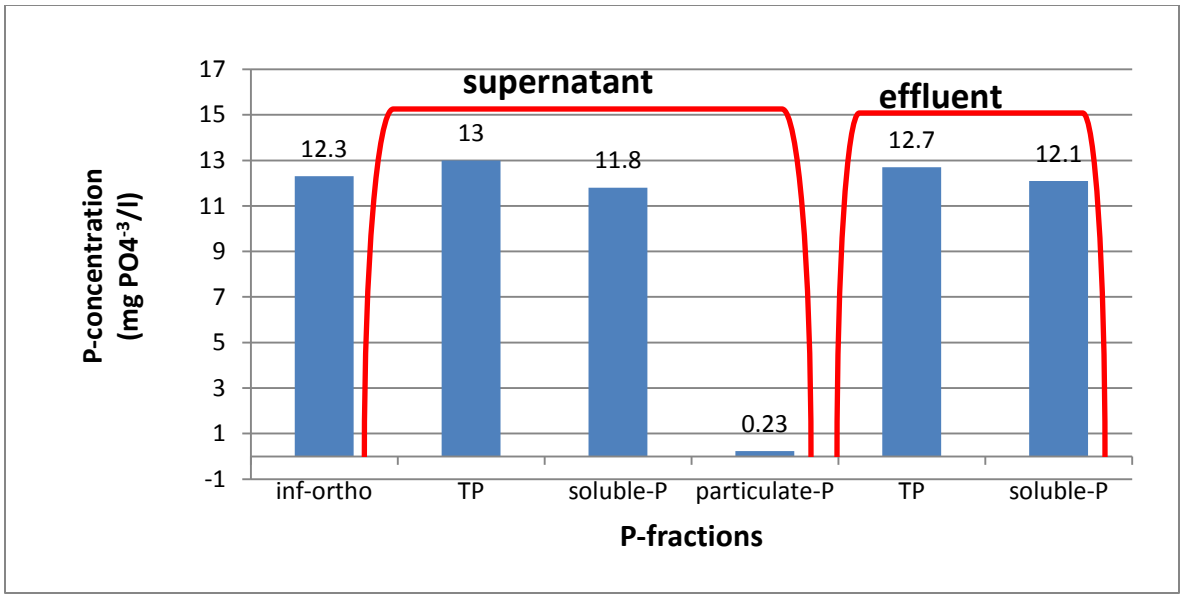

Figure 8.6: Run 2a: The concentrations of different P-fractions in the control MBR on Day 14 (TP=total P)

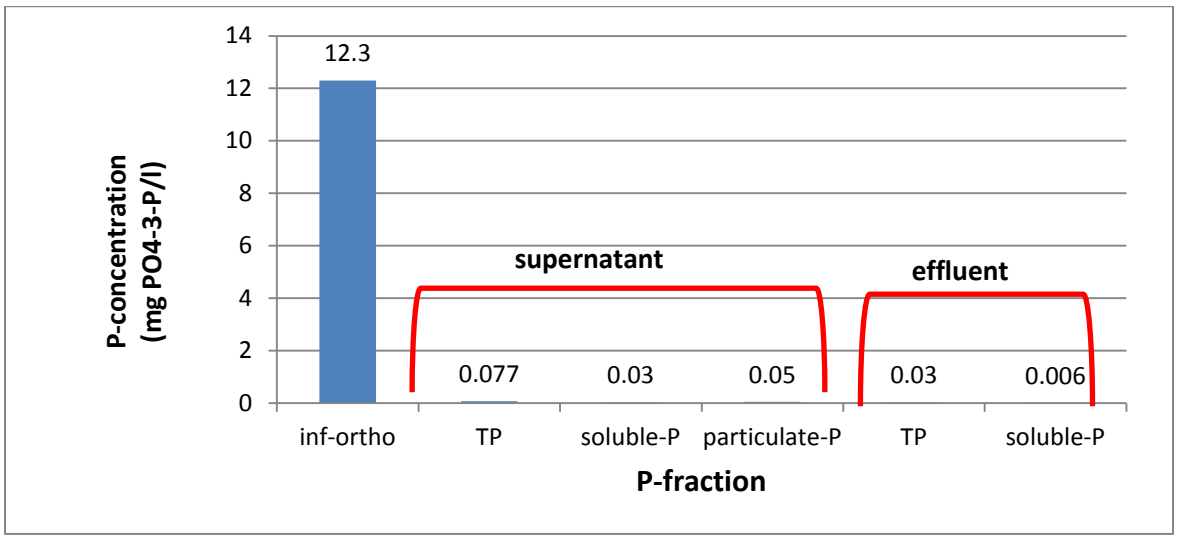

Figure 8.7: Run 2a: The concentrations of different P-fractions in the SMEBR on Day 14 (TP=total P)

Since phosphorus in the SMEBR was not found in the liquid phase of the sludge, it probably became part of the suspended solid of sludge liquor. To verify this speculation, 1 ml of sludge liquor of both reactors was sampled and analyzed to measure the P

content embedded in the solid phase within the sludge liquor. Figure 8.8 shows that the concentration of phosphorus embedded within the suspended solids was much higher in the SMEBR (355 mg PO_4^{-3}-P/1 ml MLSS) than the MBR (240 mg PO_4^{-3}-P/1 ml MLSS) after 14 days of operation. This proves that the influent orthophosphate precipitated in the form of complexed solids of aluminum phosphates ($AlPO_4$) and aluminum hydroxides.

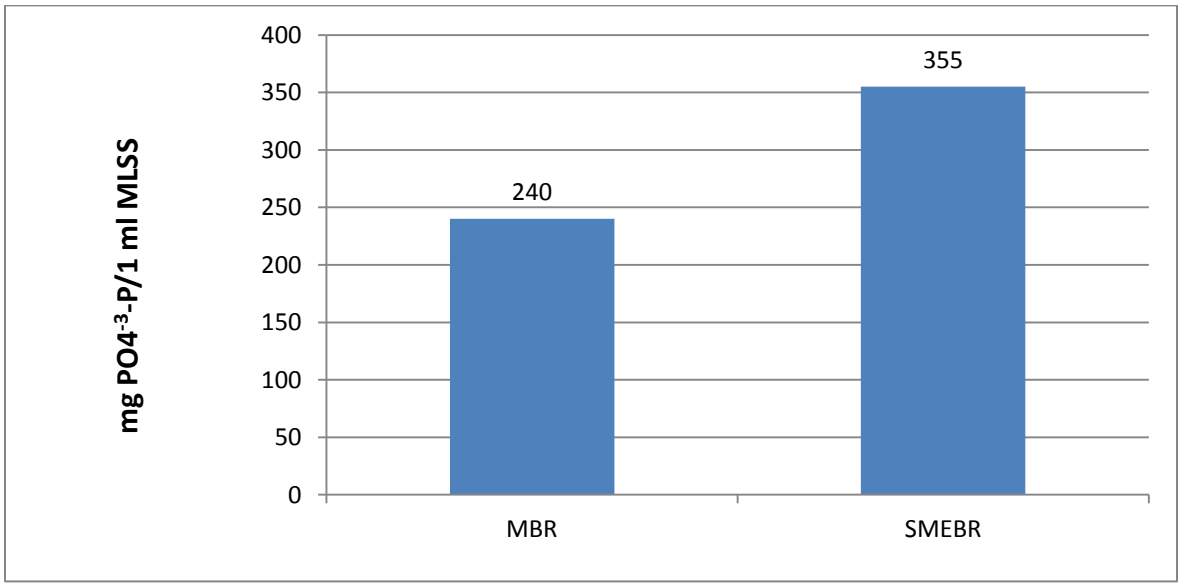

Figure 8.8: Run 2a: P content in the solid phase of 1 ml of MLSS in the MBR and SMEBR on day 14

8.3 Electrical changing of ORP

Complete transformation of N into gas in one reactor requires the fluctuation of the ORP between the anoxic/anammox and the aerobic conditions. In order to force the ORP to adequately fluctuate, the electrical operating parameters (current density, voltage gradient and exposure mode) should be adjusted with the other operating

conditions such as the organic loading, HRT and MLSS, which determines the biological oxygen demand and the diffusivity of gases in the system. Obtaining an ORP fluctuating between -150 to +150 mV could be achieved at different levels of DO based on the operating conditions. Working at low MLSS requires high DO concentration because the diffusivity of electrons in the reactor is high and can easily reach the DO and deactivate its role as the dominant electron acceptor. Likewise, at high MLSS, low DO concentration is required since the movement of the electrons is hindered by the low diffusivity of the reactor. For example, the CD of 17 A/m^2, MLSS of 10,000 mg/l and exposure mode of 5'-ON/20-OFF did not show any significant changes in ORP when the DO concentration was very high. Once the DO was reduced to 4 mg/l, a slight reduction of ORP was observed (from +250 to +130 mV) that is not enough to develop anoxic conditions (Figure 8.9a). As the DO was lowered again (2 to 3 mg/l), the ORP declined to 30 mV for a short period of time, which is not enough to cause significant denitrification of nitrate under perfect anoxic conditions (Figure 8.9b). Further reduction of DO (1.5 to 2.5 mg/l) showed more reduction of ORP down to -60 mV at the end of time-ON, at which the DO concentration was at its lowest level (Figure 8.9c). Once the time OFF started, the ORP began to recover its starting value (ORP = +155 mV). Each electrical cycle was divided into nearly 50% of typical anoxic condition followed by 50% of typical aerobic conditions. Further reduction of DO to 0.2 at the end of time-ON and up to 1.6 mg/l at the end of time-OFF permitted the ORP to drop down to -130 mV where anammox conditions developed and enhanced nitrification of ammonium is likely to take place (Figure 8.9d). Working at ORP profile fluctuating between -150 to +150 mV

was found to exhibit the best conditions for N removal. Furthermore, nitrification potential of the SMEBR reactor was higher than the control reactor (MBR) due to the activation of anammox as another pathway of nitrification.

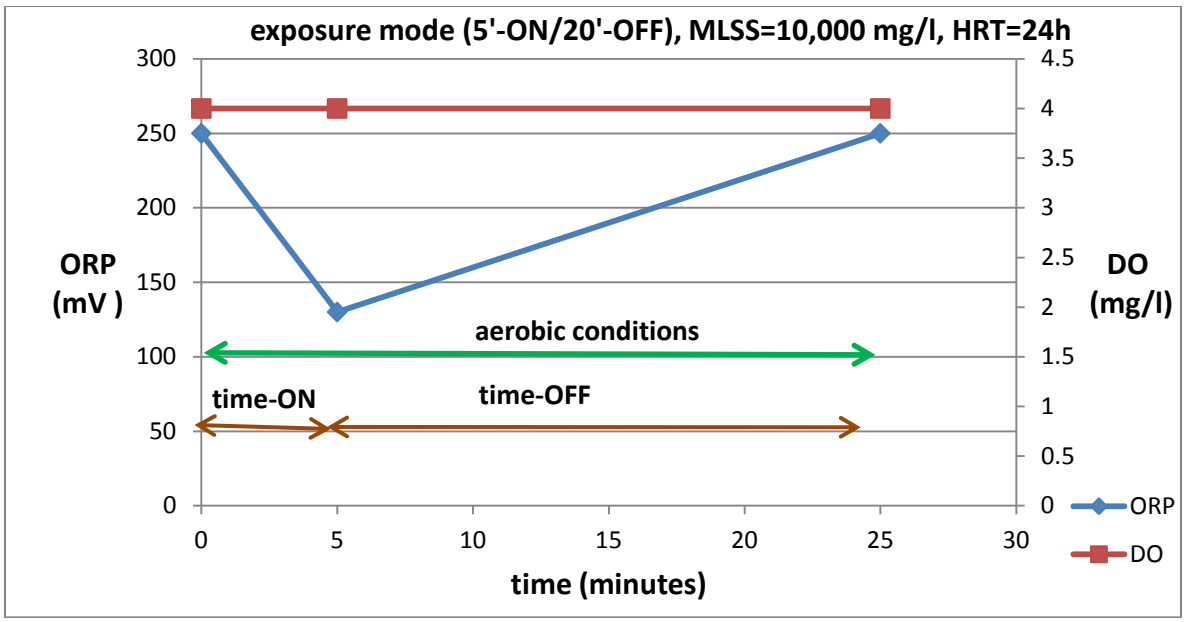

Figure 8.9a: Changing of the ORP at DO=4 mg/l and CD=17 A/m^2 during one electrical cycle (5'-ON/20'-OFF)

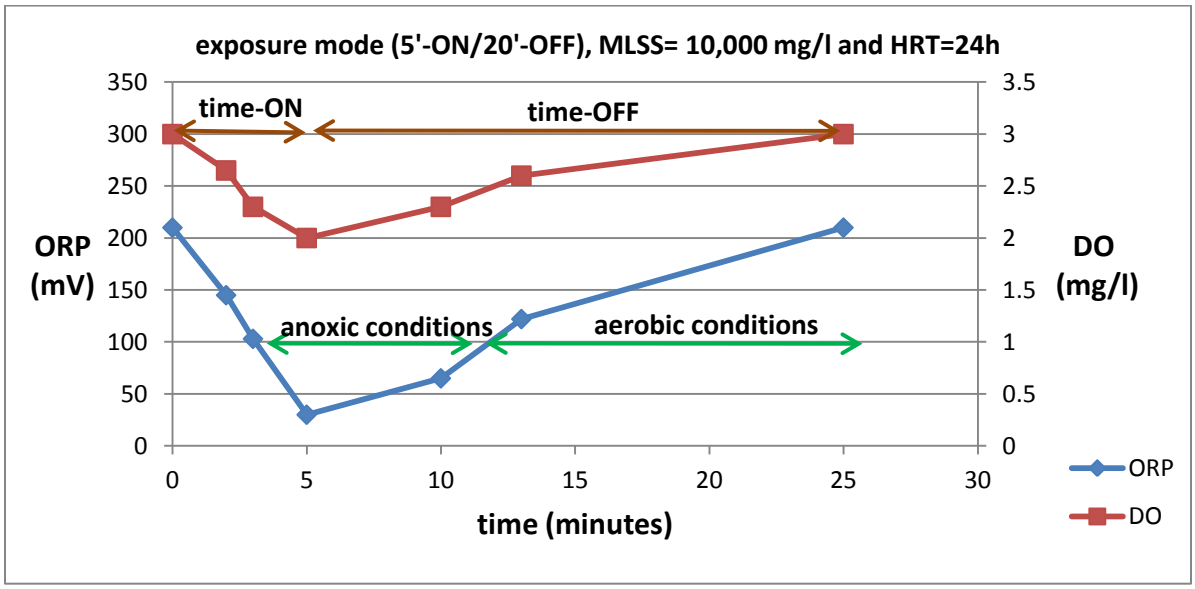

Figure 8.9b: Changing of the ORP at DO= 2 to 3 mg/l during one electrical cycle (5'-ON/20'-OFF)

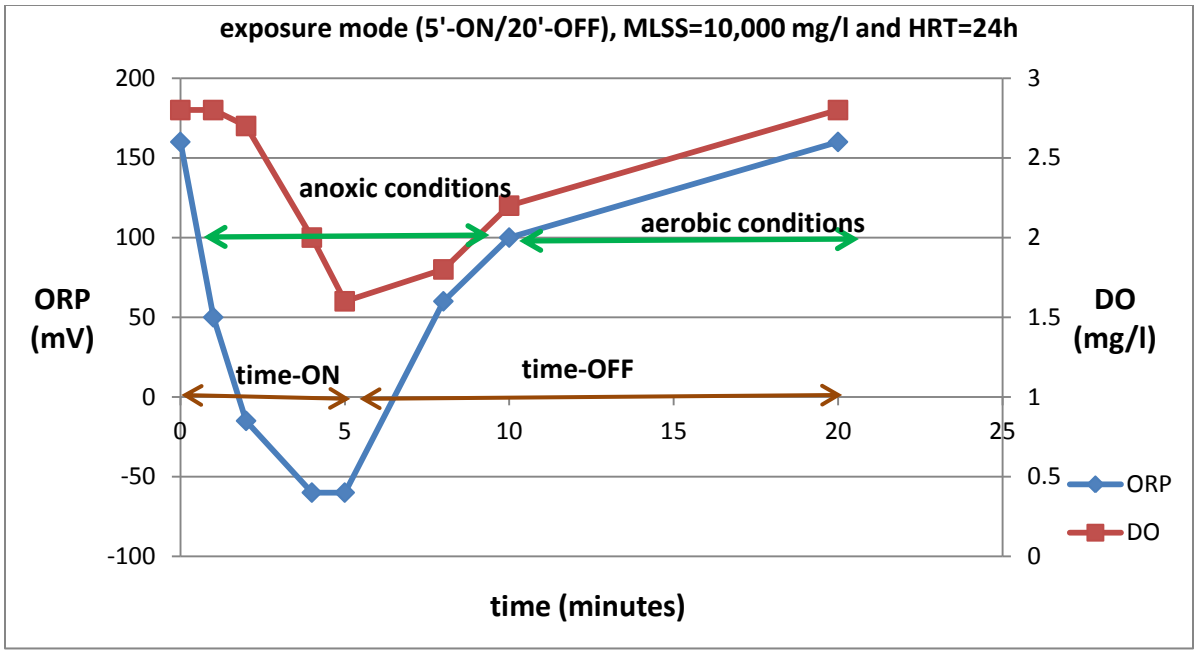

Figure 8.9c: Changing of the ORP at DO= 1.5 to 2.5 mg/l during one electrical cycle (5'-ON/20'-OFF)

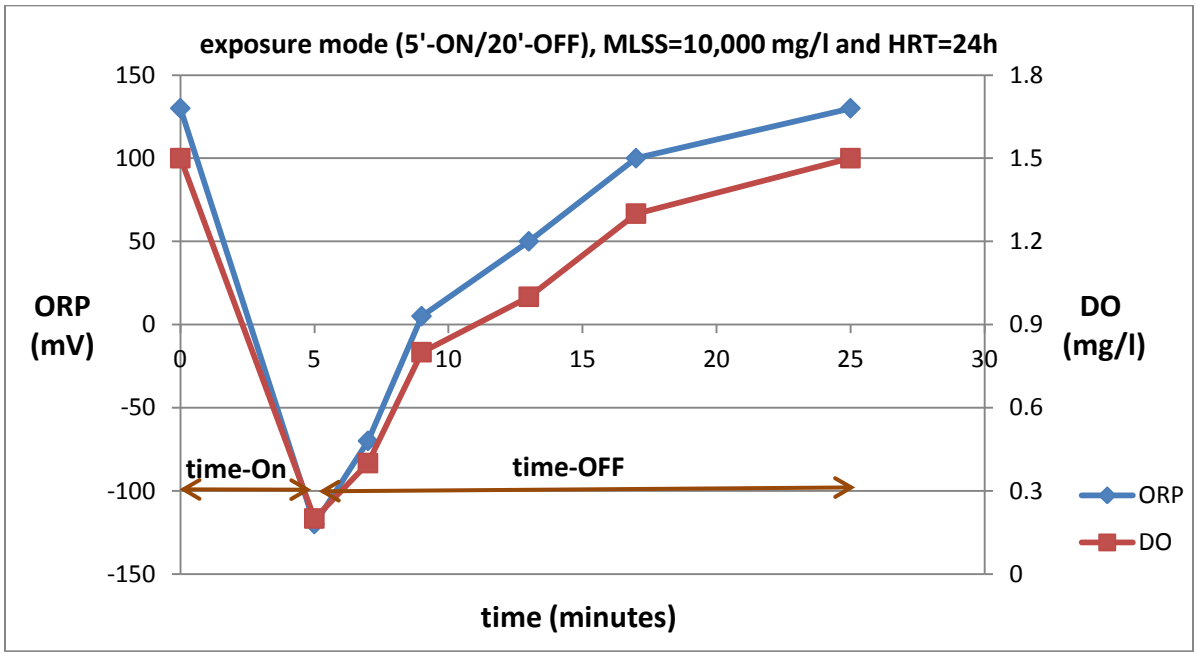

Figure 8.9d: Changing of the ORP at DO= 0.2 to 1.5 mg/l during one electrical cycle (5'-ON/20'-OFF)

8.4 Nitrogen removal

Run 1 was operated at a high influent content of organic nitrogen and 20 mg NH_4-N/l. In this run, neither the MBR (Figure 8.10) nor the SMEBR (Figure 8.11) exhibited complete nitrification until day 6. After day 6, most of the ammonium was nitrified in both reactors. However, the nitrate concentration was extremely high in the effluent of the MBR (more than 80 mg NO_3^-/l), while in the SMEBR the nitrate concentration was lower than 10 mg NO_3^-/l. The highest reduction of nitrate was achieved when the ORP of the SMEBR fluctuates between -100 to +150 mV creating the optimal conditions for the autotrophic nitrifiers and the heterotrophic denitrifiers (days 8, 9 and 10). The DO concentration required at CD=20 A/m^2 and exposure mode of 5'-ON/15'-OFF was 3 to 4 mg/l to develop this ORP profile. By the time DO concentration was increased to more than 4 mg/l, the conditions were more towards the nitrification conditions, which led to an increase of nitrate concentration in the SMEBR (days 5 to 7) and days 12 and 13.

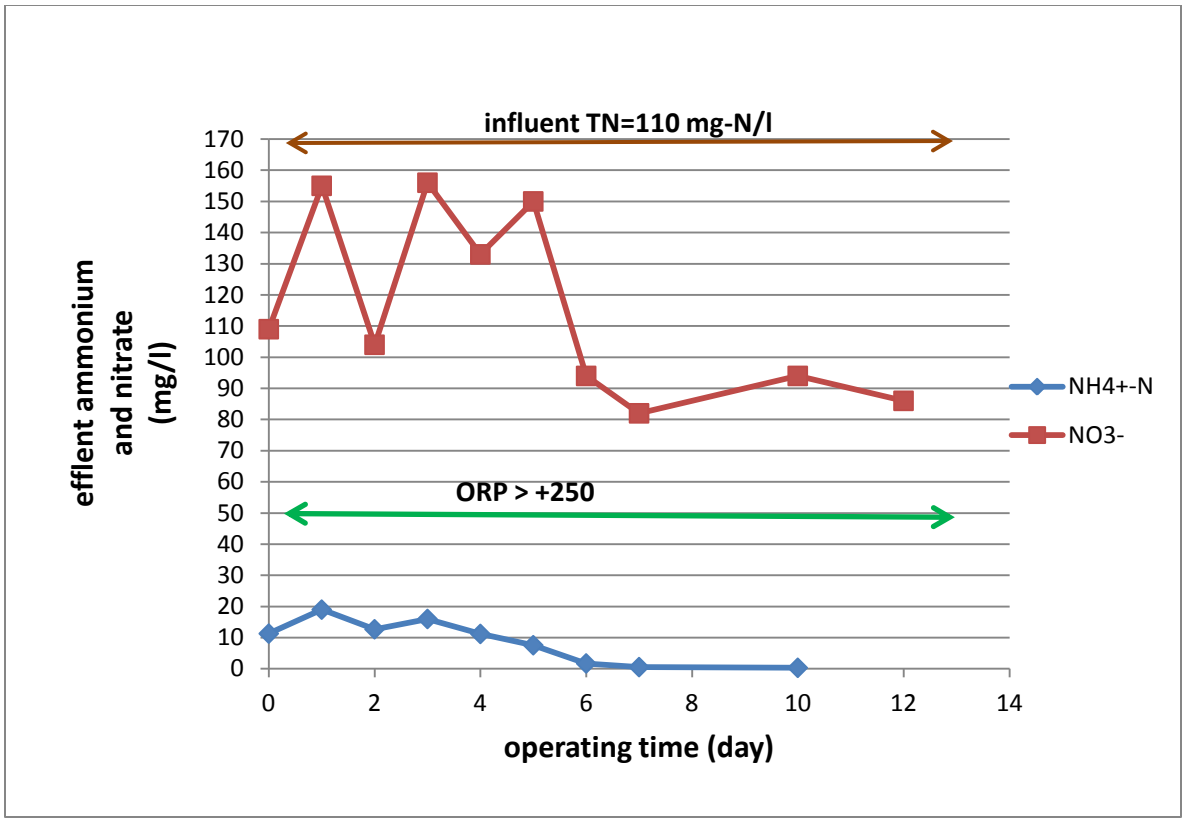

Figure 8.10: Run 1: Effluent concentrations of ammonium and nitrate in the MBR in Run 1

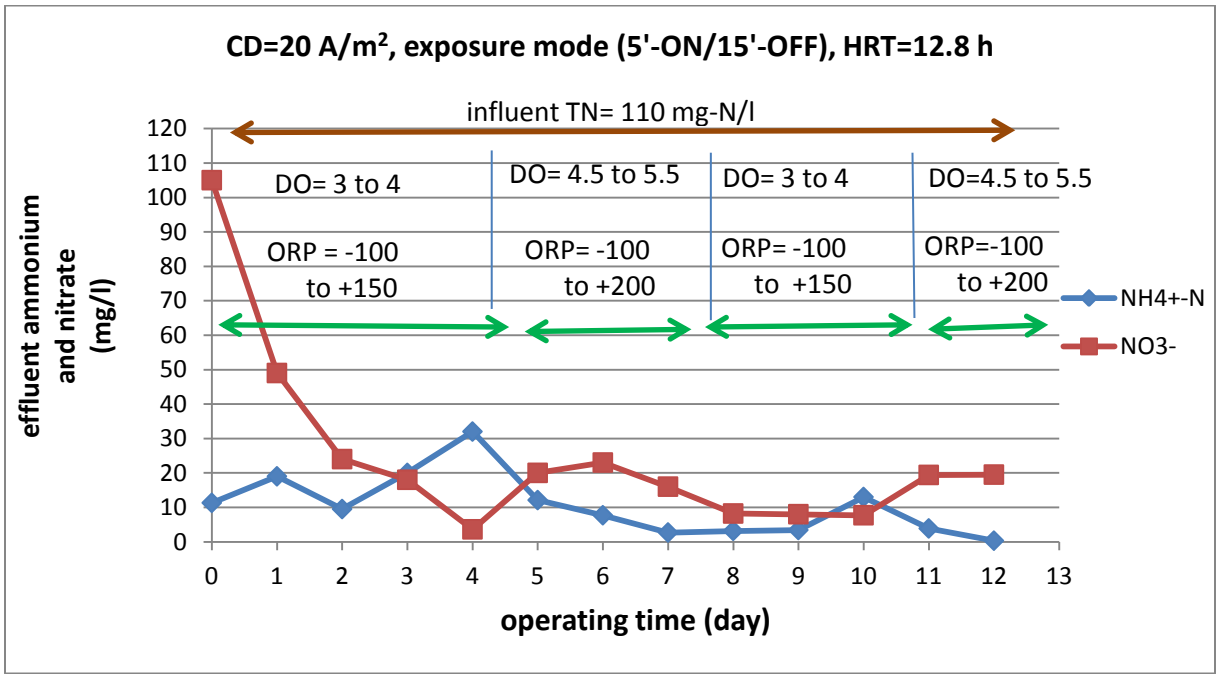

Figure 8.11: Run 1: Effluent concentrations of ammonium and nitrate in the SMEBR

Run 2 was operated at influent total nitrogen (TN) of 57 mg-N/l split between the organic N (yeast extract and peptone) and inorganic ammonium sulfate. During the first 14 days of operation, the MBR (Figure 8.12) and SMEBR (Figures 8.13) produced effluent with residual ammonium concentration between 5 to 10 mg NH_4^+-N/l because the loading of ammonium into the system is higher than their nitrification potentials at the applied operating conditions. Once the loading of N was reduced to 34 mg NH_4^+-N/l on days 15 and 16 by excluding the peptone and yeast extract from the influent wastewater, the two reactors exhibited more than 99% nitrification of ammonium. After these two days, the previous loading of TN was back, which later caused another increase of ammonium in the effluent of both reactors until day 22. When the nitrification potential of the reactors increased due to the building up of more nitrifying bacteria, the concentration of ammonium was reduced in both reactors. On the other hand, nitrate concentration in the MBR was higher than 40 mg NO_3^-/l during the whole operating period due to the high nitrification rate. Meanwhile, nitrate concentration in the SMEBR was less than 5 mg/l when the ORP profile was adjusted between -100 to +150 at DO of 1.5 to 3 mg/l, CD of 15 A/m^2 and exposure mode of 5'-ON/20'OFF. On days 15 and 16, the effluent concentrations of ammonium (0.08 mg NH_4+/l), nitrate (0.1 mg NO_3-/l), and TN (1.2 mg N/l) were the lowest with the highest removal efficiency of TN of 97%. When the SMEBR operated at high DO concentration (more than 5 mg/l) starting after day 16, the reactor was unable to reduce the ORP below +150 creating only nitrification conditions. Therefore, nitrate increased to limits equal to that of the MBR because the denitrifiers were deactivated at this level of ORP.

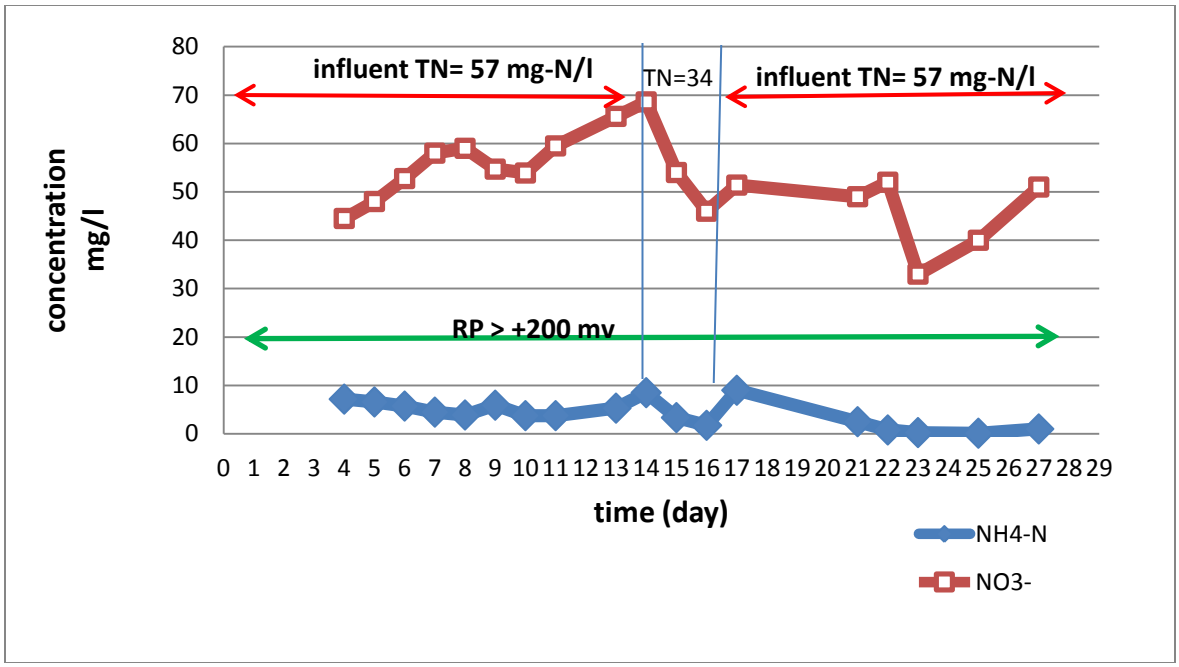

Figure 8.12: Run 2a: Effluent concentrations of ammonium and nitrate in the MBR

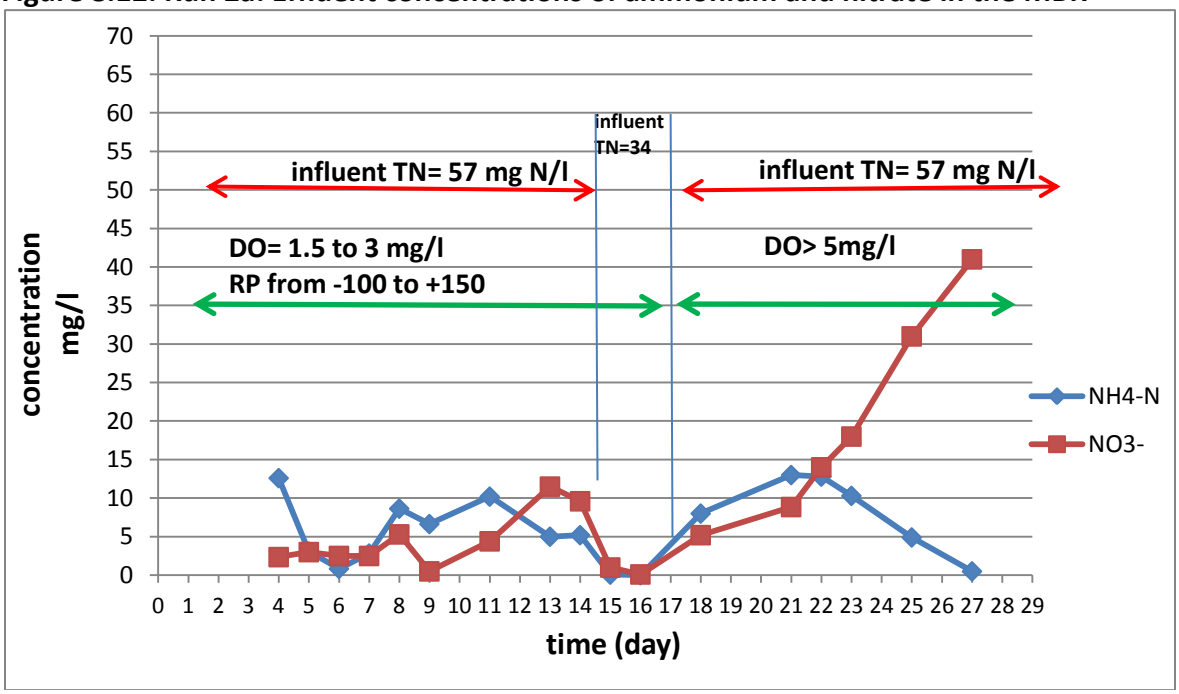

Figure 8.13: Run 2a: Effluent concentrations of ammonium and nitrate in the SMEBR

Run 2b was the continuation of Run 2a but at longer HRT of 24 h, and the ORP profile was adjusted in SMEBR between -100 to +150 mV starting on day 33 to support the simultaneous nitrification/denirtification conditions. In the MBR (Figure 8.14), typical nitrification condition led to more than 99% conversion of ammonium into nitrate, and the concentration of nitrate was almost higher than 40 mg-NO_3^-/l. The SMEBR (Figure 8.15) proved once again the possibility of achieving almost complete nitrification of ammonium and complete denitrification of nitrate if the loading of ammonium into the reactor is lower than the nitrification capacity of the system, which was the case in that run. The removal efficiency of TN was up to 97% on day 40.

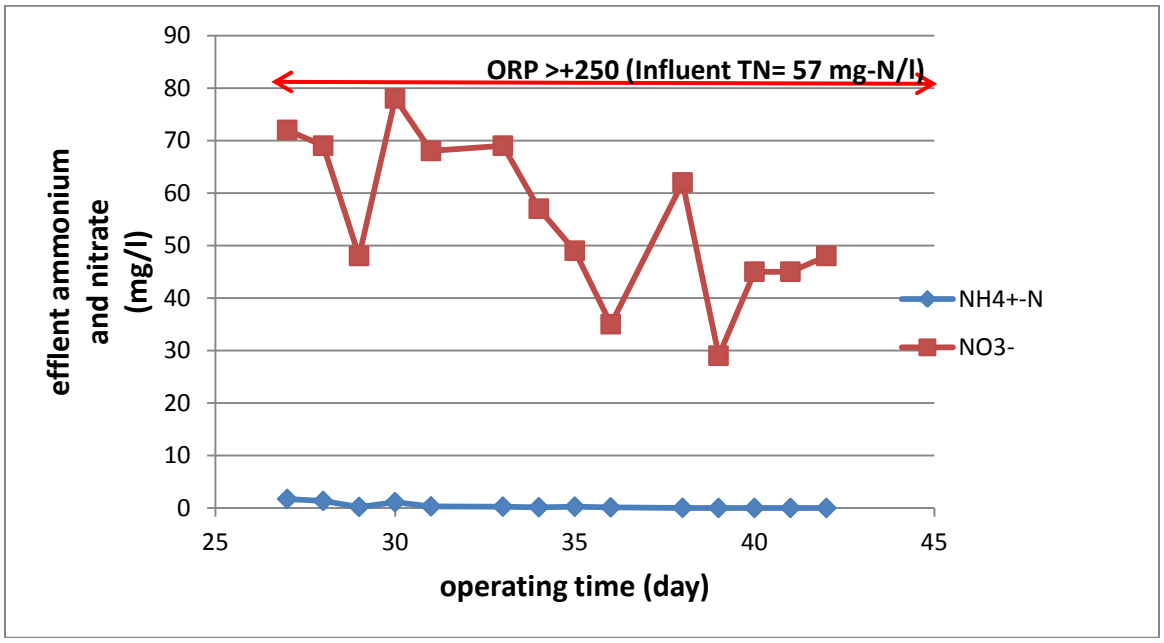

Figure 8.14: Run 2b: Effluent concentrations of ammonium and nitrate in the SMEBR

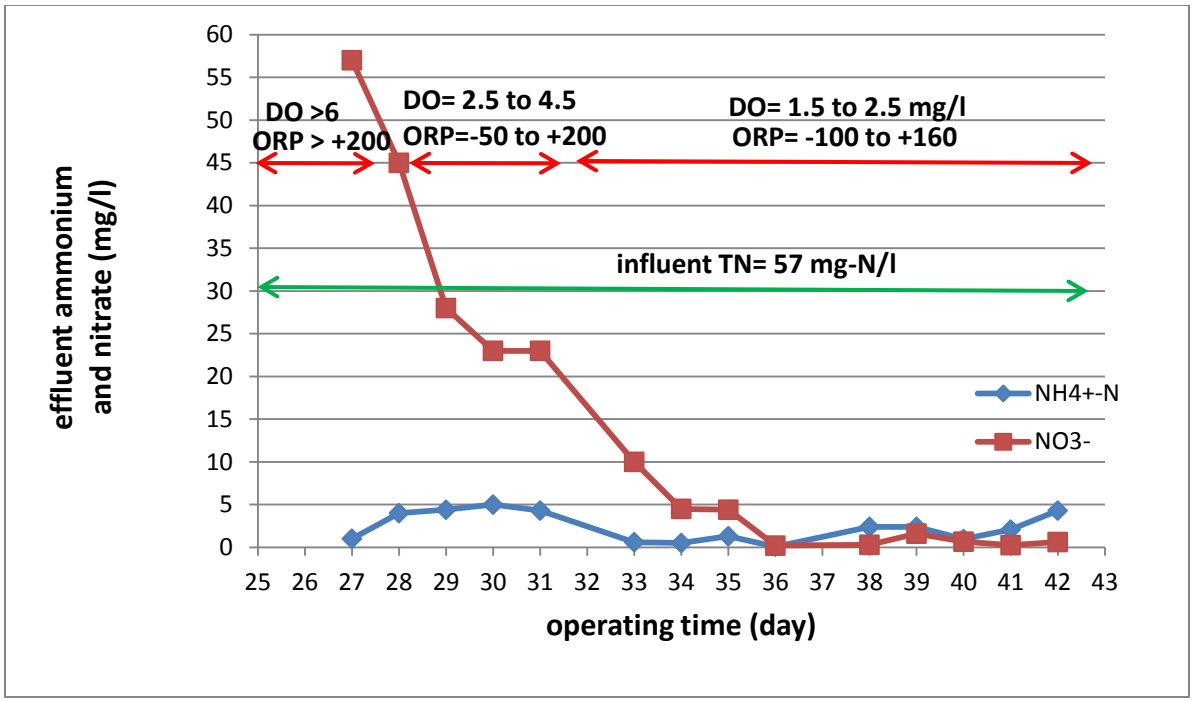

Figure 8.15: Run 2b: Effluent concentrations of ammonium and nitrate in the SMEBR

8.5 Enhancing the nitrification potential of electro-bioreactor

Run 3 was conducted to examine the nitrification potential of SMEBR and MBR. In that run, ammonium sulfate was used as the sole source of ammonium in order to assess the nitrification potential of each reactor. When the SMEBR operated at DO of 1 to 2.5 mg/l and ORP fluctuating between -100 to +150 mV, an increase of up to 10% in the nitrification potential was achieved because of the combined aerobic and anaerobic nitrification in the SMEBR compared to only aerobic nitrification in the MBR (Figures 8.16 and 8.17). On the other hand, up to 25% enhanced nitrification potential was achieved in the SMEBR as the ORP was adjusted between -130 to +130 mV at DO from 0.3 to 1.3 mg/l because more anammox bio-reactions were taking place in the reactor at that level of oxygen.

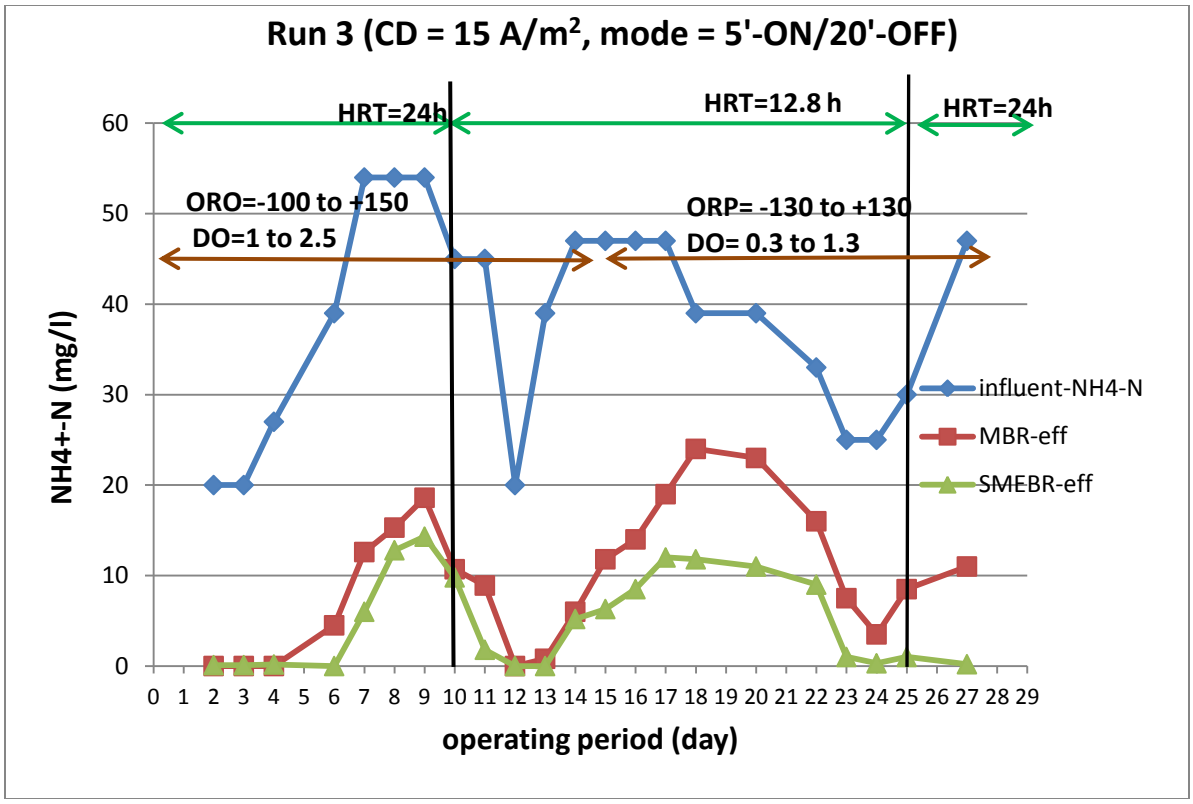

Figure 8.16: Run 3: Changes of effluent ammonium in the SMEBR and MBR at different influent ammonium concentrations

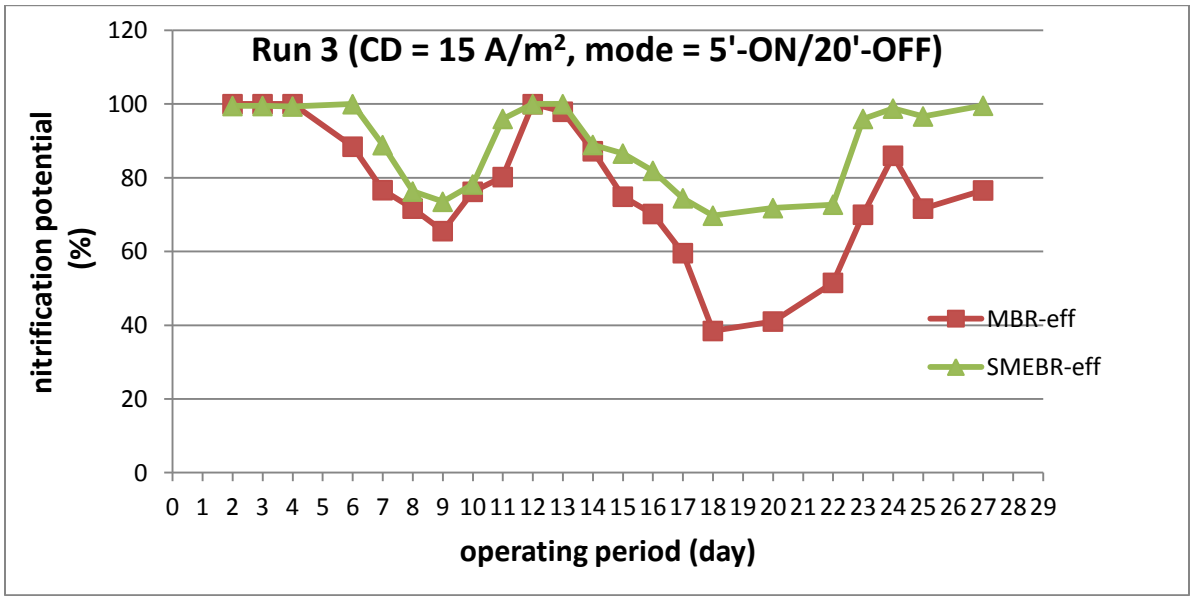

Figure 8.17: Run 3: Comparison of the nitrification potential efficiency of SMEBR and MBR when the electrical parameters were optimized

On the other hand, the enhanced nitrification was not at the expense of the denitrification. Nitrate concentration in the SMEBR effluent was very low (< 0.2 mg-NO_3^-/l) over the whole operating period (Figure 8.18). For example, on day 27, when the reactors were fed with 47 mg-NH_4-N/l, the MBR produced effluent with 11 mg- NH_4-N/l, 5 mg- NO_3^-/l and total nitrogen of 20.8 mg-N/l, while the SMEBR produced effluent with 0.2 mg NH_4-N/l, 0.02 mg NO_3^-/l and total nitrogen of 1 mg-N/l. The total nitrogen removal efficiency of the SMEBR was higher than 97% when the ammonium loading was less than 47 NH_4^+-N mg/l.d. The high fluctuation of nitrate concentration in the MBR is due to the changing of the influent ammonium. It has peaked during days 10 and 11 when the ammonium in the influent was the highest before and during that period (> 50 mg/l), Figure 8.16.

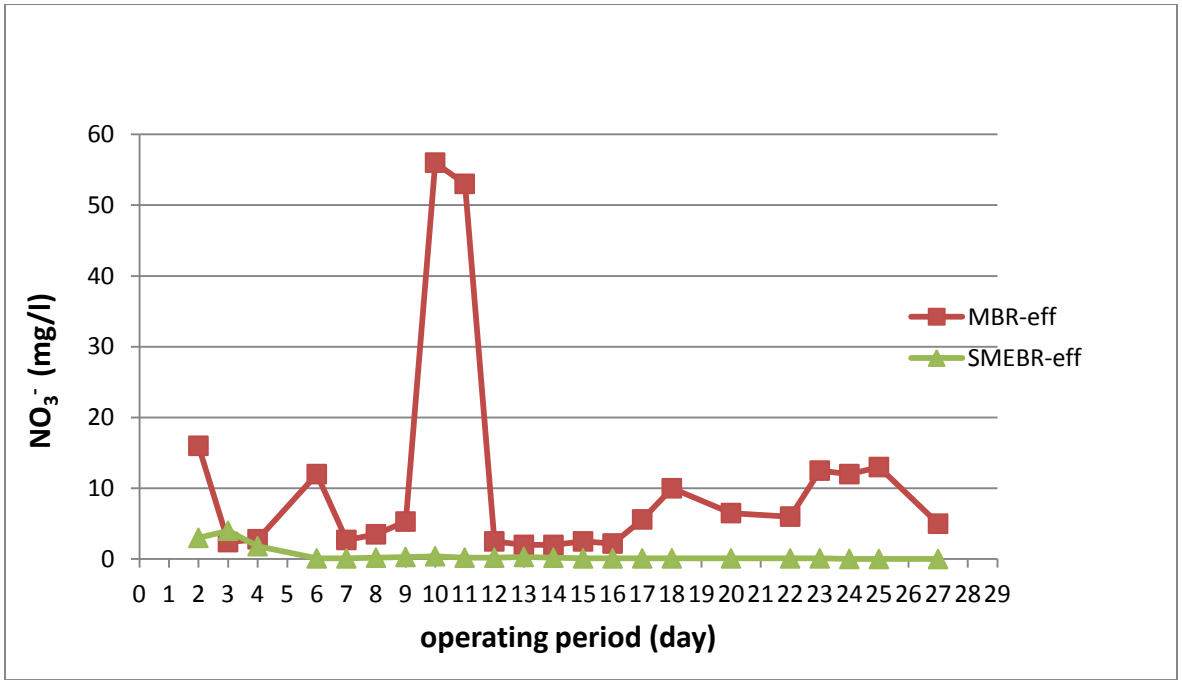

Figure 8.18: Run 3: Comparison of the nitrate concentration in the effluent of SMEBR and MBR at different influent ammonium concentrations

8.6 Denitrification processes in SMEBR and MBR

In SMEBR, denitrification is carried out in two different biological processes. The first process is the heterotrophic denitrification in which carbon is taken from the organic materials and nitrate serve as an electron acceptor. The other denitrification process in SMEBR is through the autotrophic hydrogen denitrification in which the hydrogen produced at the cathode acts as e-donor and nitrate as electron acceptor. In order to evaluate the contribution of each process in the total denitrification potential of the SMEBR, an additional lab scale experiment was conducted. In that experiment, the SMEBR was fed with an influent of high nitrate concentration and very low organic carbon source for 7 days (Figure 8.19). On day 8, the influent was enriched with organic carbon. During the first 7 days of operation where no organic materials were injected into the reactor to eliminate the heterotrophic denitrifies, a slight reduction of nitrate was obtained (up to 25 %). The reduction of nitrate concentration in the absence of organic carbon sources indicates the role of the hydrogen autotrophic denitrification, which takes its carbon needs from the inorganic sources such as carbonate and bicarbonate. On day 8 when the influent was high in organic carbon, the nitrate concentration was reduced substantially (72%). This outstanding reduction of nitrate in a short period of time confirms that heterotrophic denitrification is the major contributor of transforming nitrate into gas. However, the hydrogen autotrophic denitrification exists in the reactor and contributes to extra transformation of N into gas. In addition, the anammox process using nitrite from the incomplete nitrification as electron acceptor helped in reducing the production of nitrate in the reactor. Therefore,

anammox with the other two denitrification processes (heterotrophic and H-denitrification) working simultaneously in one reactor ensures an effluent with a very low nitrate concentration, which was the case in this study.

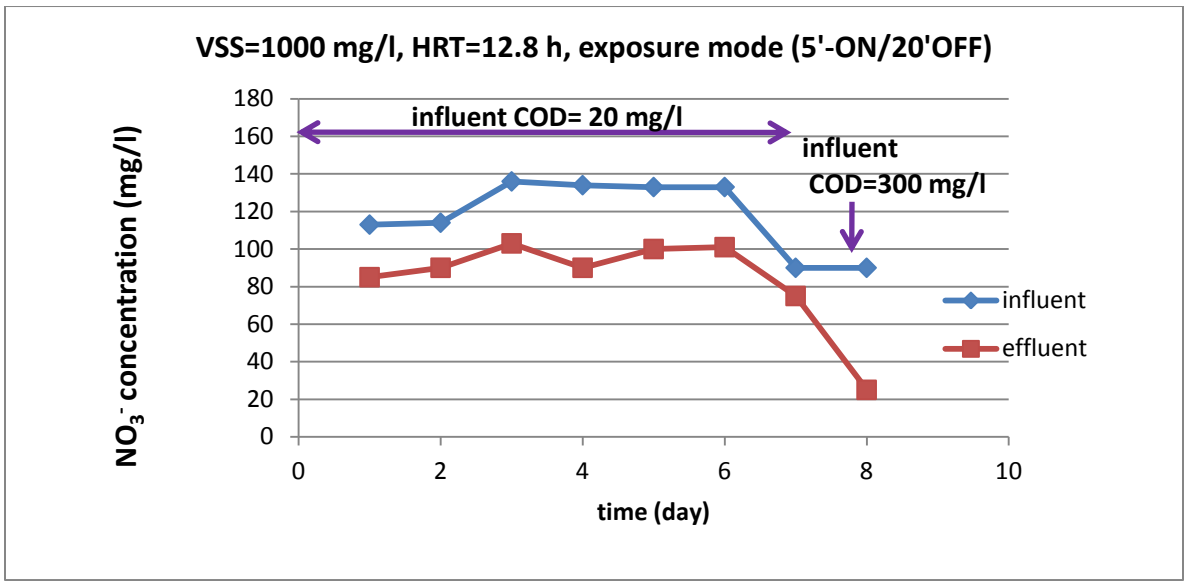

Figure 8.19: Nitrate concentrations in the influent and the effluent of SMEBR at low and high chemical oxygen demand (COD) concentrations

8.7 Conclusions

Based on this research, the electro-bioreactor has proved its capability for high removal efficiency of the unwanted nutrients (N and P) in addition to C in one single operation unit. The studies showed removal efficiencies up to more than 97% for all nutrients when the electrical parameters and the other operating conditions (HRT, MLSS, DO and organic loading) were adjusted for that purpose. Carbon was removed through biomass oxidation, phosphorus was removed through the formation of aluminum phosphate complexes, while N was transformed into nitrogen gas through changing the ORP between -150 to 150 mV to promote the simultaneous nitrification/denitrification

processes in the reactor. Nitrification potential was enhanced up to 25% in the SMEBR due to the activation of anammox as another nitrification process working in harmony with the aerobic nitrifiers, while the MBR does the nitrification only through the autotrophic nitrification.

Chapter 9

Phase 2(Stage 1): Results and discussion - sludge properties

This chapter discusses the changes of sludge characteristics inside the SMEBR. Understanding these changes enable the understanding of membrane fouling reduction, which will be discussed in Chapter 10.

9.1 Sludge pH

As illustrated in Chapter 3, hydroxide ions are generated at the cathode through the production of hydrogen gas (Equation 3.3) and the reduction of oxygen molecules (Equation 3.4). The formation of hydroxide ions and then the increasing of sludge pH are proportional to the CD and the length of time-ON. However, at the applied electrical parameters in Phase 1, the increase of sludge pH was between 1 to 2 orders (Figure 9.1 and 9.2) over the whole operating period. Though, the final magnitude of pH was still around neutrality that ensures a favorable condition for microbial growth.

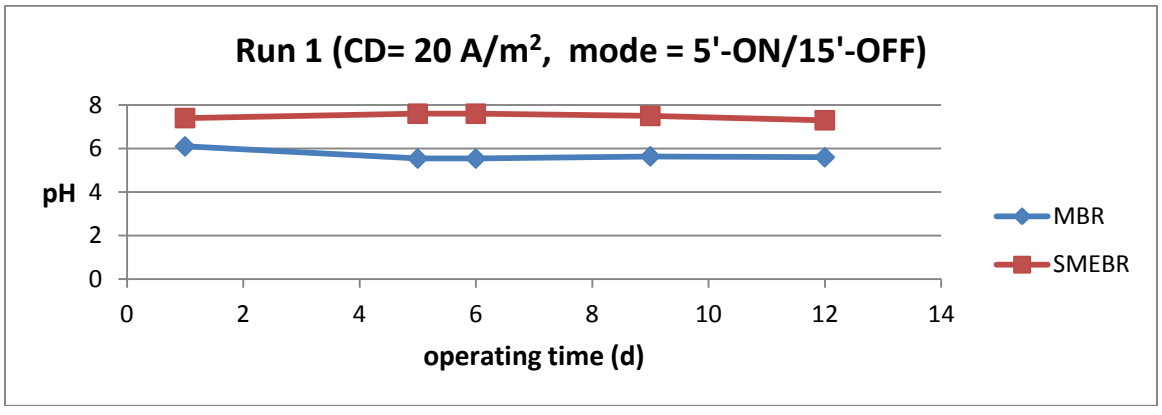

Figure 9.1: Run 1: Changes of sludge pH over time in the SMEBR and MBR

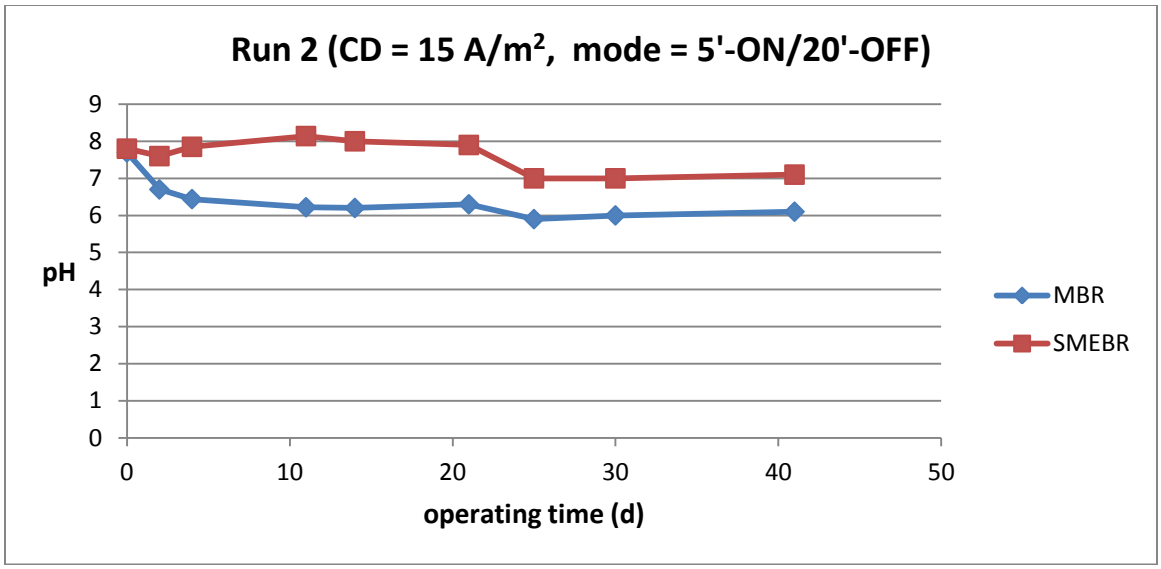

Figure 9.2: Run 2: Changes of sludge pH over time in the SMEBR and MBR

9.2 Sludge electrical conductivity (EC)

The concentration of soluble salts (ions) represented as EC decreased in the SMEBR within a range of 50 to 150 µs/cm compared to MBR (Figures 9.3 and 9.4). Two major mechanisms are contributing for this reduction. Firstly, the electro-migration that causes the deposition of ions on the electrodes surfaces or the other solid surfaces in the sludge liquor. Secondly, due to the removal of nitrate through the denitrification process once the system is adjusted to work at low DO concentration and low ORP. The existence of soluble ions in the sludge liquor is crucial because of its role in conducting the current. Higher concentrations of ions require less voltage gradient to obtain the required CD, which is better in terms of cost and its impact on biomass activity. However, the reduction of EC in the SMEBR should be accompanied by a slight increase in the voltage gradient to maintain the same operating CD.

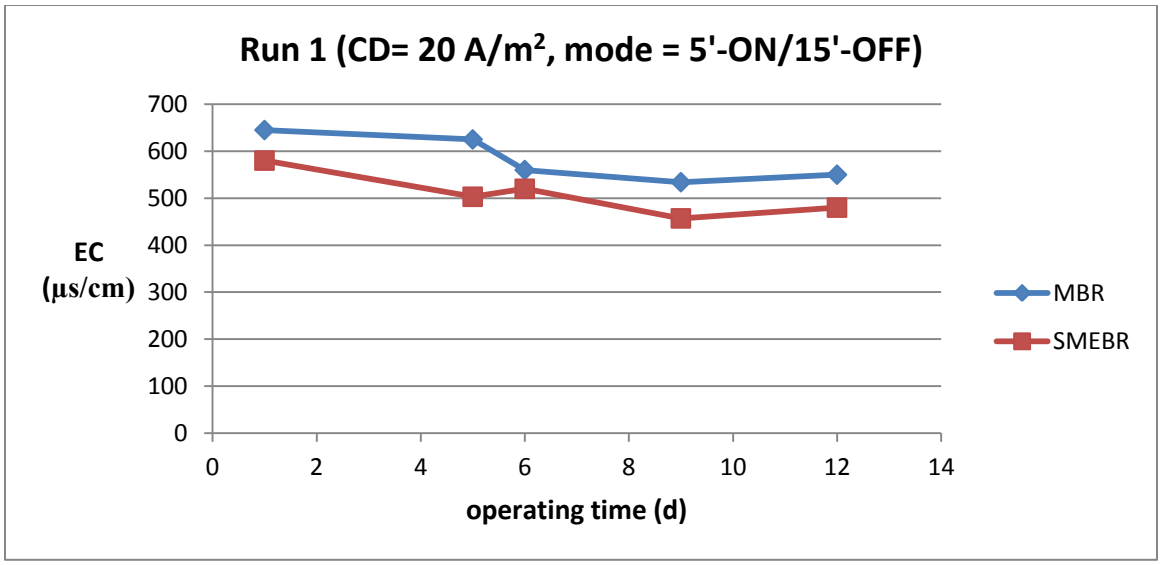

Figure 9.3: Run 1: Changes of sludge EC over time in the SMEBR and MBR

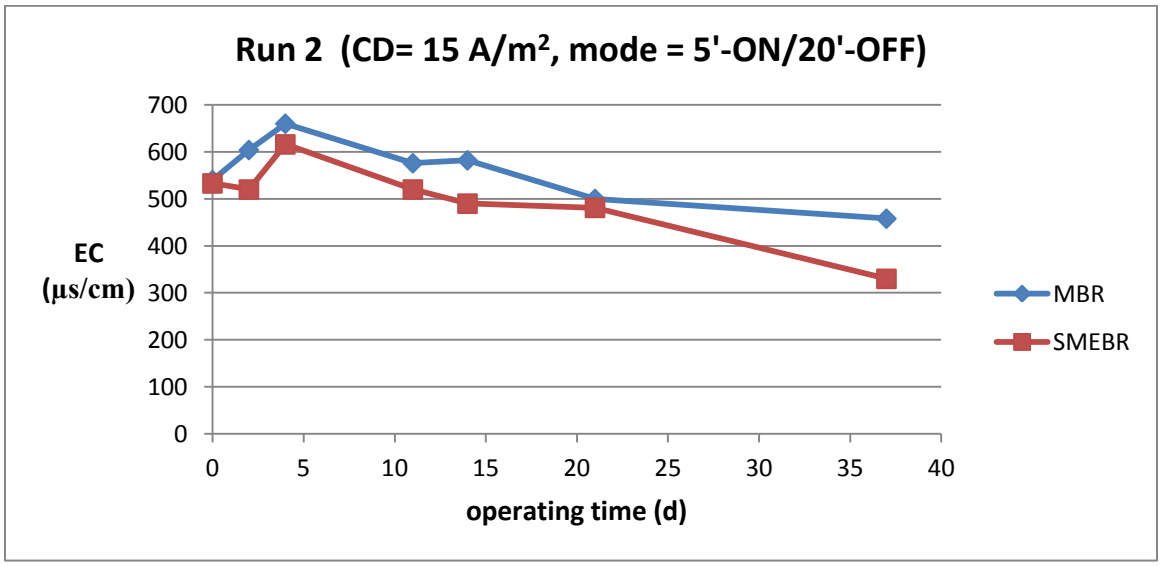

Figure 9.4: Run 2: Changes of sludge EC over time in the SMEBR and MBR

9.3 Sludge solids

The electro-coagulation process involves the production of Al^{+3} from the anode followed by the formation of aluminum hydroxides. These hydroxides are considered as

suspended solids and a part of the sludge to be wasted in the treatment plant. Thus, the CD and electrical mode that operate the SMEBR should be selected at levels that do not produce much of this inorganic sludge. Despite that the production of this type of sludge is indispensable, the production rate is controllable. In Run 1, the concentration of the fixed suspended solids (FSS) in MBR over the operating period was almost stable at around 500 mg/l (Figure 9.5) and the percentage of the volatilized suspended solids (VSS) was around 85% (Figure 9.7) of the total MLSS. On the other hand, the situation in the SMEBR was very different. The FSS due to the accumulation of aluminum hydroxides in the SMEBR increased up to 9000 mg/l (Figure 9.6). This increase of the FSS led to 30% contribution of the VSS of the total MLSS (Figure 9.7). This rate of FSS production in Run 1 is very high and unacceptable. Therefore, the electrical operating conditions of Run 1 should be adjusted so that the FSS production rate is minimized. This was the reason behind ending up that run after 13 days and starting Run 2 at lower CD and longer time-OFF.

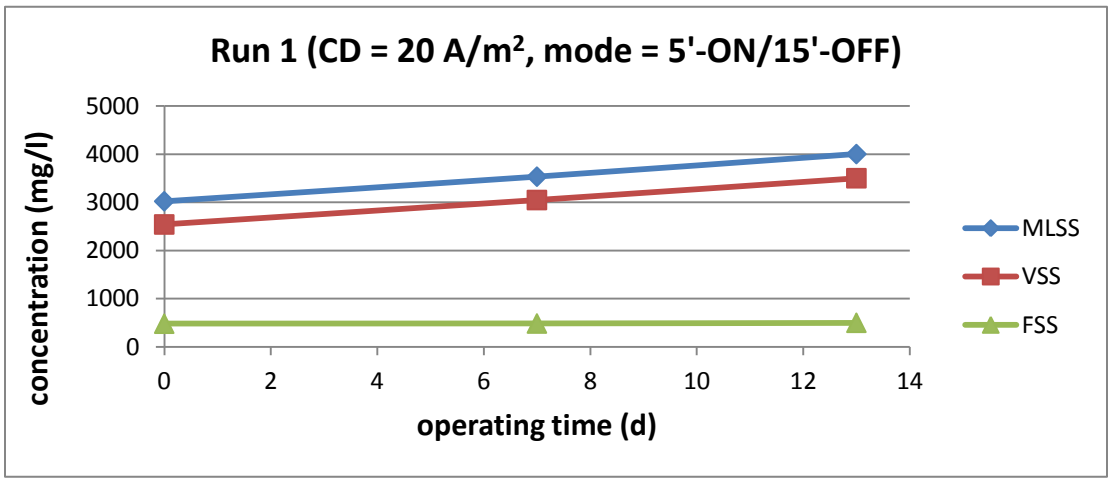

Figure 9.5: Run 1: Changes of MLSS, VSS and FSS concentrations over time in the MBR

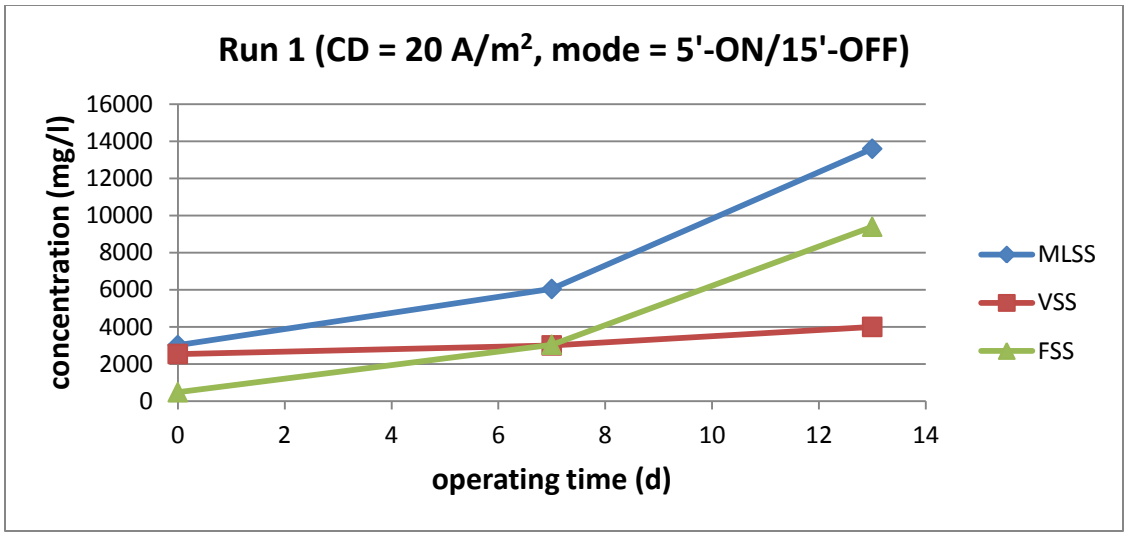

Figure 9.6: Run 1: Changes of MLSS, VSS and FSS concentrations over time in the SMEBR

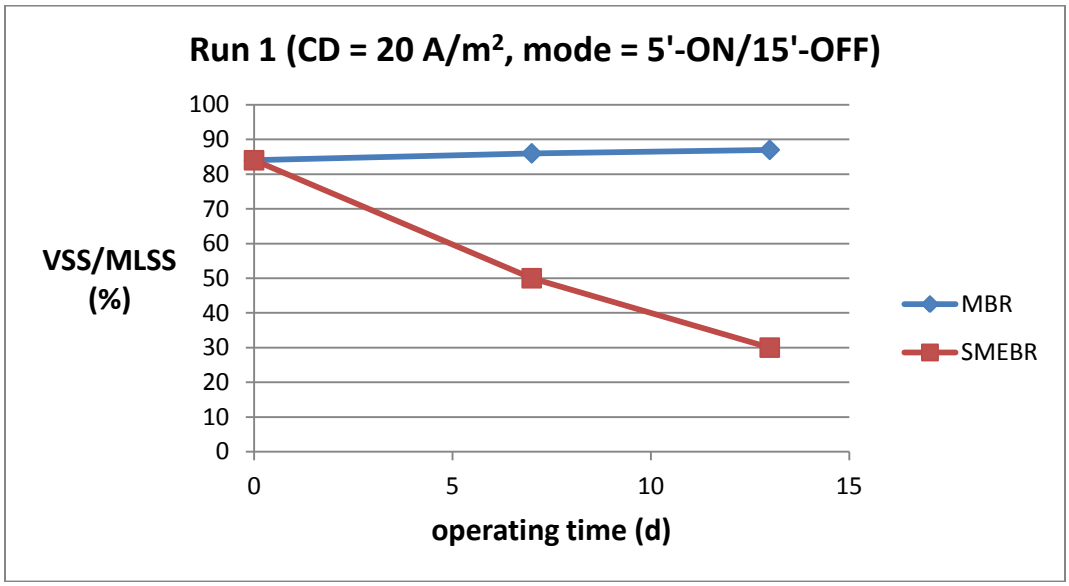

Figure 9.7: Run 1: Changes of the (VSS/MLSS) percentage in the SMEBR and MBR over time

In Run 2, the concentration of MLSS in the MBR increased over the operating time and peaked at a level equal to 9000 mg/l with nearly 85% contribution of VSS (Figure 9.8). Sludge liquor was diluted 50% on day 35 to minimize the high fouling rate at that level of suspended solids. In SMEBR, the concentration of VSS was almost the same as in the

MBR at nearly 9000 mg/l (Figure 9.9), but the concentration of FSS was almost 9 times higher than that in the MBR due to the formation of aluminum hydroxides and contributed to nearly 50% of the MLSS (Figure 9.10). Running the SMEBR at CD = 15 A/m^2 and electrical mode of 5'-ON/20'-OFF sounds reasonable regarding the benefits gained at that amount of inorganic sludge produced. However, the sludge produced has a better dewaterability nature than the MBR that reduces the ultimate volume of sludge to be disposed.

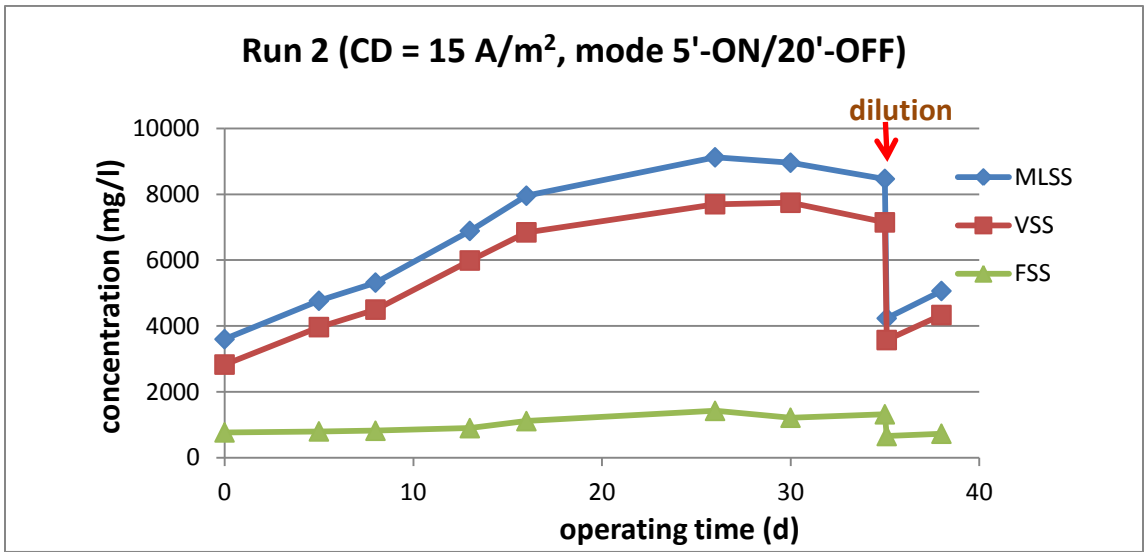

Figure 9.8: Run 2: Changes of MLSS, VSS and FSS concentrations over time in the MBR

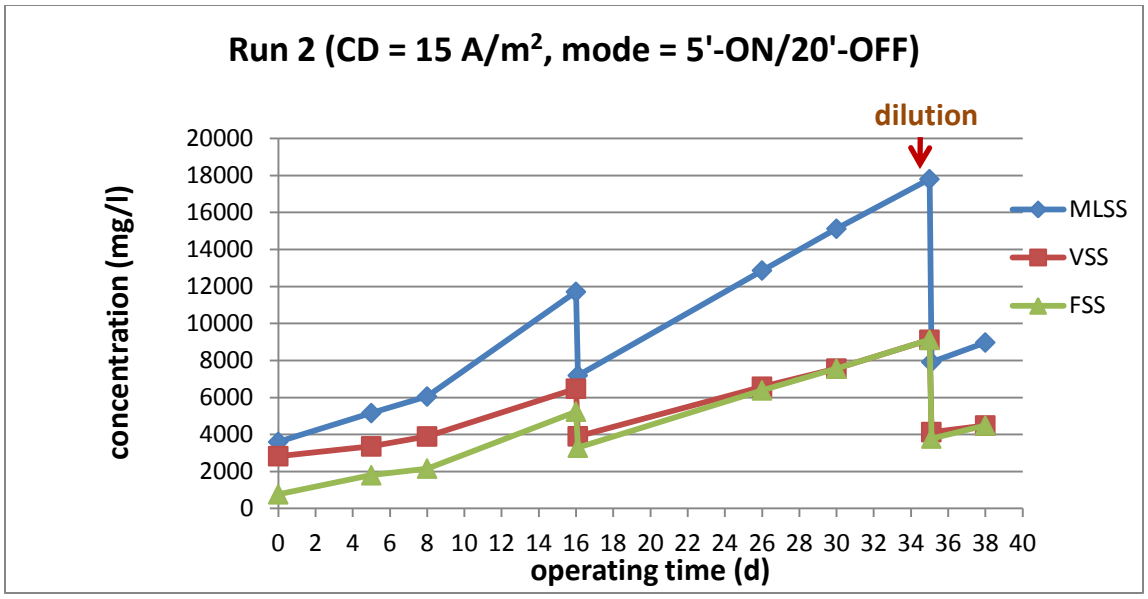

Figure 9.9: Run 2: Changes of MLSS, VSS and FSS concentrations over time in the SMEBR

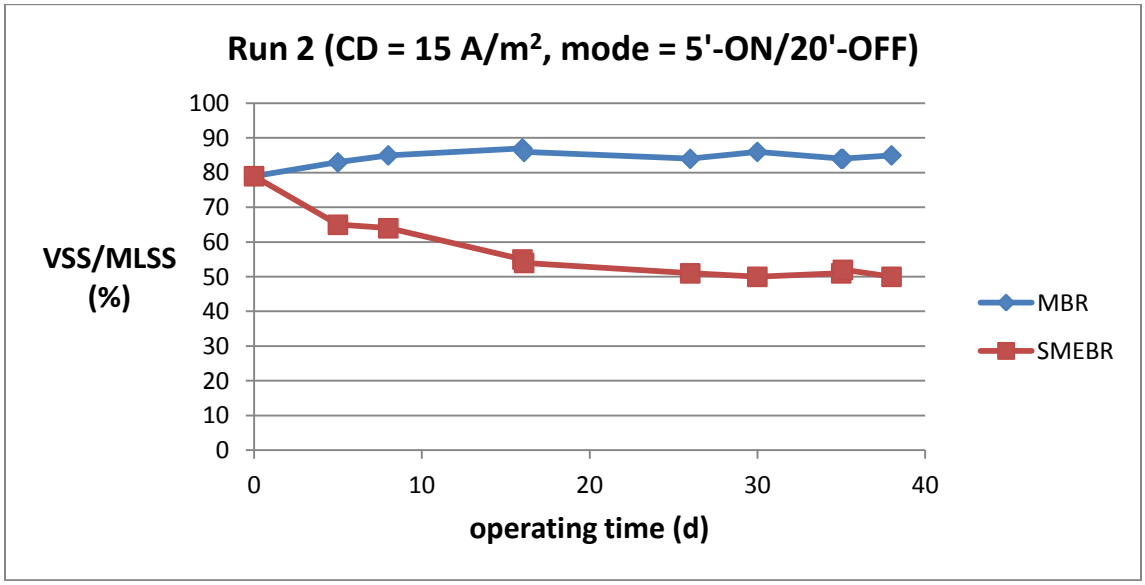

Figure 9.10: Run 2: Changes of the VSS/MLSS percentage in the SMEBR and MBR over time

Run 3 was operated at the same electrical operating conditions of Run 2 but at variable HRT and ammonium concentration in the influent. Results were similar to that of Run 2 (Figures 9.11 to 9.13). The SMEBR at the end of 24 days of operation ended up at nearly 50% of both FSS and

VSS. lower amounts of inorganic sludge could be produced at lower CD and longer time-OFF. But, going into this direction is restricted to the concentration of phosphorus concentration in the influent wastewater. In our study, it was found that neither the decrease of CD nor the increase of time-OFF was a solution to reduce the sludge production and maintain high removal efficiency of phosphorus.

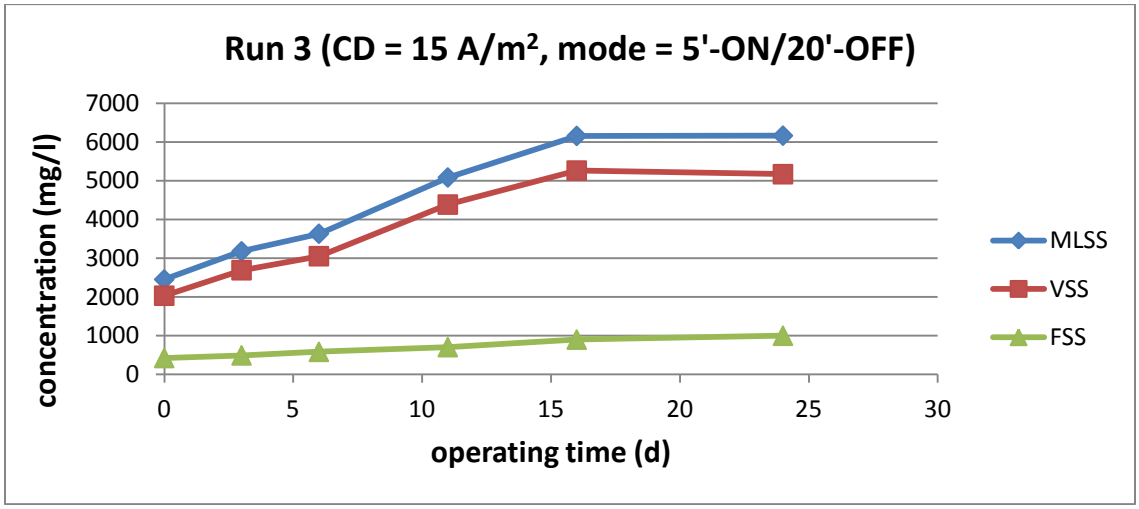

Figure 9.11: Run 3: Changes of MLSS, VSS and FSS concentrations over time in the MBR

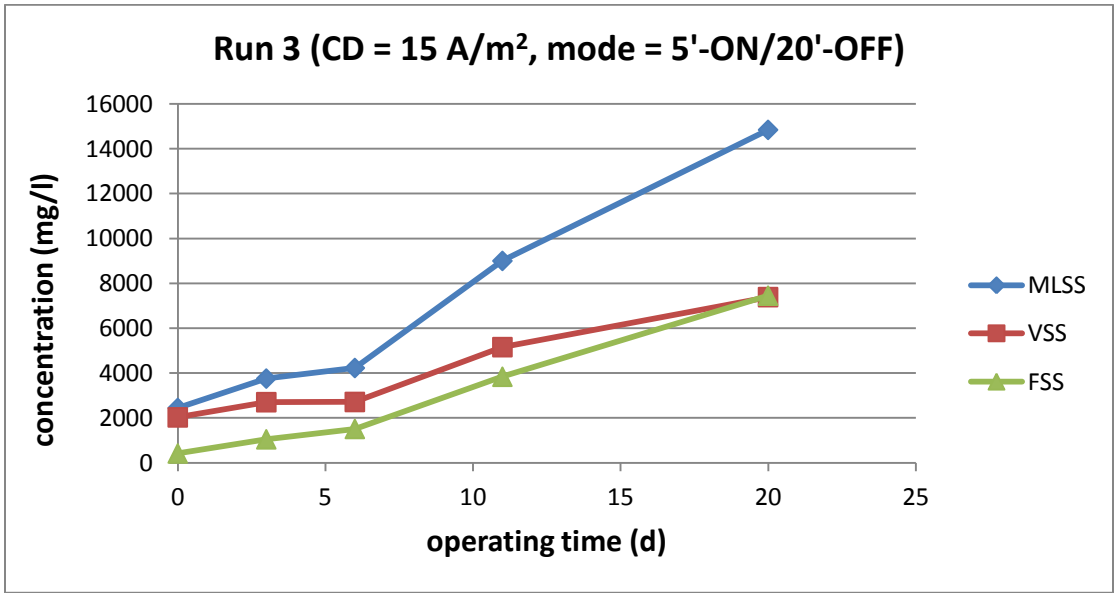

Figure 9.12: Run 3: Changes of MLSS, VSS and FSS concentrations over time in the SMEBR

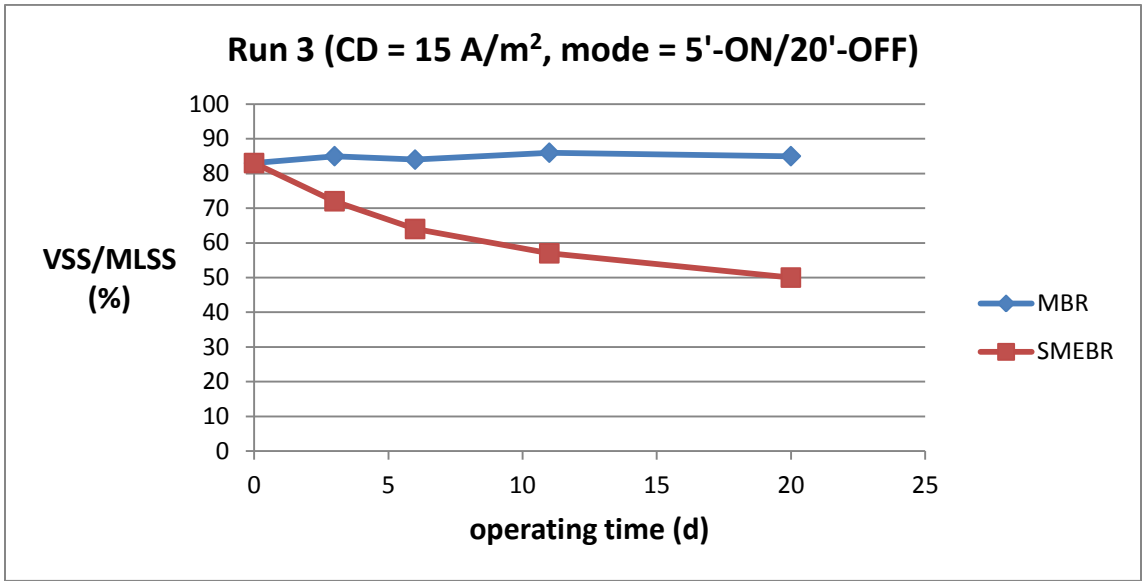

Figure 9.13: Run 3: Changes of the VSS/MLSS percentage in the SMEBR and MBR over time

9.4 Colloidal materials

SMEBR exhibited a substantial removal of colloidal materials due to the electro-coagulation processes (Figures 9.14 and 9.15). The removal of colloids was almost complete in the SMEBR. This high removal of colloids is a big reason of improving the effluent quality and reducing the membrane fouling, particularly, the irreversible fouling.

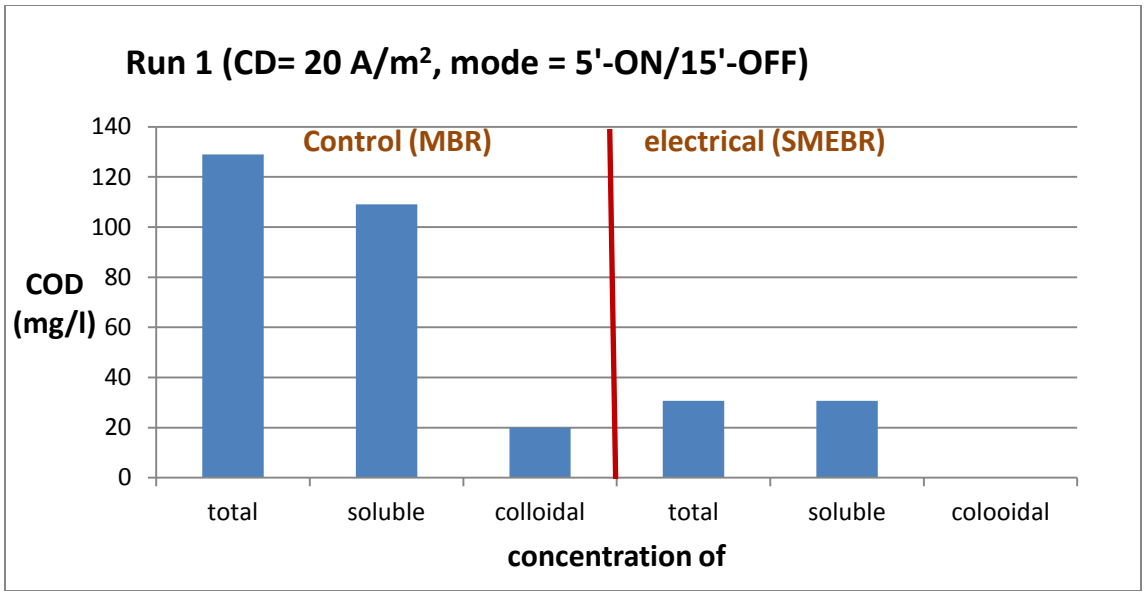

Figure 9.14: Run 1: The concentrations of (total, soluble and colloidal) COD in the sludge supernatant on day 7

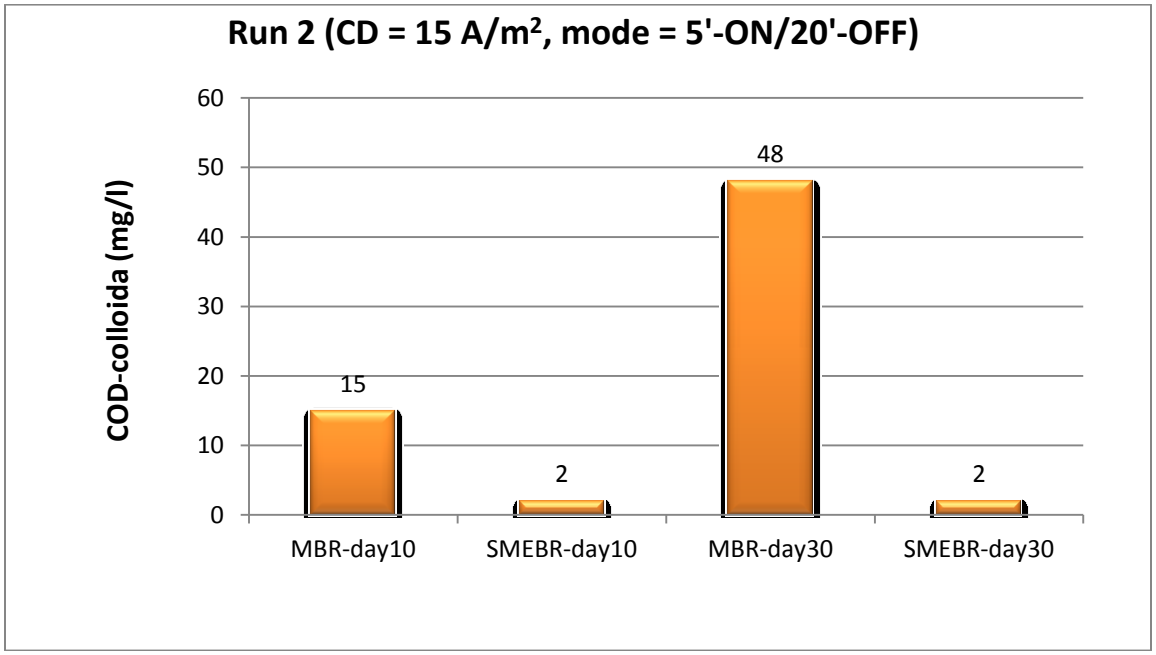

Figure 9.15: Run 2: The concentrations of the colloidal COD in the sludge supernatant on days 10 and 30 in the SMEBR and the MBR

9.5 SMP (protein)

Run 1 (Figure 9.16) showed a substantial removal of protein from the sludge supernatant. The first days did not exhibit a big difference between the MBR and SMEBR, but after 6 days of operation the removal starts becoming obvious up to nearly 55% on day 12 (Figure 9.17). Protein concentration in the sludge supernatant in this run was higher than the other runs due to the high concentration of protein in the influent. This high protein concentration increases membrane fouling as will be discussed later.

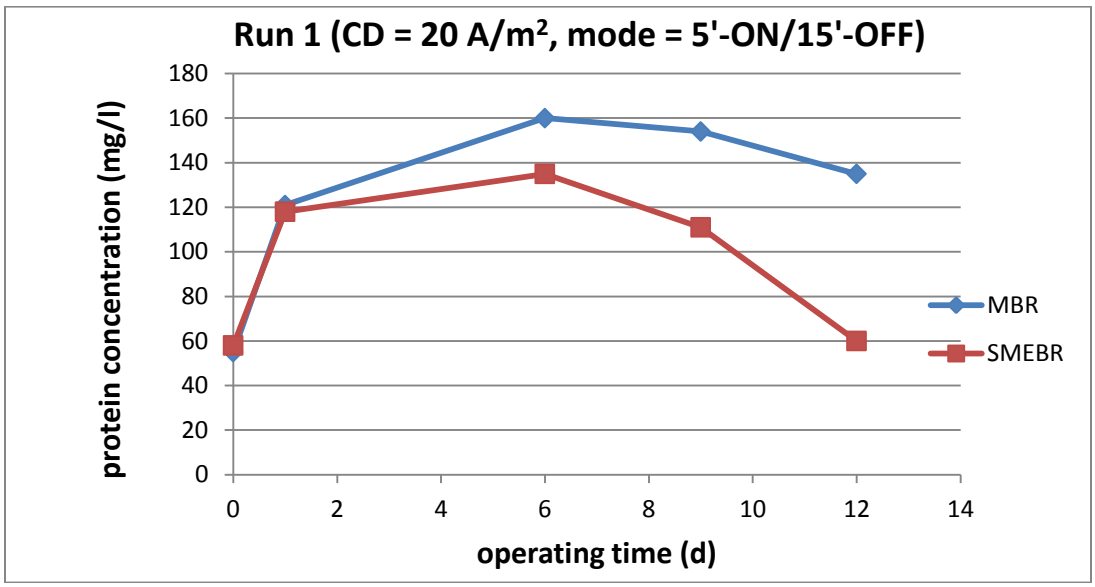

Figure 9.16: Run 1: Protein concentrations in the supernatant of SMEBR and MBR

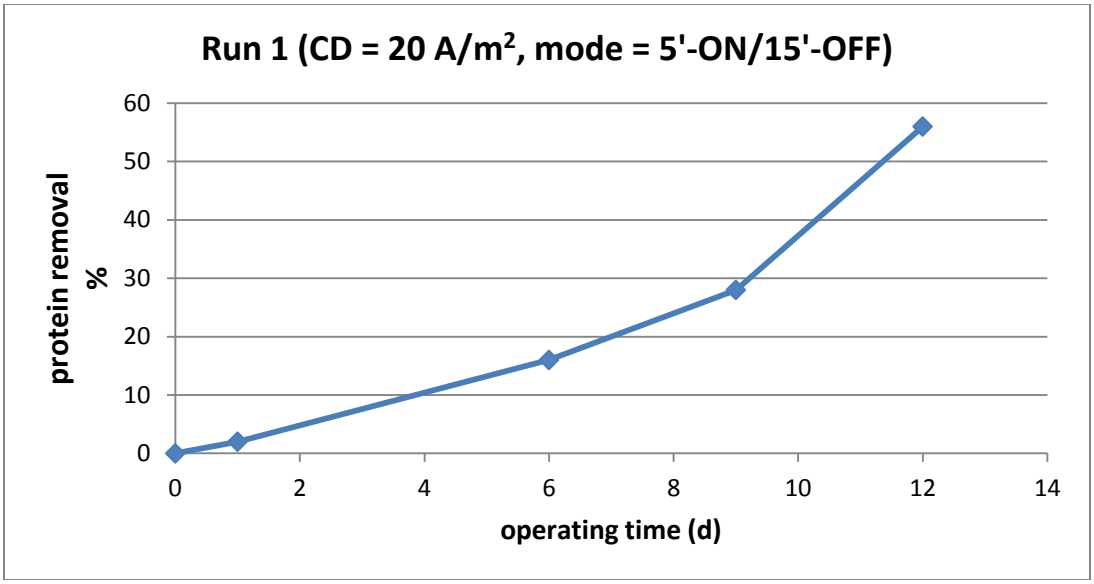

Figure 9.17: Run 1: Protein removal percentage in the SMEBR compared to that of the MBR

In Run 2, protein removal from the SMEBR sludge supernatant to a level lower than that of the MBR started on day 12 (Figure 9.18). Afterward, the removal efficiency was almost around 40% over the whole operating period (Figure 9.19). Run 2 showed that the effluent in each reactor has a slightly lower concentration of protein than it is in the sludge supernatant. This indicates that the majority of the protein molecules have molecular size less than the membrane pore size (0.04 µm) that permitted the passage of protein through the membrane into the effluent.

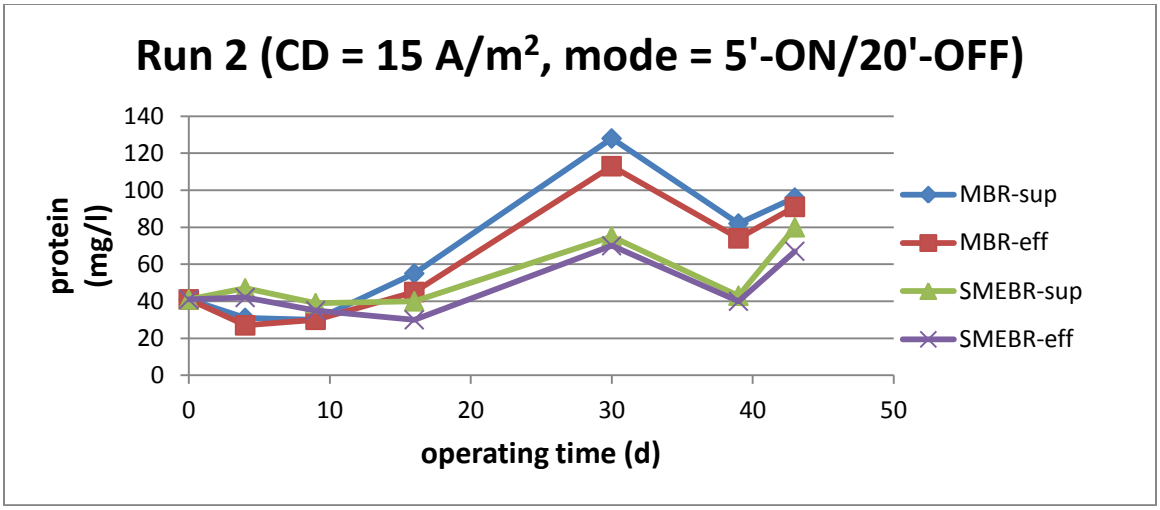

Figure 9.18: Run 2: Protein concentrations in the supernatant and effluent of SMEBR and MBR

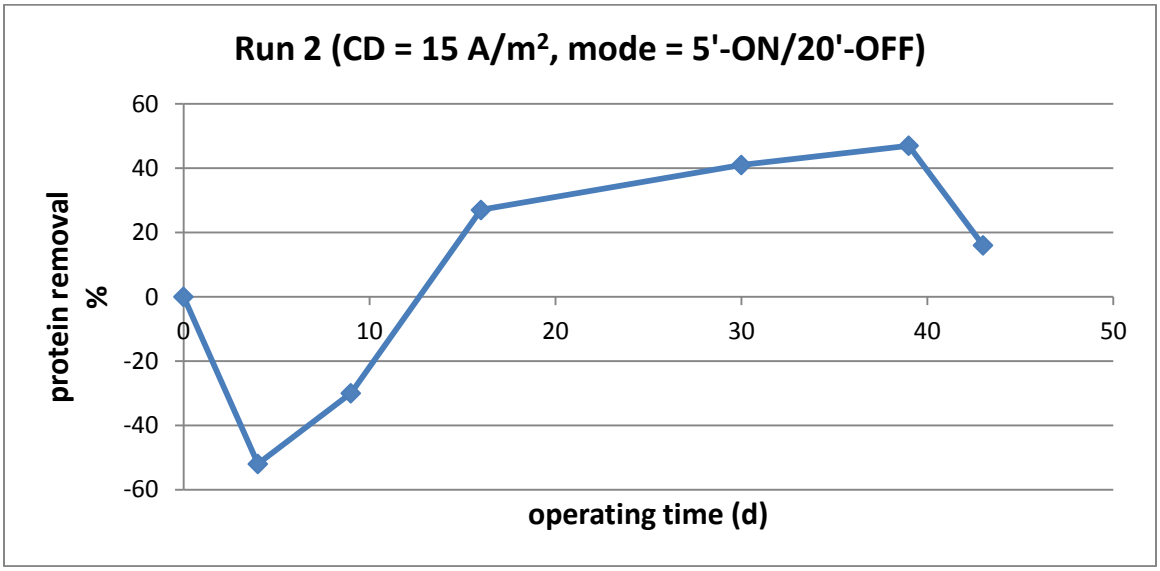

Figure 9.19: Run 2: Protein removal percentage in the SMEBR compared to that of the MBR

Results of Run 3 showed the same trend of Run 1 and Run 2. The first few days of operation showed an increase of protein in the sludge supernatant (Figure 9.20). This initial increase of protein witnessed in the three runs of Phase 2 is likely due to the initial reaction of the microbial biomass to the electrical shock that led to the release of some protein. After nearly a week of adaptation period, a substantial removal of protein

was observed. The removal percentage of protein was between 25 to 55 % over the whole operating period (Figure 9.21).

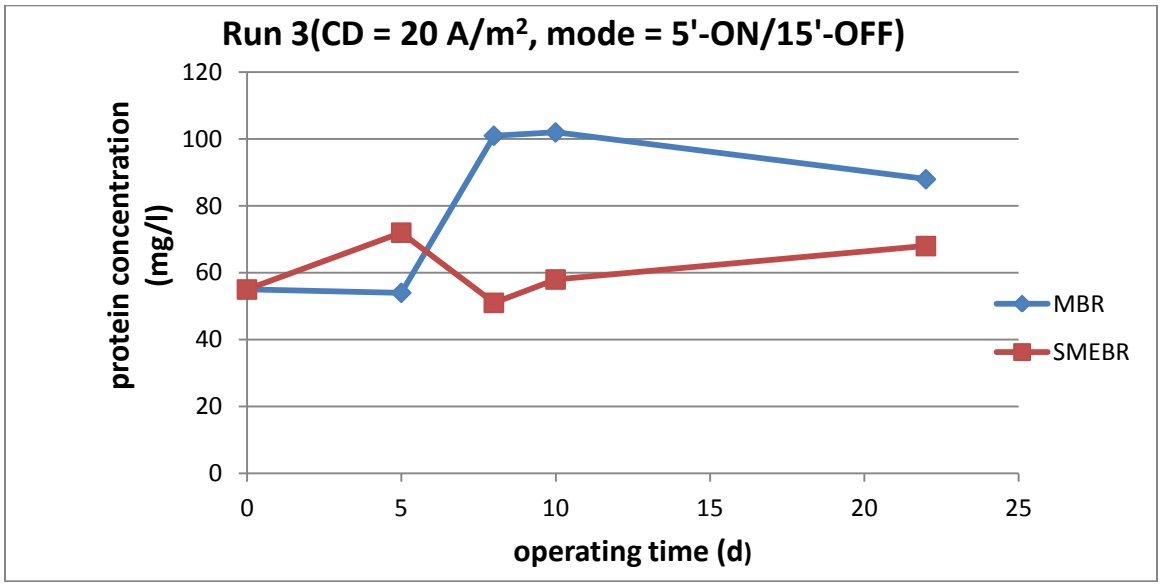

Figure 9.20: Run 3: Protein concentrations in the supernatant of SMEBR and MBR

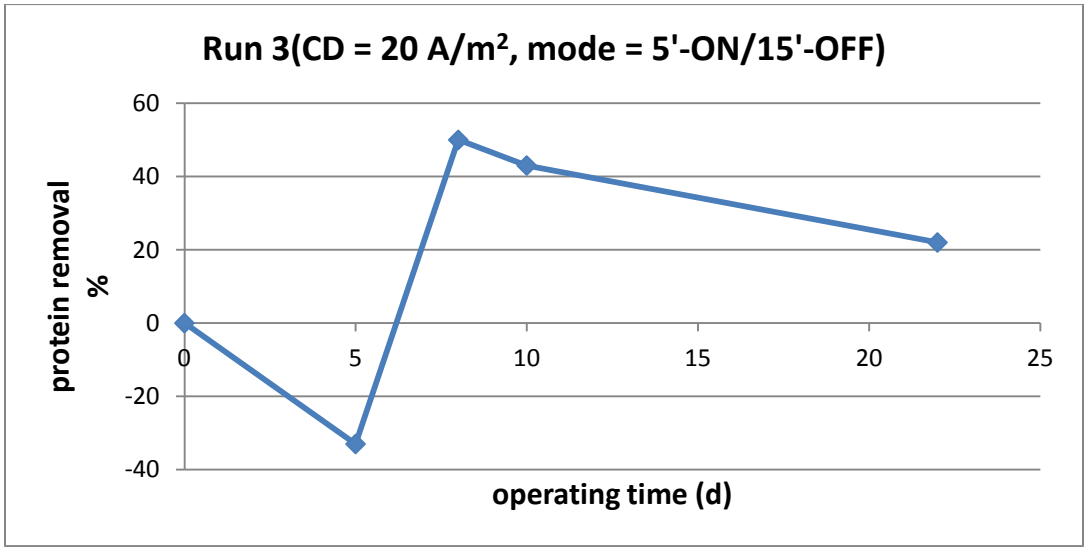

Figure 9.21: Run 3: Protein removal percentage in the SMEBR compared to that of the MBR

9.6 SMP (polysaccharides)

SMEBR exhibited substantial removal of polysaccharides than the MBR in all runs of Phase 2 (Figures 9.22 to 9.24). The behavior of polysaccharides in the MBR and SMEBR is different from protein in several ways. Firstly, the removal efficiency was much higher than that of protein. The removal efficiency of polysaccharides was up to 90 % (Figures 9.25 to 9.27), while the maximum removal efficiency of protein was around 50%. Secondly, MBR (Run 2 and Run 3) showed a big difference between the concentration of polysaccharides in the effluent and supernatant; it was much higher in the supernatant. However, the concentration of polysaccharides was nearly the same in the effluent and the supernatant of the SMEBR. These results are justified by the higher molecular weight of polysaccharide molecules than the protein. Organic materials with higher molecular weight and larger surface area are easier to coagulate with other solid surfaces in the sludge liquor and easier to be retained by the membrane pore size so that they don't pass through. Thirdly, a polysaccharide increase was not observed during the first days of operation unlike the protein. On the contrary, the removal was there from the beginning. It is likely that the microbial biomass initially responds to the electrical shock by secreting enzymes of protein nature to defend or adapt with the new system. Its high removal efficiency masked any likely release of polysaccharide during the adaptation period.

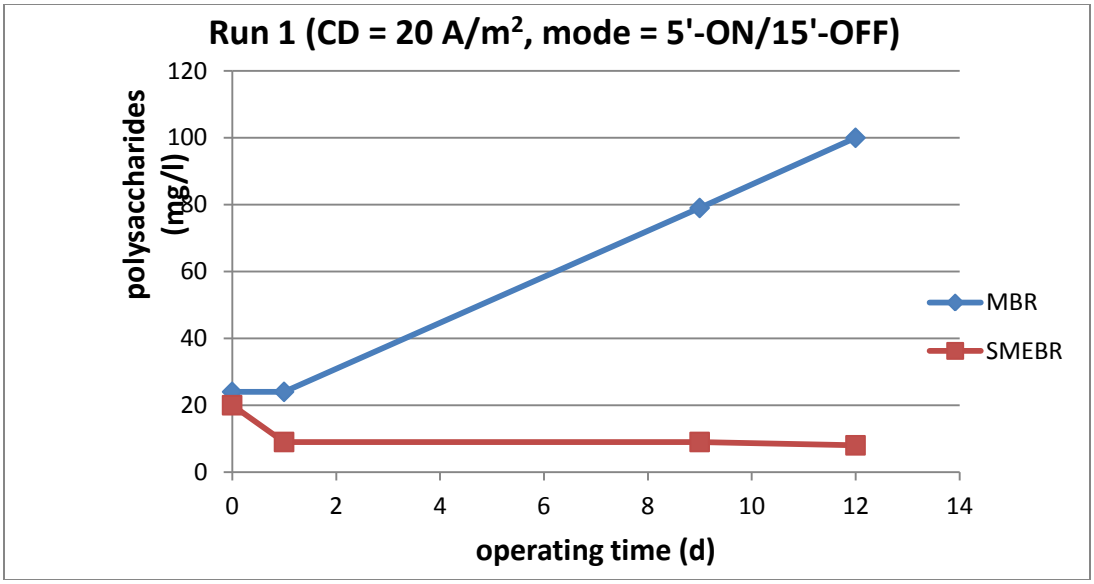

Figure 9.22: Run 1: Polysaccharides concentrations in the supernatant of SMEBR and MBR

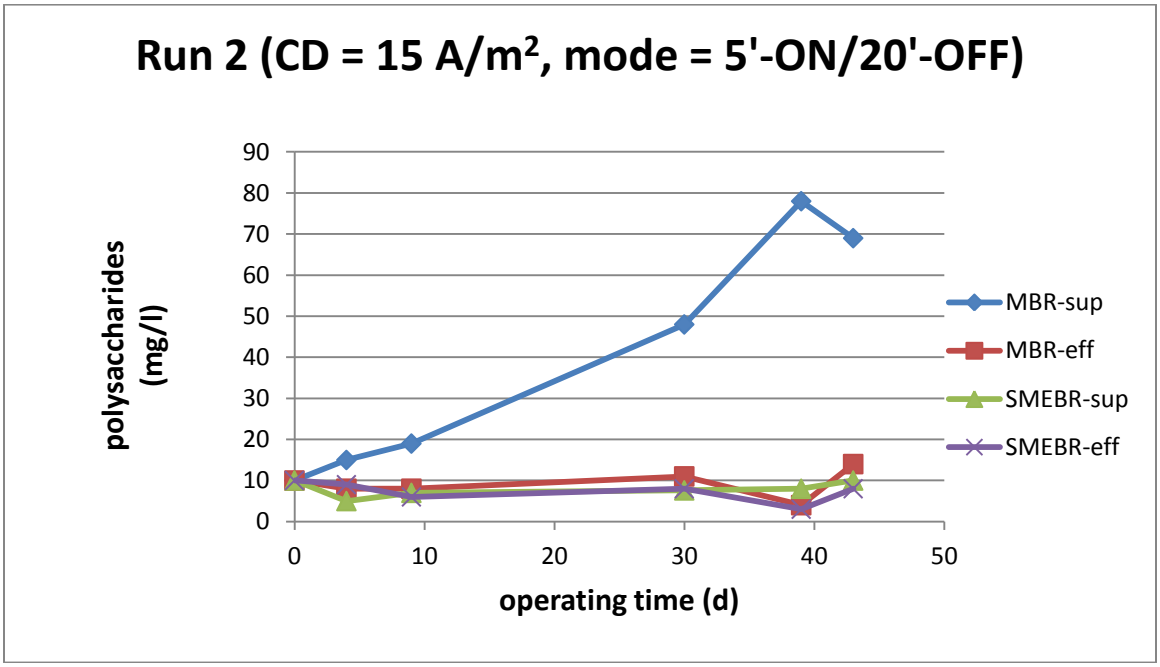

Figure 9.23: Run 2: polysaccharide concentrations in the supernatant and effluent of SMEBR and MBR

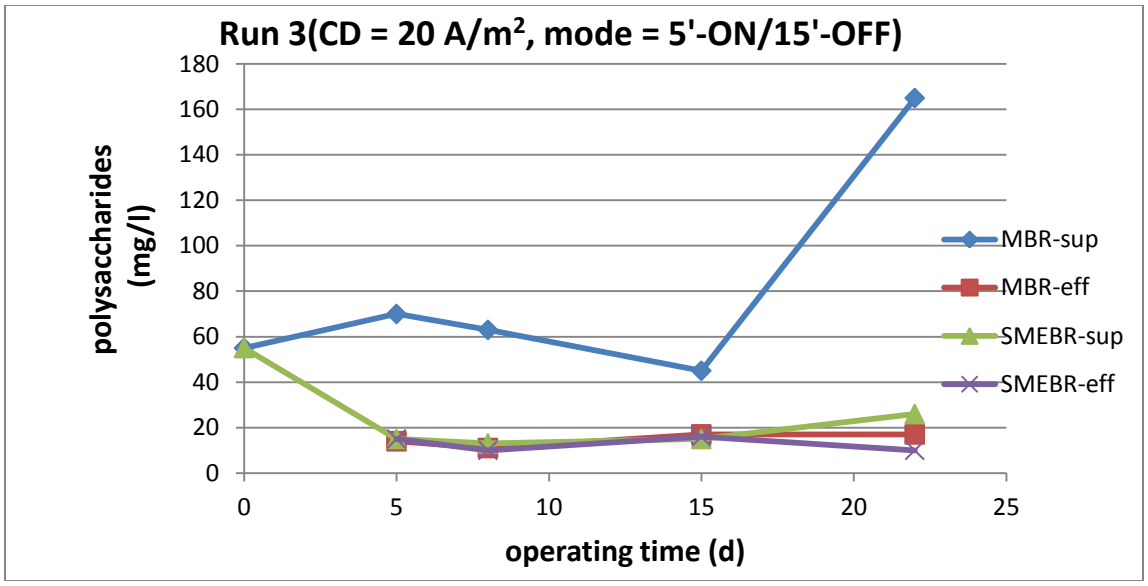

Figure 9.24: Run 3: Polysaccharide concentrations in the supernatant and effluent of SMEBR and MBR

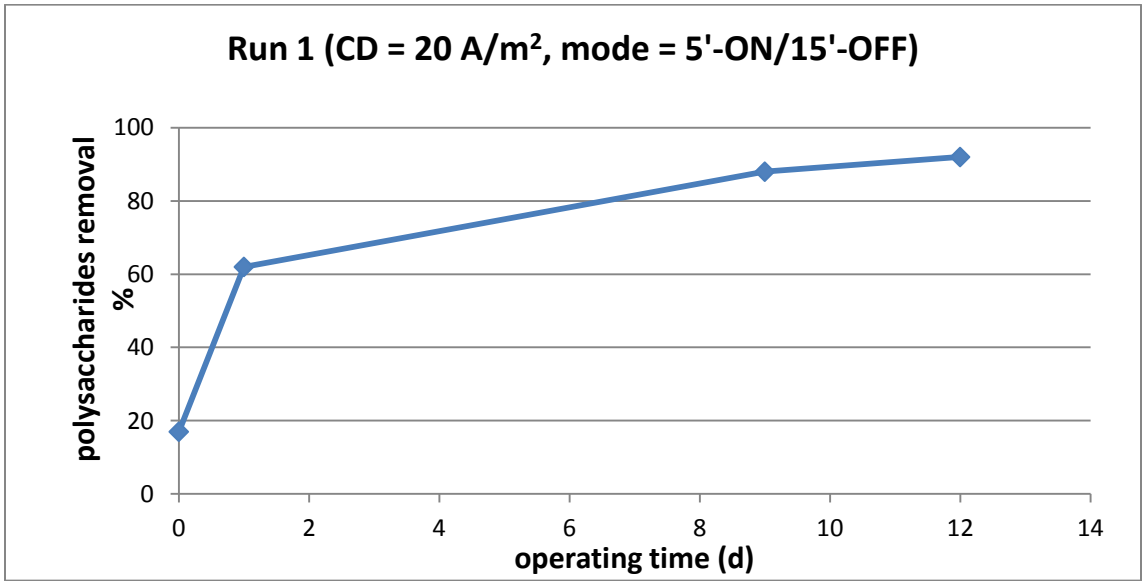

Figure 9.25: Run 1: Polysaccharide removal percentage in the SMEBR and the MBR

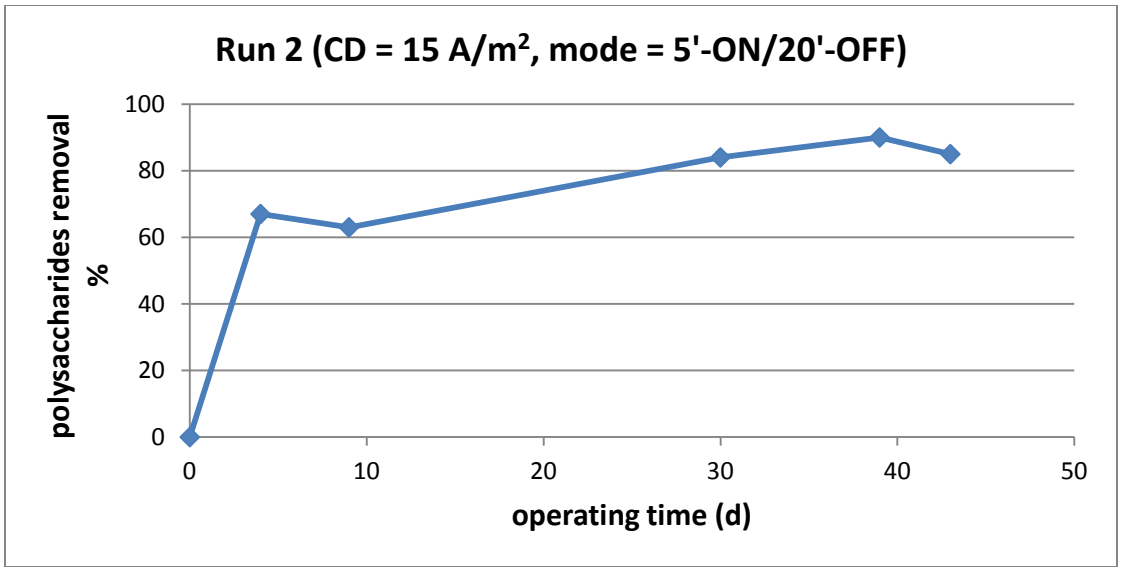

Figure 9.26: Run 2: Polysaccharide removal percentage in the SMEBR and the MBR

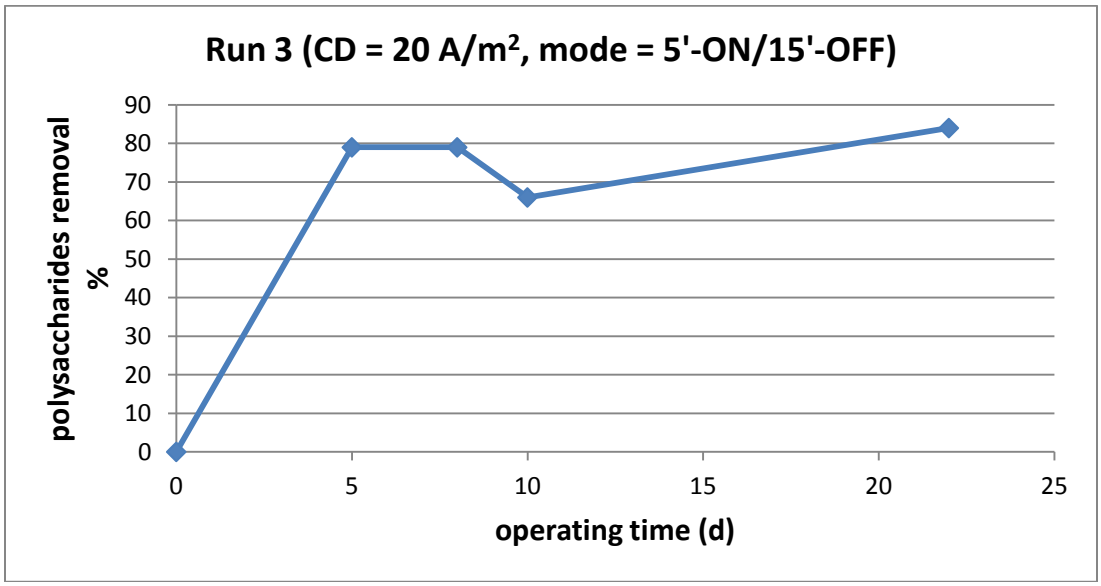

Figure 9.27: Run 3: Polysaccharide removal percentage in the SMEBR and the MBR

9.7 Tightly bound water

Tightly bound water represents the amount of water that is still retained by the sludge after the physical extraction of water. In MBR, the amount of tightly bound water was higher than 20 g.water/g.SS, while in the SMEBR, it was around 6 g.water/g.SS over the whole operating period for all runs of Phase 2 (Figures 9.28 to 9.30). The reduction of tightly bound water in the suspended solids (SS) is attributed to the removal of water from the electrical double layer through the electro-osmosis. Also, due to the changes in the structure of the SS. The SS in the SMEBR have a higher percentage of inorganic solids, which is likely to have less electrostatic attraction forces to water than the organic materials. However, less bound water in the sludge means less volume and lower cost in the treatment facilities.

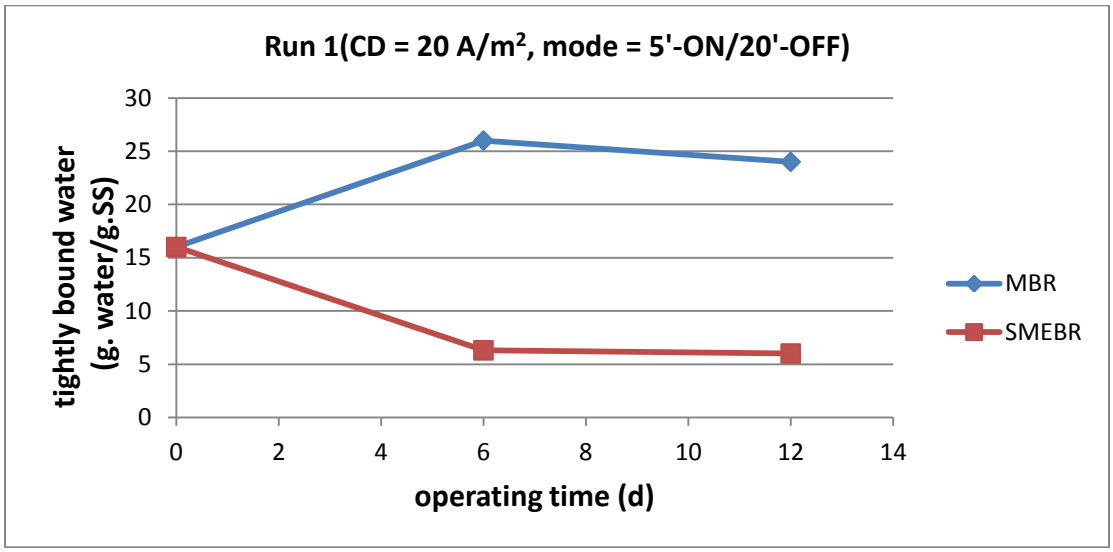

Figure 9.28: Run 1: Comparison of the tightly bound water in SMEBR and MBR

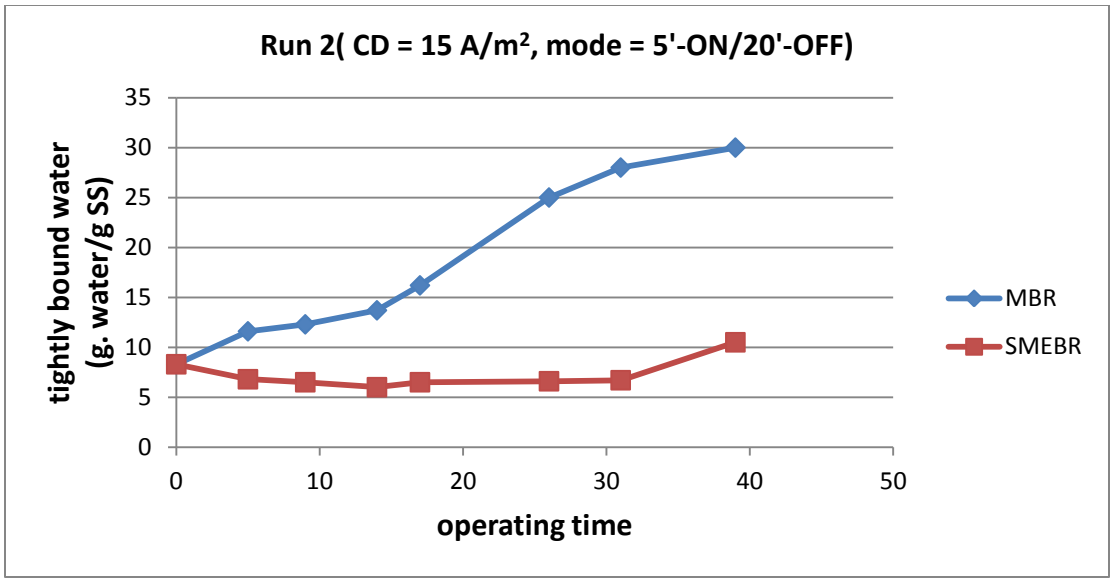

Figure 9.29: Run 2: Comparison of the tightly bound water in SMEBR and MBR

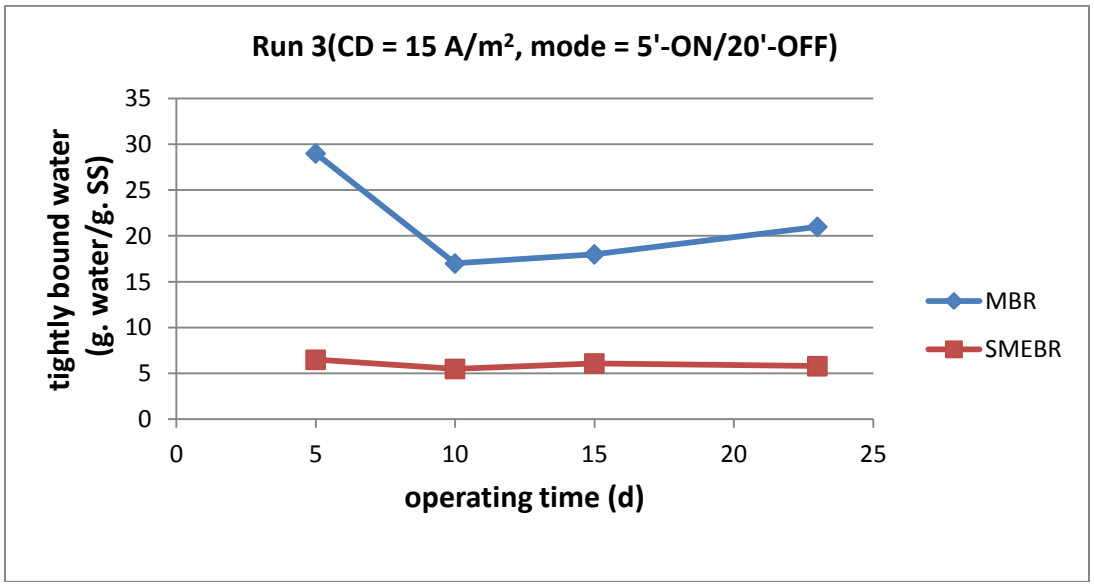

Figure 9.30: Run 3: Comparison of the tightly bound water in SMEBR and MBR

9.8 Specific resistance to filtration (SRF)

Lower specific resistance to filtration (SRF) leads to easier sludge dewaterabilty and less membrane fouling rate. The applied CD and the electrical modes in this phase showed a substantial reduction of SRF in all runs (Figures 9.31 to 9.33). The reduction of SRF in the SMEBR is fast and requires only a few days to reach its maximum reduction, afterward the SRF was stabilized. On the other hand, MBR exhibited an increase of SRF over time. For example, in Run 2, the SRF of the sludge liquor in the SMEBR reduced from 27×10^{12} to 2.4×10^{12} m/kg after 5 days of operation. The SMEBR maintained a low value of SRF between 4 to 9 $m.10^{12}$/kg over the whole operating period. Meanwhile, the SRF in the MBR kept increasing up to 690×10^{12} m/kg, at which the SMEBR showed lower resistance by 141 times (Table 9.1). This increase in the MBR is due to the increase of the MLSS and the concentration of SMP in the sludge supernatant. The electrical field is likely to exhibit improved SRF at higher MLSS and higher concentration of SMP due to its capability to extract the tightly bound water through electroosmosis and to remove the SMP through electrocoagulation.

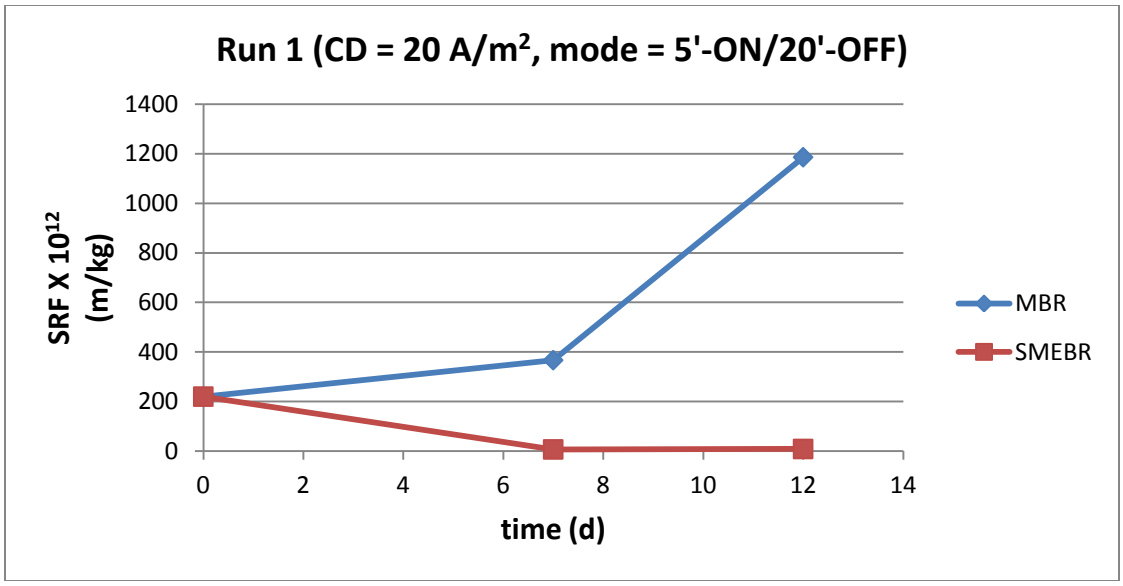

Figure 9.31: Run 1: Changes of SRF over time for SMEBR and MBR

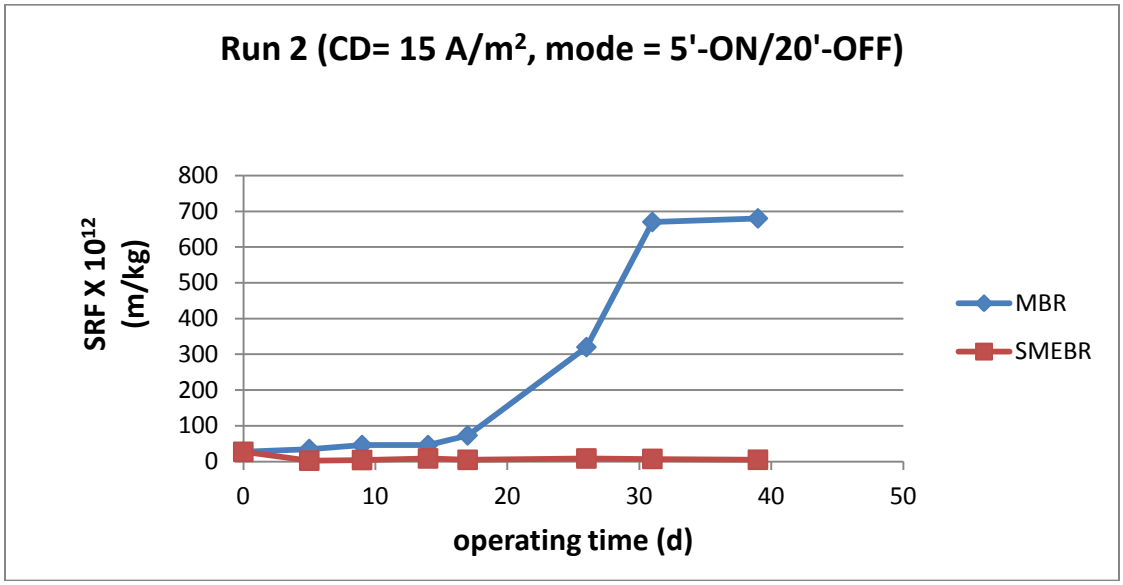

Figure 9.32: Run 2: Changes of SRF over time for SMEBR and MBR

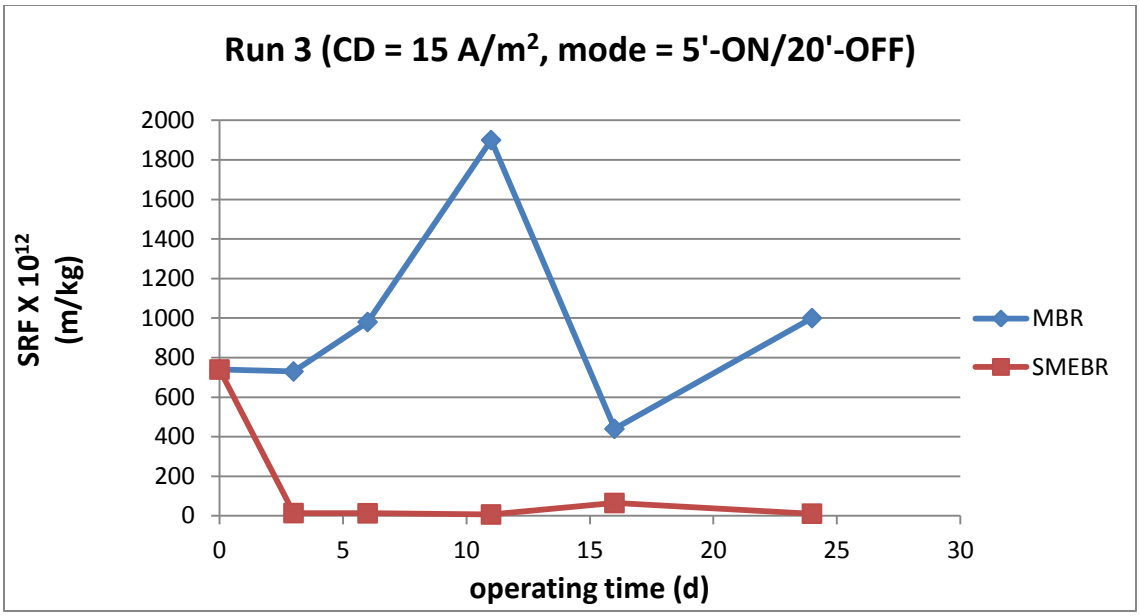

Figure 9.33: Run 3: Changes of SRF over time for SMEBR and MBR

Table 9.1: Comparison of the SRF (m/kg) of the SMEBR to that of MBR in Run 2

Time (d)	MBR X 10^{12}	SMEBR X 10^{12}	(SRF-MBR/SRF-SMEBR)
0	27	27	1
5	35	2.4	14
9	46	4.2	10
14	46	8.6	5.3
17	73	4.7	15
26	320	8.4	38
31	670	7.2	93
39	680	4.8	141

Pictures of the SMEBR and MBR sludge after the vacuum physical extraction of loosely bound water (Figure 9.34) demonstrate the nature of each sludge type. The sludge of the SMEBR shows less bound water content that reached the cracking point very fast. On the other hand, the MBR sludge looks very rich in water, sticky and without any cracks.

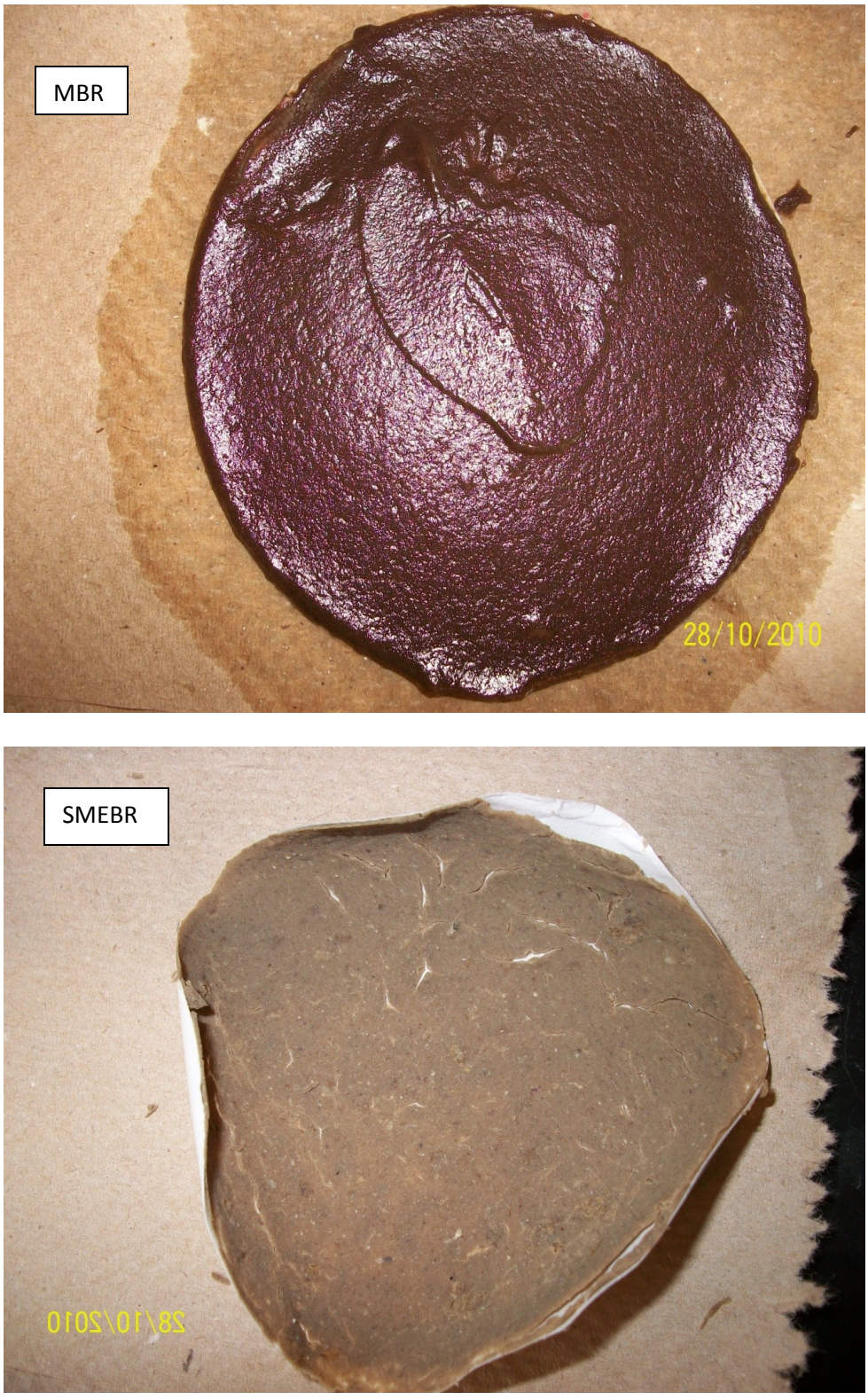

Figure 9.34: Photos of SMEBR and MBR sludge after vacuum filtration

9.9 Zeta potential

The results of Phase 1 showed that zeta potential could be reduced substantially through the production of Al^{+3} that neutralize the negative charge on the solid surfaces. Similarly, Phase 2 showed a reduction of the magnitude of zeta potential in the SMEBR. However, this reduction was not large because the SMEBR operated at low CD and long time-OFF. In all runs, the range of zeta potential in the SMEBR was between -20 to -25 mV, while in the MBR it was between -30 to -35 mV. Magnitude of zeta potential in Run 2 is given in Figure 9.35, but the same trend and values were observed in Run 1 and Run 3.

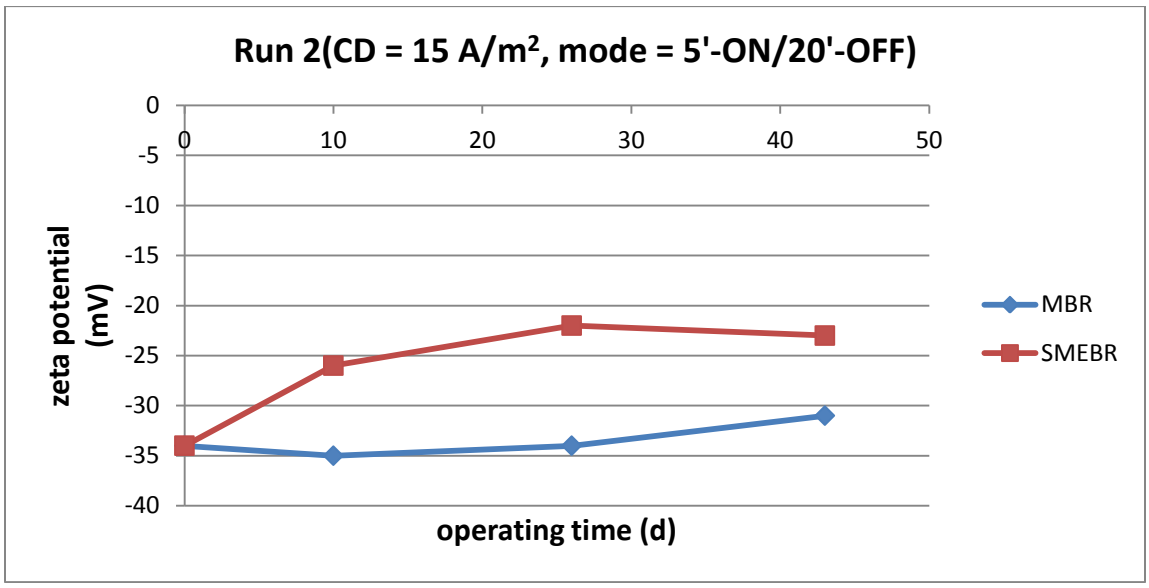

Figure 9.35: Run 2: Changes of floc zeta potential (mV) over the operating period

9.10 Particle size distribution (PSD)

In Phase 2, floc PSD exhibited the same trend of Phase 1; initial increase followed by a recession. However, the magnitude of the increase is different from one run to another. In Run 2 (Figure 9.36), the mean floc PSD increased from 115 to nearly 200 μm after 13 days of operation, while in Run 1 (Figure 9.37) and Run 3 (Figure 9.38) the increase was much lower than that (from 40 to 50 μm). Each run has a different initial floc size (from 50 to 120 μm) because the sludge was brought from the treatment plant at different times over year. The summer sludge has better quality and larger floc size, because of the impact of temperature on the microbial growth. The reason why each run peaks at different magnitude of PSD is unclear. However, the reason could be attributed to the mixing of the sludge within the reactor and its movement into and out of the electrical zone between the electrodes. Nevertheless, the magnitude of the peak value is not a big concern compared to the trend over the time. The peak size does not last too long as it started to decline after a few days. These changes of floc size reflect the dynamics of the system of the electrical bioreactor. Therefore, floc size increasing, either small or big, followed by a reduction is the trend that dominates the system. The initial increase of floc size is caused by the reduction of zeta potential that forces the flocs to come together, in addition to the enhanced movement of the charged solid surfaces as affected by the electrical field. On the other hand, the extraction of the tightly bound water from the inside of the flocs reduces its size. Another important factor contributes in reducing the floc size over the time is the production of aluminum hydroxides. These hydroxides eventually form flocs of their own or combine with the other solids in the

system. These formed inorganic suspended sloid flocs in the SMEBR with their smaller size compared to the microbial flocs reduces the measured mean PSD. In the end, the floc size is likely to stabilize at a certain value based on the average size of the hydroxide complexes produced.

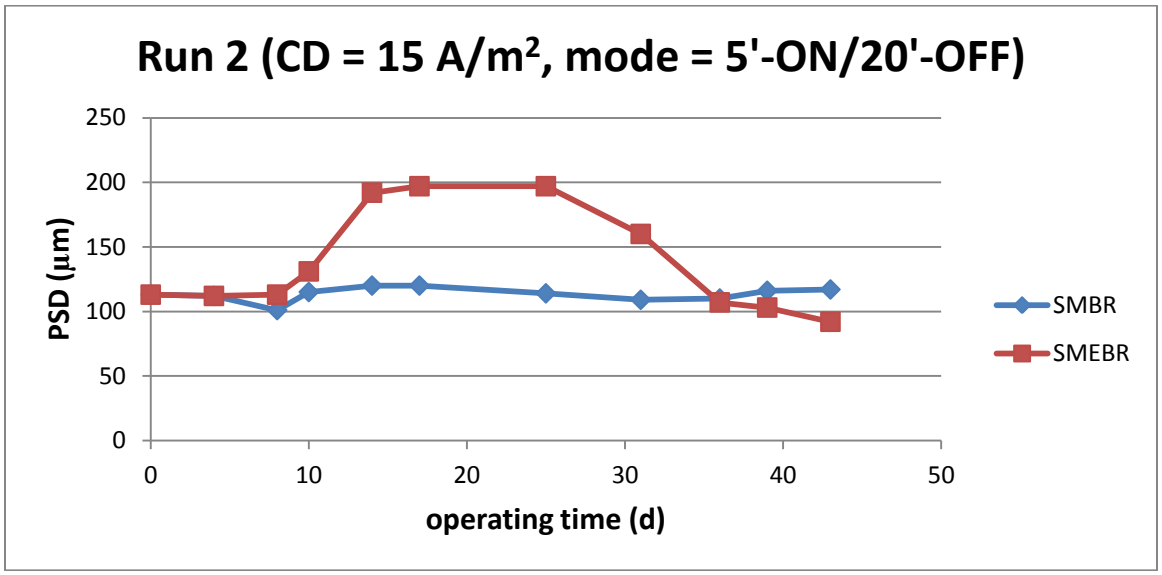

Figure 9.36: Run 2: Changes of the mean PSD in the SMEBR and MBR over time

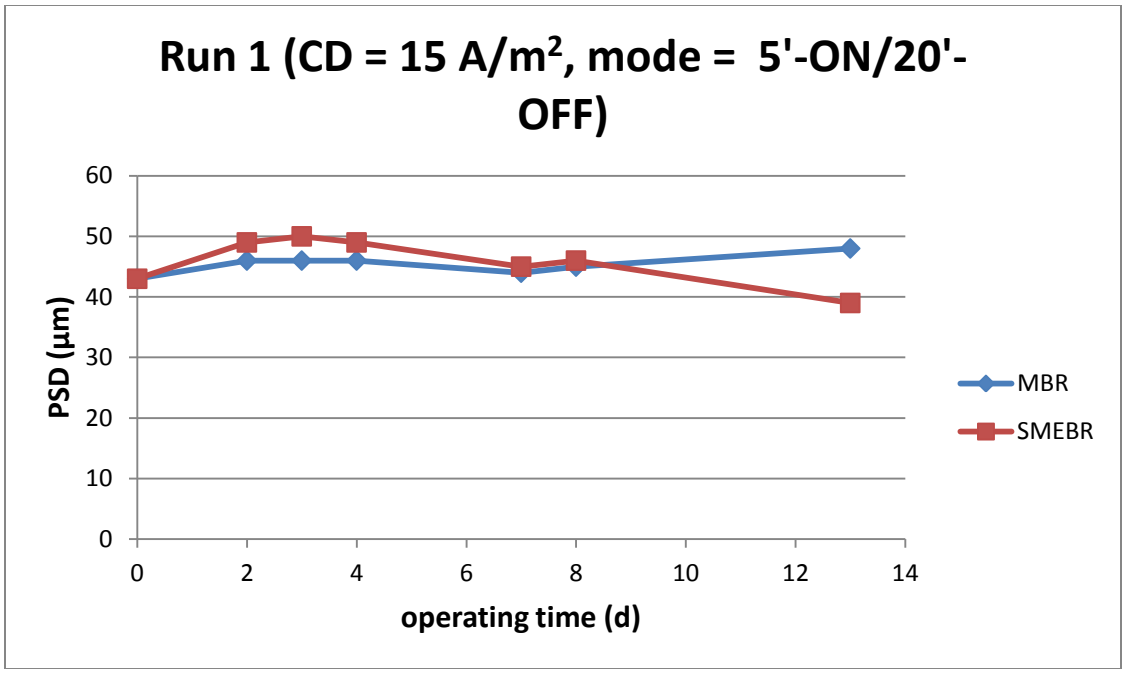

Figure 9.37: Run 1: Changes of the mean PSD in the SMEBR and MBR over time

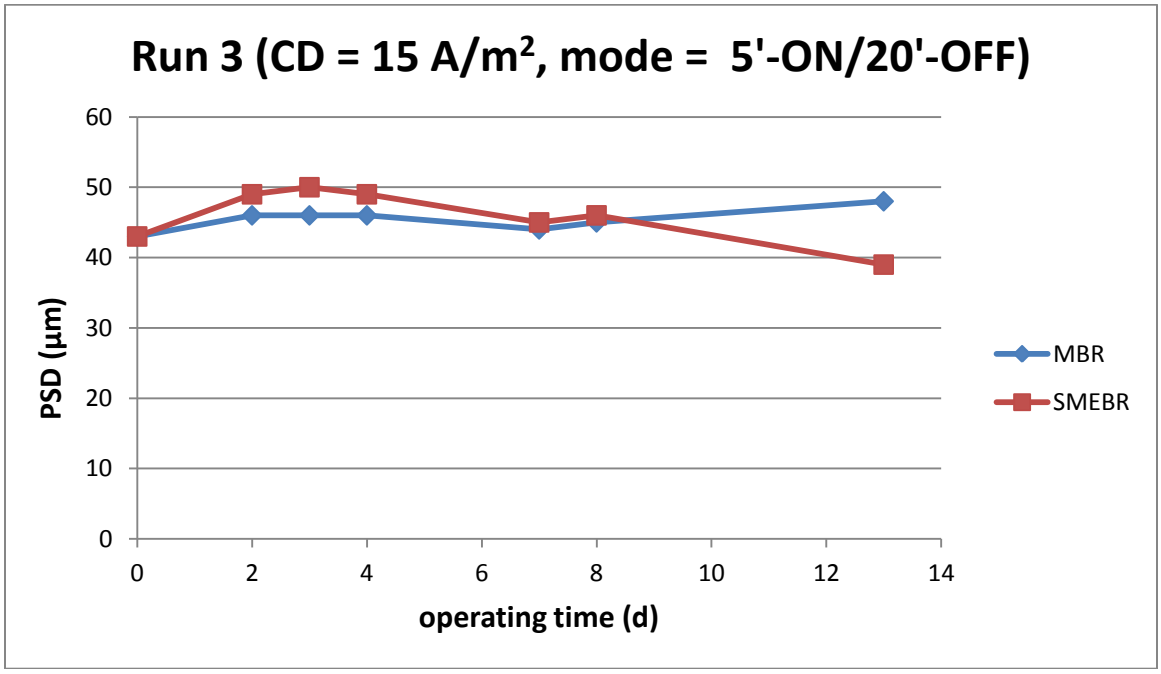

Figure 9.38: Run 3: Changes of the mean PSD in the SMEBR and MBR over time

9.11 Viscosity

Sludge dynamic viscosity of the effluent and the supernatant of both reactors was almost the same around 1 mPa.s. Although, SMEBR was expected to reduce the viscosity due to its ability to remove the viscous materials from the sludge supernatant through coagulation, no changes were observed. This is clearly because the viscosity of the sludge used in the experiments was low and close to that of clean water.

Chapter 10

Phase 2 (stage 1): Results and discussion - membrane fouling

This chapter discusses the reduction of membrane fouling in the SMEBR as a result of improving sludge properties.

10.1 Membrane critical flux

The specifications of the membrane modules used in this research are illustrated in Table 10.1. The membrane critical flux was determined before starting the experiments using the flux stepping method. The changes of trans- membrane pressure (TMP) over 20 minutes of filtration period were recorded for each flux. The minimum flux that causes an increase of TMP within that period determines the critical flux value. The critical flux was determined at two different MLSS. At MLSS of 6,000 and 10,000 mg/l, the critical flux was 13 $l/m^2.h$ (Figures 10.1 and 10.2).

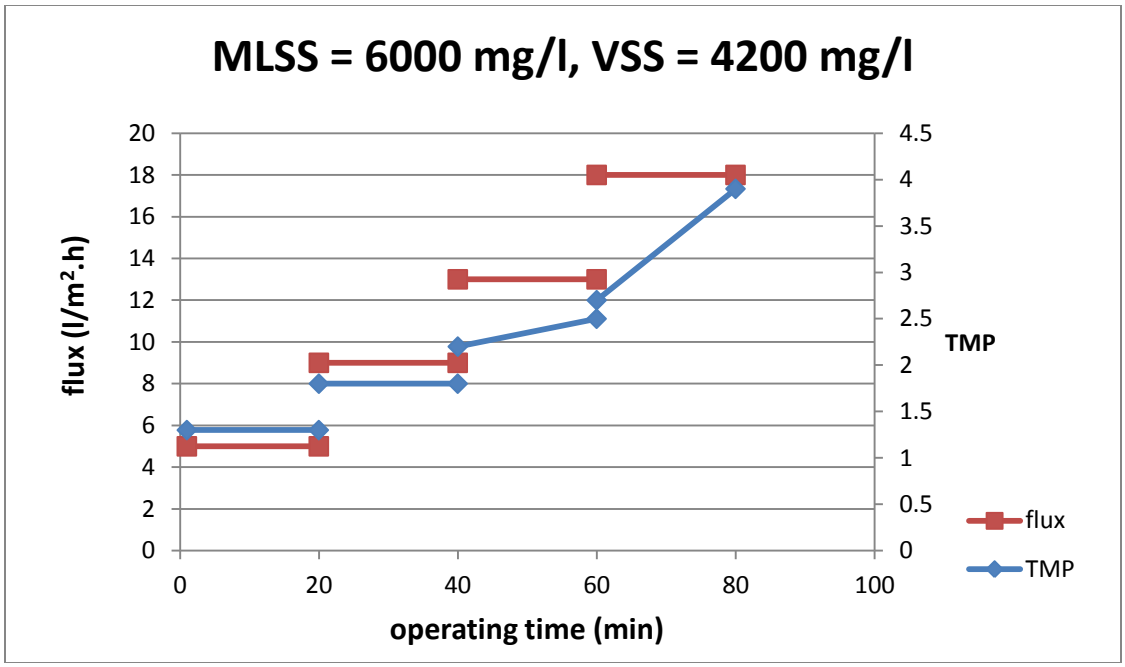

Figure 10.1: Determination of the membrane critical flux using the stepping method

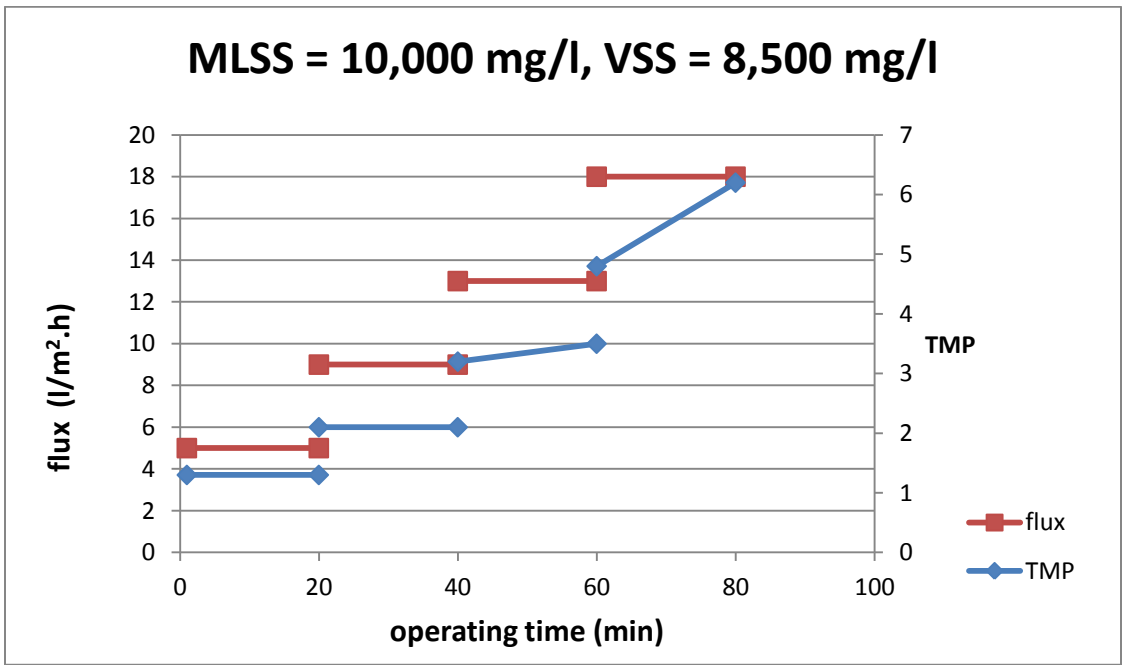

Figure 10.2: Determination of the membrane critical flux using the stepping method

10.2 Membrane fouling

All runs of Phase 2, except Run 2b, were operated at a flux of 13 l/m^2.h in order to achieve the required 12.8 h HRT. Since this flux is equal to the measured membrane critical flux, the membrane fouling frequency was high. Run 2b was operated at HRT of 24 h at a flux equal to 6 l/m^2.h and showed a much lower fouling propensity. All runs of Phase 2 proved that the membrane fouling propensity in the SMEBR was less than the MBR. However, the magnitude of membrane fouling mitigation differed from one run to another. The level of mitigations depended on the sludge characteristics. In cases where the sludge had a high fouling potential, the SMEBR showed substantial reduction of membrane fouling rate compared to the MBR. Likewise, when the sludge had low fouling potential, the SMEBR exhibited a noticeable improvement but not as much as that when lower sludge quality was used. In this research it was found that high concentrations of SMP, colloidal materials and VSS are the key components that determine the sludge quality and its fouling potential. In Run 1, at which the SMEBR and the MBR were fed by high protein concentration, the reduction of membrane fouling was much better in the SMEBR than the MBR. Over the 13 days of operation of Run 1, the membrane in the MBR was cleaned 6 times compared to only 2 times for the SMEBR (Figure 10.3). Cleaning was carried out whenever the TMP is higher than 10 kPa, because a TMP higher than that level led to a fast reduction of membrane flux which changed the operating HRT. This low limit of TMP above which the flux was deteriorating rapidly is due to the membrane characteristics and its low critical flux.

Membrane fouling rate was 13.1 kPa/d in the MBR compared to 1.8 kPa/d in the SMEBR (Figure 10.4). The reduction of membrane fouling rate was 7 times better in the SMEBR.

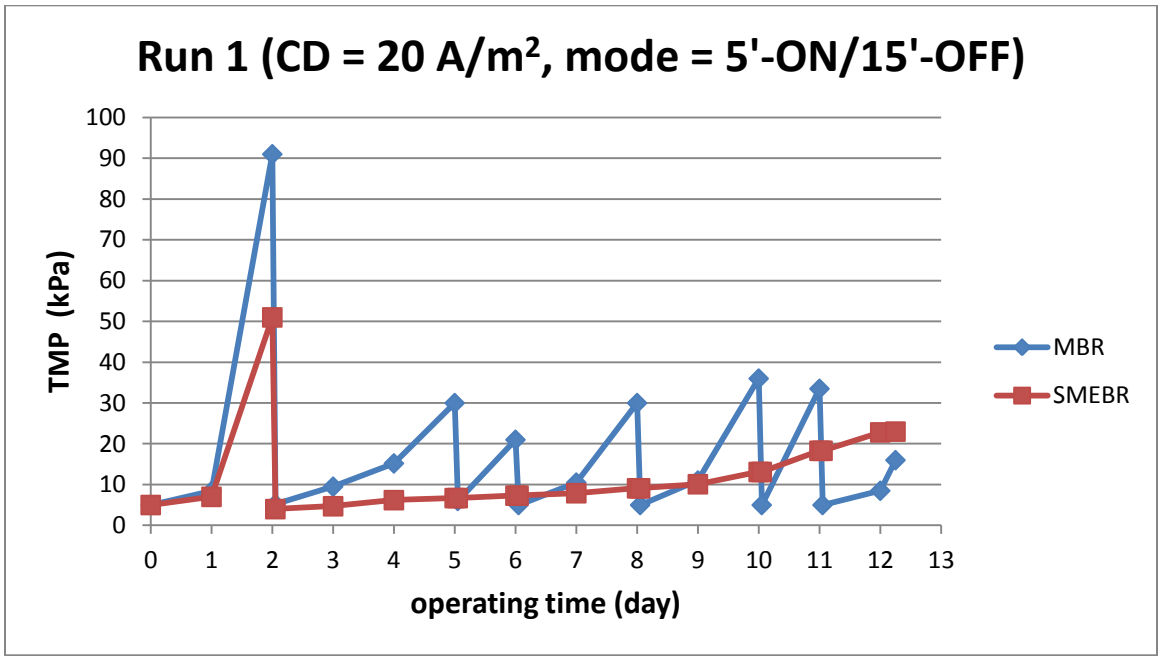

Figure 10.3: Run 1: Changes of TMP in the SMEBR and MBR over operating time

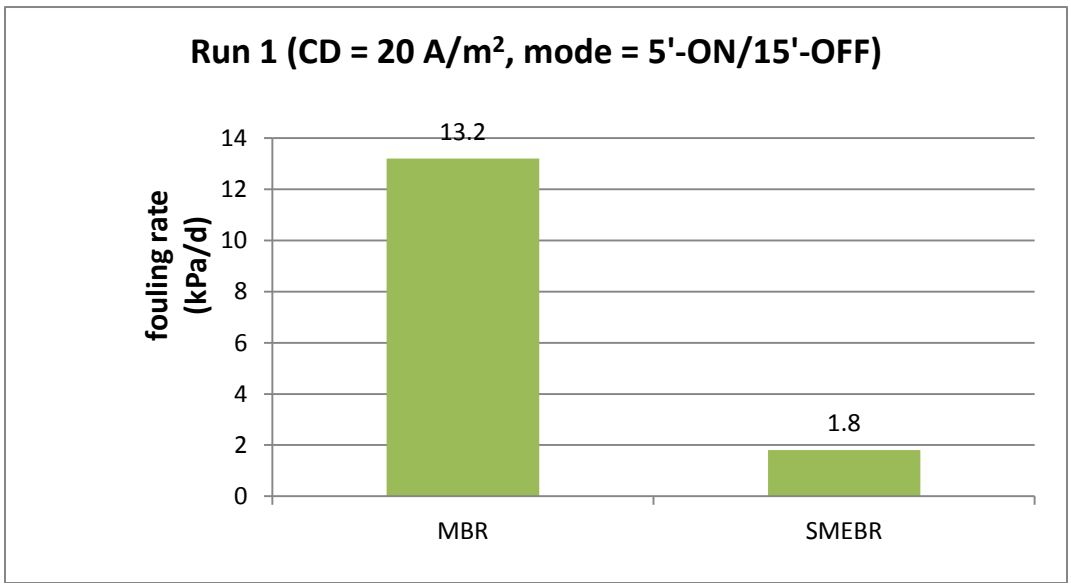

Figure 10.4: Comparison of membrane fouling rate in the SMEBR and MBR

Run 2 exhibited less membrane fouling than Run 1 because the reactors were fed by synthetic wastewater with lower protein concentration. Protein concentration in the sludge supernatant of the MBR in Run 1 was almost between 140 to 160 mg/l, while in Run 2 it was between 20 to 120 mg/l. The SMEBR was cleaned 8 times compared to 13 times of MBR over 40 days of operation (Figure 10.5). During the first 20 days of operation, the SMEBR showed a very slight improvement of membrane fouling than the MBR. Afterward, the improvement in the SMEBR was substantial. This discrepancy of membrane fouling improvement over time is related to the concentration of SMP in the sludge supernatant. During the first 20 days of operation, the polysaccharide concentrations in the sludge supernatant were between 10 to 30 mg/l and the protein concentrations were between 30 to 60 mg/l. during the next 20 days of operation, polysaccharide concentrations increased in the MBR up to 30 to 80 mg/l and protein concentrations increased to 60 to 120 mg/l. In the second half of operation of Run 2, the removal of protein and polysaccharides from the sludge supernatant through the electrocoagulation in the SMEBR has improved the sludge quality, which is then reflected in a lower fouling frequency. During the first 20 days of operation, membrane fouling rate in the MBR was 3.2 kPa/d and reduced to 2.6 kPa/d in the SMEBR (Figure 10.6). Nearly 1.2 times lower fouling rate than the MBR. In the next 20 days of operation, the improvement was much greater up to more than 5 times. This substantial improvement that started after day 20 is related to the accumulation of SMP in the MBR. In the SMEBR, the SMP concentration was much less in the supernatant because of the removal through electrocoagulation and other electrokinetic processes.

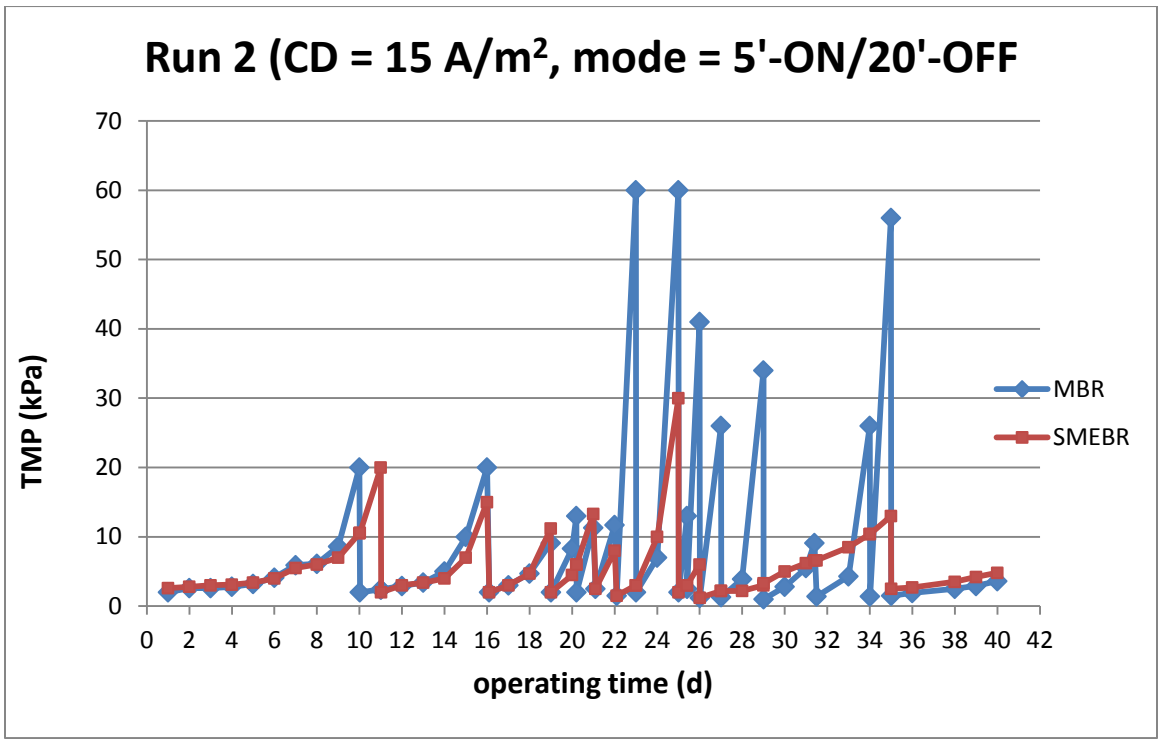

Figure 10.5: Run 2: Changes of TMP in the SMEBR and MBR over operating time

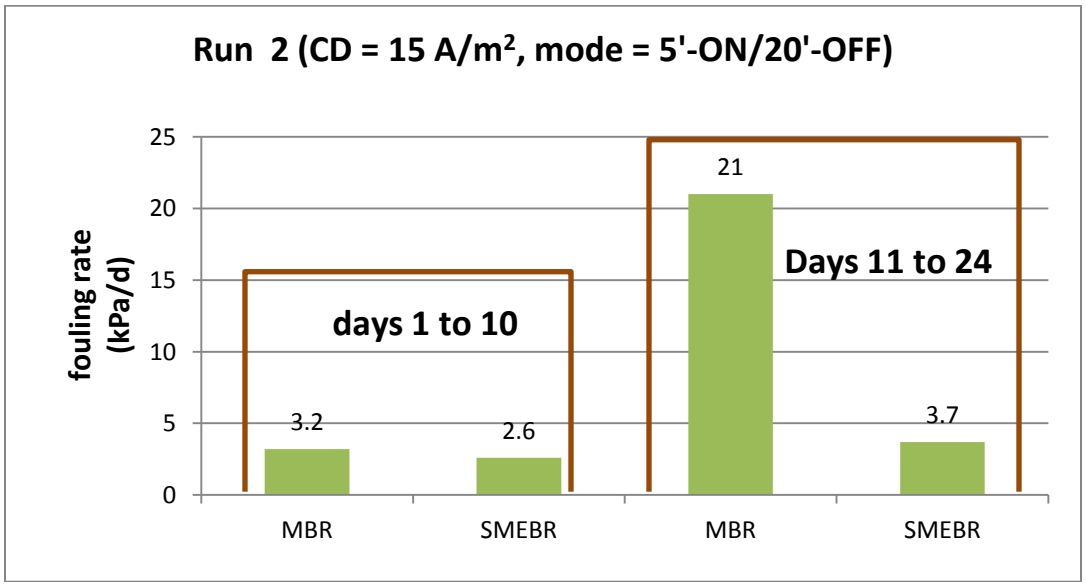

Figure 10.6: Run 2: Comparison of membrane fouling rate in the SMEBR and MBR

In Run 3, membrane fouling rate was very close to that of Run 2. The SMEBR was cleaned 6 times compare to 11 times in the MBR over a period of 24 days (Figure 10.7).

Cleaning frequency was higher in the MBR than the SMEBR at the end of the run due to the accumulation of SMP. membrane fouling rate started to get higher after 9 days of operation than at the beginning due to the increase of SMP concentration in the sludge supernatant (Figure 10.8). However, the improvement of membrane fouling in the SMEBR was at least 4 times over the whole period of operation.

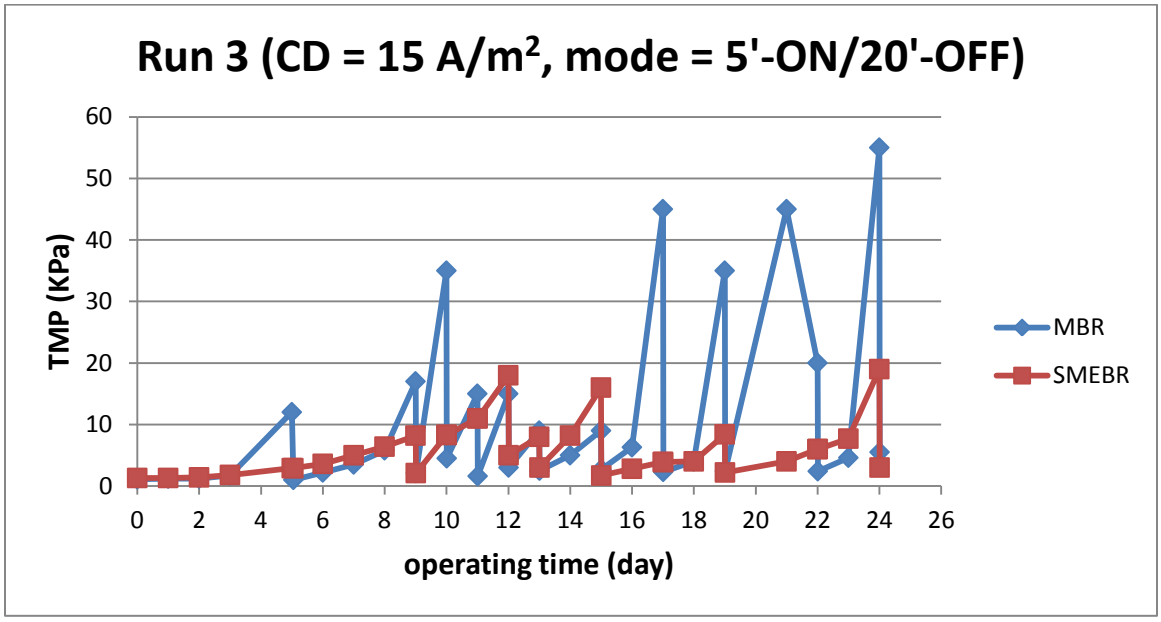

Figure 10.7: Run 3: Changes of TMP in the SMEBR and MBR over operating time

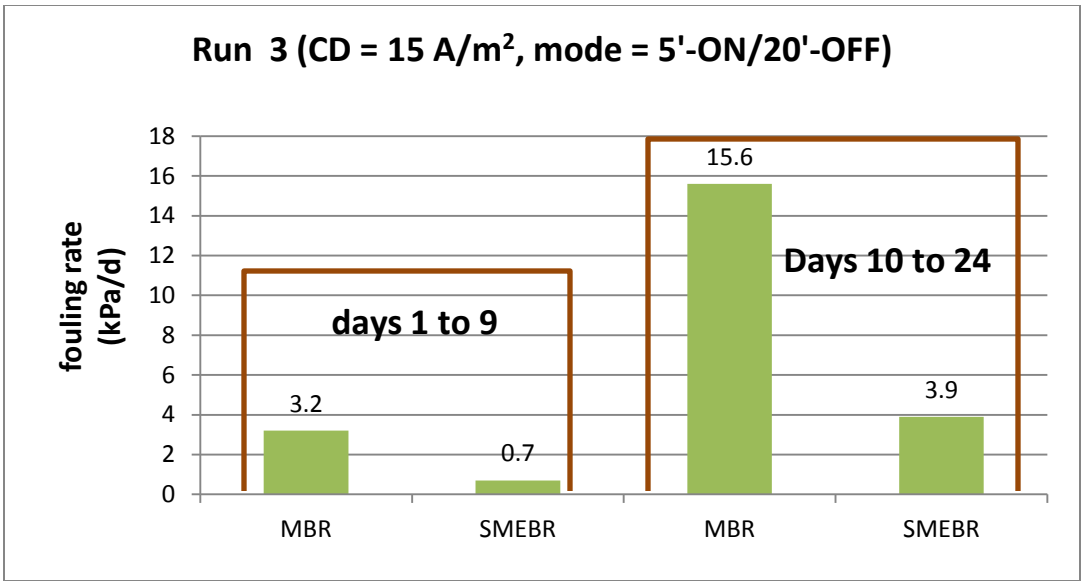

Figure 10.8: Run 3: Comparison of membrane fouling rate in the SMEBR and MBR

10.3 Combined effect of SMP and VSS on membrane fouling

Membrane fouling rate was found to be affected mainly by the concentration of SMP in the sludge supernatant and to the concentration of VSS. The tested runs of Phase 2 were divided into periods according to their SMP and VSS concentrations; results are summarized in Table 10.1. These results will be used to determine the relationship between the combined effects of SMP and VSS on membrane fouling.

Table 10.1 Membrane fouling rate (kPa/d) in the SMEBR and MBR over time

Run #	Period (d)	VSS (mg/l)	PN supernatant (mg/l)	PS supernatant (mg/l)	SMP (PN + PS) (mg/l)	Average SMP (mg/l)	Fouling rate (kPa/d)
Run 1 (MBR)	2 to 12	2500 to 3500	120 to 160	40 to 100	160 to 260	210	13.4
Run 1 (SMEBR)	2 to 12	2500 to 3000	60 to 120	10 to 20	70 to 140	105	1.8
Run 2 (MBR)	1 to 20	2500 to 7000	30 to 60	10 to 30	40 to 90	65	3.2
Run 2 (SMEBR)	1 to 20	2500 to 6000	30 to 45	5 to 10	35 to 55	45	2.6
Run 2 (MBR)	21 to 35	7000 to 8000	60 to 120	30 to 80	90 to 200	145	21
Run 2 (SMEBR)	21 to 35	5000 to 8000	40 to 80	5 to 10	45 to 90	68	3.7
Run 3 (MBR)	1 to 9	2000 to 4000	50 to 80	60 to 70	110 to 150	130	3.2
Run 3 (SMEBR)	1 to 9	2000 to 4000	50 to 70	15 to 20	65 to 90	78	0.7
Run 3 (MBR)	11 to 24	4000 to 5500	90 to 100	40 to 160	130 to 260	195	15.6
Run 3 (SMEBR)	11 to 24	4000 to 7000	55 to 70	15 to 25	70 to 95	83	3.9

PN=protein, PS=polysaccharide

Since there is yet no consensus in the literature on the impact of VSS on membrane fouling, particularly within the range between 3,000 to 10,000 mg/l, the combined impact of SMP and VSS will be investigated hereafter in an attempt to better understand the relationship between these components. At almost equal SMP concentration in the sludge supernatant (130 to 145 mg/l), the increase of VSS from

3000 to 7500 mg/ in the MBR was accompanied by significant increase in membrane fouling (Figure 10.9). The fouling rate was increased from 6.4 to 21 kPa/d.

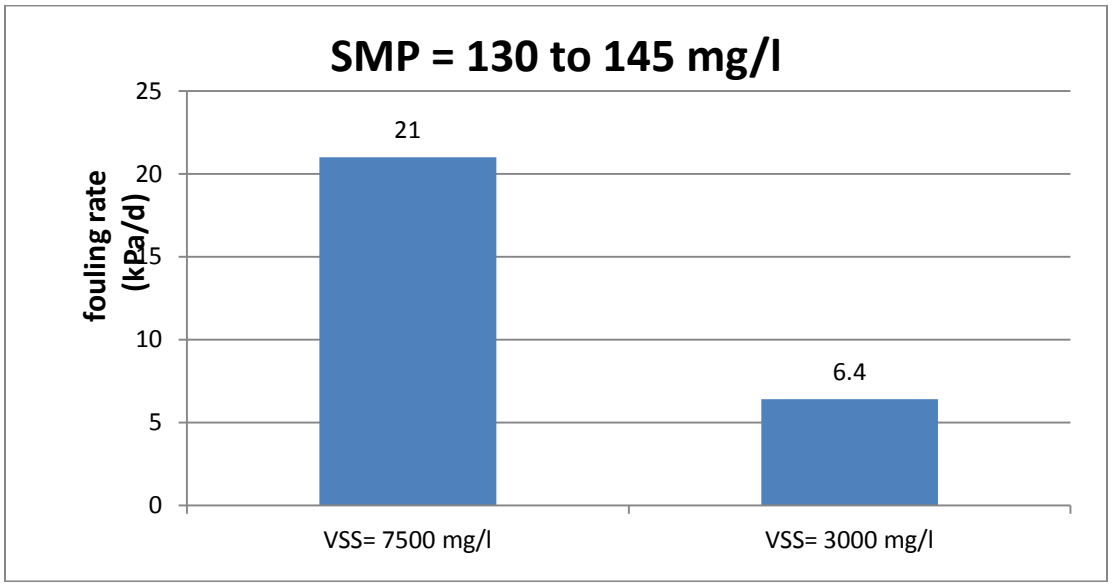

Figure 10.9: Comparison of membrane fouling rate in the MBR at different VSS and nearly equal SMP

When the supernatant SMP concentration in the SMEBR was within the range of 70 to 85 mg/l, the membrane fouling rate was lower at VSS of 3000 mg/l (0.7 kPa/d) than at 5500 mg/l (3.9 kPa/d) and 6500 mg/l (3.7 kPa/d) as illustrated in Figure 10.10. However, the fouling rate was much less than the previous case where SMP concentration was much higher.

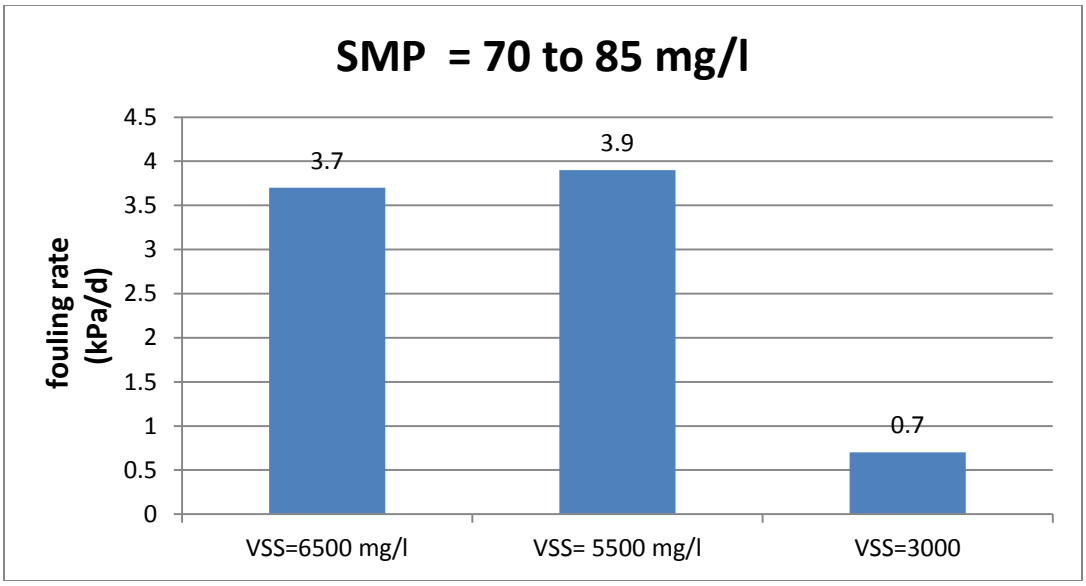

Figure 10.10: Comparison of membrane fouling rate in the SMEBR at different VSS but equal SMP concentration

On the other hand, at almost equal concentration of VSS, the increase of SMP was accompanied by a further increase of membrane fouling rate. For example, at VSS between 2000 to 4000 mg/l, the membrane fouling at SMP concentration of 65 mg/l was 3.2 kPa/d. The membrane fouling rate increased to 6.4 and 13.4 kPa/d after increasing the concentration of supernatant SMP to 130 and 210 mg/l, respectively (Figure 10.11).

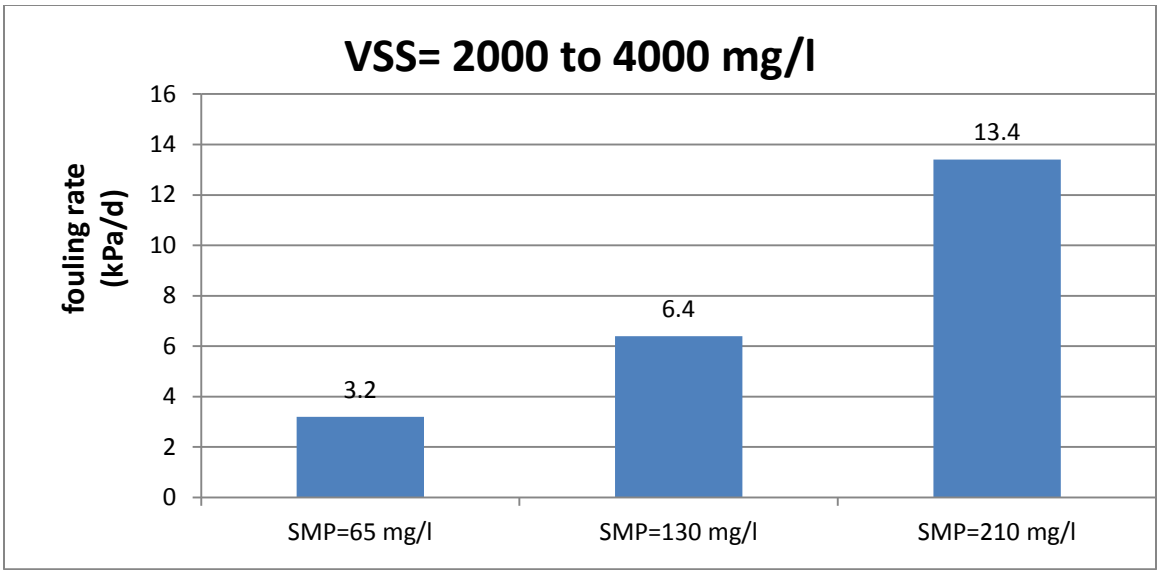

Figure 10.11: Comparison of membrane fouling rate in the MBR at equal VSS but different SMP concentrations

The importance of considering the combined effect of SMP and VSS on membrane fouling is clarified in the following case. The membrane fouling rate was much higher (13.4 kPa/d) at VSS of 3000 mg/l than the fouling rate (3.2 kPa/d) at VSS of 4750 mg/l. This is because the concentration of supernatant SMP at the lower concentration of VSS was 210 mg/l compared to 65 mg/l at the higher concentration of VSS equal to 4700 mg/l (Figure 10.12). The increase of SMP caused more fouling than the increase of VSS.

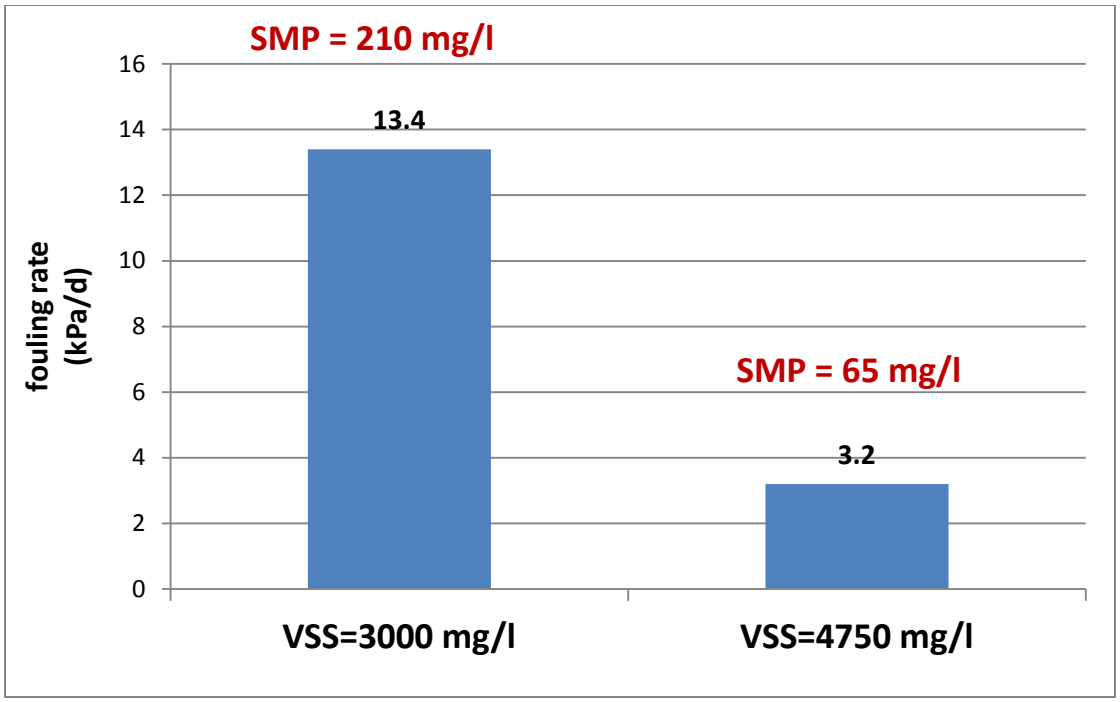

Figure 10.12: Comparison of membrane fouling at different VSS and different SMP in the MBR.

In order to further investigate the relationship between the SMP and membrane fouling, the critical flux test was conducted for the sludge in the MBR and the SMEBR on day 11 of Run 2. On that day, the concentration of SMP was minimal and almost equal in the two reactors. The test indicated that the membrane critical flux for both reactors was 22 $l/m^2.h$ (Figure 10.13). This value was higher than the initially measured 13 $l/m^2.h$ critical membrane flux, because the SMP concentration was higher. However, the rate of TMP changes was much higher in the MBR than in the SMEBR at 27 $l/m^2.h$ membrane flux. This difference is mainly due to the impact of electro-kinetic processes on improving sludge characteristics.

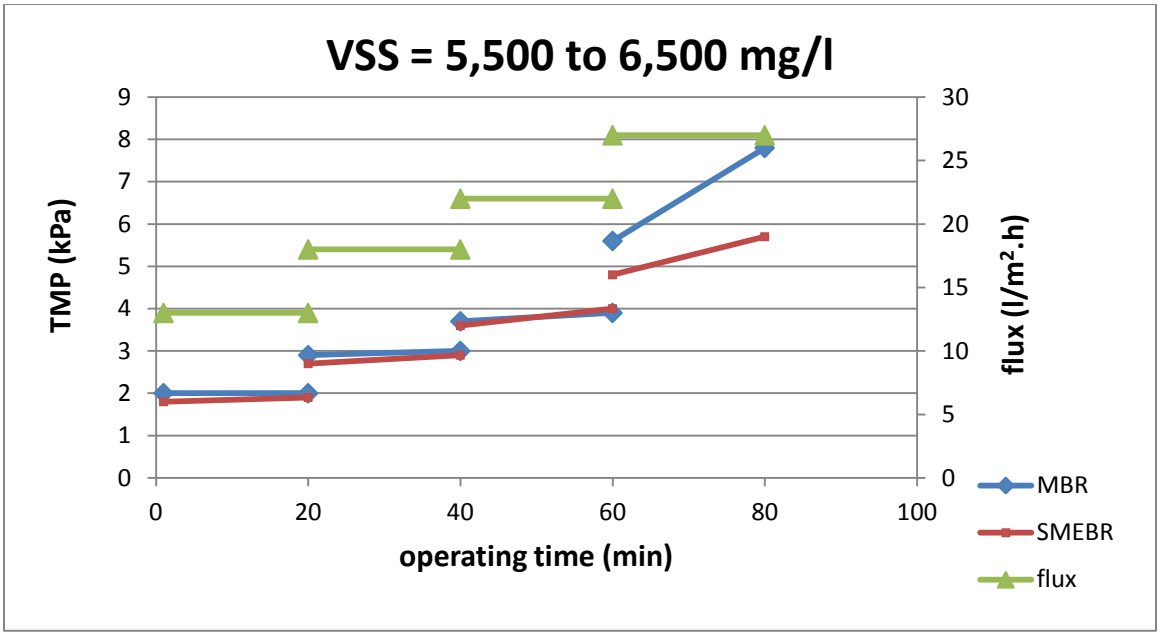

Figure 10.13: Run 2: Critical flux determination in the MBR and SMEBR on day 11

10.4 Conclusions

The reduction of membrane fouling in the SMEBR was not a direct process. The reduction of membrane fouling rate was done indirectly through the removal of the materials that have high fouling potential (SMP and colloids), in addition to the extraction of the tightly bound water from the suspended solids. VSS and SMP are interrelated in their effect on membrane fouling. Considering their effect separately is a misleading approach that resulted in controversial conclusions on the relationship between VSS and membrane fouling.

Chapter 11

Phase 2 (Stage 2): Results and discussion

This chapter discusses the results of the two runs (Run 4 and Run 5) of Stage 2 in three aspects: nutrient removal, sludge characteristics and membrane fouling. Stage 2 was conducted at different conditions than Stage 1. However, the results of both stages where analyzed together to evaluate the reproducibility of results for the nutrient removal and membrane fouling reduction.

11.1 Carbon removal

The removal of carbon through oxidation by microbial biomass was very high in both reactors (> 97%) in Run 4 and Run 5 over the whole operating period. Though, the SMEBR showed a slight decrease of COD concentrations in the effluent than that of the MBR. Results of the effluent COD of Run 4 for both reactors are given in Figure 11.1.

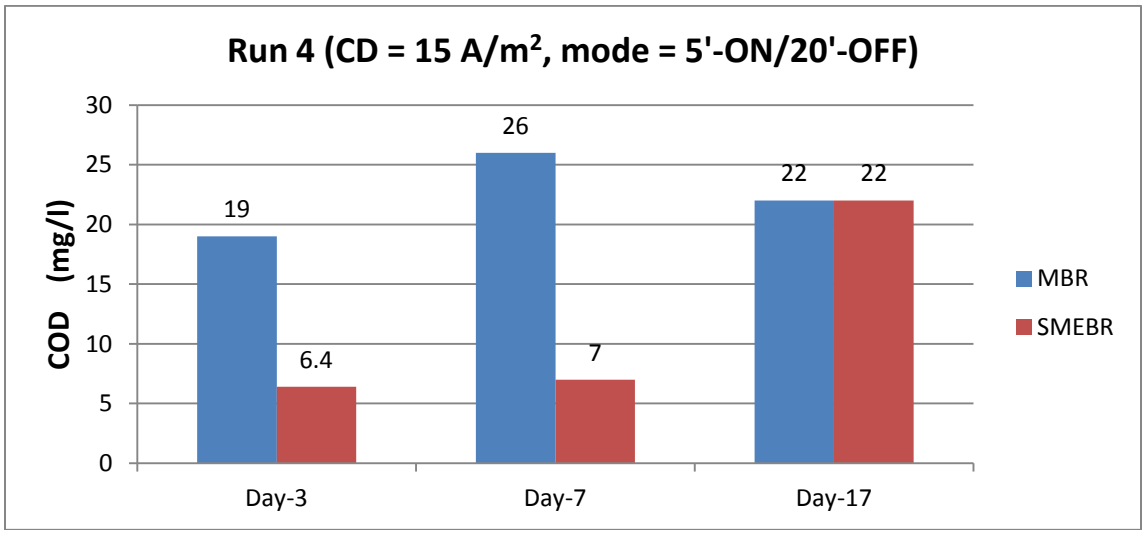

Figure 11.1: Run 4: Effluent COD concentrations in the SMEBR and MBR

11.2 Phosphorus removal

Phosphorus removal was very high in the SMEBR in Run 4 and Run 5 compared to the MBR (Figure 11.2). The removal efficiency was above 99% over the whole operating period in Run 4 (Figure 11.3) and Run 5. In MBR, the increase of P concentration over time reduced the removal efficiency to 44% on day 17. This accumulation of phosphorus in the MBR is due to the higher loading of P than the biomass needs. These results are consistent with the findings of Phase 2 (Stage 1). SMEBR through the formation of phosphate hydroxide complexes is a very powerful system for removing soluble phosphorus from the wastewater.

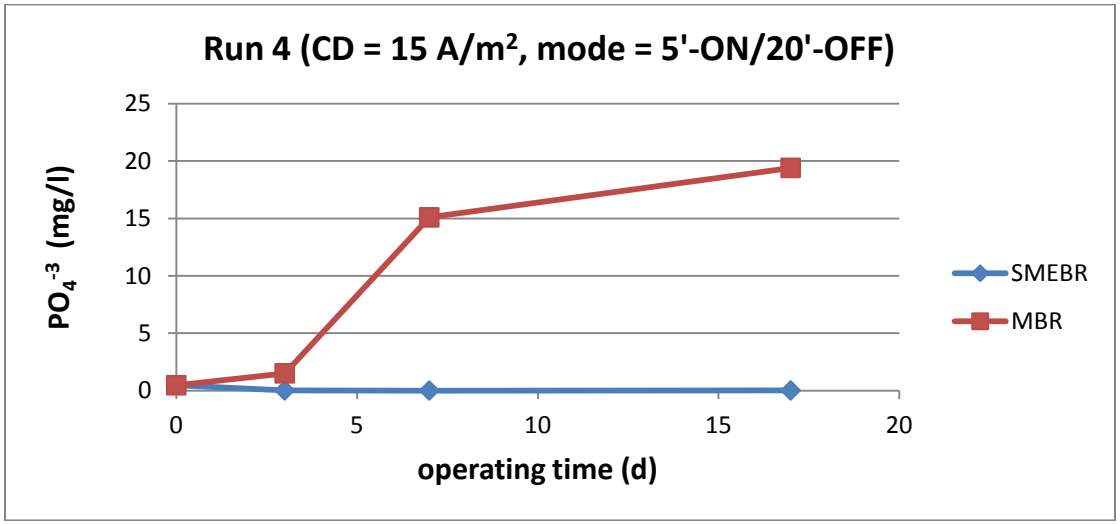

Figure 11.2: Run 4: Concentration of effluent orthophosphate in the SMEBR and MBR

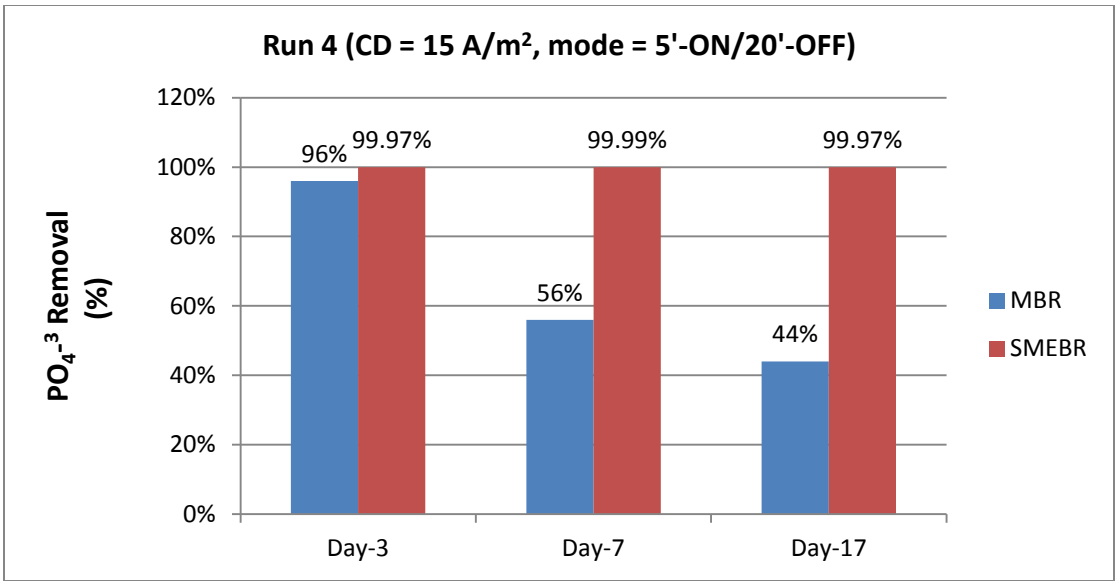

Figure 11.3: Run 4: Orthophosphate removal efficiency in SMEBR and MBR

11.3 Nitrogen removal

Run 4 and Run 5 exhibited the same behavior of nitrogen components witnessed in Phase 2 (Stage 1). The MBR in Run 4 and Run 5 showed a typical conversion of ammonium to nitrate, while the SMEBR showed a constant conversion of ammonium to nitrogen gas through the simultaneous nitrification/denitrification processes. Over the first 9 days of operation, the SMEBR and the MBR of Run 4 produced an effluent with very low ammonium concentration (< 1 mg/l). Afterward, the effluent ammonium concentration increased in both reactors due to the increase of ammonium concentrations in the influent from 22 to 29 mg/l (Figure 11.4); the system was working at an influent ammonium concentration higher than the nitrification potential capacity of the reactors. The increase was slightly higher in the SMEBR, because the system was not working at DO concentration that supports the optimum anammox conditions. During the first 9 days, the average nitrification was above 98% in both reactors. During

the second half of operation (days 10 to 18), the average nitrification was 85% in the MBR and 81% in the SMEBR (Figure 11.5). However, the slight increase of ammonium in the SMEBR was accompanied by a high nitrate removal (Figure 11.6). The nitrate concentration increased up to 80 mg/l in the MBR, while in the SMEBR it was always below 10 mg/l. The average denitrification in the SMEBR for the period starting from day 6 to the end was 96 % compared to the nitrate concentrations in the MBR (Figure 11.7). The first few days were excluded from the denitrification calculation due to the initial high nitrate concentration before activating the electric field. Run 4 proved once again the possibility of the combined ammonium and nitrate removal in the SMEBR. The SMEBR exhibited 4% reduction in the nitrification, but in return, the denitrification was almost 97% over the whole operating period.

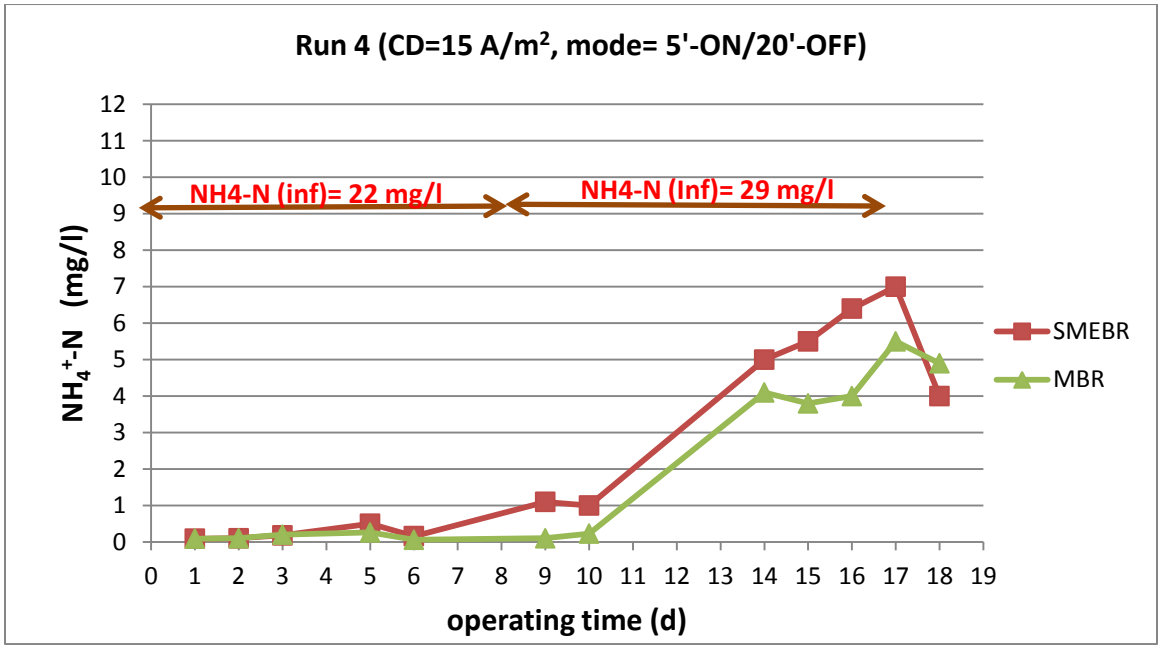

Figure 11.4: Run 4: Ammonium concentrations in the effluent of SMEBR and MBR

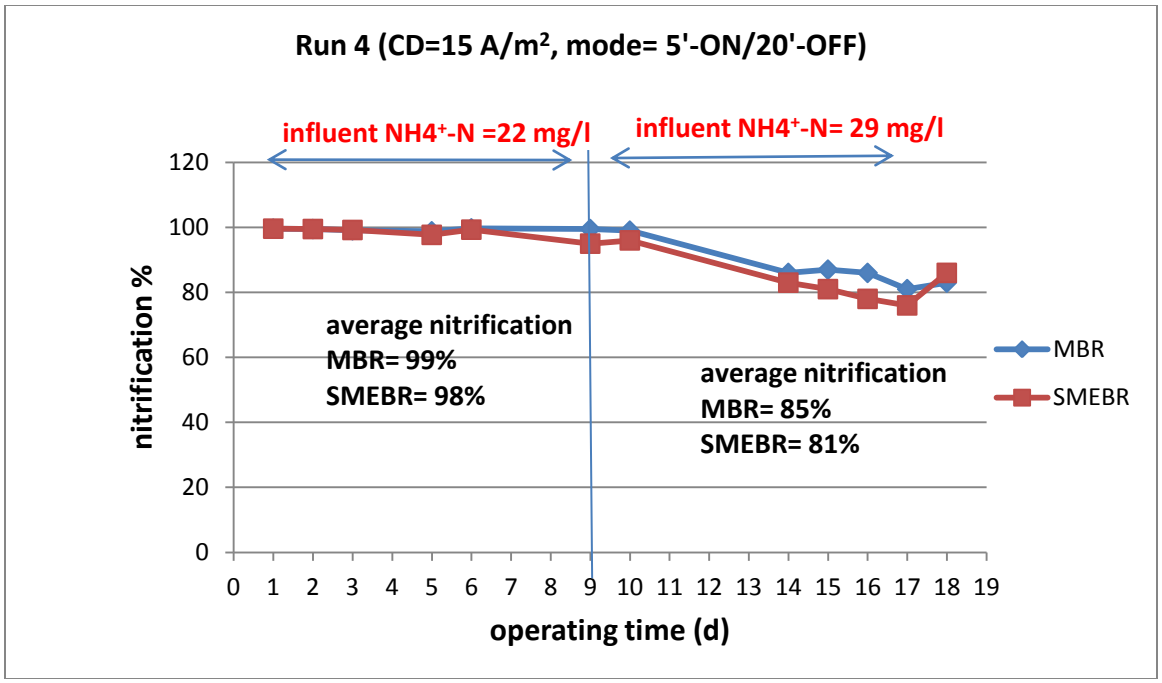

Figure 11.5: Run 4: The nitrification percentage of influent ammonium in the SMEBR and MBR

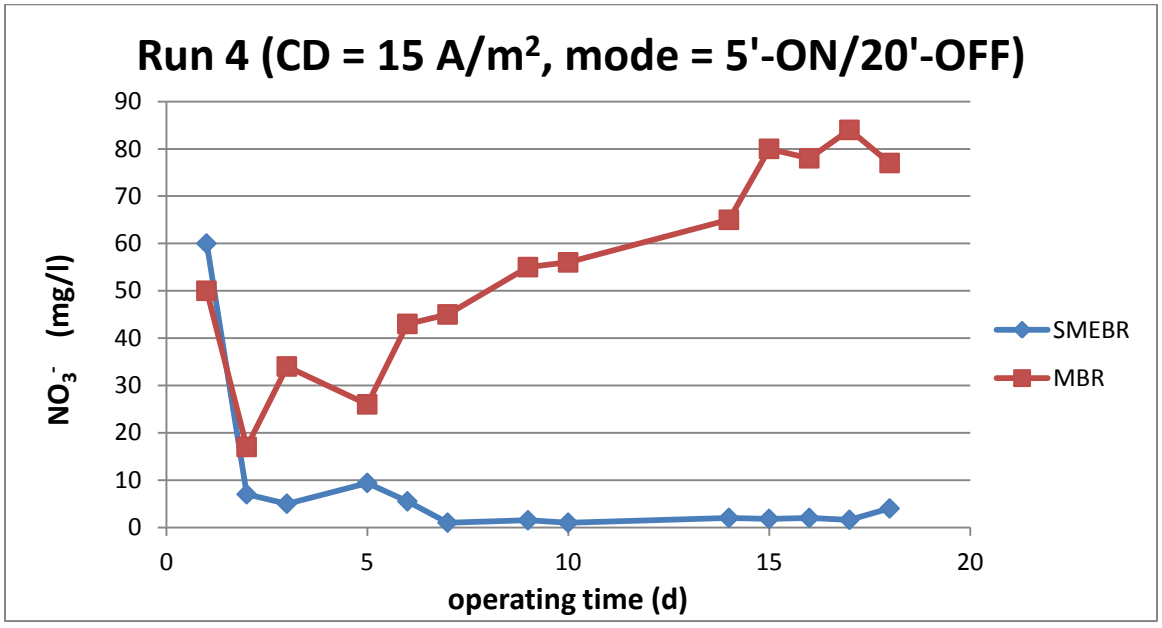

Figure 11.6: Run 4: Effluent nitrate concentrations in the SMEBR and MBR

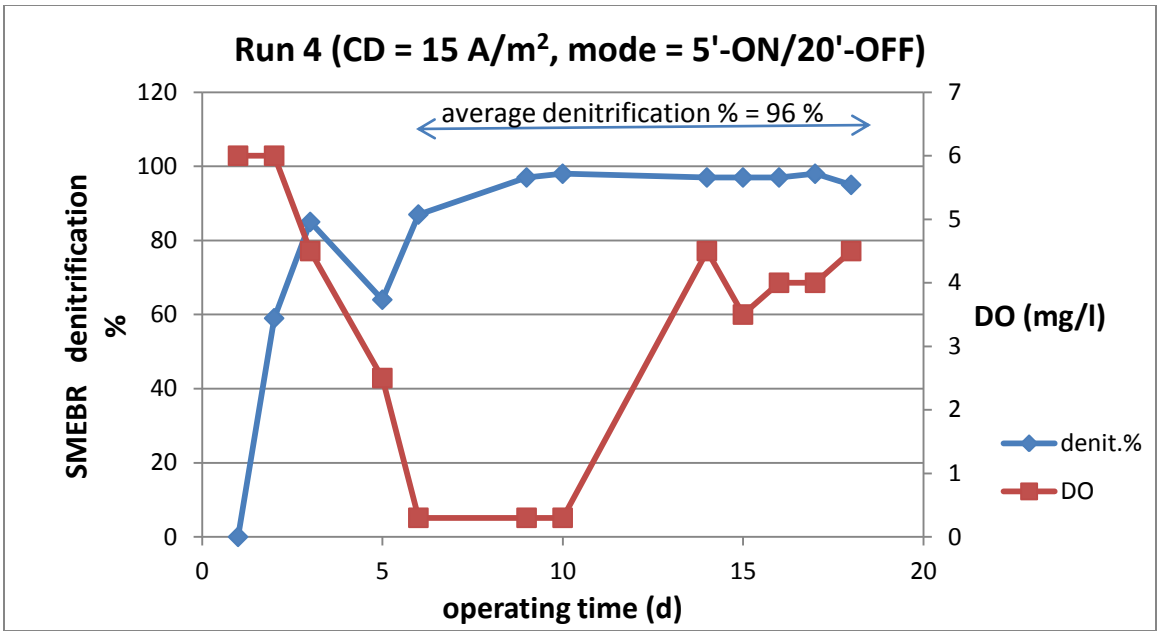

Figure 11.7: Run 4: Denitrification percentage in the SMEBR compared to MBR

Nitrogen removal in Run 5 was similar to Run 4. The MBR showed almost complete conversion of ammonium to nitrate (Figure 11.8).On the other hand, the SMEBR produced effluent with low ammonium concentration of less than 5 mg/l and nitrate concentration of less than 10 mg/l over the 30 days of operation (Figure 11.9). The average nitrification in the MBR over the 30 days of operation was 97% compared to 86% for the SMEBR (Figure 11.10). The reduction of 11% nitrification in the SMEBR was compensated by an average denitrification of 93% over the period from day 6 to day 30 (Figure 11.11). Run 5 confirms the results of Run 4 and all runs of Phase 2 (Stage 1) regarding the simultaneous removal of ammonium and nitrate in the SMEBR.

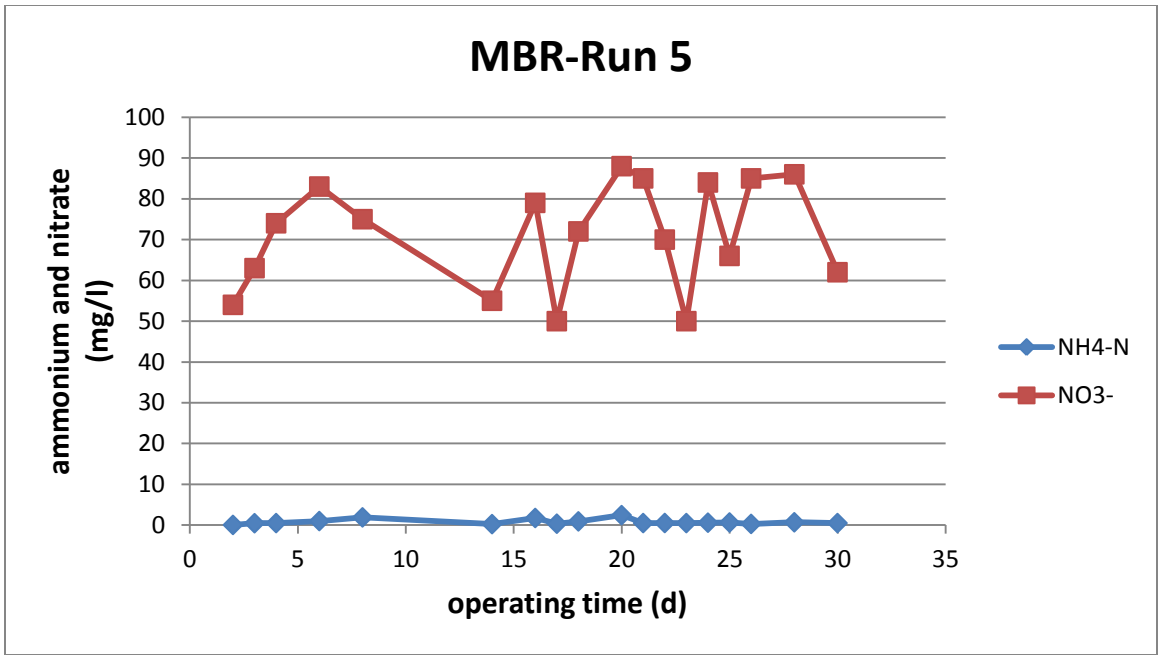

Figure 11.8: Run 5: Effluent concentrations of ammonium and nitrate in the MBR

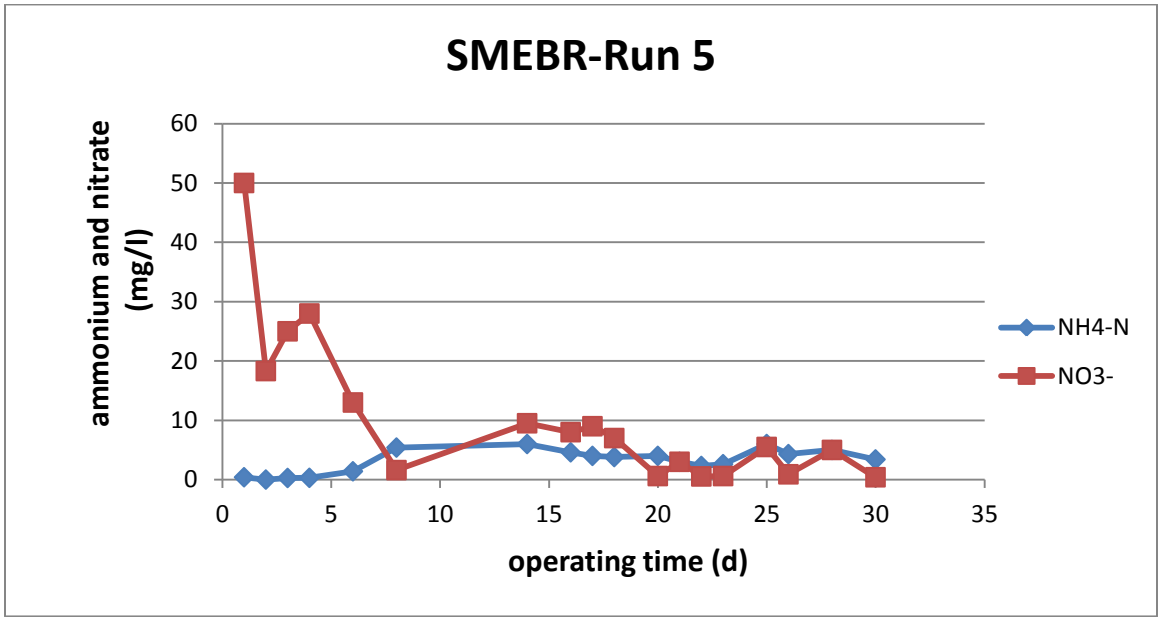

Figure 11.9: Run 5: Effluent concentrations of ammonium and nitrate in the SMEBR

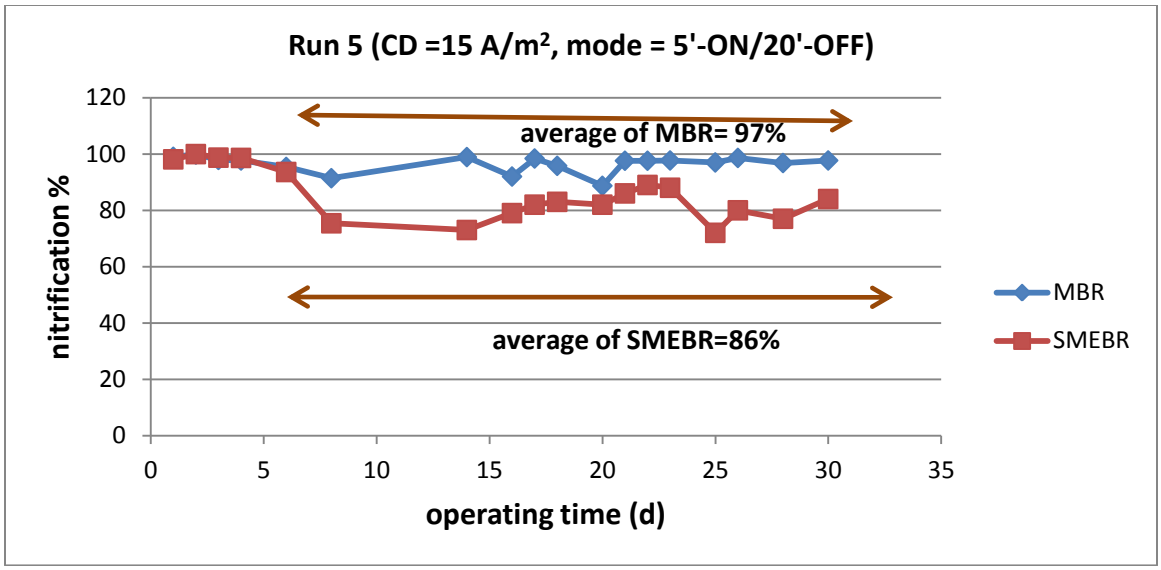

Figure 11.10: Run 5: Nitrification percentage in the SMEBR and MBR over the operating time

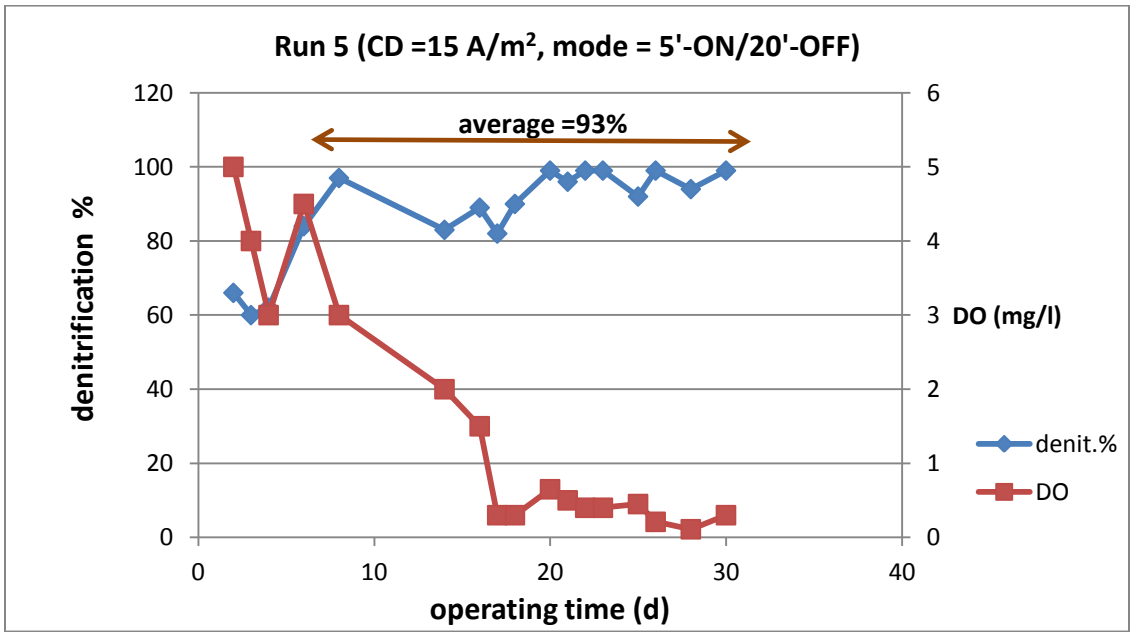

Figure 11.11: Run 5: Denitrification percentage in the SMEBR compared to that of the MBR

The SMEBR in Run 4 and Run 5 showed a reduction of the average nitrification by 4% and 11% over the operating period, respectively. However, results of Run 3 of Phase 2

(Stage 1) showed an enhancement of nitrification potential of the SMEBR (Chapter 8). This discrepancy of results between Phase 2 and Phase 3 could be related to the slow growth rate of the autotrophic bacteria performing the anammox process. Thus, working at SRT of 16 days in Phase 3 compared to infinity SRT in Phase 2 might have reduced the growth rate and impaired the reduction of nitrate through that process. Furthermore, the objective of this phase was to prove the high removal of ammonium and nitrate over a long period of time rather than to prove the superiority of nitrification in the SMEBR. For that reason, the operating conditions were not changing as long as the system was removing the bulk concentration of ammonium and nitrate. However, a slight change of the DO concentration could have increased the nitrification potential.

11.4 Sludge pH

SMEBR showed insignificant (up to 2 degrees) higher pH values than the MBR in Run 4 (Figure 11.12) and Run 5. This trend of increasing pH in both runs is similar to the trend observed in Phase 2 (Stage 1). The increase of pH in the SMEBR compared to the MBR is due to the production of hydroxide ion through the electro-chemical reactions (Equations 3.3 and 3.4).

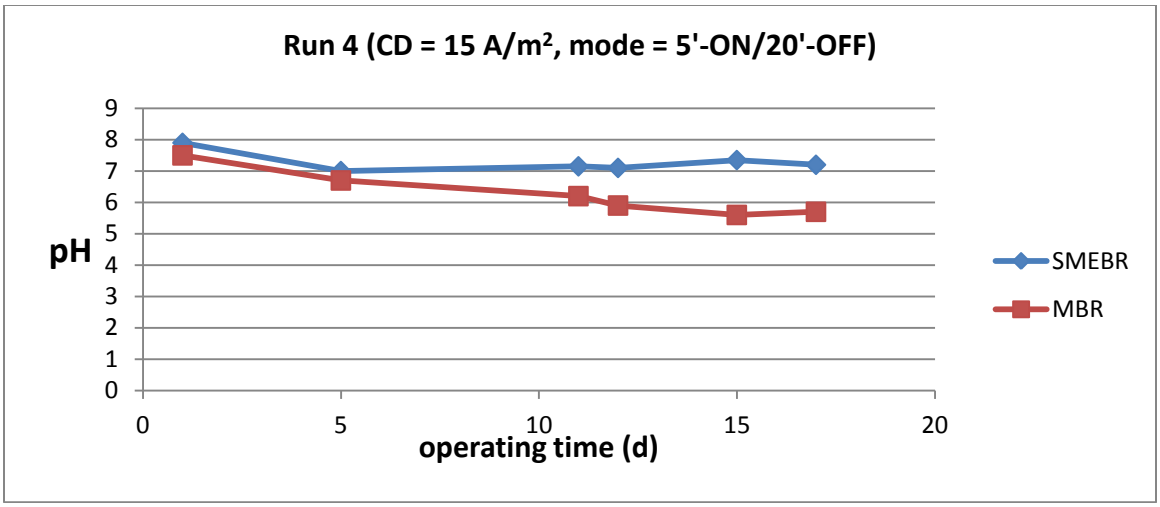

Figure 11.12: Run 4: Changes of sludge pH in the SMEBR and MBR over time

11.5 Electrical conductivity (EC)

The EC was higher in the SMEBR than the MBR by 100 to 150 μs/cm in Run 4 (Figure 11.13) and Run 5 (Figure 11.14) over the whole operating period. The same trend was observed in Phase 2. It is likely that the deposition of ions on the electrodes combined with the high removal of nitrate in the SMEBR reduced the magnitude of EC. Ions removal could be also related to their interactions between themselves and the ionic active groups on the solid surfaces that cause the precipitation of ions on the solid surfaces.

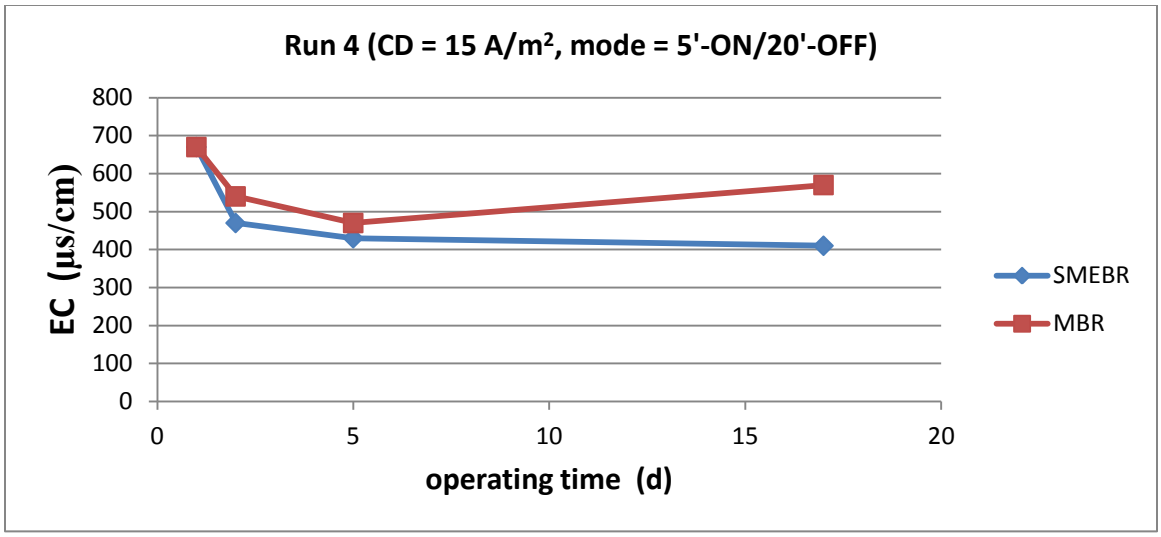

Figure 11.13: Run 4: Changes of sludge electrical conductivity (EC) in the SMEBR and MBR

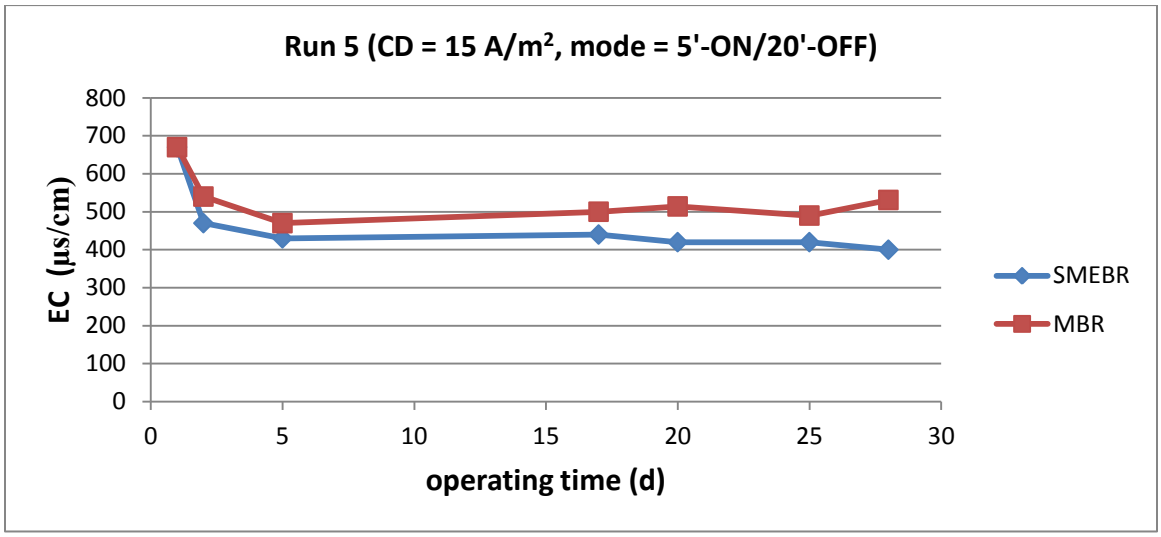

Figure 11.14: Run 5: Changes of sludge electrical conductivity (EC) in the SMEBR and MBR

11.6 Suspended solids

The concentration of MLSS in the SMEBR was almost twice as high than that of the MBR, mostly due to the formation of aluminum hydroxides. In Run 4, the MLSS was stabilized

between 7000 to 8000 mg/l and 4000 to 5000 mg/l in the SMEBR and MBR, respectively (Figure 11.15). However, the concentration of VSS was almost the same in both reactors between 4000 to 5000 mg/l. The nearly equal concentration of VSS in both reactors indicates that the biomass activity was not hindered in the SMEBR. Since the inorganic sludge production in the SMEBR was high, the ratio of the VSS/MLSS was stabilized at around 60%, while in the MBR it was around 85% (Figure 11.16). The same trend was observed in Run 5 (Figures 11.17 and 11.18). The stabilization of the VSS/MLSS around 50 to 60 % as shown in Run 4 and Run 5 is consistent with the result of Run 2 and Run 3 (Phase 2- Stage 1).

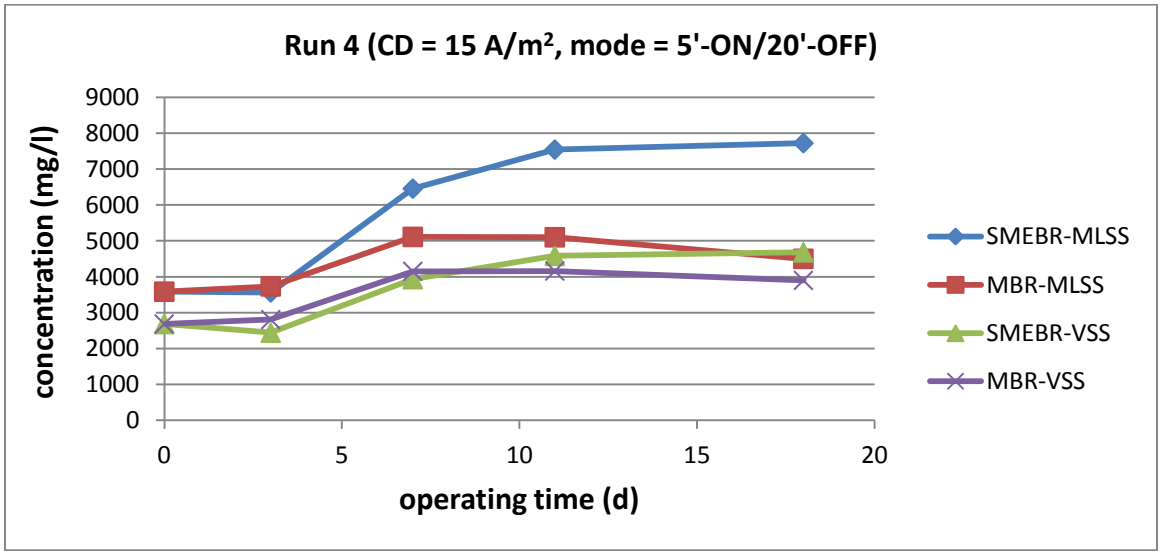

Figure 11.15: Run 4: Changes of MLSS and VSS concentrations in the SMEBR and MBR over time

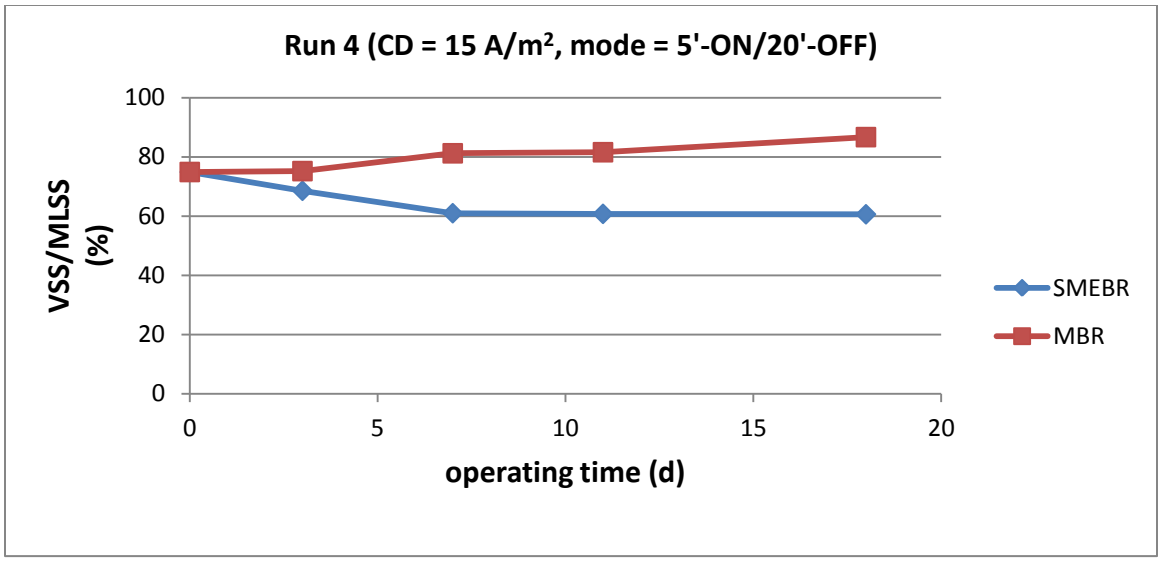

Figure 11.16: Run 4: Changes of VSS/MLSS percentage in the SMEBR and MBR over time

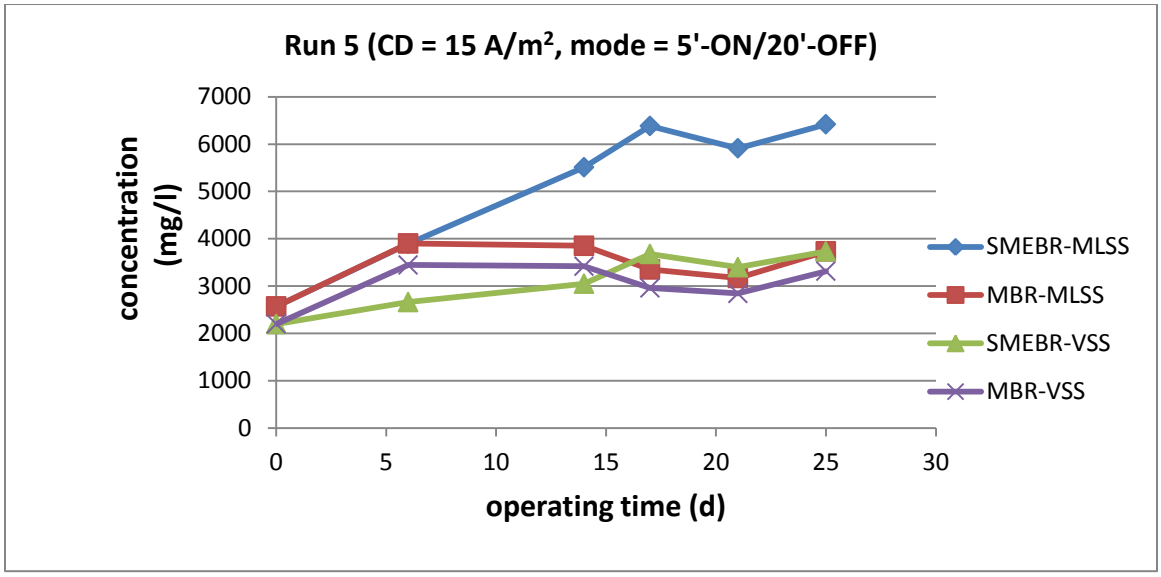

Figure 11.17: Run 5: Changes of MLSS and VSS concentrations in the SMEBR and MBR over time

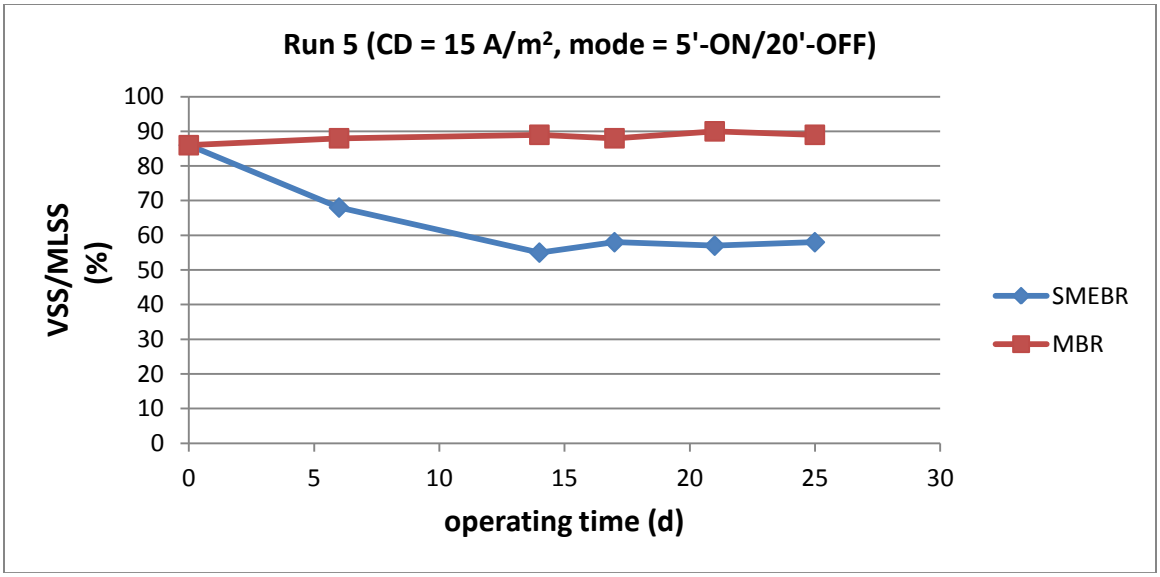

Figure 11.18: Run 5: Changes of VSS/MLSS percentage in the SMEBR and MBR over time

11.7 Particle size distribution (PSD) and zeta potential

Run 5 (Figure 11.19), unexpectedly, showed two cycles of floc particle size distribution (PSD) increase/decrease; two peaks on day 6 and day 28. Each peak was followed by a recession as it always did. This recession is due to the formation of smaller inorganic flocs composed mainly of aluminum hydroxides in addition to the extraction of bound water through electroosmosis. Changing of PSD in Run 4 (Figure 11.20) was similar to that of Phase 1 and Phase 2 (Stage 1). The mean PSD in the SMEBR peaked at 130 µm at the end of the run on day 18, while the size in the MBR was stable around 100 µm. However, the mean PSD in the SMEBR might have reduced if Run 4 was continued for longer time. The increase of PSD in the two cycles is related to the lower zeta potential in the SMEBR than the MBR and due to the enhanced movement of charged solid surfaces. The magnitude of zeta potential in the SMEBR in Run 4 and Run 5 was

between -23 to -25 mV, while in the MBR it was around -33 mV. The low CD and the long time-OFF in the electrical mode at which the SMEBR was operated did not produce enough Al^{+3} to cause further reduction in the magnitude of zeta potential.

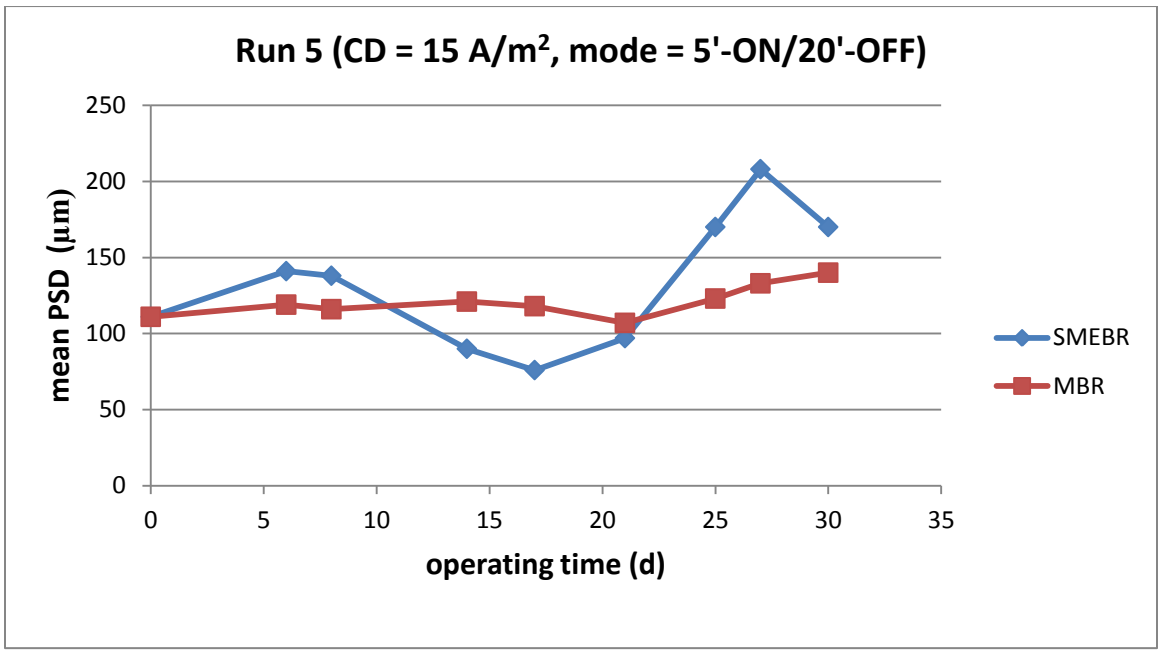

Figure 11.19: Run 5: Changes of the floc mean PSD in the SMEBR and MBR over time

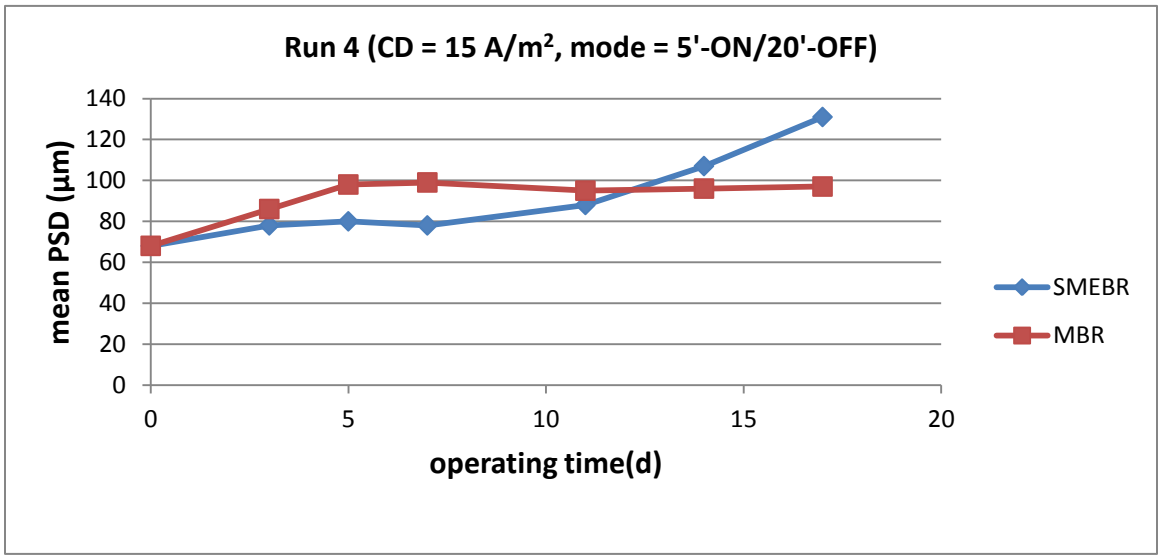

Figure 11.20: Run 4: Changes of the floc mean PSD in the SMEBR and MBR over time

11.8 Soluble microbial products (SMP) removal

Run 4 and Run 5 did not show any kind of protein removal. The concentration of protein was almost equal in the SMEBR and the MBR (Figures 11.21 and 11.22). However, this does not mean that the SMEBR is not capable of removing protein through electrocoagulation. Substantial protein removal was proved in every run of Phase 1 and Phase 2 (Stage 1). This problem was observed in the SMEBR because it was operated at low aeration intensity and low DO concentration that caused limited air movement in some zones. Limited aeration permitted the settling of the some flocs at the bottom of the reactor. The activated sludge inside the reactor was stirred manually with a rod to re-suspend the flocs every two days to ensure a complete mixing inside the reactor. It is likely that protein was released into the supernatant as the flocs were re-suspended. On the other hand, the concentration of polysaccharides in the SMEBR was lower than the MBR in Run 4 (Figure 11.23) and Run 5 (Figure 11.24). Though, the removal efficiency was not as much as the previous results of Phase 1 and Phase 2 (Stage 1). The reason why polysaccharide not protein maintained a lower concentration in the SMEBR than that in the MBR is mainly due to the higher removal percentage of polysaccharides than protein. The larger size of polysaccharide molecules makes its removal much easier than protein through electrocoagulation.

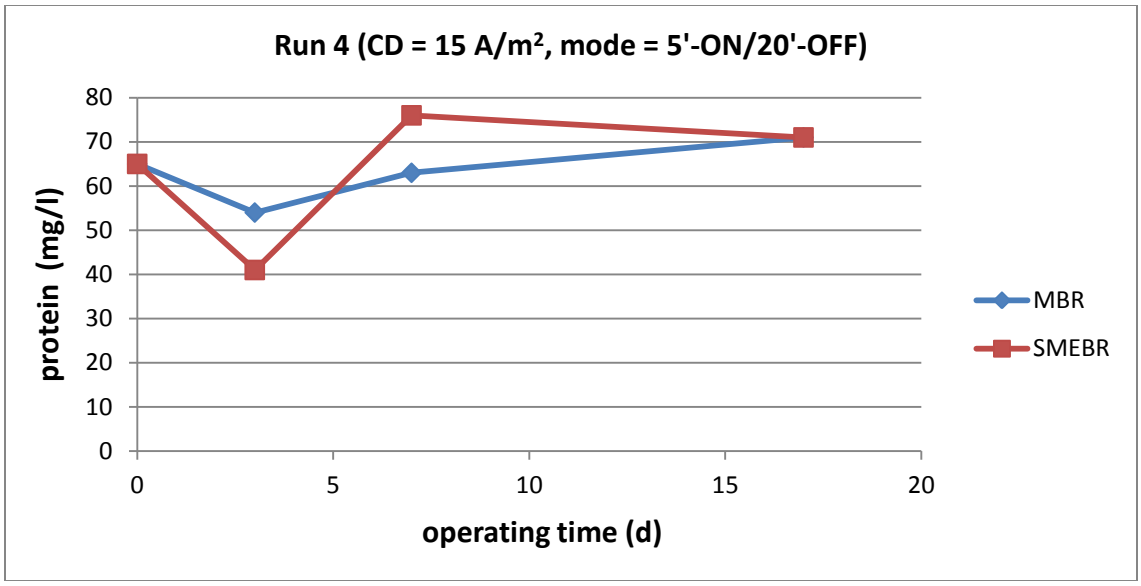

Figure 11.21: Run 4: Protein concentrations in the supernatant of SMEBR and MBR

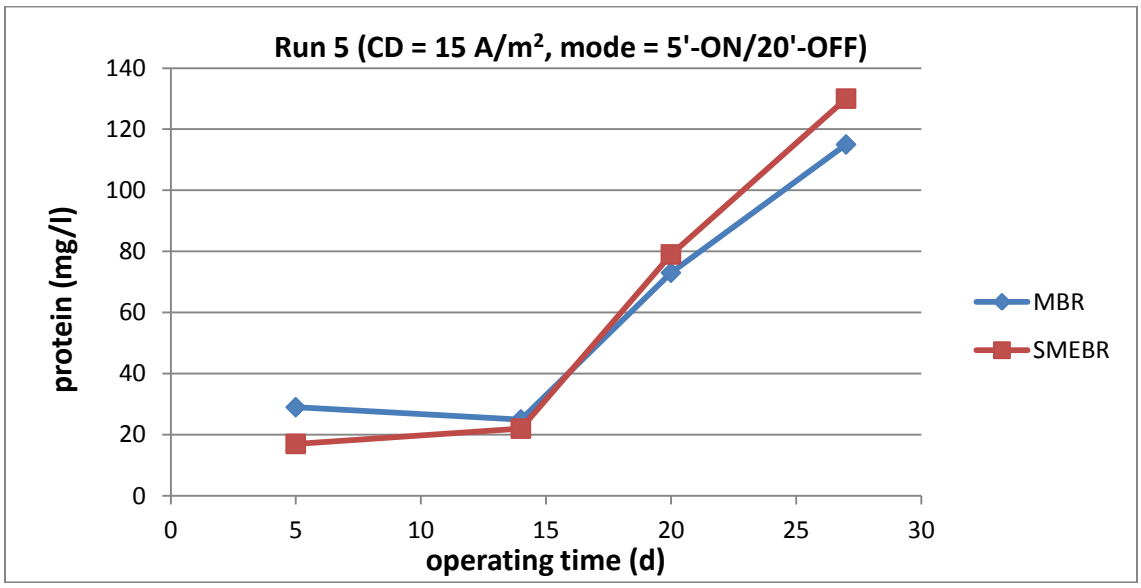

Figure 11.22: Run 5: Protein concentrations in the supernatant of SMEBR and MBR

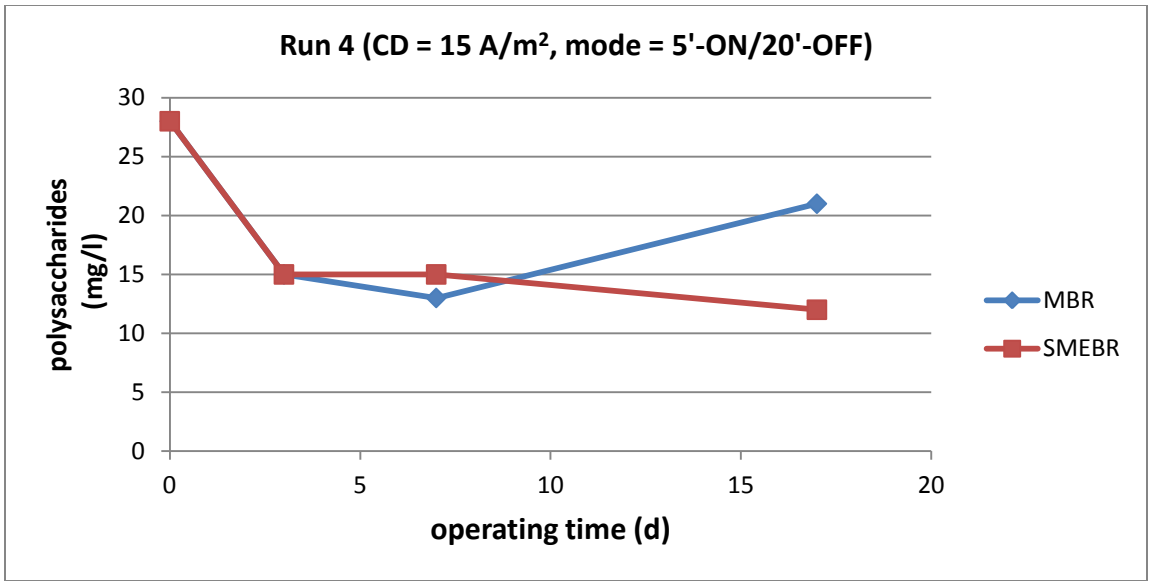

Figure 11.23: Run 4: Polysaccharide concentrations in the supernatant of SMEBR and MBR

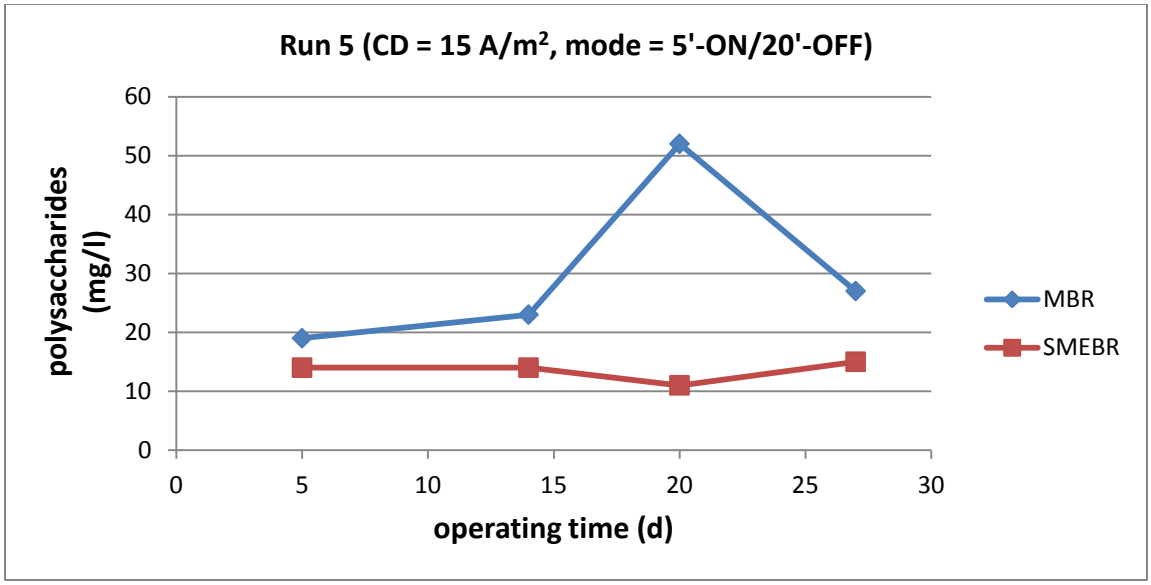

Figure 11.24: Run 5: Polysaccharide concentrations in the supernatant of SMEBR and MBR

11.9 Tightly bound water

The retained water within the flocs after the extraction of water through the physical means represents the tightly bound. Both runs showed less tightly bound water attached to the suspended solids (SS) in the SMEBR than the MBR. In the SMEBR it was between 0.5 to 0.6 g water/g.SS, while in the MBR it was between 1 to 1.5 g water/g SS (Figures 11.25 and 11.26). The extraction of tightly bound water through electroosmosis, the removal of SMP and the changes of the solids structure are the main reasons forced the SMEBR to reduce the water/solid ratio.

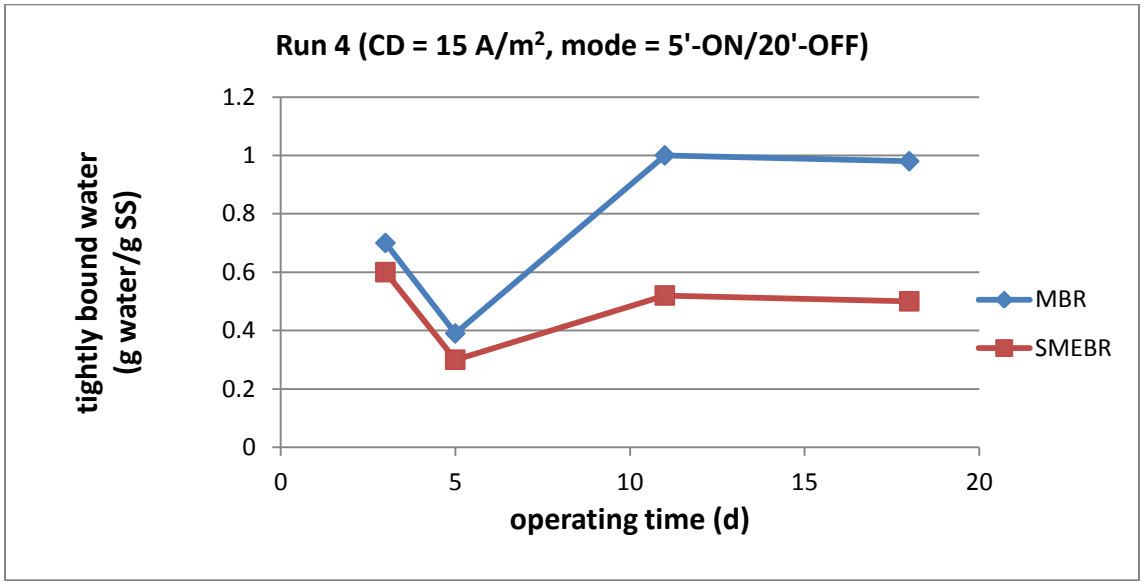

Figure 11.25: Run 4: Changes of flocs tightly bound water in the SMEBR and MBR over time

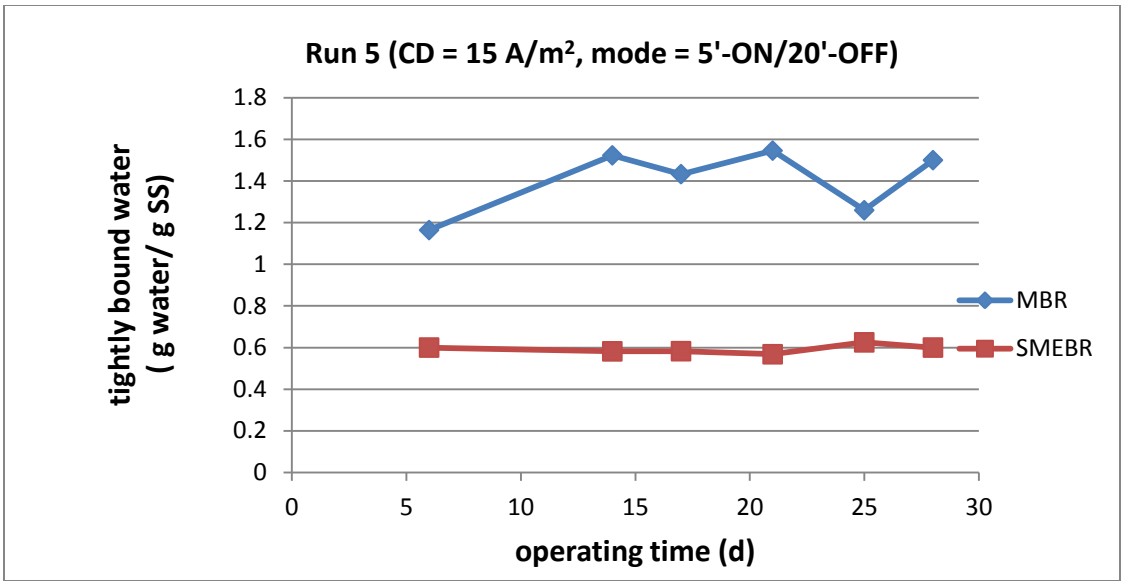

Figure 11.26: Changes of flocs tightly bound water in the SMEBR and MBR over time

11.10 Specific resistance to filtration (SRF)

Undoubtedly, the reduction of tightly bound water and the removal of SMP (excluding protein in this phase) in the SMEBR as illustrated in the previous sections should be reflected in a better sludge filterability. The specific resistance to filtration (SRF) was reduced in the SMEBR by many times over the operating period in Run 4 (Figure 11.27) and Run 5 (Figure 11.28).

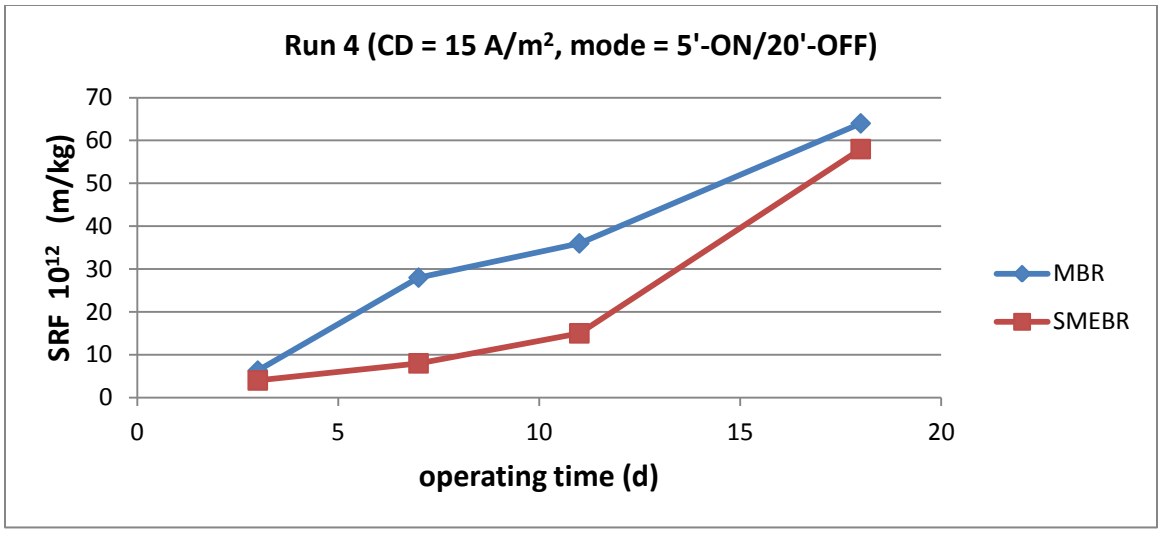

Figure 11.27: Run 4: Changes of SRF in the SMEBR and MBR over time

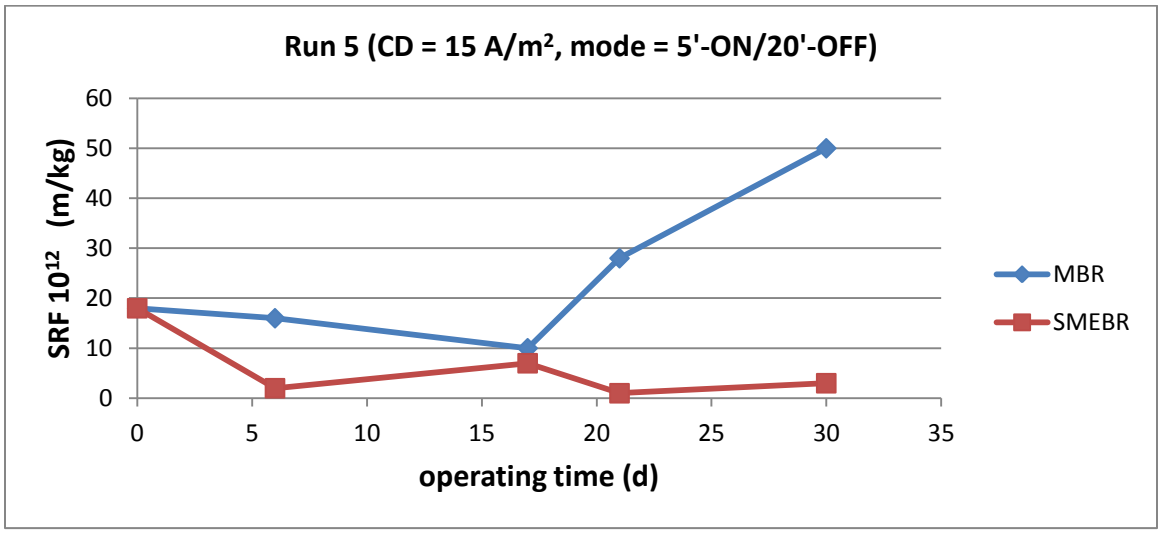

Figure 11.28: Run 5: Changes of SRF in the SMEBR and MBR over time

11.11 Membrane fouling

The impact of electrokinetics to reduce membrane fouling is an indirect process that can prevent the deposition of the flocs on the membrane surface. The removal of SMP and the tightly bound water in the SMEBR lead to a lower fouling rate. Fouling rate is expressed as the increase of trans-membrane pressure (TMP) over time. The TMP

designates the pressure difference between inside and outside the membrane. The TMP increases as the membrane is fouled due to the deposition of the microbial flocs onto its surface over the time. Once the TMP increases to a limit that causes a reduction in the membrane flux, the membrane is physically cleaned to recover its permeability. In Run 4, the membrane was cleaned 10 times compared to 7 times in the SMEBR (Figure 11.29) over the same period of time, meanwhile, the membrane fouling rate was 4.4 kPa/d in the MBR compared to 2.9 kPa/d in the SMEBR (Figure 11.30). Because the concentration of SMP in the supernatant of the two reactors was nearly equal, a slight improvement of membrane fouling in the SMEBR was observed in this run.

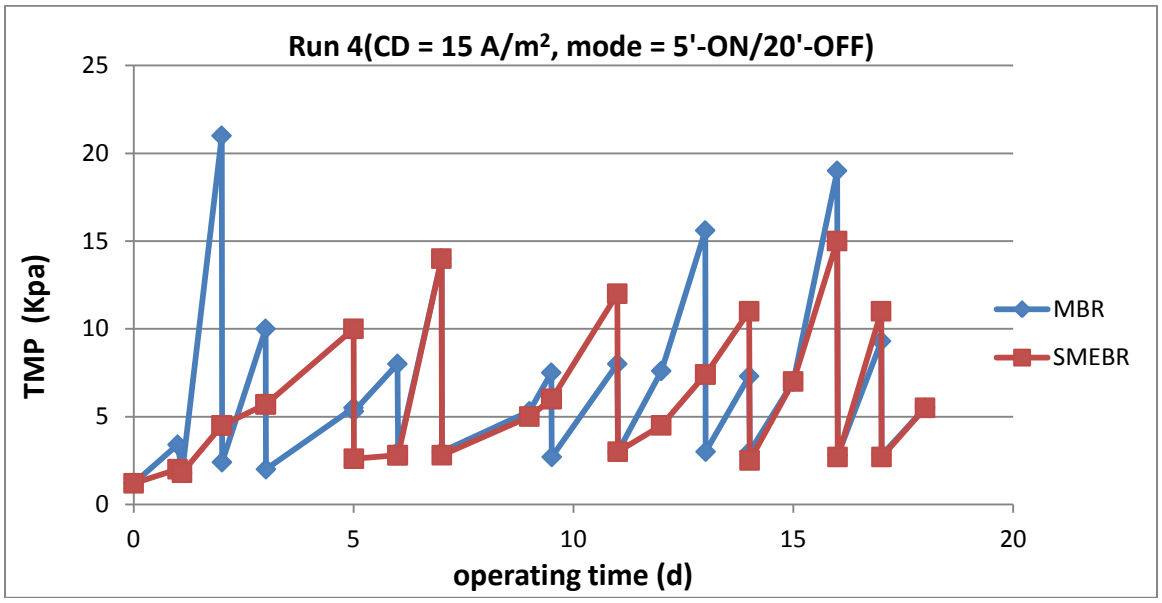

Figure 11.29: Run 4: Changes of TMP in the SMEBR and MBR over time

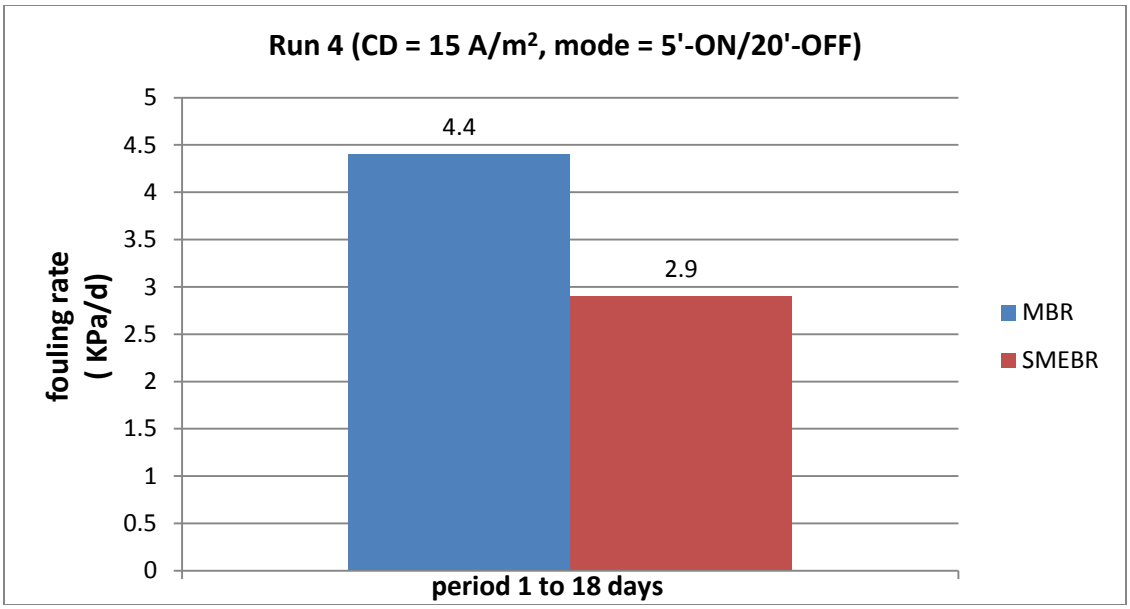

Figure 11.30: Run 4: Membrane fouling rate in the SMEBR and MBR

In Run 5, there were two distinct periods of different membrane fouling rate in both reactors. The low fouling rate period from start until day 20 and the high fouling rate period from day 21 to day 30 (Figures 11.31 and 11.32). The concentration of SMP in the last 10 days was almost 3 times higher than that in the first 20 days of operation as illustrated previously in Figure 11.22. In the MBR, the membrane cleaning was performed 17 times compared to 10 times in the SMEBR over the 30 day operation period (Figure 11.31). During the first 20 days, the membrane foulings were 1.9 kPa/d and 0.5 kPa/d in the MBR and the SMEBR, respectively. The last 10 day showed higher fouling rate in the MBR (19 kPa/d) and the SMEBR (6 kPa/d) due to the increase of SMP concentrations (Figure 11.32).

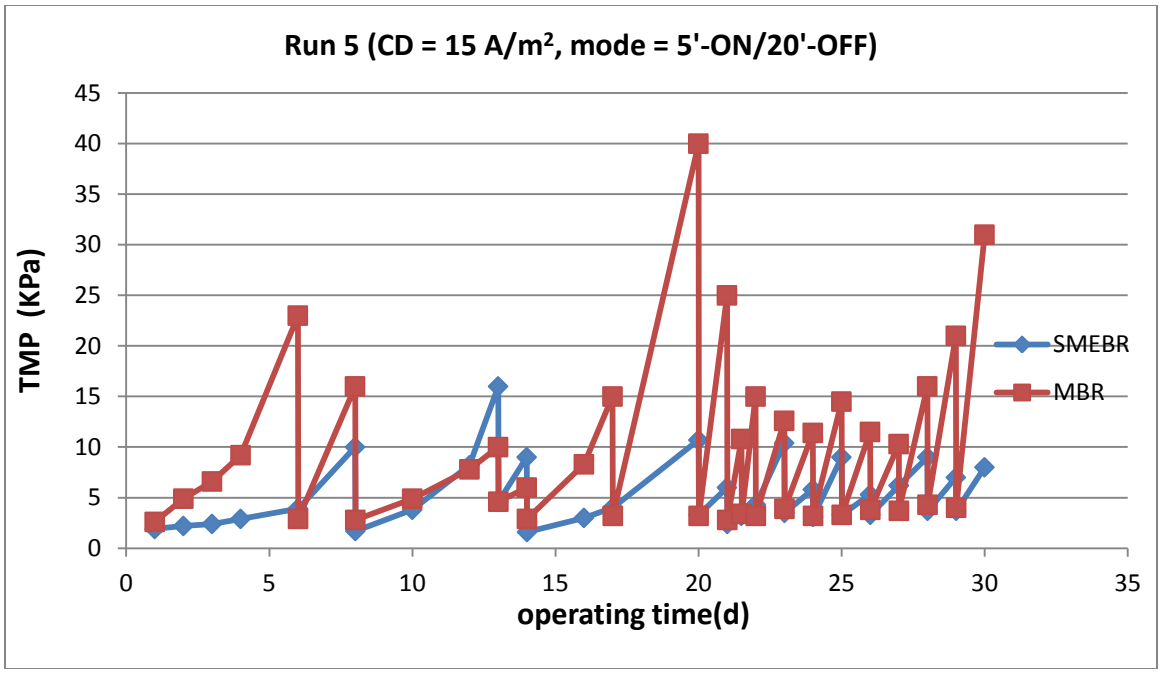

Figure 11.31: Run 5: Changes of TMP in the SMEBR and MBR over time

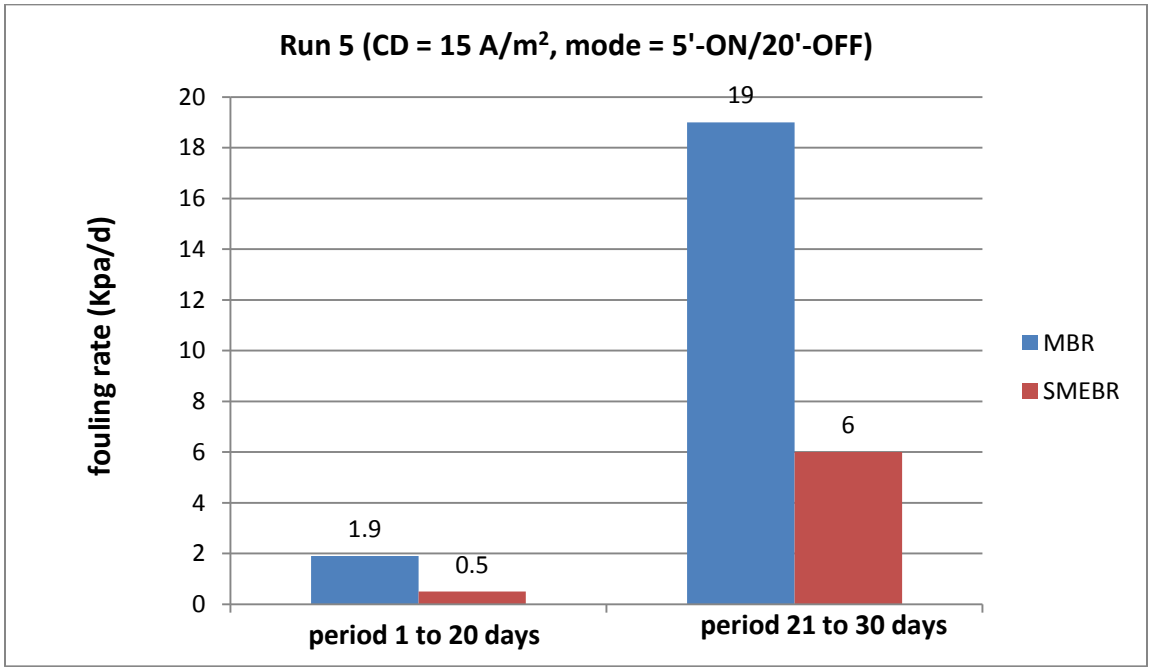

Figure 11.32: Run 5: Mean membrane fouling rate in the SMEBR and MBR

Since the concentration of VSS in Run 4 and Run 5 was almost around 3000 mg/l, it is assumed that its impact on membrane fouling is the same in both runs and both reactors. On the other hand, the concentration of SMP was different in Run 4 and Run 5. Table 11.1 was created to confirm the impact of SMP on membrane fouling propensity at almost equal VSS concentration. In the MBR, the fouling rate was 1.9, 4.4 and 19 kPa/d at SMP concentrations of 50, 77 and 135 mg/l, respectively. On the other hand, the SMEBR showed membrane fouling rates of 0.5, 2.9 and 6 kPa/d at 45, 66 and 112 mg/l of SMP, respectively. Membrane fouling rate increased with the increase of SMP concentration in the SMEBR as well as in the MBR. The capability of the SMEBR to remove the SMP from the supernatant is, undoubtedly, one of the major mechanisms contributing in the reduction of membrane fouling. The increase of SMP plays a big role in the irreversible fouling, but the results of all phases also proved the impact of the SMP on promoting reversible fouling. It is likely that the SMP acts as coherent organic materials that bridges between the flocs deposited on the membrane (cake layer). These flocs/SMP interactions make the cake layer more coherent, less porous and less permeable for the passage of water. Subsequently, higher membrane fouling rate is promoted.

Table 11.1: Correlation of the supernatant SMP and membrane fouling rate

Run #	Reactor type	Period (day)	PN (mg/l)	PS (mg/l)	Avg. SMP (PN+PS)	Fouling rate (kPa/d)
Run 4	MBR	1 to 18	50 to 70	14 to 20	77	4.4
Run 4	SMEBR	1 to 18	40 to 76	10 to 15	66	2.9
Run 5	MBR	1 to 20	20 to 40	20	50	0.7
Run 5	SMEBR	1 to 20	20 to 40	15	45	0.4
Run 5	MBR	20 to 30	80 to 120	20 to 50	135	19
Run 5	SMEBR	20 to 30	80 to 120	10 to 15	113	6

PN= protein, PS= polysaccharides

11.12 Reproducibility of results

Since many runs were tested in the two stages of Phase 2 and showed nearly the same trend, the results of all runs were evaluated together to assess the reproducibility of the results. Since carbon and phosphorus removal efficiencies were very high in all runs (above 95%), their reproducibility is clear and does not need any further evaluation. Therefore, the reproducibility of three processes will be evaluated hereafter: membrane fouling, nitrification and denitrification.

Membrane fouling was determined at high SMP concentration (130 to 210 mg/l) and low SMP (50 to 80 mg/l). Membrane fouling rate (kPa/d) was 5 ± 1.6 and 1.5 ± 0.3 times higher in the MBR than the SMEBR at high and low SMP concentrations, respectively

(Figure 11.33). This difference in membrane fouling is the average of five replicates operated at high SMP and 3 replicates at low SMP concentrations over the course of the five runs of Phase 2 (Stage 1 and Stage 2); results are summarized in Tables 11.2 and 11.3. Subsequently, at the same level of VSS, the MBR is likely to exhibit higher membrane fouling rate in the MBR than the SMEBR by 1.5 to 5 times based on the concentration of the SMP in the sludge supernatant.

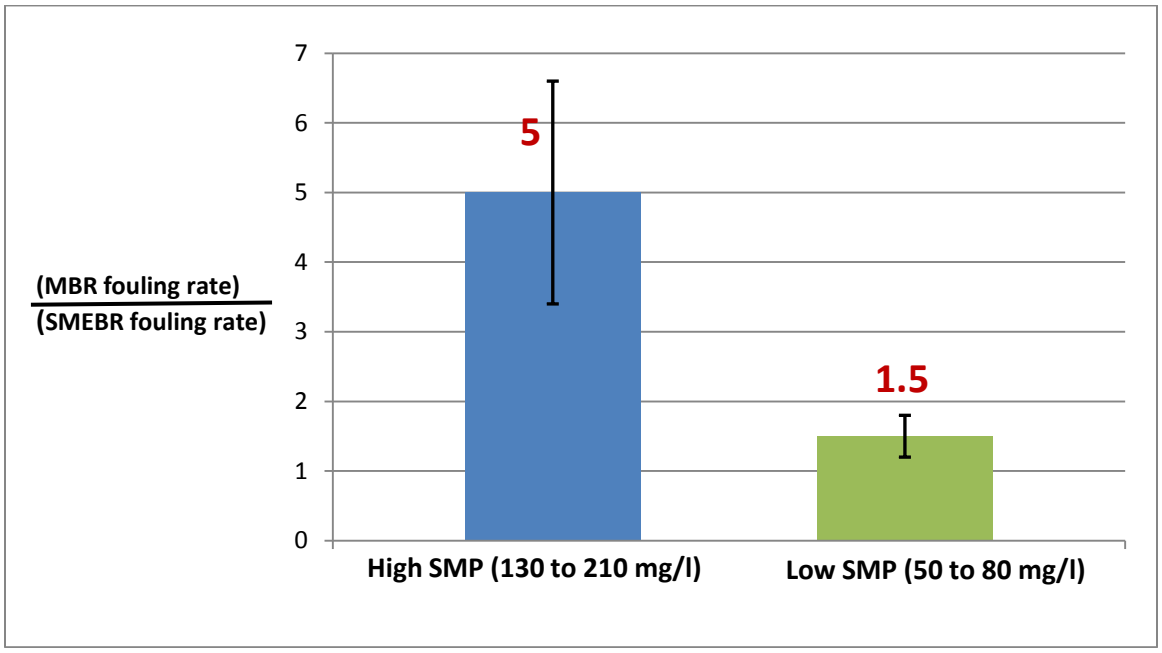

Figure 11.33: Comparison of membrane fouling rate between the SMEBR and MBR

Table 11.2: Reproducibility of membrane fouling rate (ΔTMP/d) reduction in the SMEBR compared to the MBR at SMP concentration between 130 to 210 mg/l

Replicate #	Run #	period	MBR fouling rate/SMEBR fouling rate
1	Run 1	2 to 12	(13.4/1.8) = 7.4
2	Run 2	21 to 35	(21 /3.7) = 5.6
3	Run 3	1 to 9	(3.2/0.7) = 4.6
4	Run 3	11 to 24	(15.6/3.9) = 4
5	Run 5	20 to 30	(19/6) = 3.2
			Average = 5 , SD= 1.6

SD = standard deviation

Table 11.3: Reproducibility of membrane fouling rate (ΔTMP/d) reduction in the SMEBR compared to the MBR at SMP concentration between 50 to 80 mg/l

Replicate #	Run #	period	MBR fouling rate/SMEBR fouling rate
1	Run 2	1 to 20	(3.2/2.6) = 1.2
2	Run 4	1 to 18	(4.4 /2.9) = 1.5
3	Run 5	1 to 18	(0.7/0.4) = 1.8
			Average = 1.5 , SD= 0.3

The average nitrification of five replicates in the SMEBR (89.6 ± 6.6 %) and MBR (90.2 ± 11.2 %) was almost the same (Table 11.4 and Figure 11.34). The percentage was ranging between 77 to 99 % in both reactors. The percentage was influenced by the influent

ammonium concentrations. When the influent ammonium concentration was higher than the reactor nitrification potential, the percentage dropped.

Table 11.4: Reproducibility of nitrification % in the SMEBR and MBR

Replicate #	Run #	Period (d)	MBR Nitrification %	SMEBR Nitrification%	(SMEBR nit. %)/(MBR nit.%) (%)
1	Run 2a	5 to 17	79	81	103
2	Run 2b	33 to 42	99	94	95
3	Run 3	1 to 27	77	89	116
4	Run 4	6 to 18	99	98	99
5	Run 5	1 to 30	97	86	87
			Avg. = 90.2% SD = 11.2	Avg.= 89.6% SD = 6.6	Avg. = 100% SD = 0.1

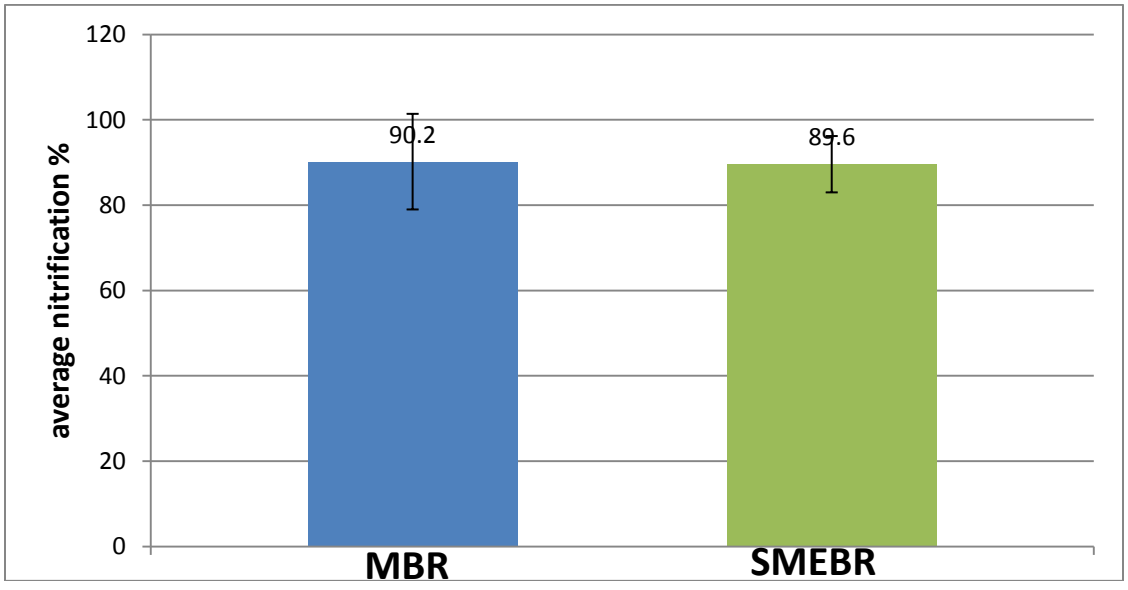

Figure 11.34: Comparison of the average of five replicates of the nitrification % in the SMEBR and MBR

Denitrification in the SMEBR was very high in all runs. The average of the five replicates was 95 ± 1.5% as illustrated in Table 11.5 and Figure 11.35. The denitrification percentage was calculated according to Equation 11.1

$$\text{denitrification } \% = \frac{([\text{nitrate}](\text{MBR}) - [\text{nitrate}](\text{SMEBR}))\ 100\%}{[\text{nitrate}](\text{MBR})} \quad (11.1)$$

The SMEBR proved in five replicates the possibility of achieving a nitrification potential as good as the MBR in addition to a simultaneous high removal of nitrate through denitrification. The results of nitrogen removal obtained in the SMEBR depend on how the system is optimized. The operating conditions that provide anammox conditions provide the maximum N removal efficiency. However, the system is still working at high efficiency even at conditions close to the anammox conditions.

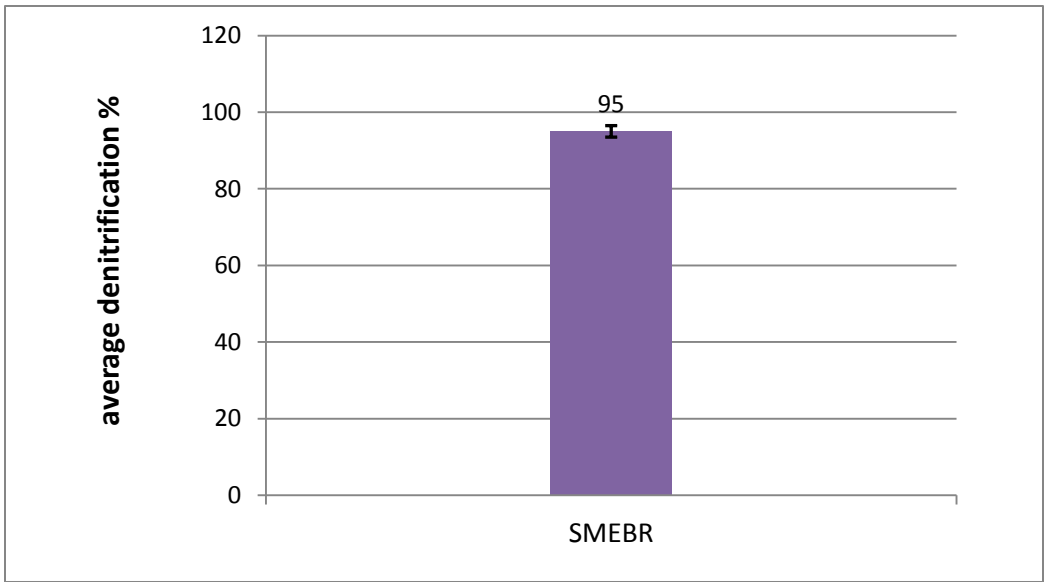

Figure 11.35: The average denitrification percentage of five replicates in the SMEBR

Table 11.5: Reproducibility of denitrification in the SMEBR compared to the MBR

Replicate #	Run #	Period (d)	Denitrification %
1	Run 2a	5 to 17	93
2	Run 2b	33 to 42	95
3	Run 3	1 to 27	96
4	Run 4	6 to 18	96
5	Run 5	1 to 30	93
			Average = 95% , SD= 1.5

Chapter 12

Phase 3: Pilot scale SMEBR

12.1 Introduction

The previous phases were conducted under lab conditions and optimum environment conditions. The temperature was around 20^{o} C and the synthetic wastewater has the same C/N ratio over the whole operating period. In reality, these conditions are changing on a daily basis all over the year. Thus, the main objective of Phase 4 was to investigate the removal of nitrogen through the simultaneous nitrification/denitrification in the SMEBR at a pilot scale level under real conditions. This phase was conducted in the wastewater treatment plant in l'Assomption, QC.

12.2. Methodology

The design of the SMEBR pilot reactor in wastewater treatment plant in the City of l'Assomption, QC was described by Hasan (2011). The configuration of the pilot SMEBR was the same as the one used in the lab, but at larger volume. The working volume of the reactor was 250 l. A PVDF hollow fiber membrane module (MUNC-600 A, Microza Asashi, Japan) was immersed in the middle of the reactor. The pore size and the surface area of that membrane are 0.1 µm and 12.5 m^2, respectively. The membrane was surrounded by perforated electrodes. The SMEBR was fed with raw wastewater after screening without any pretreatment.

Phase 3 was divided into two Runs (Run 6 and Run 7). Run 6 was operated at the real sludge reactor temperature (13° to 15° C) and will be designated in this research as low temperature. Run 7 was operated at temperature similar to that in the lab (18° to 22° C) and will be designated in this research as high temperature. The pilot experiment was conducted during the coldest period of the year in Quebec, Canada; January to March. During that period, the MLSS temperature in the reactor was between 13° to 15° C and reflected the actual sewage temperature. Since Run 7 was intended to be operated at high temperature, water heaters were immersed in the feed tank to increase its temperature and obtain the required reactor MLSS temperature of 18° to 22° C. The characteristics of the real influent wastewater and the operating conditions of each run are given in Table 12.1. The SMEBR was seeded with activated sludge of 3500 mg/l MLSS brought from the wastewater treatment plant, St. Hyacinthe, Quebec on the starting day.

Table 12.1: Operating conditions for each experimental run of Phase 4 and influent characteristics

Run #	CD (A/m^2)	Exposure mode	HRT (h)	Sludge temperature (°C)	Conc. of NH_4-N (mg/l)	Conc. Of PO_4^{-3} (mg/l)	Conc. of COD (mg/l)	Operating period (days)
Run 6	15 to 17	5'-ON/20'-OFF	11	13 to 15	15 to 50	4 to 20	70 to 250	1 to 18
Run 6	15 to 17	5'-ON/20'-OFF	24	13 to 15	15 to 50	4 to 20	70 to 250	19 to 26
Run 7	15 to 17	5'-ON/20'-OFF	11	18 to 22	15 to 50	4 to 20	70 to 250	1 to13
Run 7	15 to 17	5'-ON/20'-OFF	24	18 to 22	15 to 50	4 to 20	70 to 250	14 to 25

Because of the high cost of manufacturing such a reactor, the SMEBR was operated solely without a control MBR to compare the results. However, a small scale MBR (12 l working volume) was installed beside the pilot SMEBR to serve as a control in Run 7.

12.3 Results and Discussion

The discussion in this chapter focuses on the nutrient removal at raw wastewater and different temperatures and compares the results with the lab tests of Phase 2.

12.3.1 Carbon removal

The pilot SMEBR showed a high capability of carbon removal through oxidation when the system operated at low temperature (Run 6). The influent COD concentration was between 160 to 280 mg/l and in the effluent was less than 40 mg/l (Figure 12. 1). The average removal efficiency of COD over the whole operating period was 90 % (Figure 12.2). Theoretically, microbial activity reaches its maximum when the temperature is at the optimum level (25^{o} to 30^{o} C). Once the temperature drops below that optimum, the microbial activity deteriorates proportionally. Moreover, the impact of low temperature on microbial activity is aggravated when the biomass is subjected to the DC field as another stress factor. Based on the results of Run 6 regarding the high removal of C, it is concluded that the biomass was able to tolerate the combined stresses of low temperature and the DC field and maintained enough activity to oxidize the C to a high efficiency.

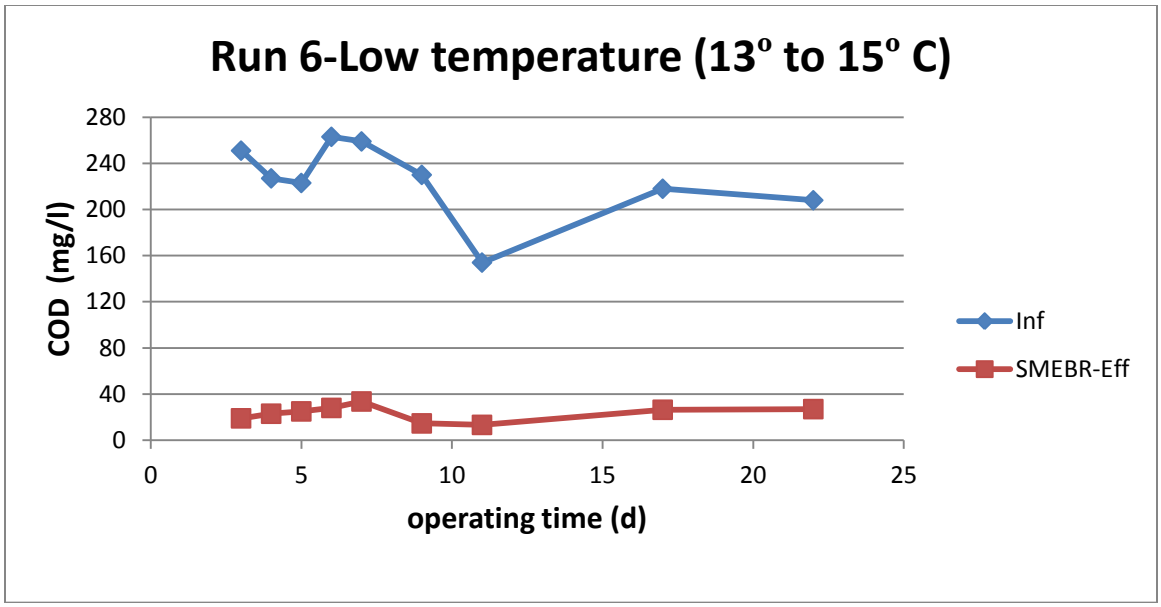

Figure 12.1: Run 6: The concentrations of COD in the influent and the effluent of the pilot SMEBR-low temp

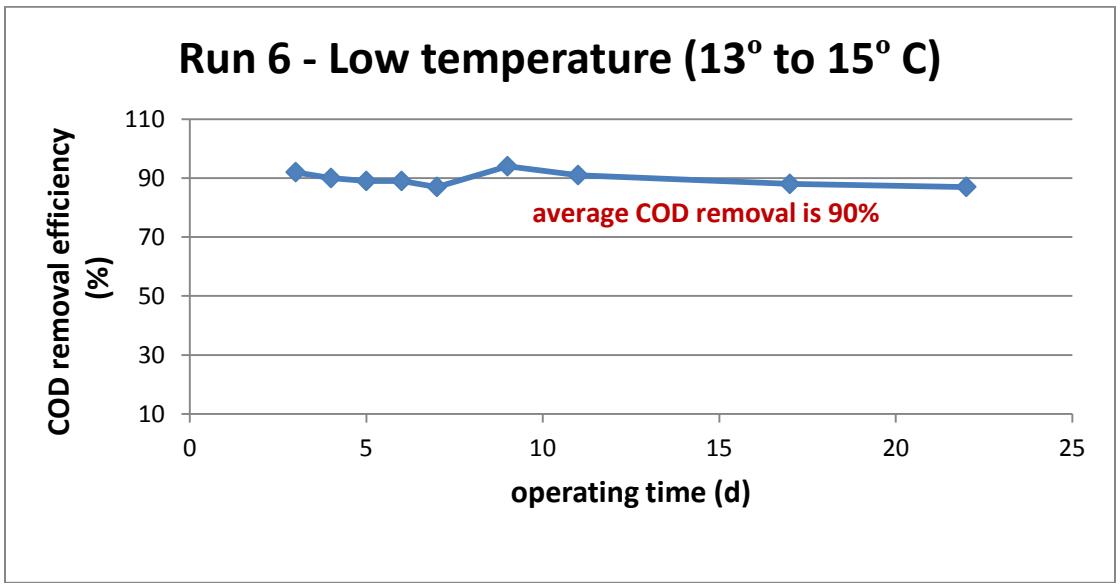

Figure 12.2: Run 6: The COD removal efficiency in the pilot SMEBR-low temperature

Run 7, operated at high temperature, showed a high reduction of the COD concentration in the effluent for the MBR and the SMEBR (Figure 12.3). However, the removal efficiency was a bit higher in the SMEBR (88%) than the MBR (85%) due to the

contribution of electrocoagulation in C removal (Figure 12.4). The COD removal efficiency at low temperature (90%) in Run 6 was higher than at high temperature (88%), because the influent of Run 6 had higher influent concentrations of COD. Meanwhile, the effluent concentrations of COD in Run 6 and Run 7 were almost the same.

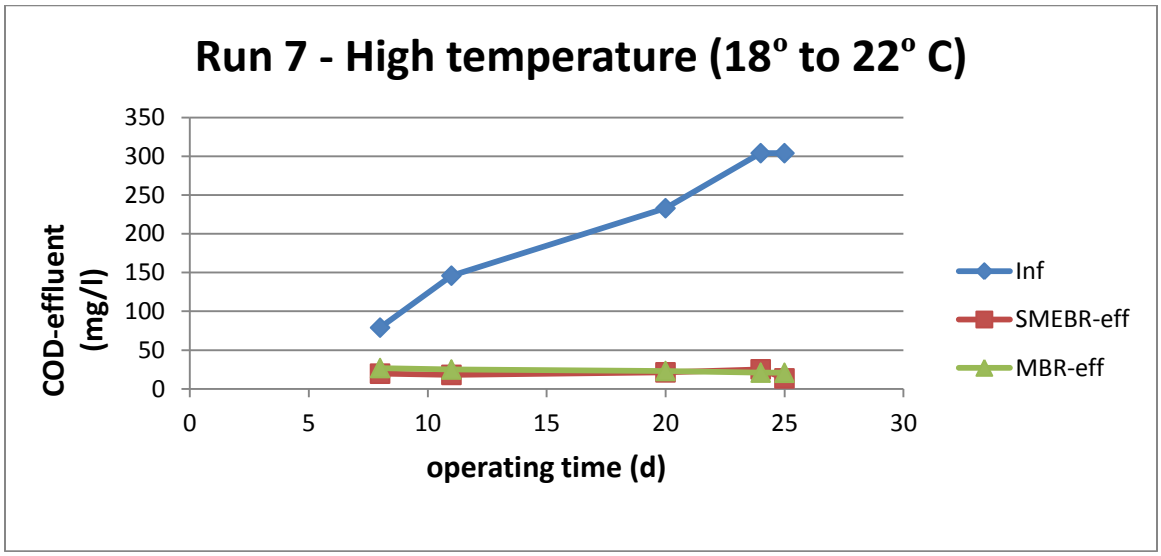

Figure 12.3: Run 7: The concentrations of COD in the influent and the effluent of the pilot SMEBR-high temperature

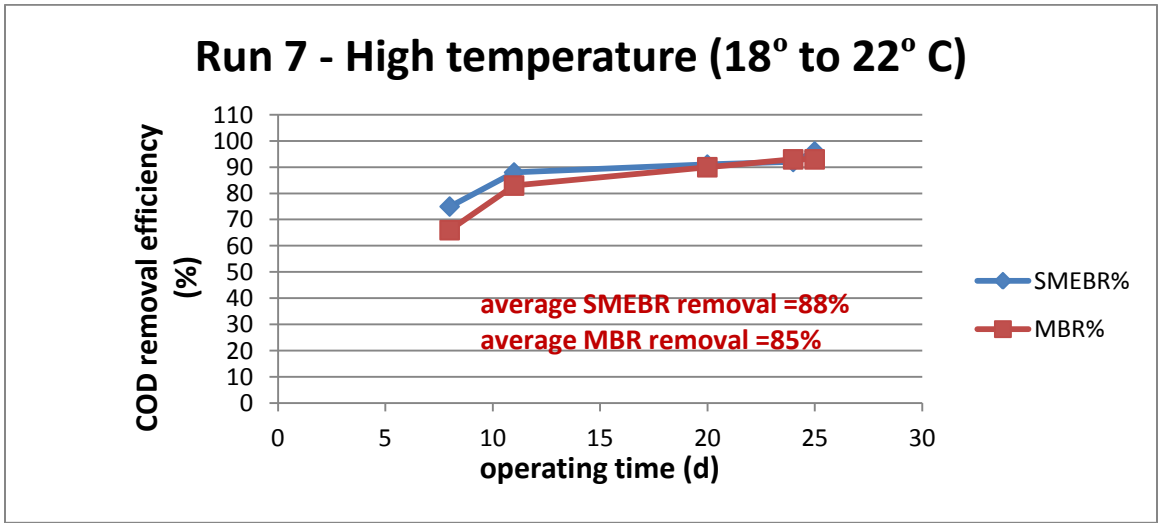

Figure 12.4: Run 7: The COD removal efficiency in the pilot SMEBR-high temperature

12.3.2 Phosphorus removal

Since phosphorus removal in the SMEBR depends mainly on the electrochemical reactions that form phosphorus hydroxide complexes rather than biological removal, the temperature did not show a significant impact on its removal. The pilot SMEBR showed a high removal efficiency of P in both runs; Run 6 (Figure 12.5 and 12.6) and Run 7 (Figures 12.7 and 12.8). However, Run 6 showed a little bit lower removal efficiency than Run 7. The contribution of P removal through the biological pathway was more substantial at high temperature in Run 7.

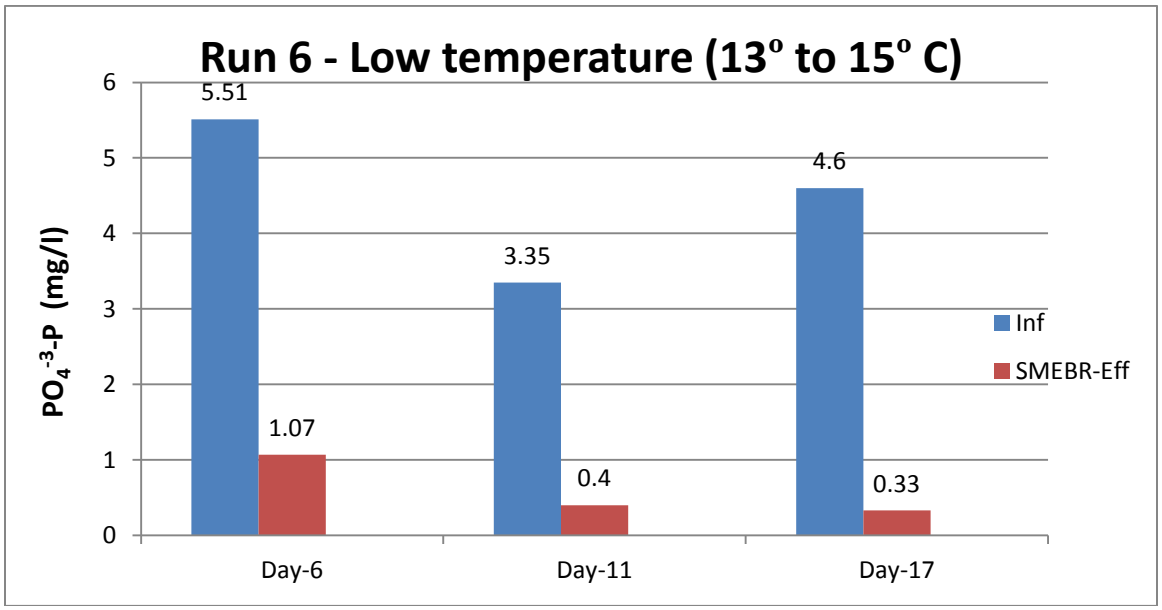

Figure 12.5: Run 6: Concentrations of orthophosphate (PO4-3) in the influent and the effluent of the pilot SMEBR – low temperature

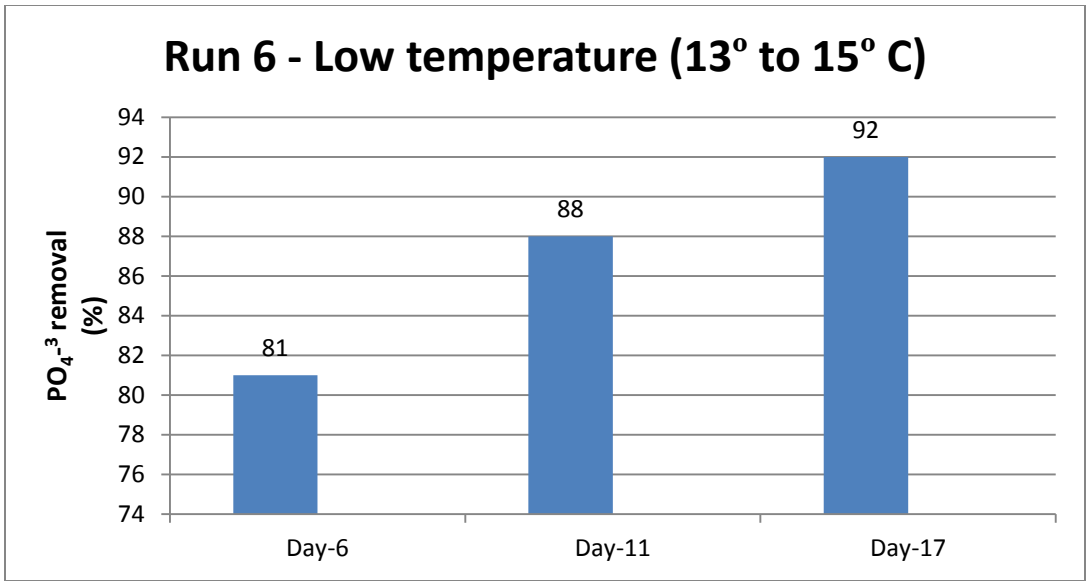

Figure 12.6: Run 6: Orthophosphate ($PO4^{-3}$) removal efficiency in the pilot SMEBR-low temp

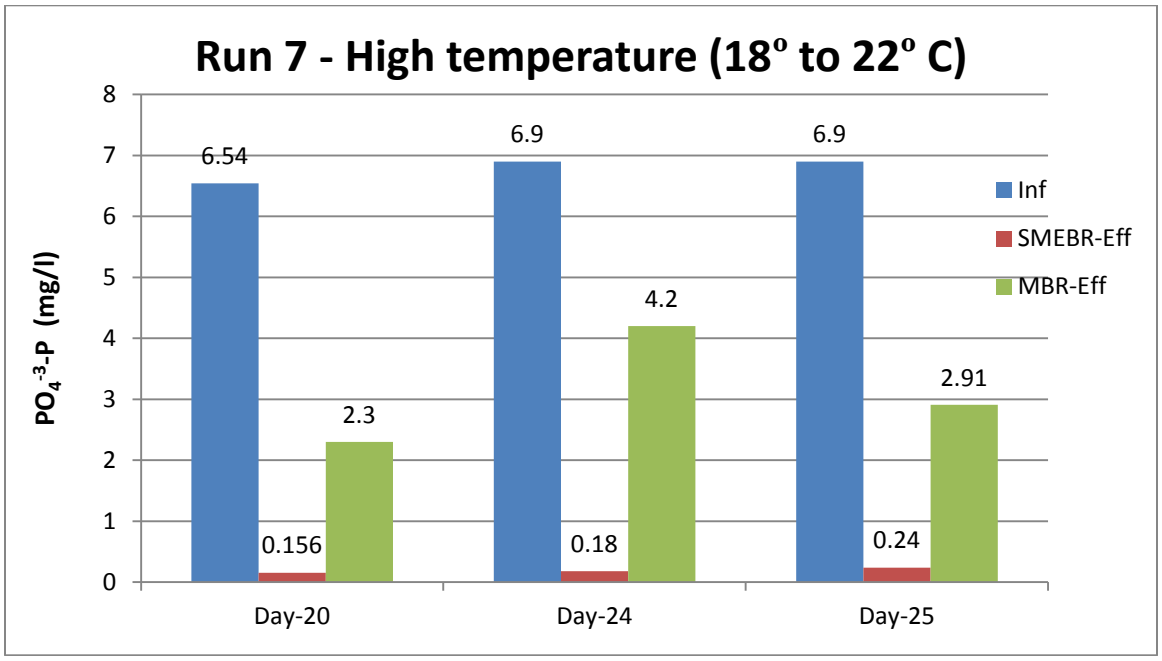

Figure 12.7: Run 7: Concentrations of orthophosphate ($PO4^{-3}$) in the influent and the effluent of the pilot SMEBR and the small scale MBR- high temperature

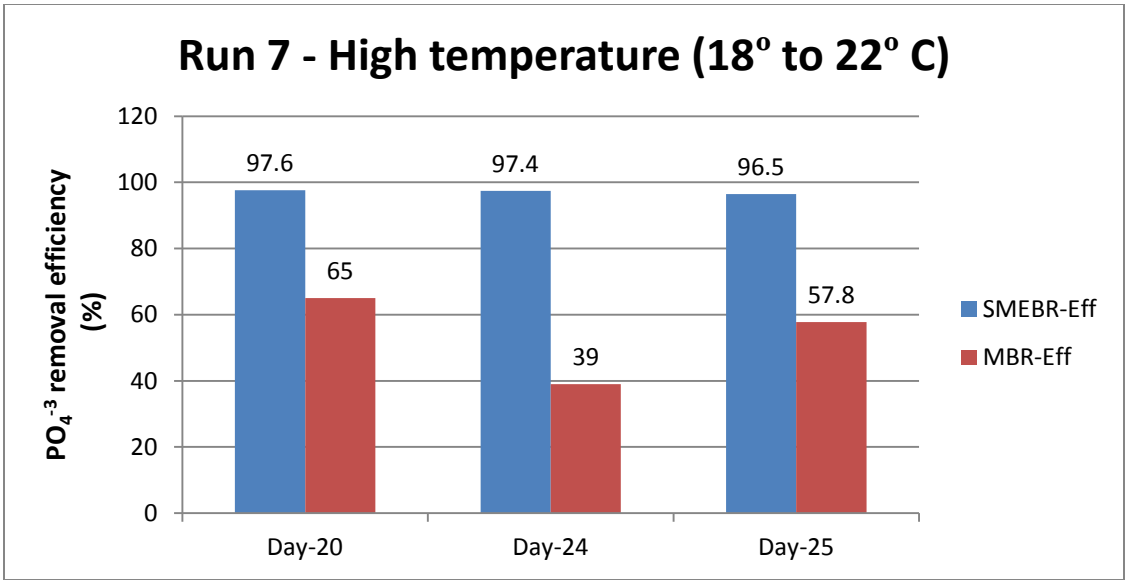

Figure 12.8: Run 7: Orthophosphate ($PO4^{-3}$) removal efficiency of the pilot SMEBR and the small scale MBR - high temperature

12.3.3 Nitrogen removal at low temperature - Run 6

Run 6 showed that the nitrogen removal in the SMEBR is severely affected at low temperature. During the first days, the ammonium concentration in the effluent was less than 3 mg/l and high nitrification percentage (> 90%) was achieved (Figure 12 .9 and 12.10). This initial high nitrification indicates that nitrifies worked at a high efficiency at low temperature. Afterward, the ammonium concentration in the effluent of the pilot SMEBR increased to more than 12 mg/l and the nitrification percentage dropped substantially. The average nitrification was around 40% over the whole operating period regardless of the DO concentration in the reactor. Starting on day 4, the DC field at that low temperature has reduced the activity of the nitrifies and therefore the nitrification process. The DC field was cut off on day 18 to give the biomass in the SMEBR enough

time to recover. The system recovery was very slow. After one week of cutting off the DC field, the nitrification percentage increased only to 50%.

Nitrogen removal in the SMEBR depends on the biological processes such as nitrification, denitrification and anammox. The performance of these processes is affected by the temperature and the applied DC field. The biomass inside the SMEBR was unable to tolerate two combined stresses; the low temperature and the DC field.

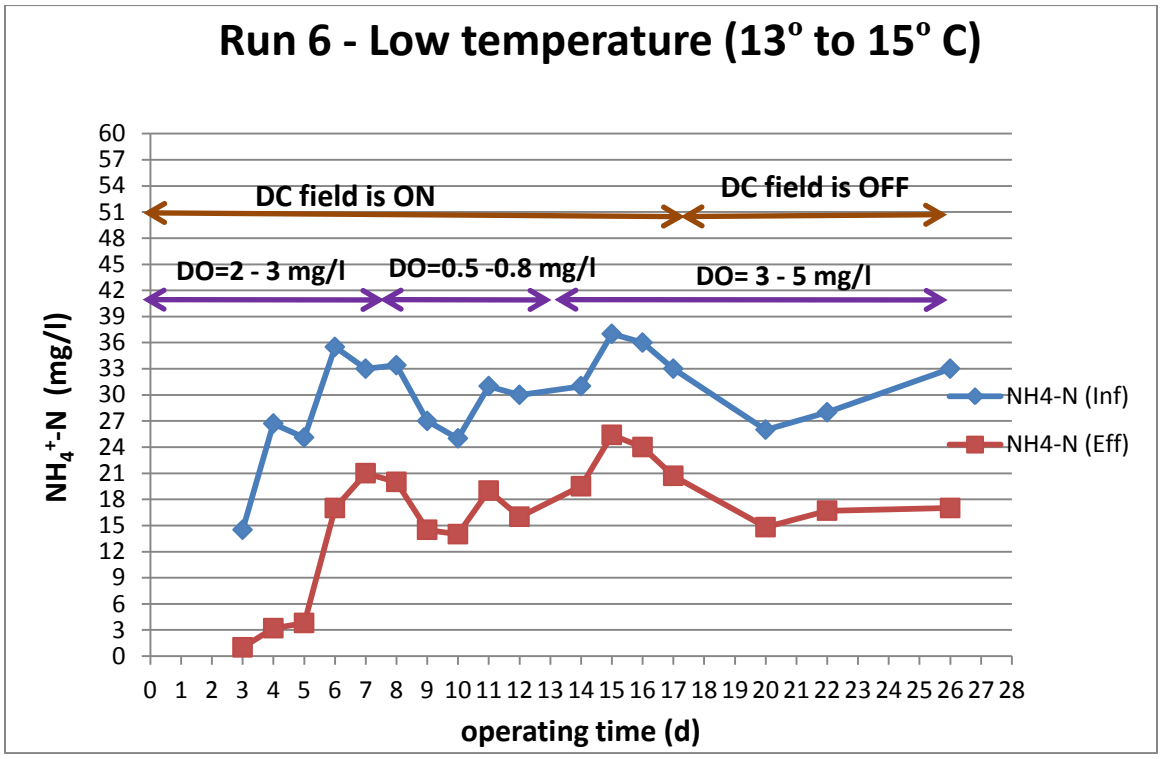

Figure 12.9: Run 6: Ammonium concentrations in the influent and the effluent of the pilot SMEBR over time

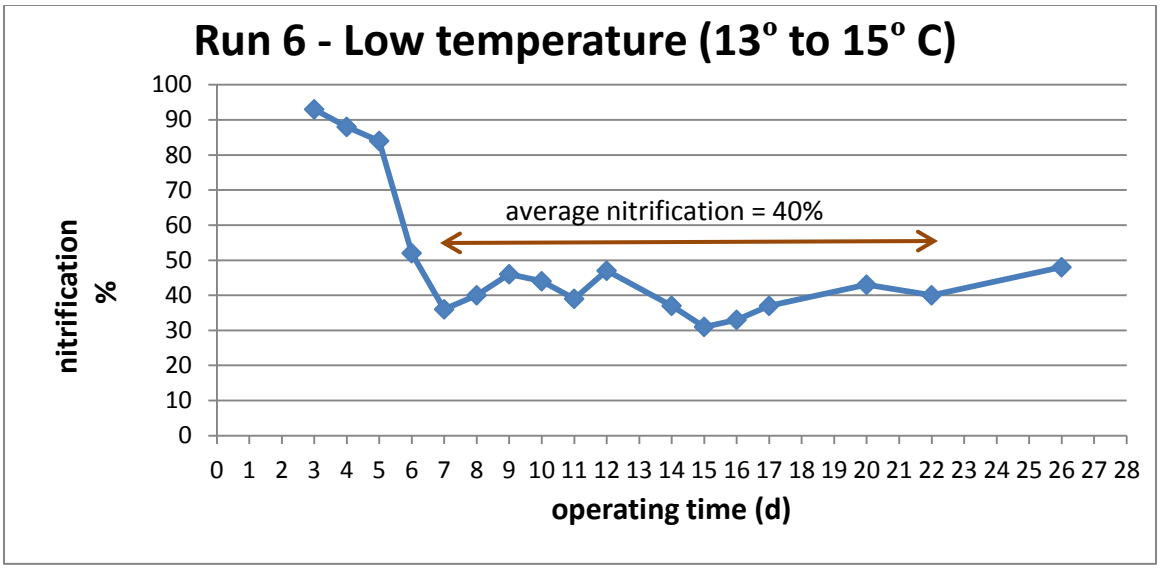

Figure 12.10: Run 6: The nitrification percentage of the pilot SMEBR over time

The pilot SMEBR was unable to remove the nitrate completely at low temperature (Figure 12.11). The nitrate concentration stabilized at 20 mg NO_3^-/l due to the reduction in the nitrification efficiency. The nitrate concentration increased to 57 mg NO_3^-/l after one week of cutting off the DC field; an indication of biomass recovery. Since there was no control reactor working simultaneously at the same conditions of the SMEBR, it is hard to evaluate how much nitrate was denitrified in the system.

Although the removal of nitrogen and carbon depends on the biological processes, nitrogen was more affected than carbon in the SMEBR. The reason of higher than 90% C removal compared to only 40% nitrification is related to the number of bacteria species responsible in each biological process. There are countless species that can oxidize the carbon and convert it into CO_2 and water. On the other hand, there are only two species responsible for the conversion of ammonium into nitrate (*Nitrosomonas* and *Nitrobacter*). The DC field impact on bacteria is the same regardless of its genotype

because they have the same size and the same structural components such as protein, polysaccharides and fatty acids. Thus, once the DC field is applied and the activity of the biomass is reduced, the biological processes that are performed by the one or two bacteria species such as the nitrification, denitrification and anammox will be affected the most. This problem did not occur with carbon removal, because of the existence of a wide spectrum of species that can use carbon as a source of energy. Collectively, even at lower activity, they can oxidize all degradable organic materials as witnessed in Run 6.

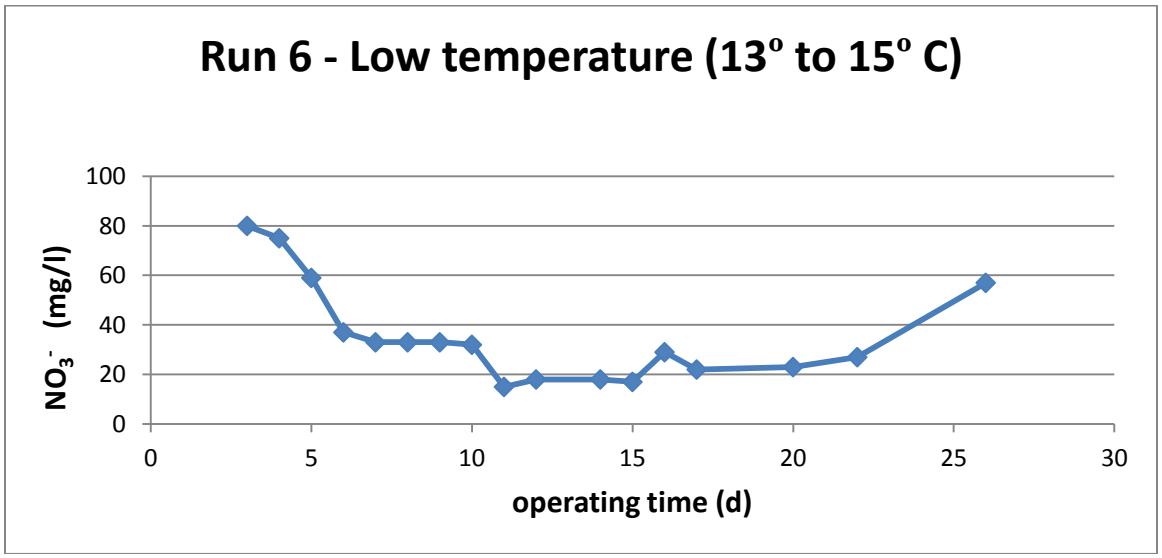

Figure 12.11: Run 6: Nitrate concentrations in the effluent of the pilot SMEBR at low temperature

12.3.4 Nitrogen removal at high temperature

The small scale MBR showed nearly complete conversion of ammonium into nitrate (Figures 12.12 and 12.13). The average nitrification over the 25 day operating period was 98.4%. The nitrate concentration stabilized around 80 mg NO_3^-/l.

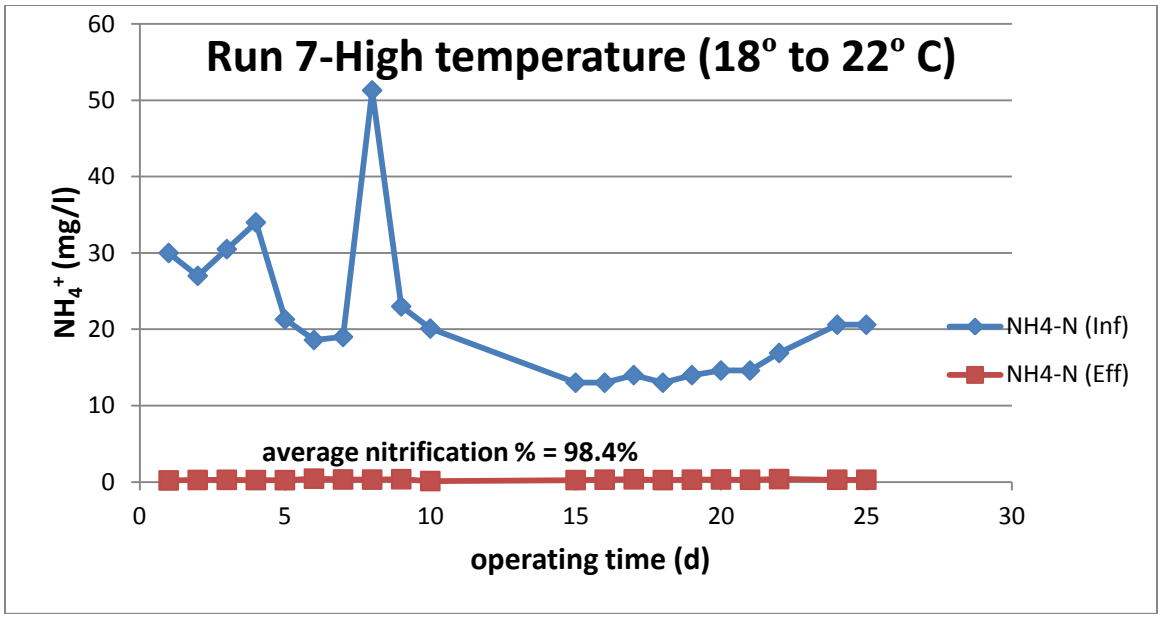

Figure 12.12: Run 7: Concentrations of ammonium in the influent and effluent of the small scale MBR-high temperature

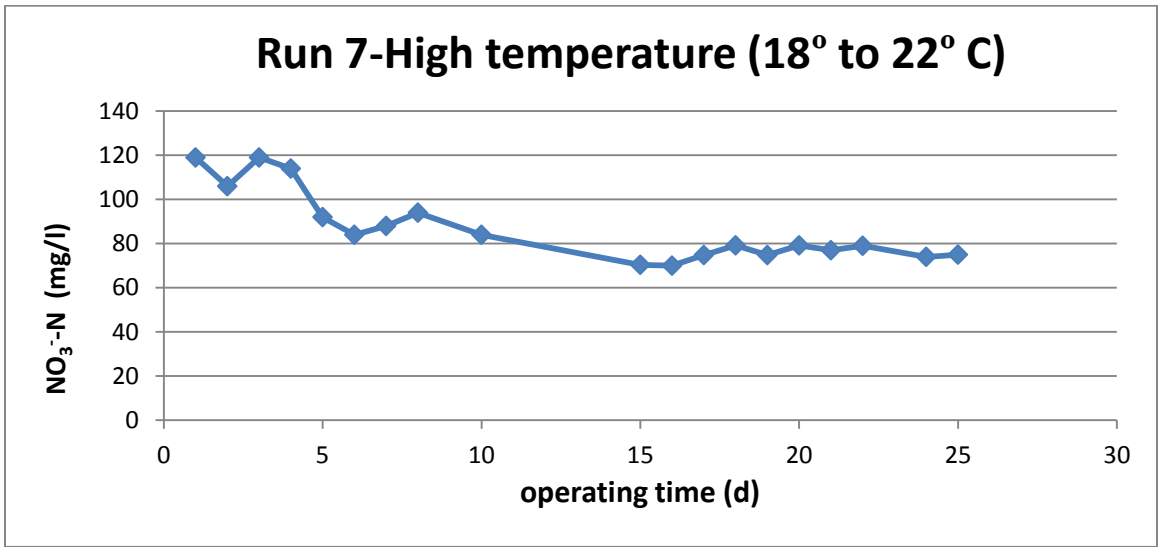

Figure 12.13: Run 7: Nitrate concentrations in the effluent of the small scale MBR-high temperature

On the other hand, the SMEBR showed a high nitrification potential over the whole period of operation (Figures 12.14 and 12.15) when the DO concentration was high enough. The results of nitrification and denitrification percentage in the pilot SMEBR as

affected by the level of DO are illustrated in Table 12.2. The SMEBR pilot system was very sensitive to the concentration of DO. A minor change of the DO concentration, either up or down, led to a major shift in the predominant biological processes. When the DO concentration in the SMEBR was above 0.7 mg/l such as on days 17, 18 and 19, the nitrification percentage was higher than 95%, meanwhile, the denitrification percentage was as low as 23%. Though, when the DO was 0.4 mg/l on days 7 and 16, the nitrification percentage reduced to around 85% and the denitrification still low (35% on average). On days 20 to 24, the DO in the reactor was reduced to 0.2 mg/l. The average nitrification during these four days was 66%, while the average denitrification increased up to 94%; this latter level of DO provided the highest N removal efficiency. The DO concentrations mentioned in this discussion represents the maximum reached at the end of the time-OFF of the electrical exposure mode. Achieving a high percentage of nitrification above 95% after 17 days of operation indicates that the system is working successfully and the microbial activity is recovering very fast at high temperature (18 to 22^{o} C).

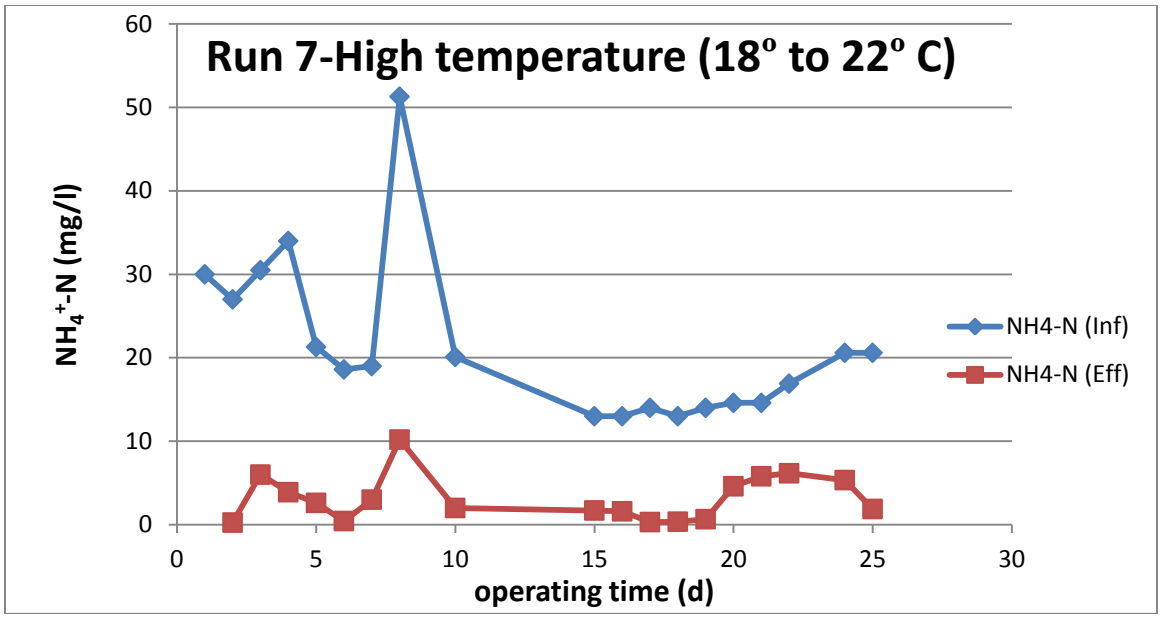

Figure 12.14: Run 7: Ammonium concentrations in the influent and effluent of the pilot SMEBR-high temperature

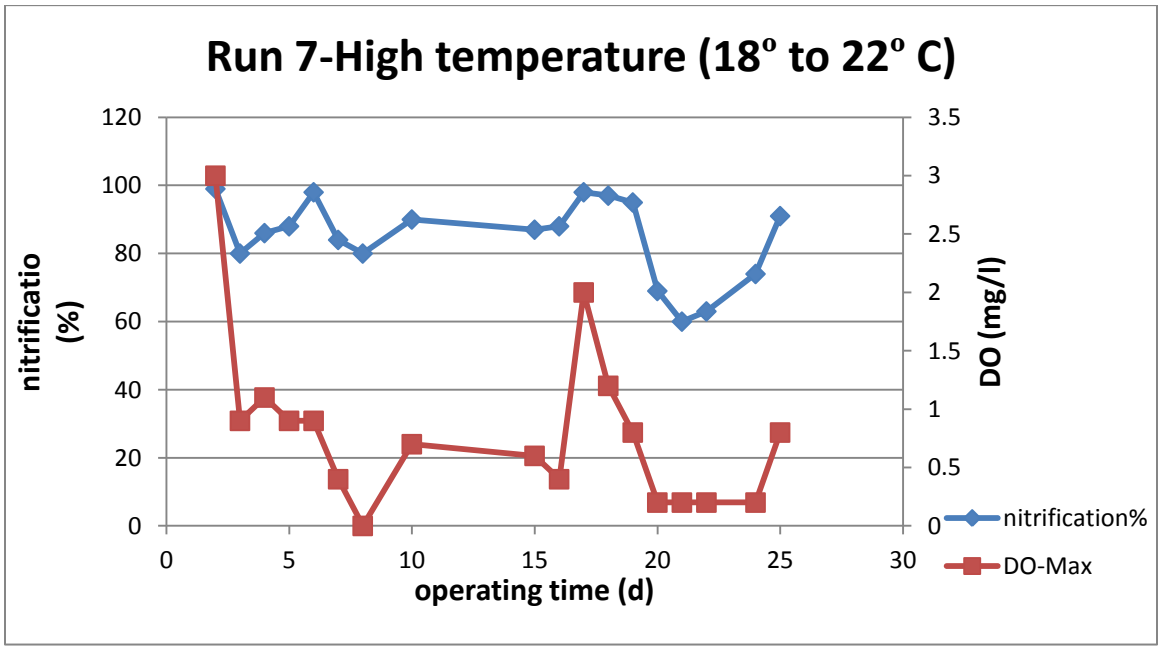

Figure 12.15: Run 7: Nitrification percentage as affected by the DO concentration in the pilot SMEBR-high temperature

Table 12.2: Changing of the nitrification % and denitrification % by the level of DO concentration in the SMEBR at high temperature

Time (d)	Max. DO (mg/l)	Inf. NH_4+-N (mg/l)	SMEBR-Eff NH_4+-N (mg/l)	SMEBR-Eff NO3- (mg/l)	MBR-Eff NO_3- (mg/l)	SMEBR Nitr. (%)	SMEBR Denit. (%)	SMEBR TN removal (%)
1		30						
2	3	27	0.25	101	106	99.07407	5	
3	0.9	30.5	6	60	119	80.32787	50	
4	1.1	34	3.89	67	116	88.55882	42	
5	0.9	21.3	2.61	50	93	87.74648	46	
6	0.9	18.6	0.435	50	86	97.66129	42	
7	0.4	19	3	47	90	84.21053	48	
8	0	51.3	10.2	22.6	94	80.11696	76	
10	0.7	20.1	2	30	85	90.04975	64	
15	0.9	13	1.7	60	72	86.92308	17	
16	0.4	13	1.6	57	70	87.69231	19	
17	3.7	14	0.312	53	75	97.77143	29	
18	1.2	13	0.355	60	78	97.26923	23	
19	0.8	14	0.655	46	76	95.32143	39	
20	0.2	14.6	4.6	4.6	80	68.49315	94	54
21	0.2	14.6	5.8	1	77	60.27397	99	
22	0.2	16.9	6.16	14	79	63.5503	82	
24	0.2	20.6	5.34	0.6	74	74.07767	99	64
25	0.8	20.6	1.88	27.4	75	90.87379	63	56

The DO concentration was deliberately forced to go up and down in Run 7, because the objective was to find out the level of DO at which the ammonium and nitrate concentrations are the lowest. During days 20 to 24, the lowest concentration of nitrate (< 5 mg NO_3^-/l) was achieved when the maximum DO concentration at the end of time-OFF was 0.2 mg/l and depleted to 0.0 mg/l at the end of time-ON of electrical exposure mode (Figure 12.16). At that level of DO, the nitrification was 60 to 75 % and the total N removal was the highest on day 24 at 64% (Figure 12.17). On day 25, the DO increased up to 0.8 mg/l. on that day, the nitrification increased to 91%, but the nitrate

concentration increased as well to 27 mg NO_3^-/l. This increase of nitrification percentage at the expense of the denitrification forced the TN removal to drop to 56%.

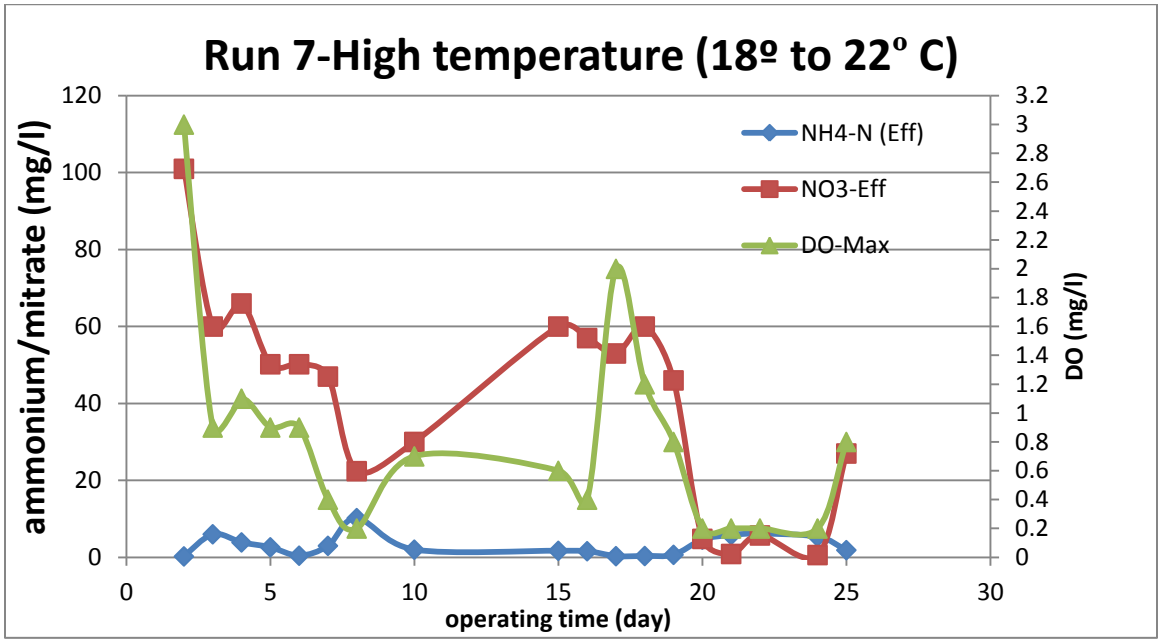

Figure 12.16: Run 7: Ammonium and nitrate concentrations as affected by the DO – high temperature

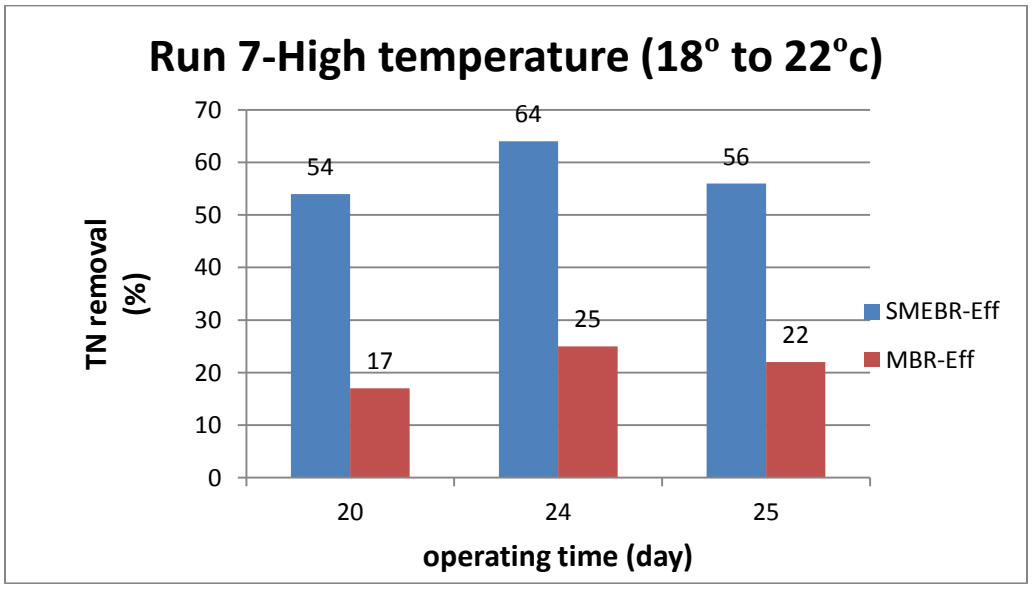

Figure 12.17: Run 7: Highest TN removal achieved in the pilot SMEBR

The results of the pilot scale SMEBR showed a maximum TN removal of 64% due to the difficulty of removing ammonium and nitrate simultaneously to low concentrations. However, in the lab scale experiments of Phase 2, the TN removal was up to 97% and the concentration of ammonium and nitrate were close to zero. Yet, the lab results were confirmed through different replicates under different operating conditions. The reason of the discrepancy between the pilot and the lab results is the concentration of carbon in the influent wastewater. In the lab tests, the influent COD was 950 mg/l, while in the pilot scale the concentration was between 50 to 300 mg/l (Figure 12.18). This low concentration is due to the snow meltdown during the month of March when Run 7 was operated. Carbon is very essential in the biological heterotrophic denitrification process that converts the nitrate into gas. Heterotrophic denitrification is the major biological process responsible for the removal of nitrate in the SMEBR. The pilot SMEBR was fed at an average influent COD of 167 mg/l. At that level of COD, the competition among microorganisms to degrade the organic carbon as a source of energy is very high. Therefore, the pilot SMEBR was unable to denitrify the nitrate at high efficiency except at maximum DO equal to 0.2 mg/l (end of time-OFF). Otherwise, any increase of DO was accompanied with an increase of nitrate concentration. At this level of DO (0 to 0.2 mg/l), the pilot SMEBR spent more time under the anoxic than the aerobic condition in each electrical cycle. This longer time of anoxic conditions allowed for a high removal of nitrate, but at the expense of the nitrification. The lab tests did not need an anoxic condition as long as that of the pilot because the carbon is readily available as required by the heterotrophic denitrifiers. In the lab runs of Phase 2, the shorter anoxic condition

period required permitted to operate the reactor at higher level of DO to create longer aerobic time within the electrical cycle that made the removal of ammonium and nitrate in the SMEBR such an easy process.

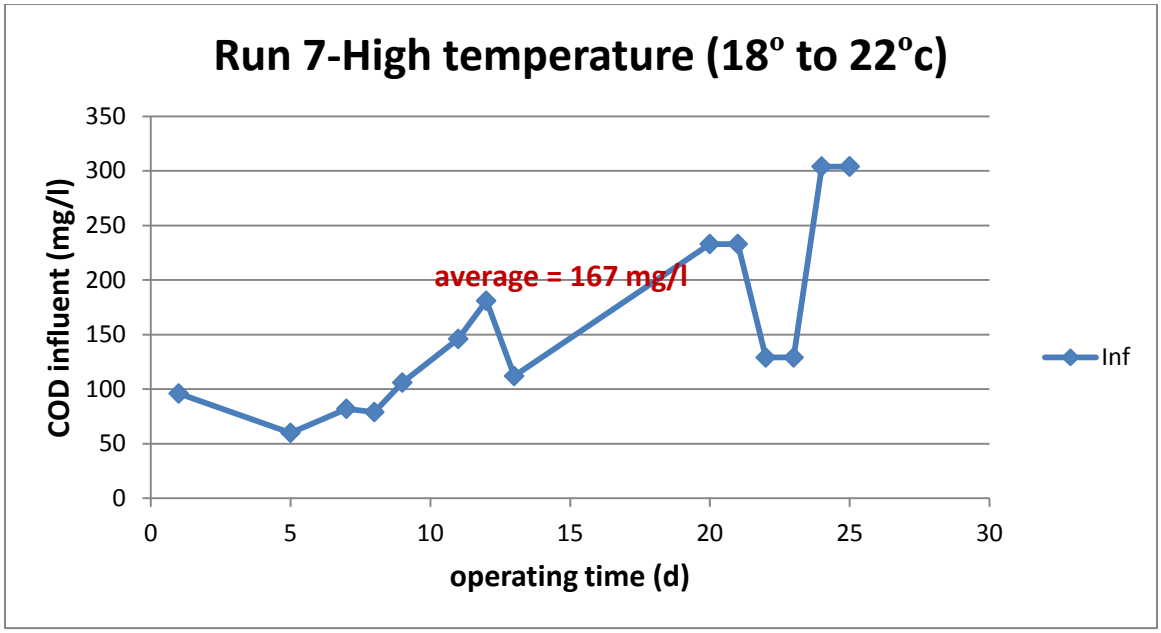

Figure 12.18: Variation of COD concentrations in the influent real wastewater

12.3.5 Membrane fouling

The pilot SMEBR operated for 2 months. During that period, the TMP increased from 5 kPa to 10 kPa. The fouling rate was very small, because the system was operated at flux lower than the critical value.

12.4 Conclusion

The pilot SMEBR proved that the removal of nitrogen in one single reactor is feasible under real conditions. The removal of nitrogen reaches its maximum when the SMEBR is

operated at high temperature (> 18° C) and high influent COD concentration. The maximum TN removal achieved was 64%. This percentage is high considering the low concentration of COD in the influent. The SMEBR has a potential to increase that percentage by increasing the COD in the influent to provide the denitrifiers with their needs of a carbon source to work more efficiently.

.

Chapter 13

Conclusions, contributions and future work

13.1 Conclusions

1- This study demonstrated a strong relation between electrical parameters and wastewater characteristics. Current densities between 15 to 25 A/m^2 with long time-OFF (5'-ON/20'-OFF) improved sludge characteristics and maintained high microbial activity. The sludge properties the electro-bioreactor can improve includes: the removal of foulants (SMP and organic colloids), the removal of tightly bound water and enhancing the dewaterability, and the removal of humic substances

2- Membrane fouling was reduced substantially in the SMEBR compared to the MBR through the removal of SMP and organic colloids. The rate of membrane fouling in the SMEBR and MBR is proportional to the concentration of SMP in the supernatant of the activated sludge and the level of VSS

3- The study showed that the ORP of the activated sludge could be controlled through adjusting the electrical operating parameters with the DO concentration, subsequently:

A- Simultaneous nitrification/denitrification conditions were established in the SMEBR

B- Anammox was stimulated in the SMEBR at low DO concentration and low ORP and contributed up to 25% increase of the activated sludge nitrification potential.

C- The removal pathway of nitrogen in the SMEBR (up to 97%) was through the combined anammox and the simultaneous nitrification/denitrification in the SMEBR

D- Nitrogen removal in the SMEBR requires enough carbon source to promote the denitrifiers

E- Nitrogen removal in the SMEBR was negatively affected at low temperature (< 15 ^{o}C)

4- The removal pathway of phosphorus in the SMEBR (> 98 %) was through the formation of complexes with aluminum when the electrical parameters were adjusted to generate enough aluminum ions.

5- The COD removal in the SMEBR (up to 99 %) was a bit higher than the MBR due to the removal of colloidal organics in addition to the biological oxidation. The high removal efficiency of COD is an indication of high microbial activity in the SMEBR despite the stress imposed by the current field.

6- Finally, the study demonstrated that the SMEBR produced high effluent quality through simultaneous and substantial removal (>95%) of carbon, phosphorus and nitrogen, while membrane fouling was minimized. Subsequently, this technology can be used to build new treatment facilities or upgrading and retrofitting of old ones.

13.2 Contributions

1- This study has demonstrated the capability of the electrokinetic processes to control the ORP of activated sludge to create simultaneous nitrification/denitrification conditions

2- This study has shown the mechanism of developing simultaneous nitrification/denitrification conditions through electrokinetic

3- This study has illustrated the mechanisms of membrane fouling reduction by electrokinetic phenomenon

4- This study proved a superior removal of carbon, phosphorus and nitrogen in one single electro-bioreactor, which has not been done before.

5- This study has proved the significant contribution of the anammox in the removal of nitrogen

6- This study has demonstrated the relationship between the electrical parameters and sludge properties

7- This study has provided the electrical operating conditions of the SMEBR that ensure high performance.

13.3 Future work

1- To study the relationship between electro-bioreactor performance and temperature to find out a solution for nitrogen removal at low temperature

2- To study in detail the relationship between the influent C/N ratio and the total nitrogen removal in the electro-bioreactors to determine the amount of carbon source that should be added to enforce completed denitrification of nitrate

3- To test different carbon sources that could be added into the SMEBR in cases of low influent C/N ratio to ensure a high removal of nitrogen with least membrane fouling impact.

Glossary

MLSS	Mixed liquor suspended solid
VSS	Volatile suspended solids
FSS	Fixed suspended solids
EPS	Extra-polymer substances
SMP	Soluble microbial products
F/M	Food/Mass ratio
COD	Chemical oxygen demand
PSD	Particle size distribution
SRF	Specific resistance to filtration
TOC	Total organic carbon
CFV	Cross flow velocity
CD	Current density
EC	Electrical conductivity
ORP	Oxidation reduction potential
TN	Total nitrogen
C	Carbon
P	Phosphorus
N	nitrogen
HRT	Hydraulic retention time
SRT	Solid retention time
Anammox	Anaerobic ammonium oxidation
DC	Direct current
A	Amperage
V	Voltage
mg	Milligrams
kg	kilograms
mPa.s	Millie pascal second
kPa	Kilo pascal
MBR	Membrane bioreactor
SMEBR	Submerged membrane electro-bioreactor

References

Adam, c., R. Gnirss, B. Lesjean, H. Buisson and M. Kraume. 2002. Enhanced biological phosphorus removal in membrane bioreactors. Water Sci. and Technol. 46(4-5):281-286

Ahmad, Z., J. Cho, B.R. Lim, K. G. Song and K. H. Ahn. 2007. Effect of sludge retention time on membrane fouling and microbial community structure in a membrane bioreactor. J. Memb. Sci. 287: 211-218

Ahn, K. H., K. G. Song, E. Cho, J. Cho, H. Yun, S. Lee and J. Kim. 2003. Enhanced biological phosphorus and nitrogen removal using a sequencing anoxic/anaerobic membrane bioreactor (SAM) process. Desalination. 157: 345-352

Amy, G., C. W. Bryant and M. Belyani. 1987. Molecular weight distribution of soluble microbial matter in various secondary and tertiary effluents. Water Sci. and Technol. 19:529-538

Arabi, S. and G. Nakhla. 2008. Impact of protein/carbohydrate ratio in the feed wastewater on the membrane fouling in membrane bioreactors. J. Memb. Sci. 324:142-150

Bai, R. and H. F. Leow. 2002. Microfiltration of activated sludge wastewater –the effect of system operation parameters. Sep. Purif. Technol. 29:189-198

Balkan, V. Y. and I. P. Kolesnikova. 1996. Influence of electrode material on the electrocoagulation. J. of Aerosol Sci. 27(supplement-1): 209-210

Bani-Melhem, K. and M. Elektrorowicz. 2010. Development of a novel submerged membrane electro-bioreactor (SMEBR): Performance for fouling reduction. Environmental Science and Technology, 44 (9): 3298-3304.

Bani-Melhem, K. and M. Elektorowicz. 2011. Performance of submerged membrane bioreactor (SMEBR) with iron electrodes for wastewater treatment and fouling reduction. J. of Mem. Sci. 379(1-2):434-439

Bani-Melhem, K. 2008. Development a submerged membrane electro-bioreactor SMEBR for wastewater treatment. Ph.D. thesis, Concordia University, Montreal, Qc, Canada

Barker, D. J. and D. C. Stukey. 1999. A review of soluble microbial products (SMP) in wastewater treatment systems. Water. Res. 33(14):3063-3082

Baskir, C. I. and G. S. Hansford. 1980. Product formation in the continuous culture of microbial populations grown on carbohydrates. Biotech. Bioeng. XXII:1857-1875

Bayramoglu, M., M. Eyvaz and M. Kobya. 2007. Treatment of the textile wastewater by electrocoagulation economical evaluation. Chem. Eng. J. 128: 155-161

Bayramoglu, M., M. Kobya, M. Eyvaz and E. Senturk. 2006. Technical and economic analysis of electrocoagulation for the treatment of poultry slaughterhouse wastewater. Sep. and Purif. Technol. 51: 404-408.

Bayramoglu, M., O. T. Can, M. Kobya and M. Sozbir. 2004. Operating cost analysis of electrocoagulation of textile dye wastewater. Sep. Purif. Technol. 37: 117-125.

Bhatta, C. P., A. Mastuda, K. Kawasaki, and D. Omori. 2004. Minimization of sludge production and stable operational condition of a submerged membrane activated sludge process. Wat. Sci. Technol. 50(9):121-128

Bin, Z., S. Baosheng, J. Min, G. Taishi, and G. Zhenghong. 2008. Extraction and analysis of extracellular polymeric substances in membrane fouling in submerged MBR. Desalination. 227:286-294

Bouhabila, F. H., R. B. Aim and H. Buisson. 2001. Fouling characteristics in membrane bioreactors. Sep. Purif. Technol. 22-23:123-132

Brooks, A., B. Jefferson, G. Guglielmi and S. J. Judd. 2006. Sustainable flux fouling in membrane bioreactor: Impact of flux and MLSS. Sep. Sci. and Technol. 41(7): 1279-1291

Bremere, I., M. Kenndy, P. Michel, P. Van Emmerik, G. Witkamp and J. Schipper. 1999. Controlling scaling in membrane filtration system using a desupersaturation unit. Desalination. 124:51-62.

Can, O. T., M. Bayramoglu and M. Kobya. 2003. Decolorization of reactive dye solutions by electrocoagulation using aluminium electrodes. Ind. Eng. Chem. Res. 42: 3391-3396

Canizares, P., F. Martinez, C. Jimenez, C. Saez and M. A. Rodrigo. 2008. Coagulation and electrocoagulation of oil-in-water emulsions. J. of Hazard. Material. 151: 44-51

Cema, G., J. Wiszniowski, S. Zabczynski, E. Zabloka-Godlewska, A. Raszka, J. Surmacz-Gorska. 2007. Biological nitrogen removal from landfill leachate by deammonification assisted by heterotrophic denitrification in a rotating biological reactor (RBR). Water Sci. Technol. 55 (8-9): 35-42

Chang, I., P. Clech, B. Jefferson and S. Judd. 2002. Membrane fouling in membrane bioreactors for wastewater treatment. J. of Environ. Eng. 128(11): 1018-1029

Chang, S. and A. G. Fane. 2001. The effect of fiber diameter on filtration and flux distribution-relevance to submerged hollow fiber modules. J. Membr. Sci. 184: 221-231

Chang, I. S., C. H. Lee and K. H. Ahn. 1999. Membrane filtration characteristics in membrane-coupled activated sludge system: The effect of floc structure on membrane fouling. Sep. Sci. Technol. 34(9):1743-1758.

Chang, I. and C. Lee. 1998. Membrane filtration characteristics in membrane-coupled activated sludge system- the effect of physiological states of activated sludge on membrane fouling. Desalination. 120:221-233

Chellam, S. and M. R. Wiesner. 1997. Particle back-transport and permeate flux behaviour in crossflow membrane filters. Water Sci. Technol. 31: 819-824.

Chiemchaisri, C. and K. Yamamoto. 1994. Performance of membrane separation bioreactor at various temperatures for domestic wastewater treatment. J. Memb. Sci. 87:119-129

Chen, G. 2004. Electrochemical technologies in wastewater treatment. Sep. Purif. Technol. 38: 11-41

Chiu Y., L. Lee, C. Chang and A. Chao. 2007. Control of carbon and ammonium ratio for simultaneous nitrification and denitrification in a sequencing batch bioreactor. International Biodeterioration and biodegradation. 59: 1-7

Cho, J., K. G. Song, S. H. Lee and K. H. Ahn. 2005. Sequencing anoxic/anaerobic membrane bioreactor (SAM)pilot plant for advanced wastewater treatment. Desalination. 178: 219-225

Choi C., M. Kim, K. Lee and H. Park. 2009. Oxidation reduction potential automatic control potential of intermittently aerated membrane bioreactor for nitrification and denitrification. Water Sci. and Technol. 60(1): 167-173

Cho, J. W., K. G. Song, S. H. Lee and K. H. Ahn. 2005. Sequencing anoxic/anaerobic membrane bioreactor (SAM) pilot plant for advanced wastewater treatment. Desalination. 28:219-225

Cho, J., G. Amy and J. Pellegrino. 1999. Membrane filtration of natural organic matter: internal comparison of rejection and flux decline characteristics with ultrafiltration and nanofiltration membranes. Water Res. 33:2517-2526

Choi, H., K. Zhang, D. D. Dionysiou, D. B. Oerther and G. A. Sorial. Influence of cross-flow velocity on membrane performance during filtration of biological suspension. J. of Memb. Sci. 248: 189-199

Christensen, B. E., W. G. Characklis. 1990. Physical and chemical properties of biofilms. In: Biofilms. Characklis, W. G. And K. Marshall eds. Wiley, NY, USA. Pp:93-130

Cote, P., H. Buisson and M. Praderie. 1998. Immersed membranes activated sludge process applied to the treatment of municipal wastewater. Water Sci. Technol. 38(4-5):437-442

Crozes, G. F., J. G. Jancenglo, C. Anselman and J. M. Laine. 1997. Impaction of ultrafiltration operating condition on membrane irreversible fouling. J. Mem. Sci. 161:63-72

Daneshvar, N., H. A. Sorkhabi and M. B. Kasiri. 2004. Decolorization of dye solution containing Acid Red 14 by electrocoagulation with a comparative investigation of different electrode connections. J. of Hazard. Mater. B112: 55-62

De Silva, D. G. V. and B. E. Rittmann. 2000a. Nonsteady-state modeling of multispecies activated sludge processes. Water Environ. Res. 72(5):554-565

De Silva, D. G. V. and B. E. Rittmann. 2000b. Interpreting the response to loading changes in a mixed-culture completely stirred tank reactor. Water Environ. Res. 72(5):566-573

Defrance, L., M. Y. Jaffrin, B. Gupta, P. Paullier and V. Geaugey. 2000. Contribution of various constituents of activated sludge sludge to membrane bioreactor fouling. Bioresource Technol. 73:105-112

Dignac, M. F., V. Urbain, D. Rybacki, A. Bruchet, D. Snidaro and P. Scribe. 1998. Chemical description of extracellular polymers: implication on activated sludge floc structure. Water Sci. Technol. 38:45-53

Dosta, J., I. Fernandez, J.R. Vazquez-Padin, A. Mosquera-Corral, J. L. Campos, J. Mata-Alvarez, R. Mendez. 2008. Short and long term effects of temperature on anammox process. J. Hazardous Materials. 154: 688-693

Drewes, J. E., M. Sprinzl, A. Soellner, M. D. Williams, P. Fox and P. Westerhoff. 1999. Tracking residual dissolved organic carbon using XDA-fractionation and C-NMR Spectroscopy in indirect potable reuse systems. Vom Wasser. 93:95-107

Drews, M., V. Vocks, B. Iversen, B. Lesjean and M. Kraume. 2005. Influence of unsteady membrane bioreactor operation on EPS formation and filtration resistance. In: Proceedings of the International Congress on Membranes and Membrane Processes (ICOM), Seoul, Korea.

Dubois, M., K. A. Gilles, J. K. Hamilton, P. A. Rebers and F. Smith. 1956. Colorimetric method for determination of sugars and related substances. Anal. Chem. 28: 350-356

Elektorowicz M., K. Bani Melhem and J. Oleszkiewicz. 2009. Submerged Membrane Electro-bioreactor- SMEBR, US patent 12/553,680

Esmaily, A., M. Elektrorowicz and J. Oleszkiewicz. 2006. Dewatering and pathogen elimination from biosolids using electrokinetic phenomena, J Environ. Eng. Sci. 5:197-202

Evenblij, H., S. Geilvoet, J. Ven der Graaf, H. F. Van der Roset. 2005. Filtration characterization for assessing MBR performance: Three cases compared. Desalination. 178:115-124

Evenblij, H. and J. Van der Graaf. 2004. Occurrence of EPS in activated sludge from a membrane bioreactor treating municipal wastewater. Water Sci. Technol. 50:293-300

Escobar, I. C., E. M. Hoek, C. J. Gabelich and F. A. DiGiano . 2005. Committee report: recent advances and research needs in membrane fouling. Journal of American Water Work Association. 97:79-89

Fan, L., J. L. Harris, F. A. Roddic and N. A. Booker. 2002. Influence of the characteristics of natural organic matter on fouling of microfiltration membranes. Water Res. 35:4455-4463

Field, R. W., D. Wu, J. A. Howell and B. B. Gupta. 1995. Critical flux concept for microfiltration fouling. J. Memb. Sci. 100(3): 259-272

Fu Z., F. Yang, Y. An and Y. Xue. 2009. Simultaneous nitrification and denitrification coupled with phosphorus removal in an modified anoxic/oxic membrane bioreactor (A/O-MBR). Biochem. Eng. J. 43: 191-196

Geng, Z. and E. R. Hall. 2007. A comparative study of fouling-related properties of sludge from conventional and membrane enhanced biological phosphorus removal processes. Water Res. 41:4329-4338

Grelier, P., S. Rosenberger and T. P. Annie. 2006. Influence of sludge retention time on membrane bioreactor hydraulic performance. Desalination. 192: 10-17

Han, S. S., T. H. Bae, G. G. Jang and T. M. Tak. 2005. Influence of sludge retention time on membrane fouling and bioactivities in membrane bioreactor system. Process Biochemistry. 40: 2393-2400

Hao, O. J. and A. O. Lao. 1988. Kinetics of microbial byproduct formation in chemostat pure culture. J. Environ. Eng. 114(5):1097-1115

Hernandez Rojas, M. E., R. Van Kaam, S. Schetrite and C. Albasi. 2005. Role and variations of supernatant compounds in submerged membrane bioreactor fouling. Desalination. 179:95-107.

Holbrook, R. D., M. J. Higgins, S. N. Murthy, A. D. Fonseca, E. J. Fleischer, G. T. Daigger, T. J. Grizzard, N. G. Love and J. T. Novak. 2004. Effect of alum addition on the performance of submerged membranes for wastewater treatment. Water Environ. Res. 76(7):2699-2702

Holt, P., G. Barton and C. Mitchel. 1999. Electrocoagulation as a wastewater treatment. The third annual Australian Environmental Engineering Research Event, 23-26 November, Castlemaine, Victoria

Hong, S. P., T. H. Bae, T. M. Tak, S. Hong and A. Randall. 2002. Fouling control in activated sludge submerged hollow fiber membrane bioreactors. Desalination. 143:219-228

How, Y. NG., T. W. Tan and S. L. Ong. 2006. Membrane fouling of submerged membrane bioreactors: Impact of mean cell residence time and the contributing factors. Environ. Sci. Technol. 40: 2706-2713

Hsieh, K. M., G. A. Murgel, L. W. Lion and M. L. Shuler. 1994. Interactions of microbial biofilms with toxic trace metals: Observation and modeling of cell growth, attachment and production of extracellular polymer. Biotechnol. Bioeng. 44:219-231

Huang J., M. Elektrorowicz and J. Oleszkiewicz. 2008, Response of aerobic and anaerobic sludge to dewatering and disinfection using elektrokinetics (EK), Water Sci. and Technol. 57 (2) 231-236

Ibeid S., M. Elektorowicz and J. Oleszkiewicz. 2010a. Impact of electro-coagulation on the fate of soluble microbial products (SMP) in submerged membrane electro-bioreactor (SMEBR). 11th international Environmental Specialty Conference, Winnipeg, Manitoba, Canada.

Ibeid S., M. Elektorowicz and J. Oleszkiewicz. 2010b. Modification of activated sludge characteristics due to applying Direct Current (DC) field. International Water Association (IWA) conference, Montreal, Canada.

Isaka, K., T. Sumino, S. Tsuneda. 2007. High nitrogen removal performance at moderately low temperature utilizing anaerobic ammonium oxidation reactions. J. Biosci. Bioeng. 103(5): 486-490

Isaka, K., Y. Date, T. Sumino, S. Yoshie, S. Tsuneda. 2006. Growth characteristic of anaerobic ammonium-oxidizing bacteria in an anaerobic biological filtrated reactor. Appl. Microbiol. Biotechnol. 70: 47-52

Itango, T., K. Kimura and Y. Watanabe. 2004. Influence of suspension viscosity and colloidal particles on permeability of membrane used in membrane bioreactor (MBR). Water Sci. Technol. 50(12):301-309

Ivanovic, I., T. Leikenes and H. Odegaard. 2008. Fouling control by reduction of submicron particles in a BF-MBR with an integrated flocculation zone in the membrane reactor. Sep. Sci. and Techno. 43: 1871-1883

Jang, N., R. S. Trussel, R. P. Merlo, D. Jenkins, S. W. Hermanowics and I. S. Kim. 2005. Fractionation of EPS(extracellular polymeric substances) molecular weight and filtration resistance as F/M (food/microorganisms) in submerged membrane bioreactor. In: Proceedings of the International conference on membranes and Membrane Processes (ICOM), Seol, Korea

Jiang, T., M. D. Kennedy, B. F. Guinzbourg, P. A. Vanrolleghem and J. C. Schipers. 2005. Optimizing the operation of a MBR pilot plant by quantitative analysis of the membrane fouling mechanism. Water Sci. Technol. 51: 19-25

Jin, B., B. Wilen and P. Lant. 2004. Impacts of morphological, physical and chemical properties of sludge flocs on dewaterability of activated sludge. Chem. Eng. J. 98:115-126

Jinsong, Z., C. H. Chuan, Z. Jiti and A. G. Fane. 2006. Effect of sludge retention time on membrane bio-fouling intensity in a submerged membrane bioreactor. Sep. Sci. and Technol. 41: 1313-1329

Jonsson C. and A. S. Jonsson. 1995. Influence of the membrane material on the adsorptive fouling of ultrafiltration membranes. J. Memb. Sci. 108:79-87.

Jorand, F., P. Guicherd, V. Urbain, J. Manem and J. C. Block. 1994. Hydrophobicity of activated sludge flocs and laboratory growth bacteria. Water Sci. Technol. 30(11):211-218

Hasan, S. 2011. Desige and performance of a Pilot Submerged Membrane Electro-bioreactor (SMEBR) Wastewater Treatment. Ph.D. thesis, Concordia University, Montreal, QC, Canada

Hasar, H., C. Kinaci, A. Unlu and U. Ipek. 2001. Role of intermittent aeration in domestic wastewater treatment by submerged membrane activated sludge system. Desalination. 142: 287-293

Jianlong W., Yongzen P., Shuying W and Yongqing G. 2008. Nitrogen removal by simultaneous nitrification and denitrification via nitrite in a sequence hybrid biological reactor. Chineese Journal of Chem. Eng. 16(5): 778-784

Kang, S., E. M. V. Hoek, H. Choi and H. Shin. 2006. Effect of membrane surface properties during the fast evaluation of cell attachment. Sep. Sci. and Technol. 41:1475-1487

Karr, P. R. and T. M. Keinath. 1978. Influence of particle size on sludge dewaterability. J. Wat. Pollut. Control Fed. 50:1911-1930

Kim, J., I. Chang, D. Shin and H. Park. 2008. Membrane fouling control through the change of the depth of a membrane module in a submerged membrane bioreactor for advanced wastewater treatment. Desalination. 231: 35-43

Kim, J. S. and C. H. Lee. 2003. Effect of powdered activated carbon on the performance of an aerobic membrane bioreactor: comparison between cross flow and submerged membrane systems. Water Environ. Res. 75: 300-307

Kim, J. and F. A. DiGiano. 2006. Defining critical flux in submerged membranes: Influence of length distributed flux. J. Memb. Sci. 280: 752-761

Kim, J. S., C. H. Lee and I. S. Chang. 2001. Effect of pump shear on the performance of a crossflow membrane bioreactor. Water Res. 35(9): 2137-2144

Kim H., H. Jang, H. Kim, D. Lee and T. Chung. 2010. Effect of an electro phosphorus removal process on phosphorus removal and membrane permeability in a pilot-scale MBR. Desalination. 250: 629-633

Knoell, K., J. Safarik, T. Cormack, R. Riley, S. W. Lin and H. Ridgway. 1999. Biofouling potentials of microporous polysulfone membranes containing a sulfonated polyether-ethersulfone/polyethersulfone block copolymer: Correlation of membrane surface properties with bacterial attachment. J. of Mem. Sci. 157:117-138

Kobya, M., H. Hiz, E. Senturk, C. Aydiner and E. Demirbas. 2006. Treatment of potato chips manufacturing wastewater by electrocoagulation. Desalination. 190:201-211

Larue, O., E. Vorobiev, C. Vu and B. Durand. 2003. Electrocoagulation and coagulation by iron of latex particles in aqueous suspension. Sep. Purif. Technol. 31: 177-192

Laspidou, C. S. and B. E. Rittmann. 2002. A unified theory for extracellular polymeric substances, soluble microbial products, and active and inert biomass. Water Res. 36:2711-2720

Le-Clech, P., V. Chen and T. A. G. Fane. 2006. Fouling in membrane bioreactors used in wastewater treatment. J. of Mem. Sci. 284: 17-53.

Le-Clech P., A. Fane, G. Leslie and A. Childress. 2005. The operator's perspective. Filtration Sep. 42: 20-23

Le-Clech, P., B. Jefferson and S. J. Judd. 2003. Impact of aeration, solids concentration and membrane characteristics on the hydraulic performance of a membrane bioreactor. J. Memb. Sci. 218:117-129

Lee, S. M., J. Y. Jung and Y. C. Chung. 2001. Novel method for enhancing permeate flux of submerged membrane system in two phase anaerobic reactor. Water Res. 35:471-477

Lee, W., S. Kang and H. Shin. 2003. Sludge characteristics and their contribution to microfiltration in submerged membrane bioreactor. J. Memb. Sci. 216:217-227.

Lesjean, B., S. Rosenberger. C. Laabs, M. Jekel, R. Gnirss and G. Amy. 2005. Correlation between membrane fouling and soluble/colloidal organic substances in membrane bioreactor for municipal wastewater treatment. Water Sci. Technol. 51(6-7):1-8

Leung, R. P. C. 2003. Effect of extracellular polymeric substances (EPS) of activated sludge and diatom blooms on their biofloculation behaviour. Hong Kong University. MSc Thesis, Hong Kong.

Li, H., a. G. Fane, H. G. L. Coster and S. Vigneswaran. 1998. Direct observation of particle deposition on the membrane surface during cross flow microfiltration. J. Memb. Sci. 149:83-97

Li, J., F. Yang, Y. Li, F. Wong and H. C. Chua. 2008. Impact of biological constituents and properties of activated sludge on membrane fouling in a novel submerged membrane bioreactor. Desalination. 225:356-365.

Li, X. Y. and S. F. Yang. 2007. Influence of loosely bound extracellular polymeric substances (EPS) on the flocculation, sedimentation and dewaterability of activated sludge. Water Res. 41:1022-1030

Liao, B. Q., D. G. Allen, I. G. Droppo, G. G. Leppard and S. N. Liss. Surface properties of sludge and their role in bioflocculation and settlability. Water Res. 35:339-350.

Lim, A. L. and R. Bai. 2003. Membrane fouling and cleaning in microfiltration of activated sludge wastewater. J. Memb. Sci. 216:279-290

Liming, S., H. E. Peipei, Y. U. Guanghui and H. E. Pinjing. 2009. Effect of protein, polysaccharides, and particle sizes on sludge dewaterability. J. Environ. Sci. 21:83-88

Lin, C. J., S. L. Lo, C. Y. Kuo and C. H. Wu. 2005. Pilot-scale electrocoagulation with bipolar aluminum electrodes for on site domestic greywater reuse. J. Environ. Eng. 131(3): 491-495

Liu, Y. and H. H. P. Fang. 2003. Influences of extracellular polymeric substances (EPS) on flocculation, settling and dewatering of activated sludge. Crit. Rev. Environ. Sci. Technol. 33:237-273.

Liu, R., X. Huang, Y. F. Sun and Y. Qian. 2003. Hydrodynamic effect on sludge accumulation over membrane surfaces in a submerged membrane bioreactor. Process Biochemistry. 39: 157-163

Liu, R., X. Huang, C. W. Wang, L. J. Chen and Y. Qian. 2000. Study on hydraulic characteristics in a submerged membrane bioreactor. Process Biochemistry. 36: 249-254.

Lowery, O. H., N. J. Rosebrough, A. L. Farr and R. J. Randall. 1951. Protein measurement with the folin phenol reagent. J. of Bio. Chem. 193:265-275

Lubbecke, S., A. Vogelpohl and W. Dewjanin. 1995. Wastewater treatment in a biological high-performance system with high biomass concentration. Water Res. 29: 793-802.

Meng, F., B. Shi, F. Yang and H. Zhang. 2007. New insights into membrane fouling in submerged membrane bioreactor based on rheology and hydrodynamics concepts. J. Memb. Sci. 302: 87-94

Meng, F., H. Zhang, F. Yang, S. Zhang, Y. Li and X. Zhang. 2006. Identification of activated sludge properties affecting membrane fouling in submerged membrane bioreactors. Sep. Purif. Technol. 51:95-103

Mishima, I. and J. Nakajima. 2009. Control of membrane fouling in membrane bioreactor process by coagulant addition. Water Sci. and Technol. 59(7): 1255-1262.

Mollah, M. Y. A., R. Schennach, J. P. Paraga and D. L. Cocke. 2001. Electrocoagulation (EC)- science and applications. J. Hazard. Mater. B84: 29-41

Morra, M. and C. Cassinelli. 1997. Bacterial adhesion to polymer surfaces: a critical review of surface thermodynamic approaches. J. Biomater. Sci. 9(1):55-74

Novak, J. T., G. L. Goodman, A. Pariroo, and J. Huang. 1988. The blinding of sludges during filtration. J. of Water Pollut. Control Federal. 60(2): 206-214

Nagaoka, H., S. Ueda and A. Miya. 1996. Influence of bacterial extracellular polymers on the membrane separation activated sludge process. Water Sci. Technol. 34(9):165-172

Ng, C. A., D. Sun, J. Zhang, H. C. Chua, W. Bing and S. Tay. 2004. Fane. Strategies to improve the sustainable operation of membrane bioreactors. In: Proceedings of the Water Environment-Membrane Technology Conference, Seoul, Korea

Nielsen, P. H., A. Jahn and R. Palmgren. 1997. Conceptual model for production and composition of exopolymers in biofilms. Water Sci. Technol. 36:11-19

Nielson, P. H. and A. Jahn. 1999. Extraction of EPS. In: Microbial extracellular polymeric substances: Characterization, structure and function. Wingenders, Neu TR, Fleming H-C editors. Berlin, Germany

Ognier, S., C. Wisniewski and A. Grasmick. 2004. Membrane bioreactor fouling in sub-critical filtration conditions: a local critical flux concept. J. Memb. Sci. 229: 171-177

Pasmore, M., P. Todd, S. Smith, D. Baker, J. Silverstein, D. Coons and C. B. Bowman. 2001. Effect of ultrafiltration membrane surface properties on Pseudomonas aerugginosa biofilm initiation for the purpose of reducing biofouling. J. of Memb. Sci. 194:15-32

Petsev, D. N., V. M. Starvo and I. B. Ivanov. 1993. Concentrated dispersions of charged colloidal particles: sedimentation, ultrafiltration and diffusion. Colloidal Surf. A. Physiochem. Eng. Asp. 81:65-81

Pribyl, M., F. Tucek, P. A. Wilderer and J. Wanner. 1997. Amount and nature of soluble refractory organics produced by activated sludge micro-organisms in sequencing batch and continuous flow reactors. Water Sci. Technol. 35(1):27-34

Pollice, A., G. Laera, D. Saturno and C. Giordano. 2008. Effects of sludge retention time on the performance of a membrane bioreactor treating municipal sewage. J. Memb. Sci. 317: 65-70.

Prosnansky, M., Y. Sakakibara and M. Kuroda. 2002. High rate denitrification and SS rejection by biofilm-electrode reactor (BER) combined with microfiltration. Water Res. 36: 4801-4810

Psoch, C. and S. Schiewer. 2008. Long-term flux improvement by air sparging and backflushing for a membrane bioreactor, and modeling permeability decline. Desalination. 230: 193-204

Prieske, H., A. Drews and M. Kraume. 2008. Prediction of the circulation velocity in a membrane bioreactor. Desalination. 231: 219-226

Quanrud, D. M., R. G. Arnold, L. G. Wilson, H. J. Gordon, D. W. Graham and G. L. Amy. 1996. Fate of organics during column studies of soil-aquifer treatment. J. Environ. Eng. 122(4): 314-321

Ramsesh, A., D. J. Lee, M. L. Wang, J. P. Hsu, R. S. Juang, J. C. Liu, and S. J. Tseng. 2006. Biofouling in membrane bioreactor. Sep. Sci. and Technol. 41(7):1345-1370

Rezania B., J. A. Oleszkiewicz and N. Cicek. 2007. Hydrogen-dependent denitrification of water in an anaerobic submerged membrane bioreactor coupled with novel hydrogen delivery system. Water Res. 41:1074-1080

Rezania B., J. A. Oleszkiewicz and N. Cicek. 2006. Hydrogen-dependent denitrification of wastewater in anaerobic submerged membrane bioreactor: potential for water reuse. Water Sci. and Technol. 54(11-12):207-214

Rittmann, B. E., W. Bae, E. Namkung and C. J. Lu. 1987. A critical evaluation of microbial product formation in biological processes. Water Sci. Technol. 19:517-528

Rittmann, B. E., and P. L. McCarty. 2001. Environmental Biotechnology: principles and Applications. McGraw-Hill, Singapore

Rittmann, B. E., J. M. Regan and D. A. Stahl. 1994. Nitrification as a source of soluble organic substrate in biological treatment. Water Sci. Technol. 30(6):1-8

Rittmann, B. E., W. Bae, E. Namkung and C. J. Lu. 1987. A critical evaluation of microbial product formation in biological processes. Water Sci. Technol. 19:517-528

Rosenberger, S., H. Evenblij, S. Te Poel, T. Wintgens and C. Laabs. 2005. The importance of liquid phase analyses to understand fouling in membrane assisted activated sludge processes-six case studies of different European research groups. J. Membr. Sci. 263:113-126

Rosenberger, S. and M. Kraume. 2003. Filterability of activated sludge in membrane bioreactor. Desalination. 151:195-200.

Rosenberger, S., R. Witzig, W. Manz, U. Szewzyk and M. Kraume. 2000. Operation of different membrane bioreactors: experimental results and physiological state of the micro-organisms. Water Sci. and Technol. 41(10-11): 269-277

Silva, C. M., D. W. Reeve, H. Husain, H. R. Rabie and K. A. Woodhouse. 2000. Model for flux prediction in high microfiltration system. J. Membr. Sci. 173:87-98

Smith, C., D. Di Gregorio and R. M. Talcott. 1969. The use of membranes for activated sludge separation. 24th annual Purdue Industrial Waste Conference. Purdue University, Lafayette, Indiana, USA, pp:1300-1310

Smollen, M. 1990. Evaluation of municipal sludge drying and dewatering with respect to sludge volume reduction. Water Sci. Technol. 22(12):153-161

Song, K, Y. Kim and K. Ahn. 2008. Effect of coagulant addition on membrane fouling and nutrient removal in a submerged membrane bioreactor. Desalination. 221: 467-474

Stephenson, T., S. Judd, B. Jefferson and K. Brindle. 2000. Membrane bioreactors for wastewater treatment. IWA publishing: London

Strous, M., J. G. Kuenen, M. S. M. Jetten. 1999. Key physiology of anaerobic ammonium oxidation. Environ. Microbiol. 65(7): 3248-3250

Sunger N. and Bose P. 2009. Autotrophic denitrification using hydrogen generated from metallic iron corrosion. Bioresource Technol. 100: 4077-4082

Sutherland, I. W. 2001. Exopolysaccharides in biofilm flocs and related structures. Water Sci. Technol. 43:77-86

Tarnaki, K., S. Lyko, T. Wintgens, T. Melin and F. Natau. 2005. Impact of extracellular polymeric substances on the filterability of activated sludge in membrane bioreactors for landfill leachate treatment. Desalination. 179:181-190

Trigo C., J. L. Campos, J. M. Garrido and R. Mendez. 2006. Start up of the anammox process in a membrane bioreactor. Journal of Biotechnology. 126: 475-487

Tsushima, I., Y. Ogasawara, T. Kindaichi, H. Satoh and S. Okabe. 2007. Development of high rate anaerobic ammonium oxidizing (anammox) biofilm reactors. Water Res. 41: 1623-1634

Ueda, T., K. Hata, Y. Kiknoka and O. Seino. 1997. Effects of aeration on suction pressure in a submerged membrane bioreactor. Water Res. 31: 489-494.

Udert K. M., E. Kind, M. Teunissen, S. Jenni and T. Larsen. 2008. Effect of heterotrophic growth on nitritation/anammox in a single sequencing batch reactor. Water Sci. and Techno. 58(2): 277-284

Van de Graaf, A. A., P. de Bruijin, L. A. Robertson, M. S. M. Jetten, J. G. Kuenen. 1996. Autotrophic growth of anaerobic ammonium-oxidizing microorganisms in a fluidized bed reactor. Microbiology. 142: 2187-2196

Van Loosdrecht, M. C. M., J. Lyklema, W. Norde, G. Schraa and A. J. B. Zehnder. 1987. Electrophoretic mobility of hydrophobicity as a measure to predict the initial steps of bacterial adhesion. App. Environ. Microbio. 53:1898-1901

Vesilind, P. A. and C. J. Martel. 1990. Freezing of water and wastewater sludges. J. Environ. Eng.-ASCE. 116:854-862.

Visvanathan, V., B. S. Yang, S. Muttamara and R. Maythanukhraw. 1997. Application of air backflushing technique in membrane bioreactor. Water Sci. Technol. 36: 259-266

VrijenHoek, E. M., S. Hong and M. Elimelech. 2001. Influence of membrane surface properties on initial rate of colloidal fouling of reverse osmosis and nanofiltration membranes. J. Memb. Sci. 188:115-128

Wang, Z., Z. Wu, X. Yin and L. Tian. 2008. Membrane fouling in a submerged membrane bioreactor (MBR) under sub-critical flux operation: Membrane foulant and gel layer characterization. J. of Mem. Sci. 325:238-244

Watanabe, Y. and K. Kimura. 2006. Influence of dissolved organic carbon and suspension viscosity on membrane fouling in submerged membrane bioreactor. Sep. Sci. and Technol. 41:1371-1382.

Wilen, B. M., B. Jin and P. Lant. 2003. The influence of key chemical constituents in activated sludge on surface and flocculating properties. Water Res. 37:2127-2139

Wisniewski, C. 1996. Etude du comportmement de cultures mixtes en bioreacteur a membrane. Cinetque reactionnelles et filtrabilite. Ph.D. thesis, University of Montpellier II, Montpellier, France.

Wisniewski, C. and A. Grasmick. 1998. Floc size distribution in a membrane bioreactor and consequences for membrane fouling. Colloids surfaces A: Physicochemical and engineering aspects. 138:403-411

Wisniewski, C. and A. Grasmick. 1998. Floc size distribution a membrane bioreactor and consequences for membrane fouling. Colloids surf. A. 138:403-411

Wu C., Z. Chen, X. Liu and Y. Peng. 2007. Nitrification-denitrification via nitrite in SBR using real time control strategy when treating domestic wastewater. Biochem. Eng. J. 36: 87-92

Yamato, N., K. Kimura, T. Miyoshi and Y. Watanabe. 2006. Difference in membrane fouling in membrane bioreactors (MBRs) caused by membrane polymer materials. J. Memb. Sci. 280:911-919

Yamamoto, K, M. Hiasa, T. Manhood and T. Matsuo. 1989. Direct solid-liquid separation using hollow fiber membrane in an activated sludge aeration tank. Water Sci. Technol. 21(4-5):43-54

Yang J., L. Zhang, Y. Fukuzaki, D. Hira and K. Furukawa. 2010. High rate nitrogen removal by the anammox process with a sufficient inorganic carbon source. Bioresource Technol. 101: 9471-9478

Yoo, H., K. H. Ahn and H. J. Lee. 1999. Nitrogen removal from synthetic wastewater by simultaneous nitrification and denitrification (SND) via nitrite in an intermittently-aerated reactor. Water Res. 33(1); 145-154

Yoon, S. H., H. S. Kim and I. T. Yeom. 2004. The optimum operational condition of membrane bioreactor (MBR): Cost estimation of aeration and sludge treatment.

Yun, M. K. Yeon, J. Park, C. Lee, J. Chun and D. Lim. 2006. Characterization of biofilm structure and its effect on membrane permeability in MBR for dye wastewater treatment. Water Res. 40:45-52